The University Of Sheffield.

The adaptive significance of avian eggshell architecture

Duncan Jackson

A thesis submitted in partial fulfilment of the requirements for the degree of Doctor of Philosophy

The University of Sheffield
Faculty of Science
Department of Animal and Plant Sciences

December 2019

Contents

Summary

The avian eggshell plays a critical role in reproduction, providing the primary defence for the developing embryo against the outside world. The aim of this thesis is to understand how and why eggshell microstructure varies. I focus on one particular species, the common guillemot, which incubates its egg in a harsh environment – an exposed dirty, wet rock ledge – without a nest. I also make comparisons with other members of its family, the Alcids.

Across Alcids, eggshell thickness increases with adult (parental) body mass. I find eggshells are thicker at the equator in Alcid species that lay more elongate eggs and those that incubate their egg(s) on rock. A putative consequence of enhanced shell thickness at the equator (and potentially pointed end) is that fewer pores are able to form there, and as a result, the thinner blunt end may require a higher pore density to satisfy gas exchange demands. In common guillemot eggs pore density is indeed negatively related to shell thickness. I find that total pore number relates to egg size – but not incubation period – across the Alcids.

As eggshell pores are open channels from the outside into the egg, they pose a risk if they allow foreign matter to enter the eggshell. I show that shell accessory materials on common guillemot eggs provide protection, preventing foreign material from entering and blocking pores. I suggest that eggshells with a rough surface, particularly at the equator, may be better able to keep shell accessory material adhered to the shell, minimising the impact of abrasion from hard rock substrates. Intriguingly, I also show that surface microstructure relates to eggshell colour and pattern.

Overall, these findings provide a detailed insight into how eggshell structure varies within and between individuals and species, with important implications for our understanding of avian eggshell function.

Acknowledgements

When I first began studying common guillemot eggs in 2014, I did not expect to be still researching them five years later after being enticed into pursuing a scientific career and carrying out a PhD. I owe my sincere thanks to my supervisors, Dr Nicola Hemmings and Professor Tim Birkhead, for their guidance and support throughout that time, including the duration of this PhD. Their assistance was crucial to gaining funding for this PhD as well as ensuring exciting avenues of research could be pursued. Nicola and Tim's invaluable advice and consistent enthusiasm for my ideas and research has kept me motivated throughout this PhD, and their constructive feedback has helped to dramatically improve my scientific thinking, critical analysis, writing and presentation skills.

During my time in Sheffield several members of staff have also provided crucial support and guidance. Most notably, Jamie Thompson, who has provided invaluable assistance and stimulating discussion which has helped shape the nature and direction of my research. Jamie and Tim also collected all the common guillemot eggs from Skomer Island used during my research, and I am thankful that they were the ones abseiling down the precarious cliffs rather than myself. I would also like to thank Dr. Marie Attard for thought-provoking discussions about bird's eggs during this project. I owe thanks to Dr Chris Cooney for outstanding advice and assistance in performing phylogenetic analyses.

I am deeply thankful to all the researchers, their field crews and research assistants who supplied eggshells or helped with getting them imported into the UK including Nora Rojek, Mark Hipfner, Aevar Peterson, Mark Harris, Hallvard Strøm, Akiko Shoji, Kuniko Otsuki, Andrew Power, Ian O'Connor, David Mazurkiewicz, Linnea Hall and René Corado. Without their cooperation, much of the research here would not have been possible.

I am also thankful to Douglas Russell – the curator of eggs and nests at the Natural History Museum, Tring – for many helpful discussions throughout my PhD, including guidance on how to successfully import eggshells into the UK.

I am grateful to the Skelet.AL lab in the Royal Hallamshire Hospital for the use of their microCT scanner and also to the members of staff who work there for their support during the many intense months of scanning eggshells.

Finally, I must thank my partner, Abbie, for being incredibly supportive during both the highs and lows of my research and her patience in listening to me incessantly talk about bird eggs and imaging methods over the course of this project.

This PhD research would not have been possible without a University of Sheffield Faculty of Science Studentship Award.

Declaration

I, the author, confirm that the Thesis is my own work, except where work that has formed part of jointly authored publications has been included. I am aware of the University's Guidance on the Use of Unfair Means (www.sheffield.ac.uk/ssid/unfair-means). This work has not been previously been presented for an award at this, or any other, university.

Acknowledgement of previously published work in this thesis

Chapter 4 was published in The Journal of Experimental Biology:

> **Jackson, D., Thompson, J. E., Hemmings, N. and Birkhead, T. R.,** (2018). Common guillemot (*Uria aalge*) eggs are not self-cleaning. *The Journal of Experimental Biology*. **221**(23), jeb188466.

Article posted online on the 15 October 2018 and the final version was published on the 27 November 2018. Access the published version at:

http://jeb.biologists.org/lookup/doi/10.1242/jeb.188466

No permission is required to include this published work in this thesis, as indicated by The Journal of Experimental Biology's copyright policy: https://jeb.biologists.org/content/rights-permissions also see relevant user licence https://www.biologists.com/user-licence-1-1/

Appendix A1 was published in IBIS:

> **Birkhead, T. R., Thompson, J. E., Jackson, D. and Biggins, J. D.,** (2017). The point of a Guillemot's egg. *Ibis.* **159**(2), 255-265.

A license was granted by John Wiley and Sons for the reuse of this article in this thesis. License number: 4825960048339.

Chapter 1:

Introduction

The adaptive significance of avian eggshell architecture

Birds are one of the most evolutionarily successful vertebrate taxa, exploiting a vast array of ecological opportunities and colonising all terrestrial habitats around the world (Rahn 1991; Benson *et al.* 2014). The secret to their success is, at least in part, their reproductive strategy of laying hard-shelled, dessication-resistant eggs, in nests (or incubation sites) that are generally attended by a parent (Rahn 1991; Deeming 2002; Reynolds & Deeming 2016). This combination of a protective egg and nest, along with parental incubation behaviours, ensures optimal conditions for embryo development, even in extreme environments where other terrestrial vertebrates cannot reproduce (Rahn 1991; Deeming & Reynolds 2016).

The egg provides the primary form of protection and resources to the developing avian embryo, facilitating growth, development and survival until hatching (Romanoff & Romanoff 1949). Of particular importance to all of these processes is the eggshell. Far from being an inert container for the embryo, yolk and albumen, the eggshell is a finely tuned life support system that fulfils multiple functions, including physical and chemical protection, transmission of heat and light, regulation of gas exchange, and provision of inorganic minerals, primarily calcium, necessary for embryonic muscle, brain and skeleton development (Board & Sparks 1991; Deeming 2002; Karlsson & Lilja 2008; Birkhead 2016; Deeming & Reynolds 2016). As the eggshell is the boundary between the internal egg contents and the external environment, it is typically well-adapted to ensure the embryo is protected and nourished during incubation.

In this thesis, I focus on the microstructural adaptations of eggshells in bird species that incubate their egg(s) in harsh environmental conditions. I consider the importance of (1) shell thickness, (2) microscopic gas exchange pores, and (3) shell surface structure in providing protection and maintaining optimal conditions for the embryo during incubation, and how and why these features vary across different regions of the eggshell.

Eggshell thickness

The thickness of the shell is an important determinant of egg strength (Carnarius *et al.* 1996; Bain 2005). Large eggs laid by heavy birds need to be stronger than smaller eggs laid by small birds, to withstand the physical pressure associated with contact incubation by the parent. Their shells are thus relatively thick (Ar *et al.* 1974; Rahn *et al.* 1975; Ar *et al.* 1979; Rahn & Paganelli 1989; Birchard & Deeming 2009; but see Maurer *et al.* 2010). Eggs that are at risk of damage, such as those from species that incubate on hard substrates, in confined spaces, or that risk being punctured and ejected, also require thicker shells to prevent shell breakage (Uspenski 1958; Belopol'skiĭ 1961; Williams *et al.* 1982; Picman 1989; Mallory & Weatherhead 1990; Boersma *et al.* 2004; Spottiswoode & Colebrook-Robjent 2007; Spottiswoode 2010; Pirie-Hay & Bond 2014). Shell thickness may also play a role in regulating the diffusion of respiratory gases through microscopic pores in the shell, since shell thickness presumably determines the distance gases have to diffuse to get in or out of the egg (Wangensteen *et al.* 1970; Wangensteen & Rahn 1970; Ar *et al.* 1974). However, empirical evidence to support a role for shell thickness in mediating gas exchange is lacking (Simkiss 1986; Rokitka & Rahn 1987; Clark *et al.* 2010; Portugal *et al.* 2010; Maurer *et al.* 2012; Portugal *et al.* 2014). This may be because thicker eggshells typically contain larger pores, and this compensates for any reduction in gas exchange rate due to pores being longer (Rahn & Paganelli 1990). The number of pores in the shell may be a more important determinant of eggshell gas exchange efficacy (or conductance) than shell thickness or pore size (Ar & Rahn 1985; Rokitka & Rahn 1987; Rahn & Paganelli 1990).

Gas exchange pores

Eggshell gas conductance primarily relates to an egg's requirement to lose water as vapour – typically 10 - 22% of the egg's initial mass – during incubation, rather than specifically to the embryo's oxygen requirements (Rahn & Paganelli 1990; Ar & Deeming 2009). Losing adequate water is essential for the formation of the air cell within the egg, as well as for normal embryonic growth and hatchability (Ar & Rahn 1980; Ar 1991). It is therefore essential that the egg loses water throughout the incubation period, whereas an influx of oxygen from the external environment is only likely to become crucial towards

the end of incubation (Rahn & Paganelli 1990). Since water production from metabolic processes is directly related to oxygen consumption, the eggshell's gas conductance requirements for optimum water loss throughout incubation should also provide adequate oxygen gain even when oxygen requirements peak towards the end of incubation (Ar & Rahn 1980; Ar & Rahn 1985; Rahn & Paganelli 1990; Ar & Deeming 2009).

Three main factors influence the optimum rate of eggshell gas conductance across birds: (1) egg size, (2) incubation period and (3) environmental conditions (Ar & Rahn 1985). Eggshell porosity (specifically, total pore number) drives differences in gas conductance, so the effects of these three factors are often manifested as changes in total pore number (Ar & Rahn 1985; Rahn & Paganelli 1990). For example, larger eggs containing more water need a larger number of pores than small eggs do, in order to lose the optimum amount of water by the end of incubation (Rahn & Ar 1974; Tullett & Board 1977; Ar & Rahn 1985; Rahn & Paganelli 1990). Species with longer incubation periods typically require eggs with fewer pores than those with shorter incubation periods, to slow the rate of water loss and avoid desiccation (Rahn & Ar 1974; Rahn *et al.* 1976; Roudybush *et al.* 1980; Vleck & Kenagy 1980; Whittow 1980; Whittow *et al.* 1980; Grant *et al.* 1982; Ricklefs 1984; Tullett 1984; Ar & Rahn 1985; Rahn & Paganelli 1990; Zimmerman & Hipfner 2007). Variation in eggshell porosity can also be explained by two important components of the incubation environment: humidity (often mediated by the nest) and atmospheric pressure at different altitudes, both of which influence the rate of egg water loss (Packard *et al.* 1977; Rahn *et al.* 1977; Rahn *et al.* 1982; Vleck *et al.* 1983; Davis *et al.* 1984; Davis & Ackerman 1985; Arad *et al*. 1988; Guerra *et al.* 1988; Carey *et al.* 1990; Hempleman *et al.* 1993; Monge *et al.* 2000; Portugal *et al.* 2014; but see Carey 2002).

Although pores are an essential feature of the avian eggshell, they represent a weakness in the egg's overall defence against the environment. Pores are essentially open channels from the egg's interior to the outside world, and can facilitate the passage of microbes into the egg that may lead to embryonic infection and mortality (Board 1982). Pores are also vulnerable to becoming blocked by debris and flooded with water, reducing gas exchange efficacy of the shell (Board 1982). These problems may be mitigated if pores are protected by, for example, features of the exterior surface of the shell.

Shell surface structure

The eggshell's surface can be broadly divided into (a) the microstructure and topography of calcium carbonate shell and (b) the shell accessory material that sits on top. Shell accessory material protects against debris (Board & Perrott 1982), water (Board & Halls 1973a, b; Sparks & Board 1984) and microbes (Wellman-Labadie *et al.* 2008; D'Alba *et al.* 2014; Gole *et al.* 2014a, b; Ishikawa *et al.* 2010; D'Alba *et al.* 2017; Chen *et al.* 2019), and potentially contributes to other functions, including to egg strength (Tyler 1969; Portugal *et al.* 2018), gas conductance (Deeming 1987; Thompson & Goldie 1990), the visual appearance of an egg (including colouration, patterning and gloss; Lang & Wells 1987; Sparks 1994; Deeming 2011; Sparks 2011; Sammiullah & Roberts 2013; Sammiullah & Roberts 2014; Igic *et al.* 2015), and therefore protection against solar radiation and harmful UV-B light (Maurer *et al.* 2015; Lahti & Ardia 2016). The role of eggshell surface microstructure and topography is less clear. When combined, a small number of studies suggest that interspecific variation in surface microstructure may exist (Mikhailov 1997), from the pitted eggshells of hoopoes (*Upupa epops*; Martín-Vivaldi *et al.* 2014), to the smooth eggshells laid by tinamous (Tinamidae; Igic *et al.* 2015), to the rough eggshells of some megapodes, ratites and dinosaurs that contain peaks and troughs (Tyler & Simkiss 1959; Sabath 1991; Grellet-Tinner *et al.* 2006; Hechenleitner *et al.* 2016; Grellet-Tinner *et al.* 2017).

Despite the lack of empirical data on the function of eggshell surface topography, there have been several hypotheses proposed for the role of surface microstructure during incubation. Indents or "crypts" in the shell's surface have been suggested to hold uropygial fluid (or preening oils) containing mutualistic bacteria, providing microbial protection on the eggshell surface (Soler *et al*. 2008; Martín-Vivaldi *et al.* 2014; Soler *et al*. 2014). Mayani-Parás *et al.* (2015) suggested that in some species, surface microstructure may help debris to adhere to the surface of eggs, aiding in "behaviourally induced camouflage" to minimise egg predation. In contrast, Steven Portugal *et al.* (Unpublished Data, https://phys.org/news/2013-07-unique-shell-guillemot-eggs-edge.html) proposed the rough surface of common guillemot (*Uria aalge*) eggs provides hydrophobicity and self-cleaning properties. Grellet-Tinner *et al.* (2017) suggested that

the eggshell surface may be rough (via surface protrusions) to protect against organic acids in the incubation environment. These observations and suggestions raise the possibility that eggshell surface topography plays an important role in mediating negative conditions in the incubation environment. A number of studies have also suggested that eggshell surface structure, including the presence or absence of shell accessory materials, influences the egg's appearance depending on how the surface reflects light (Richards & Deeming 2001; Fecheyr-Lippens *et al.* 2015; Igic *et al.* 2015; Brulez *et al.* 2016). It is currently unclear how variable surface structure is within and between bird species, and what the functional properties of different surface morphologies and roughness profiles are.

Case study: the common guillemot

The common guillemot is a species that exemplifies incubation in extreme environments. It lays its single egg on bare rock cliff ledges without constructing any nest in densely populated breeding colonies where conditions are highly unsanitary. There is a risk of eggs being dislodged from this precarious incubation site, but parental incubation behaviours and inherent stability provided by the shape of the egg limits this possibility (Tschanz 1990; Birkhead *et al.* 2018). Common guillemots lay an unusually pyriform ("pear-shaped") egg, and in Birkhead *et al.* (2017a), we suggested that this shape, along with the birds upright incubation position, ensures that the more porous blunt end is kept relatively clean and free from debris during incubation, ensuring sufficient gas exchange across the eggshell (see Appendix A1). Furthermore, we proposed that enhanced thickness at the equator compared to each end of the eggshell ensures maximum strength at the region that is in contact with hard rock, which is essential due to the impacts the egg has to endure when other guillemots imprecisely land at the colony (Uspenski 1958; Belopol'skiĭ 1961; Pirie-Hay & Bond 2014). The common guillemot's eggshell is thinner at the blunt end and therefore presumably weaker, likely allowing the chick to hatch out more easily than it would at the reinforced equator. It is possible that variation in shell thickness and porosity (primarily driven by changes in pore density) along the guillemot eggshell may be ecologically adaptive, mitigating the negative aspects of the incubation environment, but this has not yet been tested.

Variation in eggshell microstructural variation could also relate to the fundamental requirements of embryos developing in eggs. Pore densities may be higher towards the blunt end of the eggshell (Romanoff & Romanoff 1949; Rokitka & Rahn 1987) in order to compensate for the reduction in shell surface area available for gas exchange due to the equatorial region being partially covered by the incubating bird's brood patch (Reizis *et al.* 2005). This could be particularly pertinent for the guillemot's egg, which is rarely left unattended and is therefore nearly constantly covered throughout incubation (Gaston & Jones 1998). It is also possible that having more pores at the blunt end optimises air-cell formation, although egg and shell membrane structure may play a more important role in this (Mao *et al.* 2007), since even when the blunt end is covered by an impermeable material (epoxy cement), an air-cell still forms (Tazawa *et al*. 1971). Additionally, the egg's shape and/or size may lead to variation in eggshell microstructure along an egg. For example, more elongate eggs (such as the common guillemot's egg) may require a particularly thick equatorial region because elongate eggs are inherently weaker than more spherical eggs (Picman 1989; Maurer *et al.* 2012).

It is important to note that eggshell porosity, thickness, and/or surface structure may all be linked, due to the process of eggshell formation (Tullett 1975; Tullett & Board 1977; Tyler & Fowler 1978; Riley *et al.* 2014). One microstructural pattern along the eggshell may therefore emerge as a consequence of another, or even be the result of macro-egg morphological traits such as egg size or shape. For example, thicker shells tend to contain a lower density of pores (Tullett & Board 1977; Tyler & Fowler 1978), so possessing a relatively thicker equator as, for example, an adaptation to a hard incubation substrate, may have the knock-on effect of limiting the number of pores that can form at the equator and producing an unequal distribution of pores across the eggshell, as seen in the common guillemot (Birkhead *et al.* 2017a). To understand the ecological significance of regional variation in eggshell microstructure, we therefore have to identify how factors such as egg size, shape and the interconnectedness of eggshell structure contribute to the eggshell microstructure patterns we see in nature.

Research objectives

The aim of this thesis is to understand how eggshell microstructure, and particularly variation in microstructure along an egg, is adaptive in birds. To do this, I focus primarily on a species – the common guillemot – that incubates its egg in harsh environmental conditions without a protective nest. I also draw comparisons with other related species that incubate their egg(s) in a range of conditions due to variation in incubation site selection and nest type.

To address this aim, I will ask three broad questions.

1. **What is the functional significance of eggshell thickness variation along bird eggs?**

   I will test the following hypotheses:

   1a: Larger, more elongate common guillemot eggs will have thicker eggshells at the equator to reinforce strength at the region the parent primarily makes contact with during incubation (Chapter 2). Maurer *et al.* (2012) suggested that more elongate eggs require reinforcement at the equator to compensate for any structural weakness imposed by their shape and Bignert *et al.* (1995) found that larger common guillemot eggs have thicker eggshells than smaller eggs.
   1b: Species that lay their eggs on hard/abrasive substrates and/or have higher body mass and/or lay large or elongate eggs have thicker eggshells, particularly at the equatorial region, to reinforce egg strength at the region the bird applies force to during incubation (Chapter 2; see Uspenski 1958; Belopol'skiĭ 1961; Ar *et al.* 1974; Ar *et al.* 1979; Rahn & Paganelli 1989; Birchard & Deeming 2009; Maurer *et al.* 2012; Pirie-Hay & Bond 2014; Birkhead *et al.* 2017a).

2. Why does eggshell pore density vary along bird eggs?

I will test the following hypotheses:

2a: All bird eggs contain a higher density of pores at the blunt end, potentially as an adaptation to the eggshell being partially covered during contact incubation (Chapter 3; see Rokitka & Rahn 1987; Reizis *et al.* 2005).
2b: High blunt end pore densities are associated with species that breed and incubate their eggs in dirty environments where the risk of eggshell surface contamination (and pore blockage) by debris around most of the egg is high (Chapter 3; Birkhead *et al.* 2017a).
2c: Precocial birds lay eggs with high blunt end pore density compared to the rest of their egg to create a specialised respiratory site for accelerated neural development. Smart (1991) suggested that an asymmetrically pointed egg may be adaptive for precocial species to facilitate accelerated neural development by creating a specialised respiratory site at the blunt end of the egg, but only if pore densities are also higher here than along the rest of the egg. Based on this logic, egg shape and/or unequal pore distributions could facilitate the creation of a specialized site for respiration at the blunt end of an egg (Chapter 3).
2d: The distribution of pores in bird eggshells is related to regional variation in eggshell thickness. Specifically, thicker regions of shell in an egg will contain a lower density of pores due to thickness related constraints on pore formation (Chapter 3). The fact that a negative correlation between shell thickness and pore density has been found in other studies (Tullett & Board 1977; Tyler & Fowler 1978), and that the common guillemot's egg exhibits a strikingly unequal distribution of pores along its shell (Birkhead *et al.* 2017a) and also possesses a very thick equatorial region relative to the blunt end (Maurer *et al.* 2012; Birkhead *et al.* 2017a), gives credence to this hypothesis.
2e: Larger eggs will have a higher total number of pores than small eggs, with those having long incubation periods having lower than expected pore numbers (based on the size of the egg) to satisfy water loss demands (Chapter 3; see Rahn & Ar 1974; Rahn *et al.* 1976; Ar & Rahn 1980; Ricklefs 1984; Tullett 1984; Ar & Rahn 1985; Rahn & Paganelli 1990).

3. What is the adaptive significance of eggshell surface structure in the common guillemot?

I will investigate the following hypotheses and sub-questions:

3a: Due to their rough surface, common guillemot eggshells are self-cleaning to cope with incubation in a dirty environment (Chapter 4; Portugal *et al.* Unpublished Data: https://phys.org/news/2013-07-unique-shell-guillemot-eggs-edge.html).
3b: The shell accessory material layer on the common guillemot's eggshell protects pores by preventing blockage from debris allowing adequate gas conductance across the shell despite the egg becoming soiled during incubation (Chapter 4). Shell accessory material may have a similar role in other species. For example, Board and Perrott (1982) provided circumstantial, observational evidence that shell accessory material may prevent pore blockages by debris in naturally incubated guinea fowl (*Numidia meleagris)* eggs.
3c: How does surface roughness vary along the common guillemots eggshell? As the equatorial region of the egg is most frequently in contact with the abrasive, rock incubation substrate, possessing a rough surface here may potentially minimize abrasion and wear, especially of any shell accessory material. I therefore investigated whether the equator region has the greatest surface roughness compared to the blunt or pointed end to assess whether any inferences could be made about the adaptive function of eggshell surface roughness (Chapter 5).
3d: Does eggshell surface structure relate to other eggshell traits? I explored whether intraspecific variation in eggshell surface structure relates to egg size, shape, colour, patterning and shell thickness whilst also investigating how the presence of shell accessory material can alter the egg's final surface roughness and colour (Chapter 5). Other authors have suggested an egg's colour may in part be determined by its surface roughness (Fecheyr-Lippens *et al.* 2015; Igic *et al.* 2015; Brulez *et al.* 2016) and shell accessory material (Sparks 1994; Richards & Deeming 2001; Deeming 2011; Sparks 2011) therefore exploring intraspecific correlations between egg colour and surface structure may prove enlightening, especially because pigments alone do not fully explain the diversity of colour expressed in common guillemot eggs (Hauber *et al.* 2019).

The research presented here will investigate (i) how eggshell microstructure relates to other egg traits and (ii) how eggshell microstructure relates to conditions the egg experiences in the incubation environment. In order to satisfactorily answer these questions, I chose a taxon with variation in a range of parameters of interest.

Study taxon: the Alcidae

The auks (Alcidae) are a family of pelagic marine birds comprising of at least 24 extant species and numerous extinct species, including the iconic, recently extinct great auk (*Pinguinus impennis*; del Hoyo *et al.* 2019). Their name is believed to be derived from the old norse “alka”, first utilised for the razorbill (*Alca torda*) and expanded to encompass the other Atlantic Alcids, before “auk” was used to describe the entire family (Lockwood 1978). However, some authors have suggested the name comes from their “awkwardness” because in old English, they were called “awks” (Lorimer 2014). Indeed the historical saying ‘as drunk as an auk [razorbill]” probably derives from the razorbill’s unsteady gait and the swaying and stretching movement of their neck and head they perform upon returning to land (Lockwood 1978).

The Alcid family belongs to the broader Charadriiforme order. The auks can be subdivided into 6 distinct lineages or tribes; the *Aethiini* (auklets, 5 species), *Alcini* (true or typical auks and murres, 4 species), *Brachyramphini* (brachyramphine murrelets, 3 species), *Cepphini* (true guillemots, at least 3 species), *Fraterculini* (puffins, 4 species) and *Synthliboramphini* (synthliboramphine murrelets, at least 5 species; see Fig. 1; Friesen *et al.* 1996; Weir & Mursleen 2013; Smith & Clarke 2015; Smith 2016). These tribes are usually grouped into two distinct subfamilies; the Fraterculinae, consisting of the *Aethiini* and *Fraterculini* and the Alcinae comprised of the *Alcini*, *Brachyramphini, Cepphini* & *Synthliboramphini* (Fig. 1; Smith & Clarke 2015; Smith 2016).

Auks are widespread across northern latitudes, favouring cooler seas. They inhabit environments as far north as the arctic circle in Europe, Canada, North America and Russia to more intermediate, temperate latitudes, including Japan, and are even found at more southerly latitudes in the warmer climates of Mexico and California (Gaston & Jones 1998). The extant Pacific Alcids (18 species) are more speciose than their Atlantic

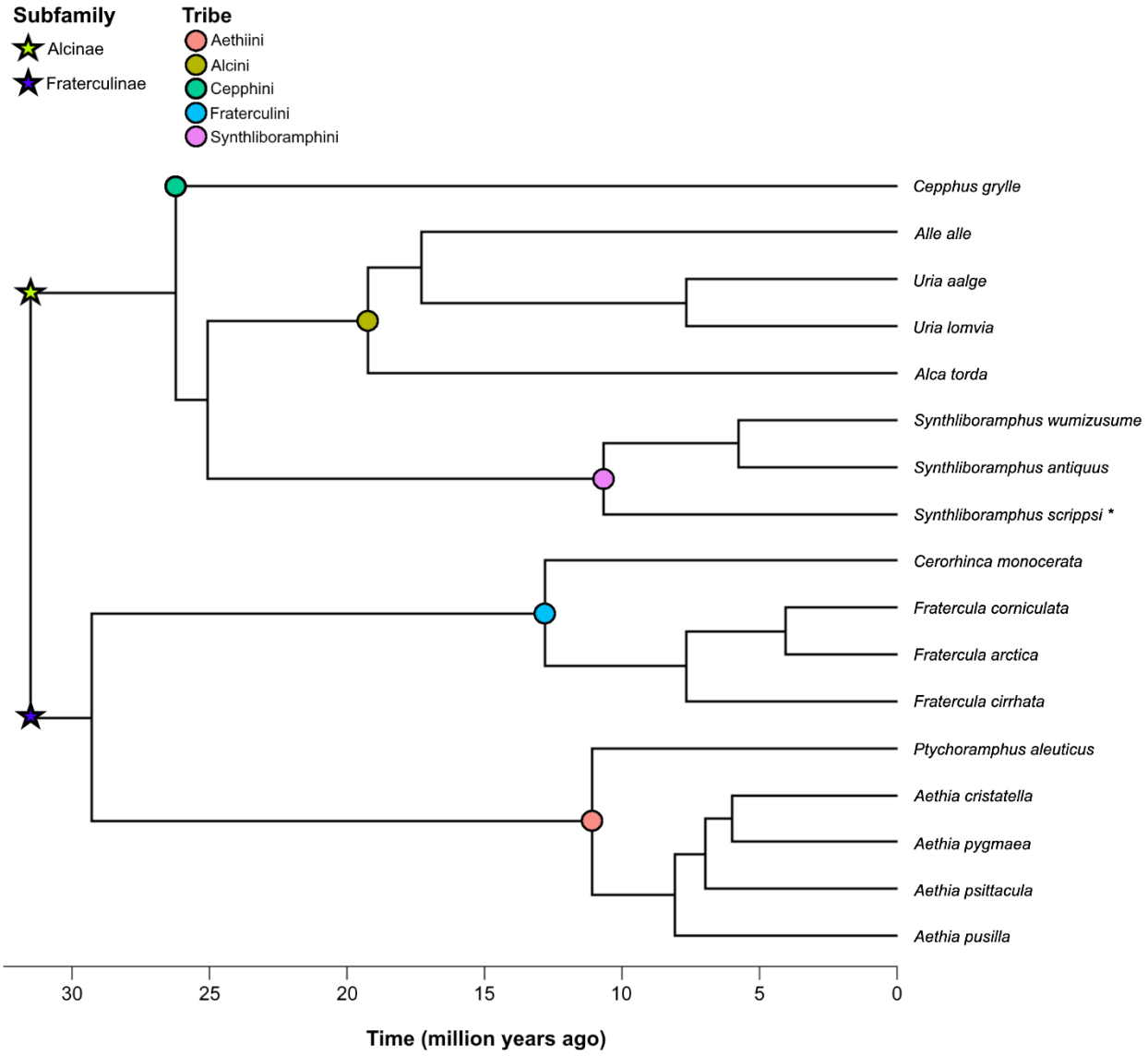

Figure 1. Phylogenetic tree of extant Alcids from Weir and Mursleen (2013), pruned to leave only the 17 species represented in our core dataset. **S. Scrippsi* previously called *S. hypoleucus scrippsi.* See Weir & Mursleen 2013 for phylogeny of extant species and Smith & Clarke 2015 for a more extensive phylogeny including extinct species.

relatives (6 species), although palaeontological evidence suggests that the Atlantic Alcids may have been far more diverse and speciose in the past (Smith & Clarke 2015). One such extinct Atlantic Alcid was the original penguin – the great auk. Its name was possibly derived from the Welsh for white head “pen gwyn” or from “pen-winged” or “pinioned”. The great auk was named before explorers and zoologists had encountered what we now consider to be modern penguins (Spheniscidae) in the southern hemisphere, which evolved convergently to the auks (Montevecchi & Kirk 2020). As a result, and because of the auks morphological similarity to the penguins, they are often referred to as the “penguins of the north”.

Alcids are exceptional swimmers. Propelled by their wings, auks can dive down to depths of up to 180m in pursuit of their prey which may include zooplankton, fish or cephalopods. Specialised wing adaptations facilitate their diving prowess, whilst allowing them to retain their ability to fly, unlike their southern hemisphere counterparts – the penguins (Gaston & Jones 1998; Weir & Mursleen 2013; Smith 2016). However, like the penguins they are less well-adapted to terrestrial life, being rather clumsy and awkward on land (Lockwood 1978; Lorimer 2014). Their leg placement and morphology typically results in an upright walking posture, and along with their webbed feet, this results in reduced agility on land (Williams *et al.* 1982). A result of this is that auks typically need to breed in locations where terrestrial predators cannot reach them, such as burrows, crevices, caves, sea cliff ledges and in the case of the marbled murrelet, in large old-growth, mature conifer trees (Williams *et al.* 1982; Gaston & Jones 1998). Auks spend most of their time out at sea, typically only returning to land to breed. With the exception of the *Brachyramphini,* the auks are colonial nesting species (Gaston & Jones 1998; del Hoyo *et al.* 2019). In fact some species, such as the common guillemot, breed at incredibly high densities, typically 20 pairs per square metre but up to 70 pairs per square metre, to allow them to defend themselves effectively against aerial predators (Birkhead 1977; Birkhead 1993).

Auks are unusual in many ways. One example is that they typically only lay one or two eggs which are usually incubated for prolonged periods of time. The time spent on incubating the chick versus rearing it post-hatch varies dramatically between species (Gaston & Jones 1998; Starck & Ricklefs 1998). Indeed, auks are unique among birds in showing more variation in several key traits than any other bird family (e.g.

developmental mode; Starck & Ricklefs 1998; Birkhead *et al.* 2019). Such diversity in morphological, life-history and behavioural traits expressed in this family makes them an ideal subject for the study of adaptation (Gaston & Jones 1998; Starck & Ricklefs 1998; Zimmerman & Hipfner 2007; Hipfner *et al.* 2010; Weir & Mursleen 2013; Smith & Clarke 2015; Smith 2016; Birkhead *et al.* 2019).

The extant auks have considerable interspecific variation in adult body size (~80g to ~1000g), egg shape (rotund to elongate and even extremely pyriform shaped), egg size (~15cm^3 to 100cm^3), egg colour (white, brown, beige, blue and green with varying degrees of maculation or patterning), reproductive mode (e.g. incubation period, precociality and clutch size) and breeding ecology, including incubation site selection and nest type from laying eggs on bare wet, dirty rocky cliff ledges without a nest, to laying eggs in mud burrows or pebble and moss-lined nests (Table 1; Gaston & Jones 1998). This variation makes the auks an ideal taxon in which to investigate the adaptive significance of egg traits (e.g. Birkhead *et al.* 2017a; Birkhead *et al.* 2019; Birkhead *et al.* 2020), including eggshell microstructure (e.g. Zimmerman & Hipfner 2007). Studying such diversity within a single family will allow us to gain greater insight into the evolutionary ecology of bird reproduction. The common guillemot in particular exhibits remarkable within-species diversity in egg shape, size, colour and shell thickness, making them an ideal model species to investigate how eggshell microstructure may be intrinsically related to other aspects of the egg (Tschanz 1990; Pirie-Hay & Bond 2014; Birkhead *et al.* 2017b).

Using X-ray micro-computed tomography to study shell structure

Traditional methods used to study eggshell microstructure have limitations, in that they, (a) are potentially inaccurate, (b) are non-specific, (c) require fragments to be taken from a shell, and/or (d) are destructive thus typically allow few structural measurements (e.g. one trait) to be collected from a single fragment (see Appendix A2). Non-destructive techniques have been developed to measure eggshell thickness on whole eggs or blown shells, however their accuracy is sometimes questionable (Gould 1972; Voisey & Hamilton 1976; Yan *et al.* 2013; Sabuncu & Akdoğan 2014; Kibala *et al.* 2015; Dong *et al.* 2017; but see Santalo 2018). In recent years, X-ray micro-computed tomography (microCT) has been applied to the study of avian eggshells and resolves many of these

Table 1. Auk summary table.

Common name	Binomial name	Adult bird mass (g)[1]	Developmental mode[2]	Incubation period (days)[3]	Breeding site[4]	Incubation site lining[4]	Eggs incubated on a rock substrate?[5]	Clutch size[6]	Egg parameters[7]		
									Volume (cm^3)	Elongation (arb)	Asymmetry (arb)
Ancient murrelet	*Synthliboramphus antiquus*	212	Fully precocial	32.5	Burrows, crevices or under boulders	Scrape or cup nest constructed out of twigs, leaves & dry grass.	Rarely	2	45.3	1.581	0.548
Atlantic puffin	*Fratercula arctica*	556	Semi-precocial	42	Burrows. Sometimes in crevices or cavities under boulders.	Substantial amount of material in nest chamber including grass, leaves, plant stalks & feathers.	Rarely	1	58.9	1.456	0.582
Black guillemot	*Cepphus grylle*	439	Semi-precocial	30	Open sites on rocky shores crevices, among boulders or talus or in burrows	Rough scrape typically lined with pebbles & snail shells.	Sometimes	2	46.4	1.485	0.578

Table continued on next page

Common name	Binomial name	Adult bird mass (g)[1]	Develop-mental mode[2]	Incub-ation period (days)[3]	Breeding site[4]	Incubation site lining[4]	Eggs incubated on a rock substrate?[5]	Clutch size[6]	Egg parameters[7]		
									Volume (cm^3)	Elongat-ion (arb)	Asymm-etry (arb)
Brünnich's guillemot[a]	*Uria lomvia*	955	Intermediate	32.5	Open cliff ledges	None. Egg directly on bare rock, snow or ice.	Usually	1	100.5	1.540	0.617
Cassin's auklet	*Ptychoramphus aleuticus*	180	Semi-precocial	38.5	Burrows, sometimes under driftwood or in dirt floored chambers	Typically none. Egg rests on dry soil. Sometimes a scape is lined with vegetation.	Rarely	1	26.8	1.468	0.554
Common guillemot[b]	*Uria aalge*	993	Intemediate	32.5	Open cliff ledges	None. Egg directly on bare rock.	Usually	1	96.1	1.574	0.631
Crested auklet	*Aethia cristatella*	260	Semi-precocial	34.5	Crevices	Sometimes on a collection of pebbles or a depression in the dirt floor	Sometimes	1	31.7	1.404	0.557
Horned puffin	*Fratercula corniculata*	574	Semi-precocial	41	Crevice or under boulders. Occasionally in a burrow.	Nest may be lined with grass & feathers.	Sometimes	1	67.4	1.480	0.580

Table continued on next page

Common name	Binomial name	Adult bird mass (g)[1]	Developmental mode[2]	Incubation period (days)[3]	Breeding site[4]	Incubation site lining[4]	Eggs incubated on a rock substrate?[5]	Clutch size[6]	Egg parameters[7]		
									Volume (cm^3)	Elongation (arb)	Asymmetry (arb)
Japanese murrelet	*Synthliboramphus wumizume*	187	Fully precocial	31	Crevice, among boulders or in a burrow.		Sometimes	2	33.3^	1.533^	0.534^
Least auklet	*Aethia pusilla*	85	Semi-precocial	30.5	Crevice.	Sometimes uses small pebbles or other detritus or may dig a slight depression if the floor is dirt & not rock.	Sometimes	1	15.6	1.438	0.564
Little auk[c]	*Alle alle*	172	Semi-precocial	29	Crevice, under boulders or amongst talus.	Bed of pebbles, sometimes small fragments of vegetation included.	Usually	1	26.7	1.447	0.576
Parakeet auklet	*Aethia psittacula*	284	Semi-precocial	35.5	Crevice, under boulders or in a burrow.	Pebbles sometimes used. Typically egg rests in a dirt scrape.	Sometimes	1	38	1.449	0.577

Table continued on next page

Common name	Binomial name	Adult bird mass (g)[1]	Developmental mode[2]	Incubation period (days)[3]	Breeding site[4]	Incubation site lining[4]	Eggs incubated on a rock substrate?[5]	Clutch size[6]	Egg parameters[7]		
									Volume (cm^3)	Elongation (arb)	Asymmetry (arb)
Razorbill	*Alca torda*	717	Intermediate	36	Open cliff ledge, crevice, under boulders or in a burrow.	Typically no nest but pebbles, vegetation or other detritus may be used.	Sometimes	1	82.4	1.561	0.597
Rhinoceros auklet	*Cerorhinca monocerata*	508	Semi-precocial	45	Typically in a burrow but may nest on the floor of caves.	Nest chambers are saucer shaped & lined with vegetation, including grass, leaves & twigs.	Rarely	1	75	1.500	0.565
Scripps's murrelet	*Synthliboramphus scrippsi*	196	Fully precocial	34	Crevice, under boulders or roots or in a burrow.		Sometimes	2	34.6	1.514	0.535
Tufted puffin	*Fratercula cirrhata*	774	Semi-precocial	45.5	Burrow, crevice or cavities under boulders or talus.	Typically on bare ground but sometimes in a rough scrape lined with plant material & feathers.	Sometimes	1	88.6	1.449	0.588

Table continued on next page

Common name	Binomial name	Adult bird mass (g)[1]	Develop-mental mode[2]	Incub-ation period (days)[3]	Breeding site[4]	Incubation site lining[4]	Eggs incubated on a rock substrate?[5]	Clutch size[6]	Egg parameters[7]		
									Volume (cm^3)	Elongat-ion (arb)	Asymm-etry (arb)
Whiskered auklet	*Aethia pygmaea*	114	Semi-precocial	35.5*	Crevices or cavities beside boulders or in densely vegetated grass slopes.	Small pebbles & detritus or a slight depression in dirt floor.	Sometimes	1	N/A	N/A	N/A

[1] Average of species values reported in Smith (2016) and del Hoyo *et al.* (2019).

[2] Sourced from del Hoyo *et al.* (2019), Gaston and Jones (1998) and Starck and Ricklefs (1998).

[3] Sourced primarily from del Hoyo *et al.* (2019), but also Gaston and Jones (1998). Value for rhinoceros auklet sourced from Gaston and Jones (1998) due to potential error in the value reported in del Hoyo *et al.* (2019).* uncertain but probably around 35-36 days.

[4] Information on auk incubation site and substrate used for categorisation (5) was obtained primarily from Gaston and Jones (1998) and del Hoyo *et al.* (2019) but also other sources in the literature (e.g. Johnsgard 1987; Olsthoorn & Nelson 1990; Tschanz 1990).

[5] Based on incubation site and whether that species lines the incubation site. Where available we also used descriptions and images of incubation sites taken by field researchers who collected eggshells for use in this study and the information available on the Audubon website (https://www.audubon.org/field-guide) to inform our categorisation. See chapter 2 for further details.

[6] Sourced from Gaston and Jones (1998).

[7] Data collected as part of this thesis except for whiskered auklet and Japanese murrelet. See chapters 2 & 3 and appendices A3 – A6 for further details on how this data was sourced or acquired.

^ Values from Birkhead *et al.* (2019) reported.

[a] Known as the thick-billed murre in North America.

[b] Known as the common murre in North America.

[c] Known as the dovekie in North America.

potential issues and limitations while providing precise and accurate microstructural measures (Riley *et al.* 2014; Willoughby *et al.* 2016; Birkhead *et al.* 2017a).

MicroCT is an advanced imaging technique that allows the structure of objects to be visualised and quantified in three-dimensional space (3D). As eggshells can be imaged in 3D, measurement of several eggshell traits from a single area of eggshell with minimal sample preparation is possible (Riley *et al.* 2014; Willoughby *et al.* 2016). This includes pore density, shape and size, and measurements of the thickness of specific shell layers such as the organic membranes, the mammillary layer and the effective shell thickness, the latter of which is the distance from the point of fusion of the mammillary bodies to the outer surface of the shell and is the measure thought to best reflect an egg's strength (Bain 2005; Riley *et al.* 2014; Willoughby *et al.* 2016; Birkhead *et al.* 2017a). MicroCT data can also provide qualitative data on eggshell surface structure (e.g. Grellet-Tinner *et al.* 2017), as well as potentially provide quantitative data on surface roughness (see Garbout *et al.* 2018), and the density of the eggshell (Riley *et al.* 2014). MicroCT techniques are generally considered non-destructive, although depending on the scanner used, fragments may need to be taken from whole eggs for imaging at high resolution (e.g. in the Bruker Skyscan 1172; Birkhead *et al.* 2017a). This technique provides accurate, precise data on a range of microstructural traits while avoiding damage to the eggshell and is therefore ideal for studying eggshell microstructure.

Thesis outline

In this thesis, I use microCT to study eggshell microstructure to understand how eggshell thickness, pore distributions, the resultant total number of pores in an egg and surface structure are adaptive in the Alcidae. A key objective of this research is to identify how microstructural variation relates to other egg traits (such as egg size or shape), but the core focus is on how eggshell microstructure varies in relation to the micro-environment in which species incubate their eggs.

Chapter 2: Patterns of eggshell thickness and their functional significance in the auks.

Here, I investigate how variation in shell thickness relates to egg size and shape within the common guillemot to test if larger or more elongate eggs have thicker shells, particularly at the equator (1a). I then explore patterns of eggshell thickness across the Alcidae in relation to egg size, shape, adult mass and incubation substrate (1b).

Chapter 3: Does the distribution of pores along a bird's egg matter?

In this chapter I characterise the distribution of pores along Alcid eggs and investigate how pore densities (and their distribution) relate to egg shape, size, developmental mode, incubation environment and variation in shell thickness along an egg (2a – d). I then assess how the distribution of pores influences predictions of the total number of pores in an egg, and how this latter variable then relates to egg size and incubation period (2e).

Chapter 4. Common guillemot (*Uria aalge*) eggs are not self-cleaning.

Here, I explore the adaptive significance of common guillemot eggshell surface structure by experimentally testing whether common guillemot eggs are self-cleaning (3a). I also investigate the role shell accessory material has in protecting the egg (3b).

Chapter 5. Dark blue-green common guillemot eggs have rougher surfaces than white eggs.

In this chapter I characterise how surface structure varies along the common guillemot's egg (3c) and then explore variation in eggshell surface structure to examine how surface roughness relates to other eggshell traits, specifically shell thickness, egg size and shape (3d). In the process of carrying out this work, I also discovered an interesting link between shell surface structure and eggshell colour in the common guillemot, and present the results of these investigations as well (3d). I also present preliminary comparisons of eggshell surface structure and roughness across the auks in Appendix A7 of this thesis.

Chapter 6. General Discussion.

In chapter 6, I discuss the main conclusions arising from the research presented in this thesis (Chapters 2 – 5) and highlight misconceptions and common assumptions in the literature about bird eggshells, which my research has indicated are likely incorrect. I also summarise the advantages of using microCT to study bird eggshells and suggest future directions for researchers interested in investigating why eggshell microstructure varies within an egg, and intra- and interspecifically.

Due to this thesis taking the form of an alternative publication format thesis, the references for each chapter will be provided at the end of each chapter rather than as a full bibliography at the end of the thesis. As per University of Sheffield recommendations, the main figures and tables will be included on the page following their initial mention in the main body of the text, instead of as a list at the end of each data chapter (i.e. manuscript) as would be typical for a paper submitted for publication. Any supplementary materials for each data chapter are included at the end of the thesis in appendices (A3 – 6) to ease readability.

Acknowledgement of collaborative work within the thesis

The candidate confirms that the work submitted is their own, except where work that has formed part of jointly authored publications has been included. The contribution of the candidate and the other authors to this work has been explicitly indicated below, as well as at the end of each chapter. The candidate confirms that appropriate credit has been given within the thesis where reference has been made to the work of others.

Chapters 2, 3 and 5:
D.J. planned and managed the research, carried out all data collection and experimental work apart from imaging common guillemot eggs from Wales which was previously done as part of other studies by J.T. (e.g. Birkhead *et al.* 2017a, b; Birkhead *et al.* 2018; Birkhead *et al.* 2019), performed all statistical analysis, and researched and wrote the manuscripts. N.H. and T.R.B. commented on manuscripts and supervised the projects.

Chapter 2:
C.R.C. provided advice on how to perform phylogenetically controlled analyses and commented on the manuscript.

Chapter 4:
D.J. carried out all microCT scanning and the self-cleaning trials, and the experiment testing how the presence of shell accessory material prevents pore blockages. J.T. used FTIR spectrometry to study how debris affects the rate of carbon dioxide conductance across dirty eggshells. J.T. performed preliminary analyses on the FTIR data, D.J. performed the final statistical analysis included in the publication. D.J. researched and wrote the initial manuscript. N.H., T.R.B. and J.T. commented and helped with further re-drafting. N.H. and T.R.B. supervised the project. Data on 5 out of 15 eggs used in self-cleaning trials were collected as a preliminary study by D.J., prior to the start of the PhD.

D.J. = Duncan Jackson, author of this thesis. N.H. = Dr Nicola Hemmings, PhD supervisor. T.R.B. = Professor Timothy R. Birkhead, PhD supervisor. J.T. = Jamie Thompson, research technician. C.R.C. = Dr Christopher R. Cooney, collaborator.

References

Ar, A., (1991). Roles of water in avian eggs. In: *Egg Incubation: Its effect on embryonic development in birds and reptiles* (eds. Deeming, D. C. and Ferguson, M. W. J.). Cambridge, UK: Cambridge University Press. pp. 229- 244.

Ar, A. and Deeming, D. C., (2009). Roles of water and gas exchange in determining hatchability success. *Avian Biology Research*. **2**(1/2), 61–66.

Ar, A., Paganelli, C. V., Reeves, R. B., Greene, D. G. and Rahn, H., (1974). The Avian Egg: Water Vapor Conductance, Shell Thickness, and Functional Pore Area. *The Condor*. **76**(2), 153–158.

Ar, A. and Rahn, H., (1980). Water in the avian egg overall budget of incubation. *American zoologist.* **20**(2), 373-384.

Ar, A. and Rahn, H., (1985). Pores in avian eggshells: Gas conductance, gas exchange and embryonic growth rate. *Respiration Physiology.* **61**(1), 1–20.

Ar, A., Rahn, H. and Paganelli, C. V., (1979). The Avian Egg: Mass and Strength. *The Condor.* **81**(4), 331–337.

Arad, Z., Gavrieli-Levin, I. and Marder, J., (1988). Adaptation of the Pigeon Egg to Incubation in Dry Hot Environments. *Physiological Zoology*. **61**(4), 293-300.

Bain, M. M., (2005). Recent advances in the assessment of eggshell quality and their future application. *World's Poultry Science Journal.* **61**(2), 268–277.

Belopol'skiĭ, L. O., (1957, translated from Russian 1961). *ecology of sea colony birds of the barents sea*. Jerusalem: Israel Program for Scientific Translations.

Benson, R. B. J., Campione, N. E., Carrano, M. T., Mannion, P. D., Sullivan, C., Upchurch, P. and Evans, D. C., (2014). Rates of Dinosaur Body Mass Evolution Indicate 170 Million Years of Sustained Ecological Innovation on the Avian Stem Lineage. *PLoS Biology.* **12**(5), e1001853.

Bignert, A., Litzen, K., Odsjo, T., Olsson, M., Persson, W. and Reutergårdh, L., (1995). Time-related factors influence the concentrations of sDDT, PCBs and shell parameters in eggs of Baltic guillemot (*Uria aalge*), 1861–1989. *Environmental pollution*. *89*(1), 27-36.

Birchard, G. F. and Deeming, D. C., (2009). Avian eggshell thickness: scaling and maximum body mass in birds. *Journal of Zoology.* **279**(1), 95–101.

Birkhead, T. R., (1977). The Effect of Habitat and Density on Breeding Success in the Common Guillemot (*Uria aalge)*. *The Journal of Animal Ecology.* **46**(3), 751-764.

Birkhead, T. R., (1993). *Great Auk Islands*. London, UK: Poyser.

Birkhead, T. R., (2016). *The Most Perfect Thing: the Inside (and Outside) of a Bird's Egg.* London, UK: Bloomsbury.

Birkhead, T. R., Russell, D., Garbout, A., Attard, M., Thompson, J. E. and Jackson, D., (2020) New insights from old eggs – the shape and thickness of Great Auk *Pinguinus impennis* eggs. *Ibis.*

Birkhead, T. R., Thompson, J. E. and Biggins, J. D., (2017b). Egg shape in the Common Guillemot *Uria aalge* and Brunnich's Guillemot *U. lomvia*: not a rolling matter? *Journal of Ornithology*. **158**(3), 679-685.

Birkhead, T. R., Thompson, J. E., Biggins, J. D. and Montgomerie, R., (2019). The evolution of egg shape in birds: selection during the incubation period. *Ibis*. **161**(3), 605-618.

Birkhead, T. R., Thompson, J. E., Jackson, D. and Biggins, J. D., (2017a). The point of a Guillemot's egg. *Ibis.* **159**(2), 255-265.

Birkhead, T. R., Thompson, J. E. and Montgomerie, R., (2018). The pyriform egg of the Common Murre (*Uria aalge*) is more stable on sloping surfaces. *The Auk*. **135**(4), 1020-1032.

Board, R. G., (1982). Properties of avian egg shells and their adaptive value. *Biological Reviews.* **57**(1), 1–28.

Board, R. G. and Halls, N. A., (1973a). The cuticle: A barrier to liquid and particle penetration of the shell of the hen's egg. *British Poultry Science.* **14**(1), 69-97.

Board, R. G. and Halls, N. A., (1973b). Water uptake by eggs of mallards and guinea fowl. *British Poultry Science.* **14**(3), 311-314.

Board, R. G. and Perrott, H. R., (1982). The fine structure of the outer surface of the incubated eggshells of the Helmeted guinea fowl (*Numidia meleagris*). *The Journal of Zoology.* **196**(4), 445–451.

Board, R. G. and Sparks, N. H. C., (1991). Shell structure and formation in avian eggs. In: *Egg Incubation: Its effect on embryonic development in birds and reptiles* (eds. Deeming, D. C. and Ferguson, M. W. J.). Cambridge, UK: Cambridge University Press. pp. 71-86.

Boersma, P. D., Rebstock, G. A. and Stokes, D. L., (2004). Why Penguin Eggshells are Thick. *The Auk*. **21**(1), 148-155.

Brulez, K., Mikšík, I., Cooney, C. R., Hauber, M. E., Lovell, P. G., Maurer, G., Portugal, S. J., Russell, D., Reynolds, S. J. and Cassey, P., (2016). Eggshell pigment composition covaries with phylogeny but not with life history or with nesting ecology traits of British passerines. *Ecology and Evolution*. **6**(6), 1637-1645.

Carey, C., (2002). Incubation in extreme environments. In: *Avian Incubation: Behaviour, Environment and Evolution* (eds. Deeming, D. C.). Oxford, UK: Oxford University Press. pp. 238-253.

Carey, C., Leon-Velarde, F. and Monge, C., (1990). Eggshell Conductance and Other Physical Characteristics of Avian Eggs Laid in the Peruvian Andes. *The Condor.* **92**(3), 790–793.

Carnarius, K. M., Conrad, K. M., Mast, M. G. and MacNeil, J. H., (1996). Relationship of Eggshell Ultrastructure and Shell Strength to the Soundness of Shell Eggs. *Poultry science.* **75**(5), 656–663.

Chen, X., Li, X., He, Z., Hou, Z., Xu, G., Yang, N. and Zheng, J., (2019). Comparative study of eggshell antibacterial effectivity in precocial and altricial birds using *Escherichia coli*. *PLoS ONE*. **14**(7), e0220054.

Clark., M. E., Boonstra, T. A., Reed, W. L. and Gastecki, M. L., (2010). Intraclutch Variation in Egg Conductance Facilitates Hatching Synchrony of Canada Geese. *The Condor*. **122**(3), 447-454.

D'Alba, L., Jones, D. N., Badawy, H. T., Eliason, C. M. and Shawkey, M. D., (2014). Antimicrobial properties of a nanostructured eggshell from a compost-nesting bird. *The Journal of Experimental Biology*. **217**(7), 1116-1121.

D'Alba, L., Torres, R., Waterhouse, G. I. N., Eliason, C., Hauber, M. E. and Shawkey, M. D., (2017). What Does the Eggshell Cuticle Do? A Functional Comparison of Avian Eggshell Cuticles. *Physiological and Biochemical Zoology.* **90**(5), 588-599.

Davis, T. A. and Ackerman, R. A., (1985). Adaptations of Black Tern (*Chlidonias niger*) Eggs for Water Loss in a Moist Nest. *The Auk.* **102**(3), 640–643.

Davis, T. A., Platter-Reiger, M. F. and Ackerman, R. A., (1984). Water Loss by Pied-Billed Grebe Eggs: Adaptation to a Hot, Wet Nest. *Physiological Zoology.* **57**(4), 384–391.

Deeming, D. C., (1987). Effect of cuticle removal on the water vapour conductance of egg shells of several species of domestic bird. *British Poultry Science*. **28**(2), 231-237.

Deeming, D. C., (2002). *Avian Incubation: Behaviour, Environment and Evolution.* Oxford, UK: Oxford University Press.

Deeming, D. C., (2011). A review of the relationship between eggshell colour and water vapour conductance. *Avian Biology Research.* **4**(4), 224–230.

Deeming, D. C. and Reynolds, S. J., (2016). *Nests, eggs and incubation: new ideas about avian reproduction.* Oxford, UK: Oxford University Press.

del Hoyo, J., Elliott, A., Sargatal, J., Christie, D. A. and Kirwan, G., (eds.) (2019). *Handbook of the Birds of the World Alive*. Barcelona, Spain: Lynx Edicions. (retrieved from http://www.hbw.com/ on [29/1/2019])

Dong, X., Tang, X., Peng, Y. and Dong, J., (2017). Nondestructive assessment of eggshell thickness by VIS/NIR spectroscopy. In: *2017 ASABE Annual International Meeting*. Michigan, USA: American Society of Agricultural and Biological Engineers.

Fecheyr-Lippens, D. C., Igic, B., D'Alba, L., Hanley, D., Verdes, A., Holford, M., Waterhouse, G. I. N., Grim, T., Hauber, M. E. and Shawkey, M. D., (2015). The cuticle modulates ultraviolet reflectance of avian eggshells. *Biology Open.* **4**(7), 753-759.

Friesen, V. L., Baker, A. J. and Piatt, J. F., (1996). Phylogenetic relationships within the Alcidae (Charadriiformes: Aves) inferred from total molecular evidence. *Molecular biology and evolution.* **13**(2), 359-367.

Garbout, A., Sturrock, C. J., Armenise, E., Ahn, S., Simmons, R. W., Doerr, S., Ritz, K. and Mooney, S. J., (2018). TopCap: A Tool to Quantify Soil Surface Topology and Subsurface Structure. *Vadose Zone Journal*. **17**(170091), doi:10.2136/vzj2017.05.0091.

Gaston, A. J. and Jones, I. L., (1998). *Bird Families of the World series: The Auks.* Oxford, UK: Oxford University Press.

Gole, V. C., Chousalkar, K. K., Roberts, J. R., Sexton, M., May, D., Tan, J. and Kiermeier, A., (2014a). Effect of Egg Washing and Correlation between Eggshell Characteristics and Egg Penetration by Various *Salmonella* Typhimurium Strains. *PLoS ONE.* **9**(3), e90987.

Gole, V. C., Roberts, J. R., Sexton, M., May, D., Kiermeier, A. and Chousalkar, K. K., (2014b). Effect of egg washing and correlation between cuticle and egg penetration by various *Salmonella* strains. *International Journal of Food Microbiology.* **182-183**, 18–25.

Gould, R. W., (1972). Non-Destructive Egg Shell Thickness Measurements Using Ultrasonic Energy. *Poultry Science*. **51**(4), 1460-1461.

Grant, G. S., Pettit, T. N., Rahn, H., Whittow, G. C. and Paganelli, C. V., (1982). Water loss from Laysan and Black-footed Albatross eggs. *Physiological Zoology*. **55**(4), 405-414.

Grellet-Tinner, G., Chiappe, L., Norell, M. and Bottjer, D., (2006). Dinosaur eggs and nesting behaviors: A paleobiological investigation. *Palaeogeography, Palaeoclimatology, Palaeoecology.* **232**(2–4): 294–321.

Grellet-Tinner, G., Lindsay, S. and Thompson, M. B., (2017). The biomechanical, chemical and physiological adaptations of the eggs of two Australian megapodes to their nesting strategies and their implications for extinct titanosaur dinosaurs. *Journal of Microscopy.* **267**(2), 237-249.

Guerra, C. G., Aguilar, R. E. and Fitzpatrick, L. C., (1988). Water Vapor Conductance in Gray Gulls (*Larus modestus*) Eggs: Adaptation to Desert. *Colonial waterbirds.* **11**(1), 107–109.

Hauber, M. E., Bond, A. L., Kouwenberg, A. L., Robertson, G. J., Hansen, E. S., Holford, M., Dainson, M., Luro, A. and Dale, J., (2019). The chemical basis of a signal of individual identity: shell pigment concentrations track the unique appearance of Common Murre eggs. *Journal of the Royal Society Interface.* **16**(153), 20190115.

Hechenleitner, E. M., Grellet-Tinner, G., Foley, M., Fiorelli, L. E. and Thompson, M. B., (2016). Micro-CT scan reveals an unexpected high-volume and interconnected pore network in a Cretaceous Sanagasta dinosaur eggshell. *Journal of The Royal Society Interface.* **13**(116), 20160008.

Hempleman, S. C., Adamson, T. P. and Bebout, D. E., (1993). Oxygen and avian eggshell formation at high altitude. *Respiration Physiology.* **92**(1), 1–12.

Hipfner, J. M., Gorman, K. B., Vos, R. A. and Joy, J. B., (2010). Evolution of embryonic developmental period in the marine bird families Alcidae and Spheniscidae: roles for nutrition and predation? *BMC Evolutionary Biology*. **10**, 179.

Igic, B., Fecheyr-Lippens, D., Xiao, M., Chan, A., Hanley, D., Brennan, P. R. L., Grim, T., Waterhouse, G. I. N., Hauber, M. E. and Shawkey, M. D., (2015). A nanostructural basis for gloss of avian eggshells. *Journal of The Royal Society Interface.* **12**(103), 20141210.

Ishikawa, S. I., Suzuki, K., Fukuda, E., Arihara, K., Yamamoto, Y., Mukai, T. and Itoh, M., (2010). Photodynamic antimicrobial activity of avian eggshell pigments. *FEBS letters.* **584**(4), 770-774.

Johnsgard, P. A., (1987). Diving Birds of North America: Species Accounts – Auks (Alcidae) In: *Diving Birds of North America, by Paul Johnsgard.* 11. Lincoln, Nebraska, USA: University of Nebraska Press.

Karlsson, O. and Lilja, C., (2008). Eggshell structure, mode of development and growth rate in birds. *Zoology.* **111**(6), 494-502.

Kibala, L., Rozempolska-Rucinska, I., Kasperek, K., Zieba, G. and Lukaszewicz, M., (2015). Ultrasonic eggshell thickness measurement for selection of layers. *Poultry science*. **94**(10), 2360-2363.

Lahti, D. C. and Ardia, D. R., (2016). Shedding Light on Bird Egg Color: Pigment as Parasol and the Dark Car Effect. *The American Naturalist.* **187,** 547–563.

Lang, M. R. and Wells, J. W., (1987). A Review of eggshell pigmentation. *World's Poultry Science Journal.* **43**(3), 238–246.

Lockwood, W. B., (1978). The Philogogy of "Auk", and Related Matters. *Neuphilologische Mitteilungen.* **79**(4), 391-397.

Lorimer, J., (2014). On auks and awkwardness. *Environmental Humanities.* **4**(1), 195-205.

Mallory, M. L. and Weatherhead, P. J., (1990). Effects of nest parasitism and nest location on eggshell strength in waterfowl. *The Condor*. **92**(4), 1031-1039.

Mao, K. M., Murakami, A., Iwasawa, A. and Yoshizaki, N., (2007). The asymmetry of avian egg-shape: an adaptation for reproduction on dry land. *Journal of Anatomy.* **210**(6), 741-748.

Martín-Vivaldi, M., Soler, J. J., Peralta-Sánchez, J. M., Arco, L., Martín-Platero, A. M., Martínez-Bueno, M., Ruiz-Rodríguez, M. and Valdivia, E., (2014). Special structures of hoopoe eggshells enhance the adhesion of symbiont-carrying uropygial secretion that increase hatching success. *Journal of Animal Ecology*. **83**(6), 1289-1301.

Maurer, G., Portugal, S. J. and Cassey, P., (2012). A comparison of indices and measured values of eggshell thickness of different shell regions using museum eggs of 230 European bird species. *Ibis.* **154**(4), 714–724.

Maurer, G., Portugal, S. J., Hauber, M. E., Mikšík, I., Russell, D. G. D. and Cassey, P., (2015). First light for avian embryos: eggshell thickness and pigmentation mediate variation in development and UV exposure in wild bird eggs. *Functional Ecology.* **29**(2), 209–218.

Maurer, G., Russell, D. G. D. and Cassey, P., (2010). Interpreting the Lists and Equations of Egg Dimensions in Schönwetter's *Handbuch der Oologie*. *The Auk.* **127**(4), 940–947.

Mayani-Parás, F., Kilner, R. M., Stoddard, M. C., Rodríguez, C. and Drummond, H., (2015). Behaviorally Induced Camouflage: A New Mechanism of Avian Egg Protection. *The American Naturalist.* **186**(4), E91–E97.

Mikhailov, K. E., (1997). *Avian eggshells: an atlas of scanning electron micrographs.* Hertfordshire, UK: British Ornithologists' Club Occasional Publications 3.

Monge, C. C., Ostojic, H., Aguilar, R. and Cifuentes, V., (2000). Reduced oxygen diffusion across the shell of Gray gull (*Larus modestus*) eggs. *Biological research.* **33**(3–4), 209–214.

Montevecchi, W. A. and Kirk, D. A., (2020). Great Auk (*Pinguinus impennis*), version 1.0 (text last updated 1996). In: *Birds of the World* (eds. Poole, A. F. and Gill, F. B.). Ithaca, NY: Cornell Lab of Ornithology. Available at: https://birdsoftheworld.org/bow/species/greauk/1.0

Olsthoorn, J. C. M. and Nelson, J. B., (1990). The availability of breeding sites for some British seabirds. *Bird Study*. **37**(3), 145-164.

Packard, G. C., Sotherland, P. R. and Packard, M. J., (1977). Adaptive reduction in permeability of avian eggshells to water vapour at high altitudes. *Nature.* **266**, 255-256.

Picman, J., (1989). Mechanism of increased puncture resistance of eggs of Brown-headed Cowbirds. *The Auk.* **106**(4), 577–583.

Pirie-Hay, D. and Bond, A. L., (2014). Thickness of Common Murre (*Uria aalge*) eggshells in Atlantic Canada. *The Canadian Field-Naturalist.* **128**(1), 72–76.

Portugal, S. J., Bowen, J. and Riehl, C., (2018). A rare mineral, vaterite, acts as a shock absorber in the eggshell of a communally nesting bird. *Ibis.* **160**(1), 173-178.

Portugal, S. J., Maurer, G. and Cassey, P., (2010). Eggshell Permeability: A Standard Technique for Determining Interspecific Rates of Water Vapor Conductance. *Physiological and Biochemical Zoology.* **83**(6), 1023–1031.

Portugal, S. J., Maurer, G., Thomas, G. H., Hauber, M. E., Grim, T. and Cassey, P., (2014). Nesting behaviour influences species-specific gas exchange across avian eggshells. *The Journal of Experimental Biology.* **217**(18), 3326–3332.

Rahn, H., (1991). Why birds lay eggs. In: *Egg Incubation: Its effect on embryonic development in birds and reptiles* (eds. Deeming, D. C. and Ferguson, M. W. J.). Cambridge, UK: Cambridge University Press. pp. 345-360.

Rahn, H. and Ar, A., (1974). The avian egg: incubation time and water loss. *The Condor.* **76**(2), 147-152.

Rahn, H., Carey, C., Balmas, K., Bhatia, B. and Paganelli, C., (1977). Reduction of pore area of the avian eggshell as an adaptation to altitude. *Proceedings of the National Academy of Sciences of the United States of America.* **74**(7), 3095–3098.

Rahn, H., Ledoux, T., Paganelli, C. V. and Smith, A. H., (1982). Changes in eggshell conductance after transfer of hens from an altitude of 3,800 to 1,200 m. *Journal of Applied Physiology.* **53**(6), 1429–1431.

Rahn, H. and Paganelli, C. V., (1989). Shell Mass, Thickness and Density of Avian Eggs Derived from the Tables of Schönwetter. *Journal of Ornithology.* **130**(1), 59–68.

Rahn, H. and Paganelli, C. V., (1990). Gas fluxes in avian eggs: Driving forces and the pathway for exchange. *Comparative Biochemistry and Physiology Part A: Physiology*. **95**(1), 1-15.

Rahn, H., Paganelli, C. V. and Ar, A., (1974). The avian egg: air-cell gas tension, metabolism and incubation time. *Respiration physiology*. **22**(3), 297-309.

Rahn, H., Paganelli, C. V. and Ar, A., (1975). Relation of Avian Egg Weight to Body Weight. *The Auk.* **92**(4), 750–765.

Rahn, H., Paganelli, C. V., Nisbet, I. C. T. and Whittow, G. C., (1976). Regulation of Incubation Water Loss in Eggs of Seven Species of Terns. *Physiological Zoology*. **49**(2), 245-259.

Reizis, A., Hammel, I. and Ar, A., (2005). Regional and developmental variations of blood vessel morphometry in the chick embryo chorioallantoic membrane. *The Journal of Experimental Biology.* **208**(13), 2483–2488.

Reynolds, S. J. and Deeming, D. C., (2016). Incubating new ideas about avian reproduction. In: *Nests, eggs and incubation: new ideas about avian reproduction* (eds. Deeming, D. C. and Reynolds, S. J.). Oxford, UK: Oxford University Press. pp. 1-7.

Richards, P. D. G. and Deeming, D. C., (2001). Correlation between shell colour and ultrastructure in pheasant eggs. *British Poultry Science*. **42**(3), 338-343.

Ricklefs, R. E., (1984). Prolonged incubation in pelagic seabirds: a comment on Boersma's paper. *The American Naturalist.* **123**(5), 710-720.

Riley, A., Sturrock, C. J., Mooney, S. J. and Luck, M. R., (2014). Quantification of eggshell microstructure using X-ray micro computed tomography. *British poultry science.* **55**(3), 311–320.

Rokitka, M. A. and Rahn, H., (1987). Regional differences in shell conductance and pore density of avian eggs. *Respiration Physiology.* **68**(3), 371–376.

Romanoff, A. L. and Romanoff, A. J., (1949). *The avian egg*. New York, USA: Wiley.

Roudybush, T., Hoffman, L. and Rahn, H., (1980). Conductance, pore geometry, and water loss of eggs of Cassin's Auklet. *The Condor.* **82**(1), 105-106.

Sabath, K., (1991). Upper Cretaceous Amniotic Eggs From the Gobi Desert. *Paleontologica.* **36**(2), 151–192.

Sabuncu, M. and Akdoğan, M., (2014). Utilizing optical coherence tomography in the nondestructive and noncontact measurement of egg shell thickness. *The Scientific World Journal*. https://doi.org/10.1155/2014/205191.

Samiullah, S. and Roberts, J. R., (2013). The location of protoporphyrin in the eggshell of brown-shelled eggs. *Poultry science*. **92**(10), 2783-2788.

Samiullah, S. and Roberts, J. R., (2014). The eggshell cuticle of the laying hen. *World's Poultry Science Journal*. **70**(4), 693-708.

Santolo, G. M., (2018). A new nondestructive method for measuring eggshell thickness using a non-ferrous material thickness gauge. *The Wilson Journal of Ornithology*. **130**(2), 502-509.

Simkiss, K., (1986). Eggshell conductance—Fick's or Stefan's law? *Respiration physiology*. **65**(2), 213-222.

Smart, I. H. M., (1991). Egg shape in birds. In: *Egg Incubation: Its Effects on Embryonic Development in Birds and Reptiles* (eds. D. C. Deeming and M. W. J. Ferguson). Cambridge, UK: Cambridge University Press. pp. 101-116.

Smith, N. A., (2016). Evolution of body mass in the Pan-Alcidae (Aves, Charadriiformes): the effects of combining neontological and paleontological data. *Paleobiology.* **42**(1), 8-26.

Smith, N. A. and Clarke, J. A., (2015). Systematics and evolution of the Pan‐Alcidae (Aves, Charadriiformes). *Journal of Avian Biology*. **46**(2), 125-140.

Soler, J. J., Martín-Vivaldi, M., Peralta-Sánchez, J. M., Arco, L. and Juárez-García-Pelayo, N., (2014). Hoopoes color their eggs with antimicrobial uropygial secretions. *Naturwissenschaften*. **101**(9), 697-705.

Soler, J. J., Martín‐Vivaldi, M., Ruiz‐Rodríguez, M., Valdivia, E., Martín‐Platero, A. M., Martínez‐Bueno, M., Peralta‐Sánchez, J. M. and Méndez, M. (2008). Symbiotic association between hoopoes and antibiotic‐producing bacteria that live in their uropygial gland. *Functional Ecology*. **22**(5), 864-871.

Sparks, N. H. C., (1994). Shell accessory materials: structure and function. In: *Microbiology of the Avian Egg* (eds. Board, R. G. and Fuller, R.). London, UK: Chapman and Hall. pp. 25-42.

Sparks, N. H. C., (2011). Eggshell pigments–from formation to deposition. *Avian Biology Research*. **4**(4), 162-167.

Sparks, N. H. C. and Board, R. G., (1984). Cuticle, shell porosity and water uptake through hens' eggshells. *British Poultry Science.* **25**(2), 267-276.

Spottiswoode, C. N., (2010). The evolution of host-specific variation in cuckoo eggshell strength. *Journal of Evolutionary Biology.* **23**(8), 1792–1799.

Spottiswoode, C. N. and Colebrook-Robjent, J. F., (2007). Egg puncturing by the brood parasitic Greater Honeyguide and potential host counteradaptations. *Behavioral Ecology*. **18**(4), 792-799.

Starck, J. M. and Ricklefs, R. E., (1998). Patterns of development: the altricial–precocial spectrum. In: *Avian Growth and Development* (eds. Starck, J. M. and Ricklefs, R. E.). Oxford, UK: Oxford University Press. pp. 3–30.

Tazawa, H., Mikami, T. and Yoshimoto, C. (1971). Effect of reducing the shell area on the respiratory properties of chicken embryonic blood. *Respiration Physiology*. **13**(3), 352-360.

Thompson, M. B. and Goldie, K. N., (1990). Conductance and Structure of Eggs of Adelie Penguins, *Pygoscelis adeliae*, and Its Implications for Incubation. *The Condor*. **92**(2), 304–312.

Tschanz, B., (1990). Adaptations for Breeding in Atlantic Alcids. *Netherlands Journal of Zoology.* **40**(4), 688–710.

Tullett, S. G., (1975). Regulation of avian eggshell porosity. *Journal of Zoology.* **177**(3), 339–348.

Tullett, S. G., (1984). The porosity of avian eggshells. *Comparative Biochemistry and Physiology Part A: Physiology.* **78**(1), 5-13.

Tullett, S. G. and Board, R. G., (1977). Determinants of avian eggshell porosity. *Journal of Zoology.* **183**(2), 203–211.

Tyler, C., (1969). The snapping strength of the egg shells of various orders of birds. *Journal of Zoology.* **159**(1), 65–77.

Tyler, C. and Fowler, S., (1978). The distribution of organic cores, cones, cone junctions and pores in the egg shells of wild birds. *Journal of Zoology.* **186**(1), 1–14.

Tyler, C. and Simkiss, K., (1959). A study of the egg shells of ratite birds. *Proceedings of the Zoological Society of London*. **133**(2), 201-243.

Uspenski, S. M., (1958). *The Bird Bazaars of Novaya Zemlya.* Canada, Ottawa: Department of Northern Affairs and Natural Resources, Canadian Wildlife Service (translated from Russian).

Vleck, C. M. and Kenagy, G. J., (1980). Embryonic Metabolism of the Fork-Tailed Storm Petrel: Physiological Patterns during Prolonged and Interrupted Incubation. *Physiological Zoology*. **53**(1), 32-42.

Vleck, C. M., Vleck, D., Rahn, H. and Paganelli, C. V., (1983). Nest Microclimate, Water-Vapor Conductance, and Water Loss in Heron and Tern Eggs. *The Auk.* **100**(1), 76-83.

Voisey, P. W. and Hamilton, R. M. G., (1976). Ultrasonic Measurement of Egg Shell Thickness. *Poultry Science*. **55**(4), 1319-1324.

Wangensteen, O. D. and Rahn, H., (1970). Respiratory gas exchange by the avian embryo. *Respiration Physiology.* **11**(1), 31-45.

Wangensteen, O. D., Wilson, D. and Rahn, H., (1970). Diffusion of gases across the shell of the hen's egg. *Respiration physiology*. **11**(1), 16-30.

Weir, J. T. and Mursleen, S., (2013). Diversity-dependent cladogenesis and trait evolution in the adaptive radiation of the auks (Aves: Alcidae). *Evolution*. **67**(2), 403-416.

Wellman-Labadie, O., Picman, J. and Hincke, M. T., (2008). Antimicrobial activity of the Anseriform outer eggshell and cuticle. *Comparative Biochemistry and Physiology Part B: Biochemistry and Molecular Biology.* **149**(4), 640–649.

Whittow, G. C., (1980). Physiological and ecological correlates of prolonged incubation in sea birds. *American Zoologist*. **20**(2), 427-436.

Whittow, G. C., Ackerman, R. A., Paganelli, C. V. and Pettit, T. N., (1982). Pre-pipping water loss from the eggs of the Wedge-tailed Shearwater. *Comparative Biochemistry and Physiology Part A: Physiology*. **72**(1), 29-34.

Williams, A. J., Siegfried, W. R. and Cooper, J., (1982). Egg composition and hatchling precocity in seabirds. *Ibis.* **124**(4), 456–470.

Willoughby, B., Steyn, L., Bam, L., Olivier, A. J., Devey, R. Maina, J. N., (2016). Micro-Focus X-Ray Tomography Study of the Microstructure and Morphometry of the Eggshell of Ostriches (*Struthio Camerus*). *The Anatomical Record.* **299**(8), 1015–1026.

Yan, Y. Y., Sun, C. J., Lian, L., Zheng, J. X., Xu, G. Y. and Yang, N., (2013). Effect of uniformity of eggshell thickness on eggshell quality in chickens. *The Journal of Poultry Science.* **51**(3), 338-342.

Zimmermann, K. and Hipfner, J. M., (2007). Egg Size, Eggshell Porosity, and Incubation Period in the Marine Bird Family Alcidae. *The Auk.* **124**(1), 307–315.

Chapter 2:

Patterns of eggshell thickness and their functional significance in the auks

Patterns of eggshell thickness and their functional significance in the auks

Duncan Jackson[1*], Nicola Hemmings[1], Christopher R. Cooney[1] and Timothy R. Birkhead[1]

[1]*Department of Animal & Plant Sciences, University of Sheffield, Sheffield, S10 2TN, UK*

*Corresponding author. Email: djackson3@sheffield.ac.uk

Key words

Egg shape, Egg size, Egg strength, Contact incubation, Alcidae, X-ray micro-computed tomography

Abstract

Birds can reproduce in harsh environments due to the combination of a protective incubation site (usually a nest), parental behaviours that buffer against the external environment, and crucially, a hard calcium carbonate eggshell. Here, we use digital egg shape analysis and X-ray micro-computed tomography to investigate how variation in eggshell thickness relates to egg size, egg shape, parental body size, and incubation environment in the Alcidae, a family of birds that incubate their eggs in a range of habitats, often without any form of protective nest. First, using an intraspecific approach, we show that variation in eggshell thickness among common guillemot eggs relates to egg size and egg shape, but this is primarily driven by differences at the equator of the eggshell. Larger eggs are absolutely thicker at their equator, while more elongate eggs and those with a sharper pointed end are thinner at their equator, with elongate (and asymmetric) eggs also thinner at the pointed end. Second, using an interspecific approach, we find similar patterns across the auks, with larger-bodied, heavier species that lay larger eggs having thicker eggshells at the equator. However, in contrast to our intraspecific findings, species that lay elongate eggs tend to have thicker shells at their equator. Finally, we show that species incubating on bare rock have particularly thick eggshells compared to those that nest on softer substrates like soil or vegetation, especially at the equator. Therefore, eggs that need to be especially strong, due to the weight of the incubating parent, their shape, and the hardness of the incubation substrate, tend to have a thicker shell, particularly at the region of the egg that is in contact with the parent’s brood patch and substrate during incubation. Our results suggest that selection on eggshell thickness is specific to each egg region, which in turn drives interspecific variation in shell thickness patterns along the egg.

Introduction

The strength of the avian eggshell is determined in part by its thickness (Romanoff & Romanoff 1949; Ar *et al.* 1974; Ar *et al.* 1979; Bain 2005). Since the majority of the parent's mass is placed on the egg during contact incubation, it has been hypothesised that the weight of the incubating parent may be a major selective force shaping variation in eggshell thickness (Ar *et al.* 1979; Birchard & Deeming 2009).

Consistent with this hypothesis, the shells of large eggs – and those incubated by large birds – tend to be relatively thick (Ar *et al.* 1974; Ar *et al.* 1979; Rahn & Paganelli 1989; Birchard & Deeming 2009). Distinguishing whether egg size (usually measured as initial mass) or the size of the incubating bird (specifically adult mass) is more important in driving variation in shell thickness across birds is not simple, because in general, adult mass and egg size are positively correlated (Rahn *et al.* 1975; Birchard & Deeming 2009). There are a few exceptions to the rule of larger eggs and those laid by large birds having thick shells, particularly in species where there is limited contact between the adult bird and the egg (Rahn & Paganelli 1989). For example, the megapodes, a family of birds that do not contact incubate their eggs, produce relatively large eggs with relatively thin shells, and there is little allometric relationship between adult bird size and shell thickness across the family (Birchard & Deeming 2009). Despite the crucial role the shell plays in preventing damage to the egg – and the embryo within it – the factors influencing how eggshell thickness varies across different regions of the egg have received less attention than overall differences in shell thickness across bird species.

Avian eggshells exhibit marked within-egg variation in thickness (Tyler 1969a). In non-passerines the eggshell is commonly thinner at the blunt end than at the equator, but this pattern is not universal across all species (Rokitka & Rahn 1987; Maurer *et al.* 2012). Large, elongate eggs tend to be particularly thick-shelled at the equator, possibly due to structural weakness caused by their elongate shape (Maurer *et al.* 2012). Theoretically, the more an egg deviates from being a perfect sphere, the weaker the eggshell will be, especially along the elongate portion of the shell (Picman 1989; Bain 1991; Smart 1991; Barta & Székely 1997; Maurer *et al.* 2012). It is therefore possible that deviations from

sphericity are compensated for via increased thickness (and therefore strength) at the equator of the eggshell (Maurer *et al.* 2012). Consistent with this idea, proportional shell mass, and therefore potentially shell thickness, relates positively to egg asymmetry (Deeming 2018). As variation in eggshell thickness at the blunt end relative to the equator across 230 bird species is only moderately explained by egg shape (adjusted R^2 value 0.24; Maurer *et al.* 2012), it is likely that other factors also influence shell thickness variation along an egg.

In species where the eggshell is vulnerable to damage, for example due to egg puncturing and other impacts in brood parasites and/or their hosts (Picman 1989; Spottiswoode & Colebrook-Robjent 2007; Spottiswoode 2010; Igic *et al.* 2011), breeding at high densities (Birkhead 1993; Birkhead *et al.* 2017a) or in confined spaces (Mallory & Weatherhead 1990; Boersma *et al.* 2004) and/or incubating on hard, abrasive substrates (Williams *et al.* 1982; Weidinger 1996; Boersma *et al.* 2004), eggshells tend to be particularly thick for the size of the egg. This phenomenon appears to be most dramatic in some members of the Alcidae, a family of pelagic birds including the guillemots, puffins, murrelets and auklets. Of this group, the common guillemot (*Uria aalge*) and Brünnich's guillemot (*Uria lomvia*) produce eggs that are, for their size, thicker than those of almost any other bird (Schönwetter 1960-92; Pirie-Hay & Bond 2014). This high relative shell thickness could in part be because these guillemot species lay single egg clutches: the full weight of the incubating parent is therefore concentrated on a single egg during incubation, rather than being distributed over many eggs. Additionally, single eggs represent a much larger proportion of the parents' reproductive potential than an egg from a multi-egg clutch, so may be under stronger selection against losses due to shell breakage (Birchard & Deeming 2009).

The incubation environment may also be an important driver of shell thickness and resultant strength. Recently, Birkhead *et al.* (2017a) demonstrated that common guillemot eggs are particularly reinforced at the point where they are in contact with the substrate, with the effective thickness of the shell (the measure that most likely reflects shell strength; Bain 1992; Carnarius *et al*. 1996; Bain 2005) being greatest at the equator of the egg. In fact, in a study of the eggs of 230 European bird species, Maurer *et al.* (2012) found that the difference in eggshell thickness between the blunt end and equator of

common guillemot eggs was one of the most extreme. A thicker shell at the equator may compensate for the relatively weak elongate, asymmetric and pointed shape of guillemot eggs, but ecological factors may also play an important role in determining intraspecific shell thickness patterns. In particular, the degree to which the equator needs to be reinforced to prevent cracking may depend on the hardness of the nesting substrate, which varies widely across bird species. While some birds lay their eggs in soft, protective nests, others lay them on soil or pebbles, and some, including the common guillemot, lay and incubate their egg directly on bare, abrasive rock with little to no nest material. Data from earlier studies provides some support for the hypothesis that thicker equator and pointed regions of the eggshell are an adaptation to nesting on hard rock substrates in some Alcids (Uspenski 1958; Belopol'skiĭ 1961). However, evidence from these early studies is limited by the relatively crude methods used to measure shell thickness and the small number of species compared.

Here we test three hypotheses regarding the adaptive function of eggshell thickness in birds by utilising X-ray micro-computed tomography (microCT) to measure shell thickness and digital image analysis methods to quantify egg size and shape. First, by taking advantage of the considerable natural variation in shape and size that exists among common guillemot eggs, we assess whether larger and more elongate, asymmetric and pointed eggs are relatively thick at the equator, thereby providing reinforcement to compensate for their relatively weak shape. We do this by (i) investigating relationships between egg shape and effective eggshell thickness across 55 eggs and (ii) by pair-matching eggs based on volume and testing the independent effects of key egg shape measures on regional shell thickness. Second, we use a comparative approach to assess the importance of egg size relative to the mass of the incubating parent in driving variation in eggshell thickness across Alcids. Third, we examine whether, after accounting for egg size, shape and the adult's mass, the hardness of the nesting substrate influences the relative thickness of the equator across the Alcidae, a bird family with extraordinary diversity of nest types and remarkable extremes in eggshell thickness.

Materials and Methods

Data and samples

Eggs from 17 Alcid species, covering 9 of 10 extant Alcid genera and 5 out of the 6 tribes (Smith & Clark 2015), were collected under licence from a range of field sites around the world between 2004 – 2018 (n = 1 – 5 eggs per species, see Supplementary Materials for details). Eggs were emptied of their contents and rinsed with distilled water, air-dried and heat treated at 56ºC to eliminate microbes before transportation to the UK. Eggs collected in the UK underwent the same procedure, with the exception of no heat treatment in 2018. Common guillemot eggs collected in 2014 – 2017 were heat treated and stored in low humidity conditions (with silica gel) to minimise fungal growth. A total of 55 common guillemot eggs were used for intraspecific comparisons; of these, five eggs collected in 2018 were randomly selected for use in our interspecific comparative analyses before they were scanned.

Adult body mass (g) was obtained from Smith (2016) and del Hoyo *et al.* (2019) and we used an average mass calculated across these two sources. Since Alcid parents typically share egg incubation duties (Gaston & Jones 1998), we used the mean mass across both sexes for each species. Information on auk incubation substrate used for categorisation was obtained primarily from Gaston and Jones (1998) and del Hoyo *et al.* (2019) but also other sources in the literature (Johnsgard 1987; Olsthoorn & Nelson 1990; Tschanz 1990). Where available we also used descriptions and images of incubation sites taken by field researchers who collected eggshells for use in this study and the information available on the Audubon website (https://www.audubon.org/field-guide) to inform our categorisation. Incubation substrate was categorised on a three-point scale based on whether species usually incubate their egg(s) directly on (1) rock or pebbles, (2) sometimes on rock or pebbles, on a scrape on a rock substrate which may be lined with vegetation or feathers, or on soil or vegetation, or (3) rarely on rock, instead typically on vegetation, soil or feathers. We prefer these categorisations to more traditional nest types (e.g. without a nest on bare rock, in a crevice, in a burrow, on scree, in a pebble nest etc; Birkhead *et al.* 2019) because they allow us to account for the substrate on which the egg is typically incubated, as well as flexibility in nest site selection within species.

Measuring egg shape and size

Maximum length and breadth were measured with calipers for all intact eggshells; for intraspecific comparisons between common guillemot eggs to the nearest 0.1mm and 0.01mm for interspecific comparisons across auk eggs. Some broken eggshells were also reconstructed using masking tape for this purpose. Those that were too fragmented to reconstruct, but still had identifiable blunt, equator, and point regions, were used for eggshell thickness measurements only (see Supplementary Material; Appendix A3).

Eggshells were imaged as described in Biggins *et al*. (2018). Briefly, silhouette images of the eggs were obtained using a light box and an Olympus OM-D Em-5 camera with an Olympus 60mm macro lens for interspecific comparisons and a Canon 600D Canon EF-S 18-135mm IS lens for intraspecific comparisons between common guillemot eggs. The eggs were levelled according to Biggins *et al.* (2018) and the cameras were mounted on a tripod which were levelled to minimise error in image acquisition. Images were analysed in R (R Core Team 2018) to obtain volume (cm^3) and shape parameters, including egg elongation, asymmetry, the degree of tapering at the pointed end (taper), a measure of roundness at the blunt end (sphericity) and elongation at the blunt end. For more information on shape and size parameters and how they are calculated, see Biggins *et al.* (2018) and Supplementary Material (Appendix A3 & Fig. S1).

Scan protocol and image processing

After whole-egg imaging, fragments of approximately 0.5 – 1 cm^2 were cut from the blunt, equator and pointed regions of eggshells (see Fig. S2) using a hand-held rotary saw, dissecting scissors, or forceps. Fragments were not washed before microCT scanning to avoid cracking and fragmenting caused by drying of the rehydrated membrane (D.J. Pers. Obs.). We previously showed that repeatability for effective eggshell thickness within an egg region was high for common guillemot and razorbill eggs (Birkhead *et al.* 2017a). Extra fragments were cut from 10 common guillemot eggs at the shoulder of the egg, flat region in between the equator and pointed end, and the tip of the egg, to examine variation in shell thickness along the entire egg (Fig. S2).

Eggshell fragments were scanned in a Bruker Skyscan 1172 set to 49kV electron acceleration energy and 179uA current. The sample was 48.9mm from the X-ray source with a 0.5mm aluminium filter, and the camera was 284mm away from the source. Camera resolution was set at 1048 x 2000 pixels, with a pixel size of 4µm leading to an area of approximately 25 – 35mm^2 of eggshell being imaged per fragment. We used the same settings for each scan, collecting a total of 499 projection images over a 180° rotation. Rotation step size was 0.4° and the detector exposure was 1475ms integrated over four averaged images, resulting in a total scan time of 62 minutes. Two eggshell fragments were scanned per session. Projection images were reconstructed in NRecon software (versions 1.6.9.4 and 1.6.10.2) and realigned in Dataviewer (1.5.6), after which image analysis was performed in CT analyser (CTAn, version 1.14.41; all the above software was provided by Bruker micro-CT, Kontich, Belgium).

Reconstruction parameters were flexible in order to achieve optimum contrast for each image set relating to a single eggshell fragment, while also reducing the influence of artefacts in the dataset. To minimise any artefacts caused by sample movement during scanning, misalignment compensation was performed manually for each eggshell fragment (twice per scan). All scans had minimal smoothing applied (level 1 Gaussian smoothing) to ensure the reconstructed images were sharp and not overly blurred. To minimise beam hardening artefacts, approximately 50% beam hardening correction was applied. Ring artefact correction varied from 0 – 20 depending on the scan but values within the range of 8 – 12 were typically used. To further reduce ring artefacts, a defect pixel mask with a threshold at 50% was applied. Images were saved as 8-bit bitmaps. After image reconstruction, each fragment was manually cut out in CTAn and the data was saved. The data for each individual fragment was then loaded in Dataviewer and re-aligned to ensure transverse slices provided accurate eggshell thickness measurements.

We measured effective shell thickness i.e. the palisade, vertical crystal and shell accessory material layers (Bain 1991; Bain 1992; Solomon *et al.* 1994; Bain 2005), as the distance between the point of fusion of the palisade columns within the mammillary body layer and the outer edge of the shell accessory material (see Birkhead *et al*. 2017a & Fig. S3). This measure of shell thickness is most likely to capture variation in eggshell

strength, particularly the ability of a shell to resist crack formation, because evidence suggests that cracks typically originate in the mammillary layer and propagate outwards (Bain 1991; Bain 1992; Soloman *et al.* 1994; Carnarius *et al.* 1996; Bain 2005; Bain *et al.* 2006; Macleod *et al.* 2006; Soloman 2010; Hahn *et al.* 2017). Preventing cracks is essential, because even a single crack in the eggshell could increase water loss and facilitate microbial infection, potentially leading to embryo mortality or a weaker (lighter) chick at hatch (Board 1982; Barnett *et al.* 2004; Khabisi *et al.* 2012; Rayan & Badri 2017).

Effective shell thickness was measured at 10 locations on the reconstructed microCT eggshell images using the line measurement tool in CTAn and averaged for each fragment (see Birkhead *et al.* 2017a). Effective shell thickness represented a large proportion of the total shell thickness (~ 55 – 75%; see Supplementary Materials) and as a result, is highly correlated with both true shell (the inorganic calcium carbonate shell, including the mammillary, palisade and vertical crystal layers) and total shell thickness (Birkhead *et al.* 2017a; Table S1 & S2). However, additional variation in total or true shell thickness may relate to factors unrelated to eggshell strength. Few published studies have measured effective shell thickness so it is unclear how our measures collected here using microCT would compare to other techniques used to measure this aspect of eggshell thickness. However, our values for common guillemot total shell thickness (mean ± SD, range; blunt end: 517µm ± 48µm, 427µm – 651µm; equator: 647µm ± 48µm, 547µm – 778µm; pointed end: 614µm ± 66µm, 466 – 756µm) lie within the range values reported for this species elsewhere (Pirie-Hay & Bond 2014). Furthermore, our values of true shell and total shell thickness measured using microCT are greater than values presented in Belopol'skiĭ (1961) for some Alcids, but are comparable to more recently published values obtained using calipers or micrometers (Ar & Rahn 1985; Zimmerman & Hipfner 2007; Maurer *et al.* 2012). It is worth highlighting that although our values tend to be similar to previously reported values, they are sometimes slightly higher (see Table S27). One reason for this difference may be that physical pressure is applied to the eggshell during measurement using traditional techniques, such as calipers or modified micrometers, and the compression of any shell accessory materials, the organic membranes or even the true shell during physical measurement could result in underestimates of total and/or true shell thickness. This is not an issue or limitation when using non-contact imaging methods, such as microCT.

Testing the relationship between egg shape and shell thickness

We exploited natural variation among common guillemot eggs in all size and shape parameters to conduct pair-wise comparisons whereby the relationship between individual egg shape parameters and variation in eggshell thickness along the egg could be assessed, while controlling for the effects of egg size (volume). Sets of five pair-matched common guillemot eggshells were identified according to shape and size, generating paired samples that primarily differed only in a single variable. Each pair differed in one of the following traits: (a) volume (by ~20 – 30cm^3); (b) elongation (by ~0.2 – 0.3 units); (c) asymmetry (by ~0.03 – 0.04 units); (d) the degree of tapering at the pointed end (by ~0.15 – 0.20 units); (e) how round the blunt end was (by ~0.15 – 0.2 units); and (f) blunt end elongation (by ~0.15 – 0.25 units, n = 6 pairs; see Fig. S4 for example pairings). For comparisons of blunt end elongation we allowed asymmetry and total egg elongation to vary, since these traits are intrinsically linked to how elongate the blunt end is (Table S3). Analysing blunt end elongation essentially allowed us to assess the interaction between asymmetry and elongation in a pair-wise manner, resulting in a comparison of more ovate to more “pear-shaped” eggs (Fig. S4). Control egg pairs (matched as closely as possible in size and shape) were created from eggs scanned for other purposes. A mixture of paired t-tests and repeated measures ANOVAs were used to determine the differences in thickness between different shaped and sized guillemot egg pairs. Linear models were also used to assess the effect of egg volume and egg shape parameters on eggshell thickness at each region for all the eggs scanned (n = 55 eggs).

Interspecific patterns of eggshell thickness

To analyse the pattern of thickness along auk eggs we took three thickness measures per egg (at the blunt, equator and pointed region) and assessed variation within eggs using a repeated measures ANOVA to control for egg identity. The ezANOVA function in the ez (Lawrence 2016) package was used to assess sphericity with Mauchly’s test and perform Greenhouse-Geisser corrections where needed. To explore which regions differed, post-hoc tests using Tukey contrasts were performed on linear mixed effects models that controlled for egg identity using the nlme (Pinheiro *et al.* 2018) and multcomp (Hothorn *et*

al. 2008) packages. Fragments of Japanese murrelet (*Synthliboramphus wumizume*) eggshell were potentially from different eggs (due to eggshell fragmentation and disorganization in transit) therefore a standard ANOVA was performed. When analysing the factors associated with differences in thickness at the blunt, equator and pointed end of the egg, each region was analysed separately. A previous study (Maurer *et al.* 2012) analysed the ratio of thickness at the blunt end to the equator, but we found that this measure could vary widely even within eggs of a single species (common guillemot) and this variation was largely due to variation in thickness at the blunt end rather than at the equator, meaning it has limited value for understanding the factors associated with relative thickening at the equator of an egg (see Supplementary Materials).

We tested the relationship between adult body mass, egg volume and effective eggshell thickness across 15 Alcid species using phylogenetic linear regression models, controlling for phylogenetic relatedness using Pagel's lambda model (Ho & Ané 2014). We used a phylogenetic tree of extant Alcids (Weir & Mursleen 2013), pruned to leave only the species represented in our dataset, and species mean values were used for each variable included in our analyses (Fig. S5). We also used this phylogenetic regression approach to test the relationship between egg volume, egg shape (elongation and asymmetry), clutch size, incubation substrate and effective eggshell thickness, while controlling for adult bird mass. We first fitted individual predictor models and then combined all individually significant predictors into a multi-predictor model. Predictors were considered to be significant if AIC values increased by > 2 units when they were removed from the multi-predictor model. R^2 values for full models, including any phylogenetic effects, and partial R^2 values associated with individual predictors were calculated using the "R2.lik" function in the R package 'rr2' (Ives 2019). We investigated differences between tribes using a similar approach, adding tribe (categorical variable) into the phylogenetically controlled linear model between adult bird mass and effective eggshell thickness to assess if intercepts differed between tribes. To assess if certain tribes (*Alcini*, n = 4 and *Fraterculini*, n = 4) were influencing the slope of the relationship between adult body mass and effective eggshell thickness, we included binary terms describing whether or not species were a member of "*Alcini*" and "*Fraterculini*" into the model. All statistical analyses were performed in R version 3.5.1 (R Core Team 2018).

Results

Intraspecific differences: egg size, shape and effective shell thickness

Although larger guillemot eggs tended to be absolutely thicker in general (across all regions and eggs studied, n = 55 eggs), the differences between eggs at the blunt end were not significantly different (thickness = 0.937*egg volume + 264; $F_{(1,53)} = 1.69$, adj-$R^2 = 0.0127$, $p = 0.199$), suggesting that increasing egg size is primarily associated with thickening of the equator and pointed end of the eggshell (equator thickness = 2.19*egg volume + 267; $F_{(1,53)} = 9.73$, adj-$R^2 = 0.139$, $p = 0.0029$; point thickness = 2.50*egg volume + 180; $F_{(1,53)} = 6.07$, adj-$R^2 = 0.0858$, $p = 0.0171$; Fig. 1). After controlling for egg volume, more elongate eggs tended to be thinner across the whole sample of common guillemot eggs, but differences at the equator and blunt end only approached significance (blunt estimate = -133, t = -1.99, $p = 0.052$; $F_{(2,52)} = 2.88$, adj-$R^2 = 0.065$, $p = 0.065$: equator estimate = -129, t = -1.98, $p = 0.054$; $F_{(2,52)} = 7.08$, adj-$R^2 = 0.184$, $p = 0.0019$; point estimate = -232, t = -2.53, $p = 0.015$; $F_{(2,52)} = 6.53$, adj-$R^2 = 0.170$, $p = 0.003$; Fig. 2). After controlling for egg volume, more asymmetric eggs tended to be thinner at the pointed end (estimate = -1382, t = -2.58, $p = 0.0127$; $F_{(2,52)} = 6.69$, adj-$R^2 = 0.174$, $p = 0.0026$; Fig. 3). No other linear regressions between egg shape and eggshell thickness were found to be significant (Tables S4 – 7).

After controlling for egg shape parameters via egg-shape matching (see Materials Methods), large common guillemot eggs were found to be significantly thicker than small eggs at the equatorial region of the shell (Tables 1 & S8; Fig. 1), as well as slightly (but not significantly: Tables 1 & S8; Fig. 1) thicker at the pointed end. Effective shell thickness at the blunt end did not differ significantly between shape matched large and small eggs. By comparing egg-shape and size matched eggs, we found that more elongate guillemot eggs were significantly thinner at their equator and pointed (but not blunt) regions than more rotund eggs (Tables 1 & S8; Fig. 2). There were no significant differences in eggshell thickness between pairs of eggs that varied in asymmetry (Fig. 3; Tables 1 & S8). Eggs with a more tapered pointed end were found to be significantly thinner at the equator (but not at the blunt and pointed end) than less tapered eggs i.e. those with rounder pointed ends, they were paired with (Tables 1 & S8; Fig. 3).

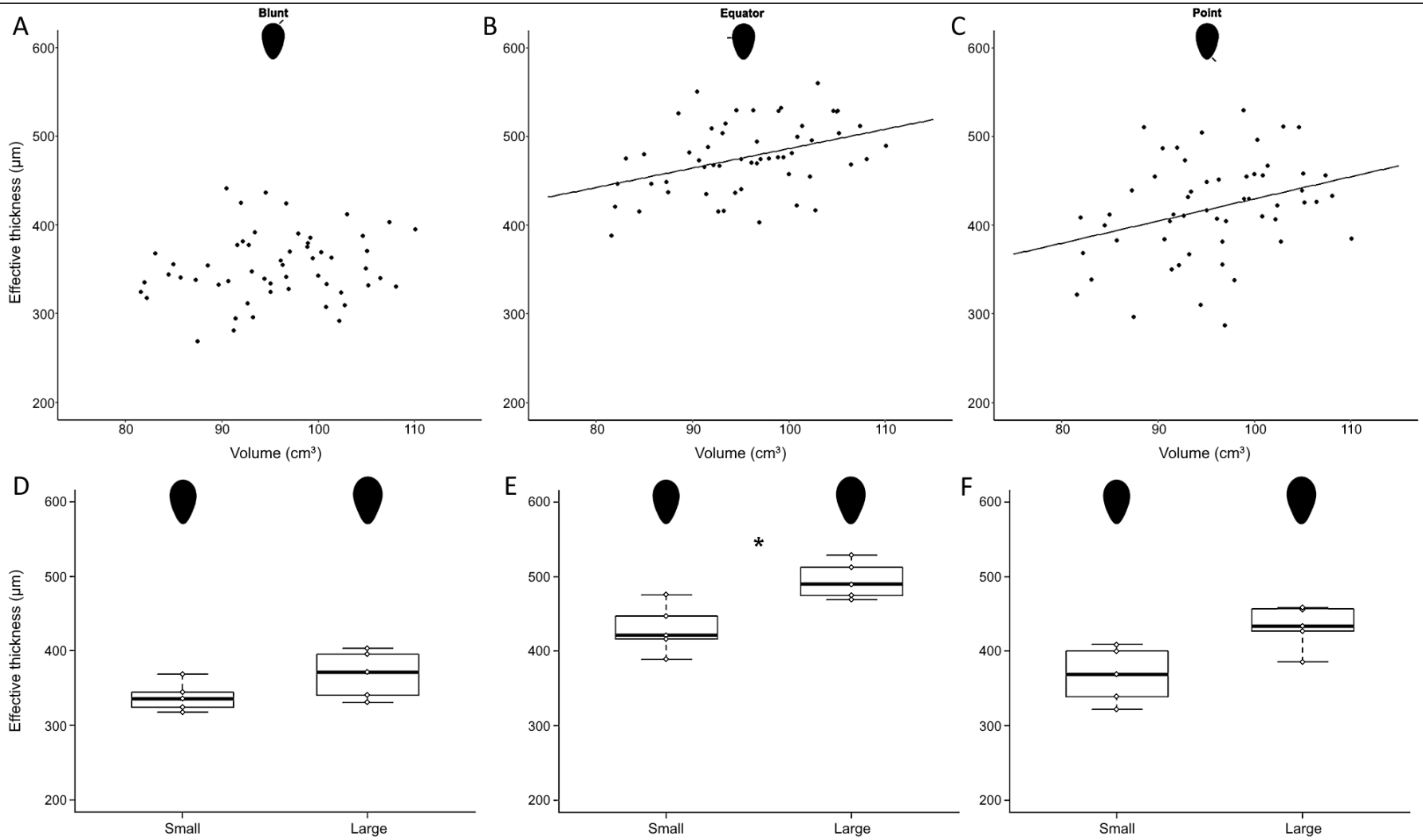

Figure 1. The relationships between eggshell thickness and egg volume at the blunt end (A & D), equator (B & E) and pointed end (C & F). (A – C) Linear regression relationships across all 55 eggs, lines are the regression relationships for the raw data. (D – F) Pairwise comparisons between five pairs of eggs. Significant differences between pairs of eggs are indicated by the presence of * above the bars. Statistics can be found in the main text and Table 1.

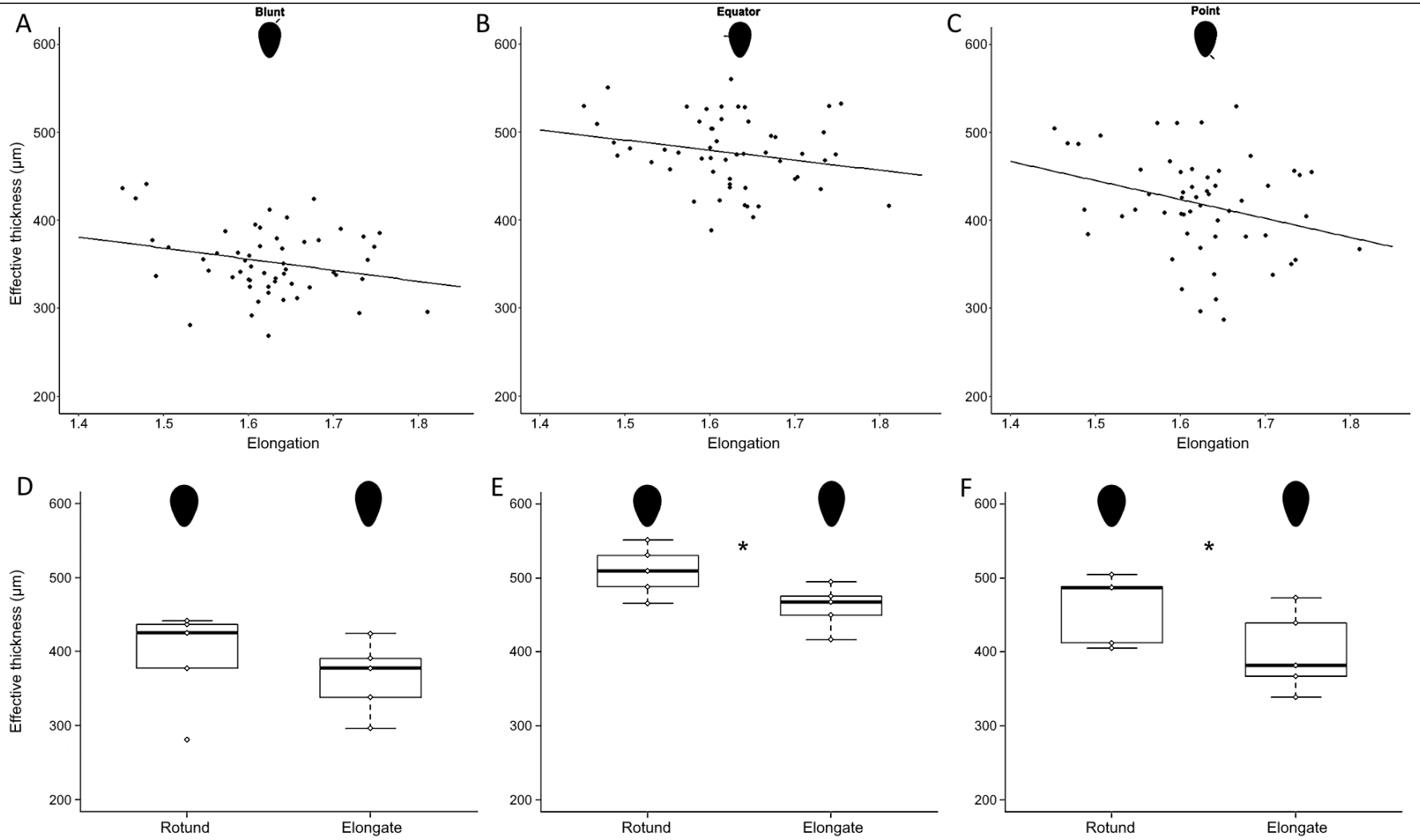

Figure 2. The relationships between eggshell thickness and egg elongation at the blunt end (A & D), equator (B & E) and pointed end (C & F). (A – C) Linear regression relationships across all 55 eggs, lines are the regression relationships for the raw data. (D – F) Pairwise comparisons between five pairs of eggs. Significant differences between pairs of eggs are indicated by the presence of * above the bars. Statistics can be found in Tables 1 and S4.

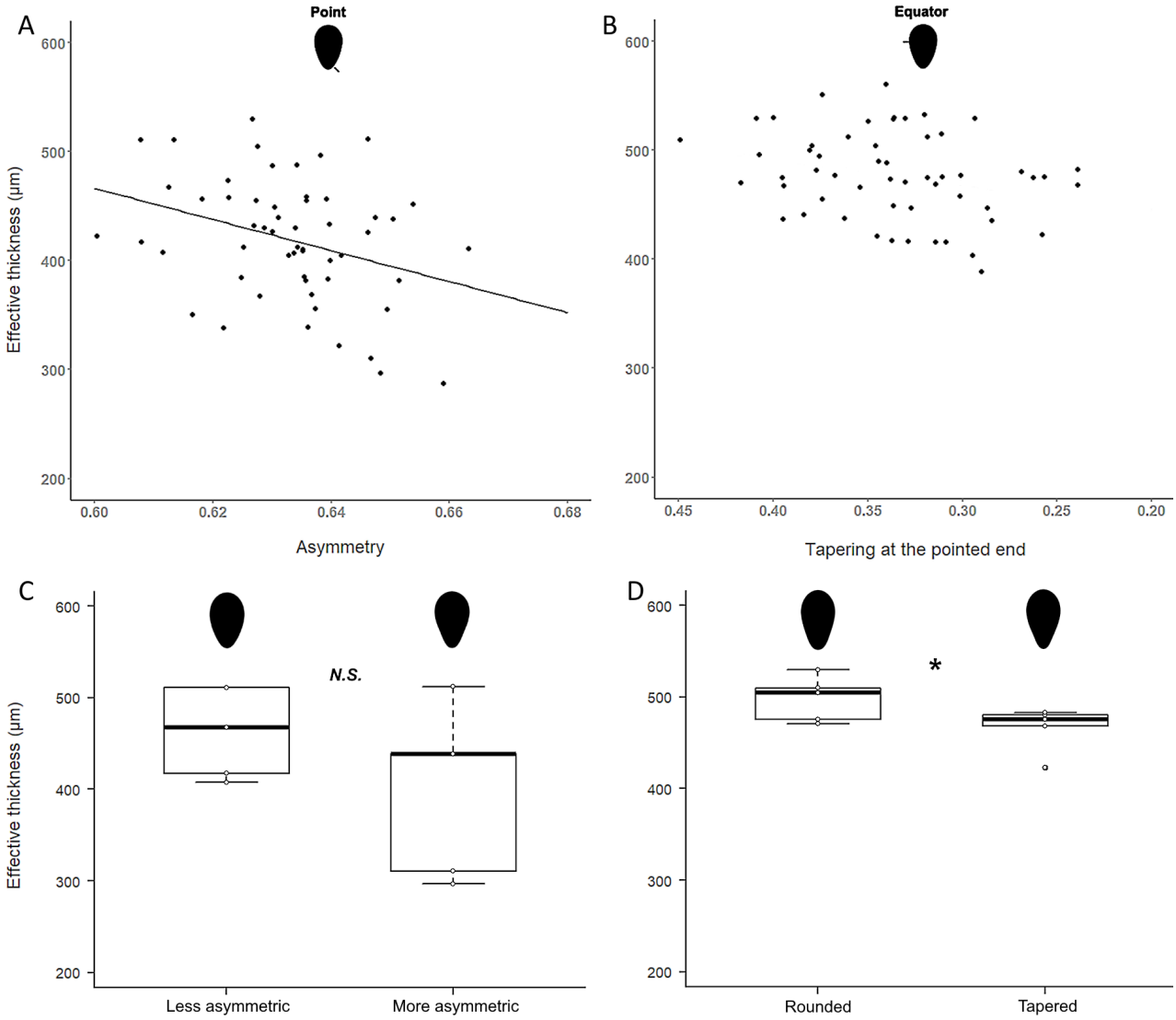

Figure 3. The relationship between eggshell thickness and asymmetry at the pointed end (A & C) and pointed end tapering on thickness at the equator (B & D). (A & C) Linear regression relationships across all 55 eggs, lines are the regression relationships for the raw data. After accounting for variation in egg volume, egg asymmetry was negatively related to effective eggshell thickness at the pointed end of an egg. At the equator, tapering at the pointed end was not significantly related to effective shell thickness at the equator but did increase the R^2 value compared to when the model only included volume (estimate = 182, t = 1.68, p = 0.099; $F_{(2,52)}$ = 6.45, adj-R^2 = 0.168, p = 0.003). (C & D) Pairwise comparisons between five pairs of eggs. Significant differences between pairs of eggs are indicated by the presence of * above the bars. Statistics can be found in Tables 1 and S4.

Table 1. Pairwise comparisons of common guillemot effective eggshell thickness (µm).

Group	Blunt end			Equator			Pointed end		
	$t_{(d.f. = 4)}$	p	Mean of the differences	$t_{(d.f. = 4)}$	p	Mean of the differences	$t_{(d.f. = 4)}$	p	Mean of the differences
Control	1.03	0.362	37.4	1.55	0.197	46.5	0.72	0.510	20.9
Volume	1.81	0.145	30.1	**9.46**	**< 0.001**	**65.4**	2.40	0.074	64.3
Elongation	-1.17	0.307	-27.2	**-2.93**	**0.043**	**-48.5**	**-4.29**	**0.013**	**-59.3**
Asymmetry	-0.22	0.840	-5.3	-0.01	0.993	-0.2	-1.34	0.251	-63.6
Taper	2.22	0.090	30.6	**3.73**	**0.020**	**32.0**	0.24	0.824	5.8
Sphere	0.74	0.499	23.7	0.69	0.528	20.4	1.97	0.120	55.7
Elongation at the blunt end[1]	-0.68	0.526	-12.1	0.39	0.715	9.9	-0.40	0.708	-16.4

Bold indicates significant difference.
[1] d.f. = 5, n = 6.

We found no significant interaction between egg asymmetry and elongation when controlling for egg size across all eggs studied (blunt estimate = 12390, t = 1.66, p = 0.103: equator estimate = 12970, t = 1.82, p = 0.075: point estimate = 13200, t = 1.34, p = 0.188). Elongation at the blunt end was not significant when included as a factor alongside egg volume (blunt estimate = -115, t = -1.47, p = 0.147: equator estimate = -51.7, t = -0.669, p = 0.507: point estimate = -53.2, t = -0.475, p = 0.637). We also found no significant difference in eggshell thickness between paired eggs that varied in how elongate the blunt end of their egg was (Table 1 & S8). No other differences in eggshell thickness were associated with egg shape (Table 1 & S4 – 8) and there were no significant differences in effective thickness between control eggs that were matched according to both size and shape (Table 1).

Despite finding variation in eggshell thickness associated with egg size and shape, the equator of an egg was still typically thicker than the rest of the shell (Table S8). Across all 55 guillemot eggs studied, the blunt end was thinnest (mean ± SD = 353 ± 38μm, range = 269 – 442μm) followed by the pointed end (mean ± SD = 419 ± 56μm, range = 287 – 530μm) and the thickest region was the equator (mean ± SD = 477 ± 40μm, range = 389 – 561μm; $F_{(2,108)}$ = 242, p < 0.0001; Greenhouse-Geisser corrected p-value due to violation of sphericity assumption; Mauchly's test p = 0.0003; ε = 0.791, adjusted d.f. = 1.58, 85.43; Tukey contrasts post-hoc p < 0.05 for all comparisons). Across 10 common guillemot eggs for which effective shell thickness was measured along the entire eggshell length, we found the equator and flat region to be thickest, followed by the pointed end, the tip of the pointed end, and the shoulder of the egg, with the thinnest region being the blunt end ($F_{(4,45)}$ = 22.9, p < 0.001; Greenhouse-Geisser corrected p-value due to violation of sphericity assumption; Mauchly's test p = 0.007; ε = 0.408, adjusted d.f. = 2.04, 18.36; Fig. 4 & S6). Post-hoc tests using Tukey contrasts revealed that the equator was significantly thicker than all other regions (p < 0.05) apart from the tip of the pointed end and the flat region (p > 0.05), the flat region was significantly thicker than the blunt end, shoulder, point and tip of the pointed end (p < 0.05), and the pointed end and shoulder were significantly thicker than the blunt end (p < 0.05).

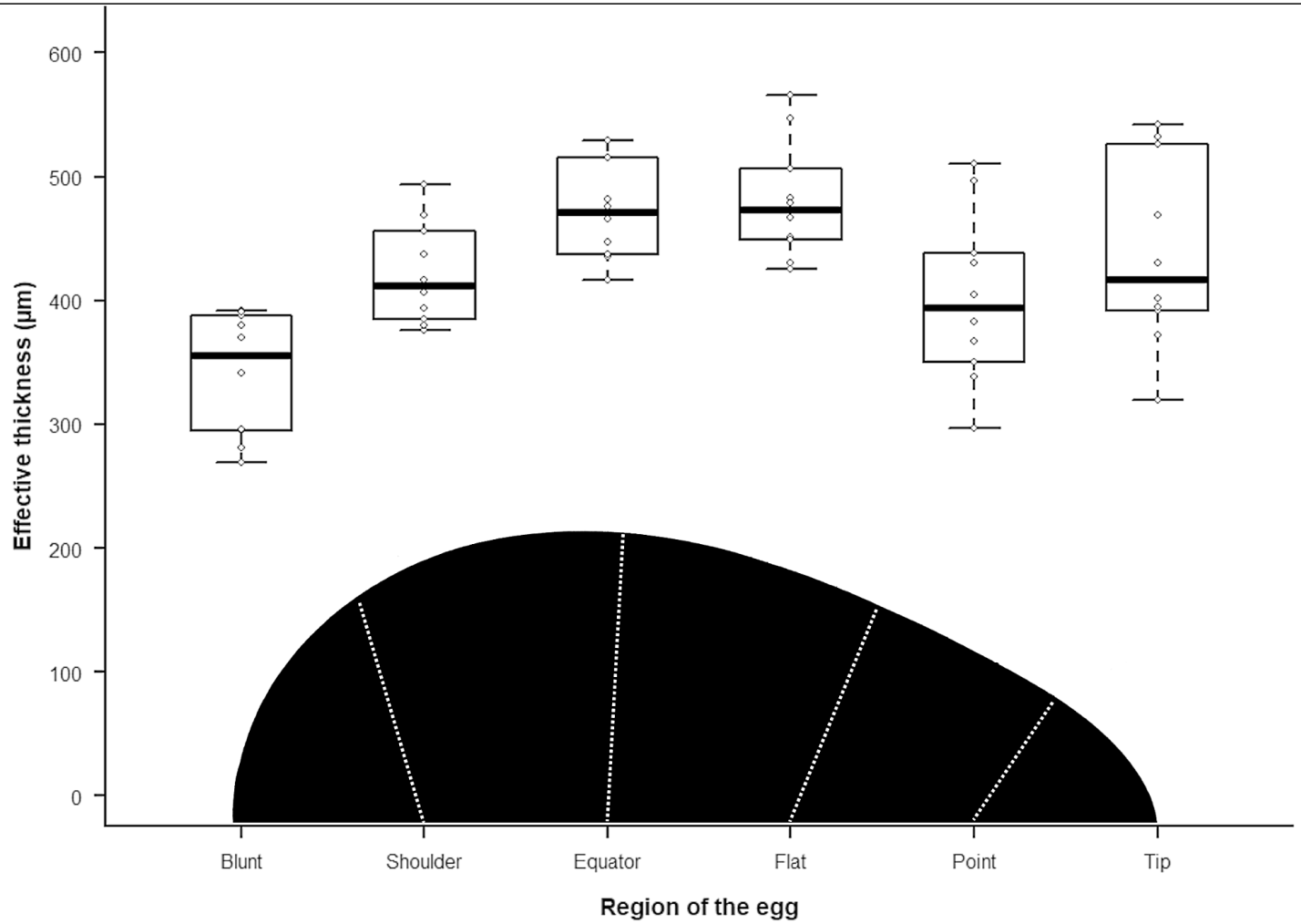

Figure 4. Effective eggshell thickness variation along common guillemot eggs. Common guillemot eggs are thickest at the equator and flat region of the egg, followed by the shoulder, tip and pointed end, with the blunt end being significantly thinner than all other regions ($F_{(4,45)} = 22.9$, $p < 0.001$; Tukey contrasts $p < 0.05$ for significant differences). The white dashed lines on the egg silhouette mark the approximate sampling locations for the shoulder, equator, flat and pointed regions of the egg.

Patterns of effective shell thickness across egg regions in the Alcids

We found variation in the patterns of shell thickness found across eggshell regions between the Alcids. Although many Alcid species tended to have a thicker equator relative to the blunt end, this difference was small and non-significant in 6 out of 17 species analysed (Atlantic puffin, *Fratercula arctica*, black guillemot, *Cepphus grylle*, Japanese murrelet, rhinoceros auklet, *Cerorhinca monocerata,* Scripps's murrelet, *Synthliboramphus scrippsi,* and Cassin's auklet, *Ptychoramphus aleuticus,* eggs; Table 2). Ancient murrelet (*Synthliborampus antiquus*) and razorbill (*Alca torda*) eggs both had significantly thicker shells at the equator and pointed end than at the blunt end (Table 2). Little auk (*Alle alle*) and common guillemot eggs were also thickest at the equator and thinnest at the blunt and pointed end (Table 2). In common guillemot eggs, the pointed end tended to be thicker than the blunt end but this difference was not significant across this small sub-sample (n = 5, post-hoc test with Tukey contrasts, p = 0.065; but see intraspecific results above). In Brünnich's guillemot eggs, the equator was significantly thicker than the pointed end, which in turn was significantly thicker than the blunt end (Table 2). The remaining species (n = 6; crested auklet, *Aethia cristatella,* horned puffin, *Fratercula coniculata,* tufted puffin, *Fratercula cirrhata,* least auklet, *Aethia pusilla,* parakeet auklet, *Aethia psittacula,* and whiskered auklet, *Aethia pygmaea*) showed no significant differences along their eggs, with the equator typically being as thick, or thinner than, the blunt end.

Interspecific differences: egg volume and the incubating bird's mass

Across the Alcidae adult mass was positively related to egg volume, with heavier birds laying and incubating larger eggs (egg volume = 0.0898*adult mass + 14.4; $t_{intercept} = 3.73$, $t_{slope} = 13.2$, $p_{intercept} = 0.0025$, $p_{slope} < 0.0001$; $R^2 = 0.940$). The lambda value (0.25) and partial R^2 values (adult mass $R^2 = 0.930$, phylogeny $R^2 = 0.007$) indicate that this scaling relationship is largely independent of phylogeny. The effective eggshell thickness was positively related to egg volume and adult mass at all three regions of the egg, however adult mass consistently explained more variation in effective shell thickness than egg volume (Fig. 5; Table 3). Despite variable lambda values, the partial R^2 value for the adult mass component of the model was consistently higher than that for phylogeny suggesting

Table 2. Regional effective eggshell thickness (mean ± SD, µm) for the Alcidae.

Species	Effective eggshell thickness (µm) at the			Pattern[1]	F (d.f.) *(d.f. adjusted)	p *(adjusted)
	Blunt end	Equator	Pointed end			
Significant variation in thickness along their eggs						
Ancient murrelet	157 ± 6.5	172 ± 9.5	174 ± 11.2	**E = P > B**	**$11.3_{(2,8)}$**	**0.005**
Brünnich's guillemot	325 ± 40.2	424 ± 24.3	366 ± 54.0	**E > P > B**	**$22.5_{(2,8)}$**	**< 0.001**
Common guillemot	399 ± 37.4	510 ± 24.5	434 ± 40.3	**E > P = B**	**$26.5_{(2,8)}$**	**< 0.001**
Little auk	187 ± 17.8	202 ± 22.7	190 ± 23.8	**E > P = B**	**$6.44_{(2,8)}$**	**0.022**
Razorbill	277 ± 17.6	327 ± 21.5	331 ± 41.7	**P = E > B**	**$11.8_{(2,8)}$**	**0.004**
Non-significant variation in thickness along their eggs						
Atlantic puffin	205 ± 6.8	212 ± 10.7	208 ± 12.0	E = P = B	$1.34_{(2,8)}$ (1.01,4.06)	0.315 (0.312)
Black guillemot	224 ± 17.7	227 ± 10.9	235 ± 14.4	P = E = B	$2.50_{(2,8)}$	0.143
Cassin's auklet	140 ± 7.9	150 ± 9.1	150 ± 5.4	E = P > B	$4.41_{(2,8)}$	0.051
Crested auklet	208 ± 41.7	210 ± 19.1	225 ± 19.2	P = E = B	$1.35_{(2,4)}$ (1.00,2.01)	0.357 (0.365)
Horned puffin	237 ± 15.8	239 ± 6.4	234 ± 17.4	E = B = P	$0.17_{(2,6)}$	0.846
Japanese murrelet	156 ± 11.0	161 ± 11.4	165 ± 6.0	E = P = B	$0.96_{(2,12)}$	0.409
Least auklet	121 ± 14.0	122 ± 11.3	127 ± 12.5	P = E = B	$0.42_{(2,6)}$	0.673
Parakeet auklet	184 ± 5.9	185 ± 15.0	183 ± 21.5	P = E = B	$0.06_{(2,4)}$	0.947
Rhinoceros auklet	210 ± 14.2	231 ± 9.3	219 ± 34.4	E = B = P	$2.72_{(2,8)}$ (1.07,4.26)	0.126 (0.171)
Scripps's murrelet	178 ± 24.6	190 ± 9.5	185 ± 14.0	E = P = B	$1.92_{(2,8)}$	0.208
Tufted puffin	286 ± 26.9	271 ± 21.2	264 ± 10.9	B = E = P	$2.93_{(2,8)}$	0.111
Whiskered auklet	150 ± 8.1	143 ± 15.4	143 ± 8.2	B = E = P	$2.81_{(2,6)}$	0.138

[1] B = blunt end, E = equator and P = pointed end. Bold patterns indicate significant differences (> or < indicates post-hoc tests with Tukey contrasts $p < 0.05$) for significant repeated measures ANOVAs controlling for egg identity.

* Greenhouse-Geisser corrected d.f. and p-values due to violation of sphericity assumption.

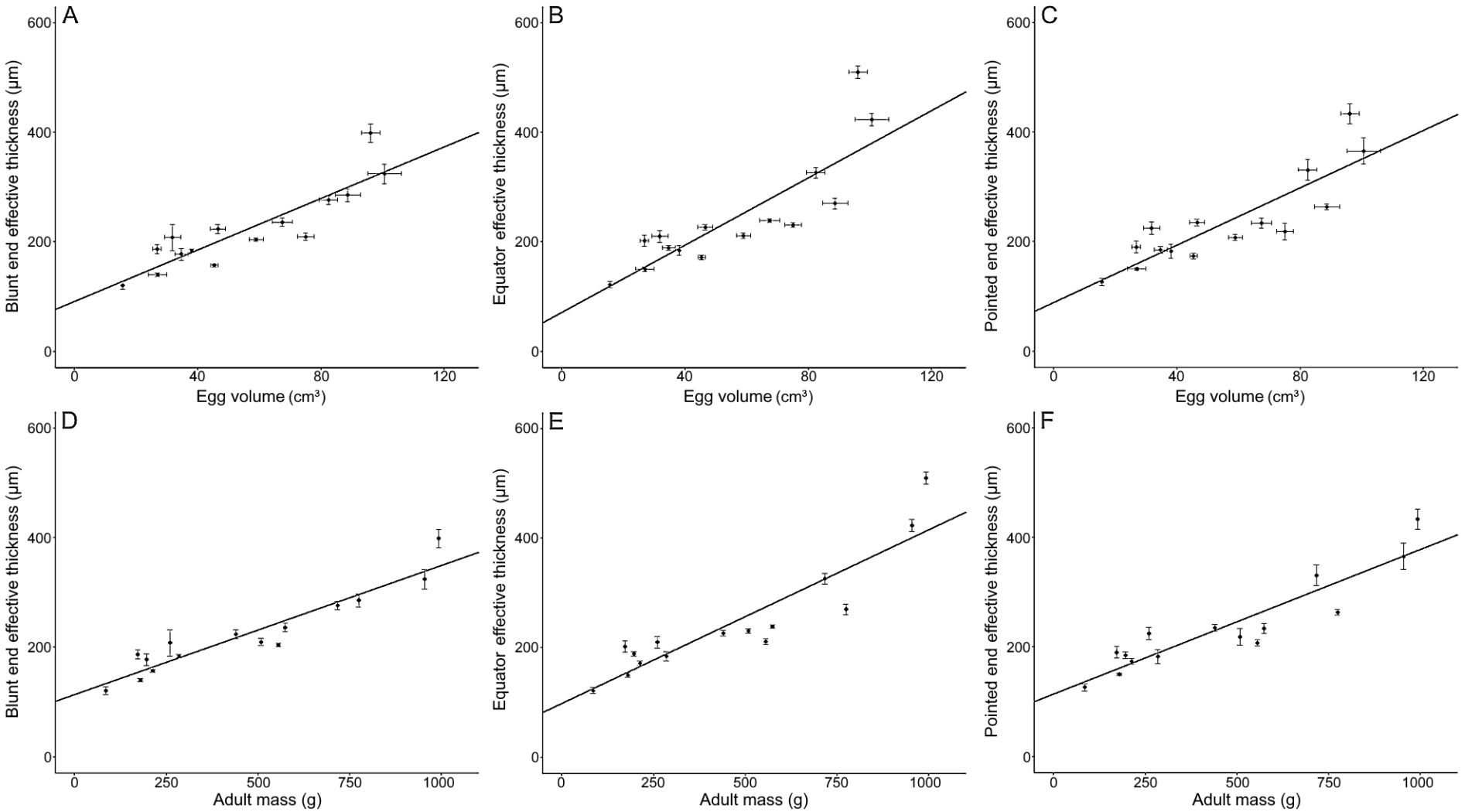

Figure 5. The relationships between effective eggshell thickness at the blunt, equator and pointed end of Alcid eggs and egg volume (A – C) or the parent's mass (D – F). The solid black line is the phylogenetic linear regression relationship and statistics can be found in Table 3.

Table 3. Phylogenetically controlled linear models for the relationship between egg volume or adult bird mass and the effective thickness of the eggshell (μm) across the Alcidae.

Size variable	Region	Lambda	Estimate		t	p	Full model R^2	Size variable R^2	Phylogeny R^2
Egg volume (cm^3)	Blunt	0.229	intercept	91.4	3.97	0.0016	0.786	0.764	0.0221
			slope	2.36	6.48	< 0.001			
	Equator	0.816	intercept	71.6	1.87	0.085	0.800	0.699	0.280
			slope	3.07	5.50	< 0.001			
	Point	0.644	intercept	89.4	3.06	0.009	0.797	0.733	0.217
			slope	2.62	5.97	< 0.001			
Adult bird mass (g)	Blunt	0.169	intercept	114	8.66	< 0.001	0.892	0.884	0.0214
			slope	0.235	9.93	< 0.001			
	Equator	0.808	intercept	98.5	4.00	0.0015	0.888	0.833	0.355
			slope	0.317	8.04	< 0.001			
	Point	0.633	intercept	114	6.22	< 0.001	0.888	0.852	0.280
			slope	0.264	8.67	< 0.001			

that the allometric scaling relationship between eggshell thickness and adult bird mass is largely independent of phylogenetic effects (Fig. 5; Table 3). The slope of the relationship between adult body mass and effective shell thickness was significantly steeper when thickness measures were taken from the equator compared to when they were taken from the blunt end of the egg (t = 2.06, p = 0.045), but not compared to when they were taken from the pointed end (t = 1.40, p = 0.17). After controlling for the allometric relationship with adult mass and phylogeny, egg volume was not significantly related to effective eggshell thickness (egg volume as an additive factor: blunt estimate = -1.27, t = -1.33, p = 0.209, equator estimate = -1.36, t = - 0.980 p = 0.346, point estimate = -1.03, t = - 0.904, p = 0.384: egg volume and adult mass interaction: blunt estimate = 0.001, t = 0.933, p = 0.371, equator estimate = 0.002, t = 1.11 p = 0.291, point estimate = 0.0001, t = - 0.092, p = 0.928). These results indicate that adult mass is more important than egg volume in explaining variation in effective eggshell thickness across the Alcidae, with the thickness of the equator scaling at a greater rate with adult mass than thickness at the blunt end.

Differences between tribes

After controlling for the allometric relationship between effective eggshell thickness and adult body mass, eggs laid by *Alcini* were significantly thicker at the equator and pointed end than those laid by the *Fraterculini* (Table 4; Fig. 6). Eggs laid by the *Fraterculini* were thinner at the equator than those laid by the *Synthliboramphini*, and at the pointed end than those laid by *Aethiini* and *Synthliboramphini* (Table 4; Fig. 6). Including whether a species belonged to the tribe *Alcini* as a binary factor (yes/no) significantly altered the slope of the relationship between adult mass and shell thickness at the equator (Fig. 7). It also altered the relationship between adult mass and effective shell thickness at the pointed end, but this difference only approached significance (estimate = 0.100, t = 2.03, p = 0.067). Including whether a species belonged to the tribe *Fraterculini* as a binary factor (yes/no) did not alter the slope of these relationships (equator estimate = -0.182, t= -1.32, p = 0.215; point estimate = -0.106, t = -1.03, p =0.327), but it did significantly alter the intercept when included as an additive factor (Fig. 7).

Table 4. Differences in effective eggshell thickness (μm) between tribes when tribe was included in the phylogenetically controlled linear model between adult mass and effective eggshell thickness

Region of the egg		Factor	Estimate	t	p
Blunt end Lambda < 0.001 Full model R^2 = 0.930	Tribe	Adult mass	0.236	6.84	< 0.001
		Fraterculini	92.1	3.83	0.004
		Aethiini	23.7	1.08	0.310
		Alcini	37.7	2.15	0.060
		Cepphini	28.3	1.02	0.333
		Synthliboramphini	27.1	1.08	0.308
Equator Lambda < 0.001 Full model R^2 = 0.951	Tribe	Adult mass	0.323	7.90	< 0.001
		Fraterculini	43.4	1.52	0.163
		Aethiini	58.4	2.23	0.052
		Alcini	93.3	4.49	0.002
		Cepphini	42.1	1.28	0.232
		Synthliboramphini	71.5	2.40	0.040
Pointed end Lambda < 0.001 Full model R^2 = 0.956	Tribe	Adult mass	0.264	8.46	< 0.001
		Fraterculini	71.7	3.29	0.009
		Aethiini	46.2	2.31	0.046
		Alcini	71.4	15.9	0.002
		Cepphini	47.3	1.88	0.092
		Synthliboramphini	54.2	2.38	0.041

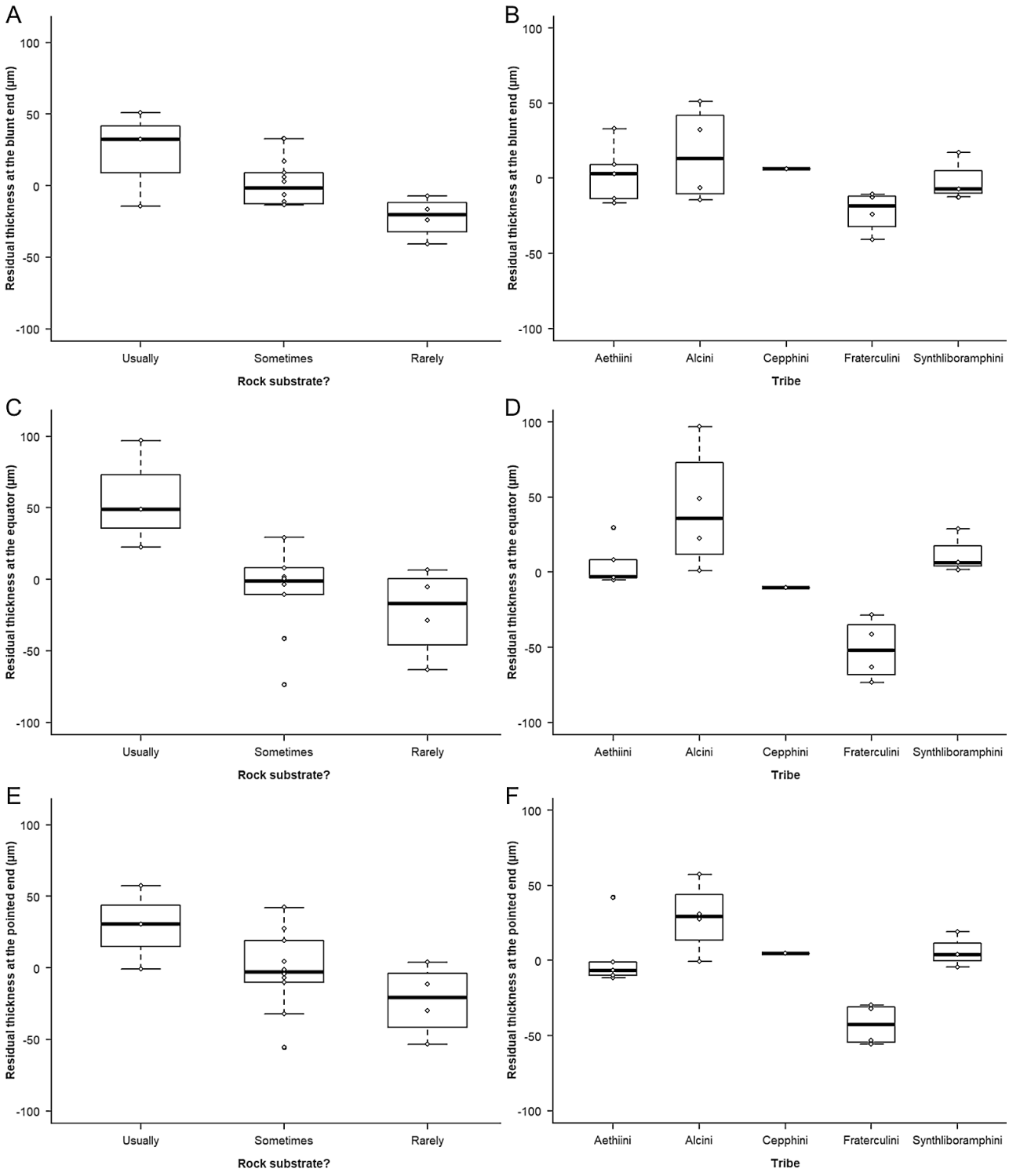

Figure 6. Residual thickness variation after accounting for the adult mass and phylogeny compared to incubation substrate (A, C, E) i.e. whether a bird usually, sometimes or rarely incubates its egg on rock and tribe at each region of the egg (B, D, F). See Tables 3 & 4 for statistics.

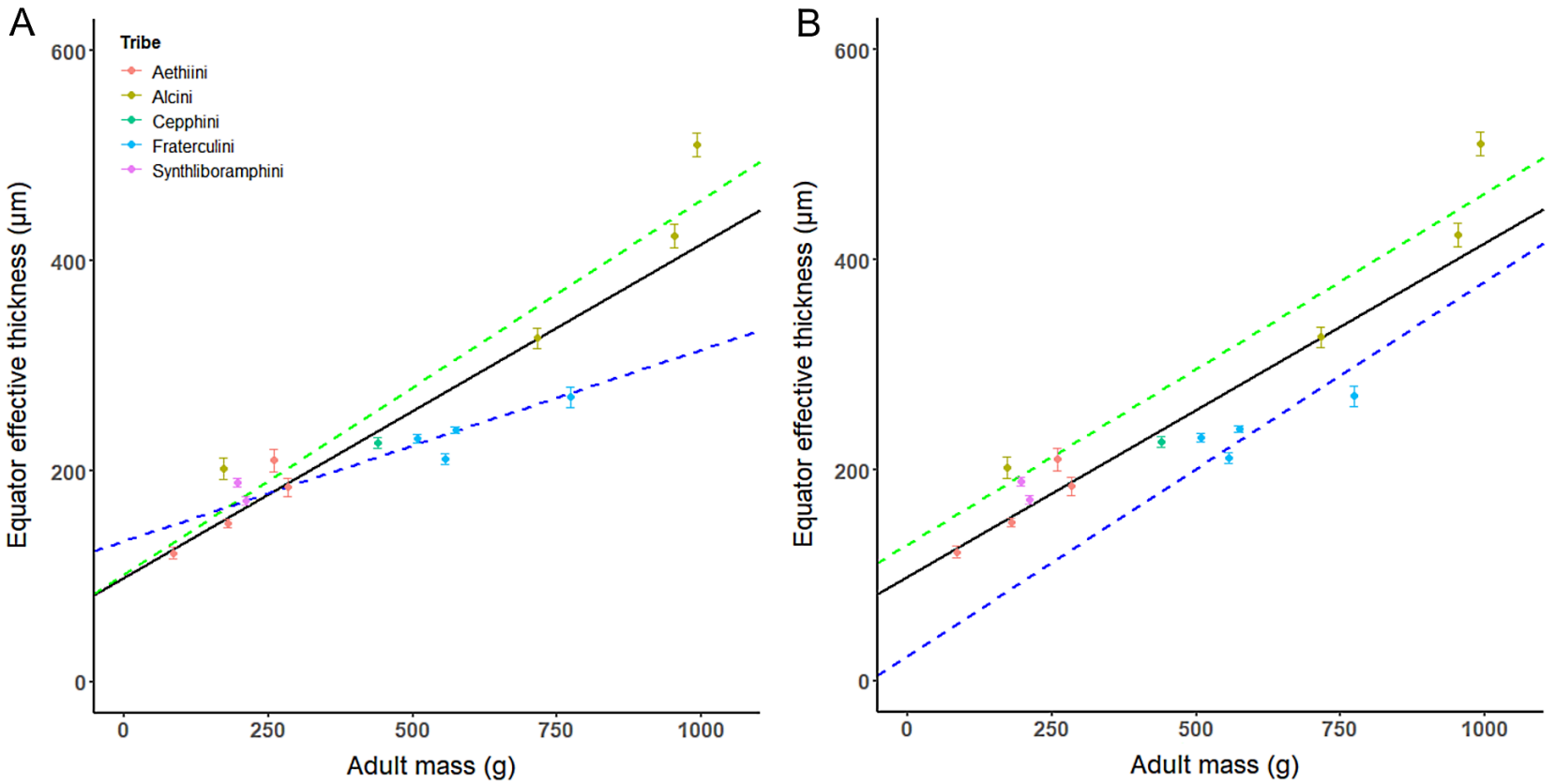

Figure 7. Tribe effects on the allometric relationship between effective eggshell thickness and the adult bird's mass at the equator of eggs. Black lines are the core regression relationship between adult mass and effective thickness at the equator when accounting for phylogeny (A) the regression relationships without the influence of the *Alcini* or *Fraterculini*. The green line is the relationship without the effect of the *Fraterculini* tribe (thickness = 0.356*adult mass + 102; $t_{intercept}$ = 7.31, t_{slope} = 13.2, $p_{intercept\ \&\ slope}$ < 0.001) and the blue line is the relationship without the effect of the *Alcini* tribe (thickness = 0.182*adult mass + 134; $t_{intercept}$ = 7.9, t_{slope} = 4.55, $p_{intercept\ \&\ slope}$ < 0.001). (B) The regression relationships for the *Alcini* and *Fraterculini*. Blue line is the relationship for the *Fraterculini* tribe (this model corresponds to the green line in (A) when *Fraterculini* or not is included as an additive factor in the allometric scaling relationship between adult mass and effective thickness; thickness = 0.356*adult mass + 24; $t_{intercept}$ = - 4.50, t_{slope} = 13.2, $p_{intercept\ \&\ slope}$ < 0.001) and the green line is the relationship for the *Alcini* tribe (this model corresponds to the blue line in (A) when *Alcini* or not is included as an interaction; thickness = 0.333*adult mass + 130; $t_{intercept}$ = - 0.109, t_{slope} = 2.631, $p_{intercept}$ = 0.915, p_{slope} = 0.0234).

Interspecific differences: incubation substrate and egg shape

After controlling for the allometric relationship between adult bird mass and effective shell thickness, eggs of species that usually incubate on a rock substrate were found to be significantly thicker at the blunt and equatorial regions of the egg than eggs of species that rarely incubate on rock. In species that sometimes incubate on rock, the thickness of the blunt end of the egg lay somewhere between that of eggs from species that usually and rarely incubate on rock, but did not differ significantly from either (sometimes compared to rarely; estimate = 25.3, t = 2.13, p = 0.056; Table 5; Fig. 6). At the equator, eggs of species that sometimes incubate on rock were thinner than those species that usually incubate on rock, but did not differ significantly from those of species that rarely incubate on rock (sometimes compared to rarely; estimate = 28.6, t = 1.63, p = 0.134; Table 5; Fig. 6). At the pointed end of the egg, adult mass was significantly related to eggshell thickness, but including incubation substrate, and egg elongation, as factors did not reduce the model AIC value by > 2, suggesting these factors did not have a significant impact on effective shell thickness at the pointed end of the egg (Table 5; Fig. 6).

In terms of egg shape, Alcid species with more elongate eggs had thicker eggshells at the equator compared to species with more rotund eggs. However, based on the model partial R^2 values, the effect of incubation substrate on effective eggshell thickness was relatively more important than the effect of egg elongation (Table 5; Fig. 6). No other factors (egg asymmetry or clutch size) were found to be significantly related to eggshell thickness.

Discussion

In this study we combined an intraspecific approach with interspecific comparative analyses to understand how egg size and shape, parental body size (mass), and the incubation substrate drive variation in eggshell thickness in the Alcids. First, we showed that within a single species with extensive variation in egg shape and size – the common guillemot – egg volume and elongation are key drivers of eggshell thickness and this is primarily reflected in changes in eggshell thickness at the equator and pointed end of the egg. Second, we show that across the Alcids, larger, heavier species, those that lay more

Table 5. Best fitting phylogenetically controlled linear models at the blunt, equator and pointed end of Alcid eggs.

Region of the egg		Factor	Estimate	t	p	Partial R^2
Blunt end AIC = 138.7 Lambda < 0.001 full model R^2 = 0.946 partial R^2 phylogeny < 0.001	Incubation substrate	Adult mass	0.209	10.8	< 0.001	0.909
		Rock: Usually	156	8.83	< 0.001	
		Rock: Sometimes	-28.8	-2.02	0.068	0.498
		Rock: Rarely	-54.0	-3.34	< 0.001	
Equator AIC = 149.6 Lambda < 0.001 full model r^2 = 0.951 partial R^2 phylogeny < 0.001	Incubation substrate	Adult mass	0.235	7.74	< 0.001	0.849
		Elongation	370	2.29	0.045	0.310
		Rock: Usually	- 349	-1.47	0.173	
		Rock: Sometimes	-71.4	-3.50	0.006	0.550
		Rock: Rarely	-100	-4.38	0.001	
Pointed end[1] AIC = 147.8 Lambda < 0.001 full model r^2 = 0.933 partial R^2 phylogeny < 0.001	Incubation substrate	Adult mass	0.202	7.05	< 0.001	0.829
		Elongation	312	2.04	0.068	0.260
		Rock: Usually	-287	-1.28	0.230	
		Rock: Sometimes	-33.5	-1.74	0.113	0.391
		Rock: Rarely	-67.2	-3.12	0.011	

[1] *N.B.* although this model was the best fitting model, the model with only adult mass had a similar AIC (149.5) - including elongation and incubation substrate did not reduce the AIC value by more than 2.

elongated eggs, and those that tend to incubate on bare rock, produce eggshells that are thicker, especially at the equator, but not necessarily at the other regions of the egg. Due to the high correlation between effective and total shell thickness (r_s = 0.95 ~ 0.97), and because the effective eggshell thickness makes up between about 55 – 75% of the total shell thickness, we obtained similar results for the total thickness of the eggshell (and true shell thickness; Supplementary Materials Tables S9 – S26). Together, our results point to a key role for shell thickness at the equator of the egg in determining egg strength and crack resistance during incubation. Our results suggest that the incubation or nesting environment may be an important driver of eggshell thickness evolution in the auks and other birds.

The role of the incubating parent's mass and egg size

At both the intra- and interspecific level, larger eggs tended to have thicker shells, especially at the equator. An increase in shell thickness likely makes an egg stronger and large eggs may therefore need to be thicker because they tend to be laid by larger, heavier birds so must withstand a greater force during contact incubation (Rahn *et al.* 1975; Ar *et al.* 1979; Rahn & Paganelli 1989; Birchard & Deeming 2009). This is especially true at the region just below the equator of the egg, which makes contact with the substrate and the incubating bird. Despite a strong correlation between egg volume and adult mass in the Alcidae, adult mass explained more variation in effective shell thickness than egg volume, suggesting that the weight of the incubating bird is more important than the size of the egg in determining effective shell thickness. Up to now it has been unclear whether shell thickness is driven by egg or parent size across all bird species (Birchard & Deeming 2009), but based on our findings and those of Castilla *et al.* (2009) in falcons (Falconidae), the size of the incubating bird appears to be most important. This is both plausible and logical given that the mass of the incubating bird determines how much force is applied to the egg(s) during incubation.

Within a single species, the common guillemot, larger eggs possessed thicker shells at the equator. It is possible that such larger eggs were laid by larger individuals, but unfortunately, we do not have individual body mass data for the common guillemots that laid these eggs. We therefore cannot rule out the possibility that egg size itself inherently

influences effective shell thickness. Producing a larger egg may involve the shell growing for a longer duration resulting in a thicker shell. Alternatively, since larger eggs are likely a greater investment by a female, thicker shells may be an adaptation against breaking, reducing the risk this investment is lost during incubation. This may be especially true in species that lay single egg clutches (Birchard & Deeming 2009).

Our method of comparing eggs matched by shape and varying only in volume allowed us to assess the relationship between egg size and effective shell thickness more rigorously than in previous studies. Our finding that larger common guillemot eggs have thicker shells is in agreement with Bignert *et al.* (1995), but contrary to that of Pirie-Hay and Bond (2014), who found no relationship between eggshell thickness and egg size. Pirie-Hay and Bond's (2014) results may have been confounded by the effect of egg shape since more elongate and asymmetric eggs tend to be larger (Birkhead *et al.* 2017b; Birkhead *et al.* 2019) but also thinner at the equator and pointed end. A decrease in thickness at the equator and pointed end associated with shape may have countered the positive effects of egg size on shell thickness. This may also explain why studies on other species (e.g. collared flycatcher *Ficedula albicollis;* Hargitai *et al.* 2011) have found non-significant trends between egg size and eggshell thickness, highlighting the potential importance of accounting for egg shape (particularly elongation) in future intraspecific studies.

The influence of egg shape on eggshell thickness

Egg elongation showed the opposite relationship with shell thickness within common guillemot eggs to what we predicted, with the equator and point being thinner in more elongate eggs (Fig. 2). Similarly, eggs with a more tapered pointed end were thinner at the equator and more asymmetric eggs were thinner at the pointed end in some cases (Fig. 3). However, consistent with our predictions, egg elongation explained some of the variation in effective eggshell thickness at the equator of the egg across the auks, providing some support for the idea that increased equatorial eggshell thickness may in part be an adaptation in species that lay eggs that are relatively weak due to their elongate shape (Maurer *et al*. 2012). Importantly, however, our intraspecific results suggest a potential cost associated with making more elongate, asymmetric, and/or

pointed eggs, since eggs of this shape are likely to be thinner and therefore weaker at regions that are under pressure during contact incubation. This finding casts doubt on the hypothesis that the common guillemot egg is strong due to its asymmetric, elongate and pointed egg shape, which has been suggested to allow forces to be dissipated more effectively across the shell due to the relatively large area of shell in contact with the substrate (Birkhead *et al.* 2017a). In contrast, producing a more elongate, asymmetric, and pointed common guillemot egg leads to an inherent weakness in the eggshell due to thinning at the equator and pointed end. It therefore seems unlikely that the common guillemot's extreme egg shape is an adaptation for greater strength. Instead, the long flat surface of the shell, which provides a greater contact area (Birkhead *et al.* 2017a), is probably more important in providing the egg with stability on sloping ledges (Birkhead *et al.* 2018) and/or allowing guillemots to incubate their egg in an upright posture (Birkhead 1993; Birkhead *et al.* 2019).

A range of other factors are known to contribute to intraspecific variation in shell thickness, most notably environmental factors including salinity, diet, and pollution – especially persistent bioaccumulating chemicals such as dichlorodiphenyltrichloroethane (DDT) and polychlorinated biphenyls (PCB; Bignert *et al.* 1995; Pirie-Hay & Bond 2014). Female condition (e.g. Castilla *et al.* 2009; Hargitai *et al.* 2011) and traits of the egg itself such as eggshell colouration and pigmentation may also be important (Hauber *et al.* 2019 but see Jagannath *et al.* 2008; López-Rull *et al.* 2008; Hargitai *et al.* 2010; Hargitai *et al.* 2011; Pirie-Hay & Bond 2014). Future studies exploring the drivers of variation in eggshell thickness within a species should control both egg size (volume) and shape, especially egg elongation, to ensure comparisons are robust. This is particularly important for factors such as diet that may also influence egg size and shape (e.g. herring gulls, *Larus argentatus*; O'Hanlon *et al.* 2019). It's important to note that although we found intraspecific variation in eggshell thickness linked to egg shape and size in the common guillemot across most of our comparison groups, eggs had a significantly thicker equatorial region compared to the blunt end (Table S8). This finding suggests that incubation conditions and/or species physiology (e.g. parent body mass) are more important in determining the pattern of thickness along the eggshell.

Incubating on rock

Our comparative analyses revealed that Alcids that incubate their egg on bare rock or pebbles tended to have thicker eggshells than expected (based on parent body mass) compared to species that sometimes or always incubate their egg on vegetation or soil. This suggests that incubation substrate is an important selective pressure shaping effective eggshell thickness variation, including changes along the egg. The pattern of thickness along the eggshell observed across the Alcidae supports the idea that incubation substrate hardness primarily drives thickening at the equator rather than at the other regions of the egg; 3 out of the 5 species whose eggs had significantly thicker equators relative to the blunt end also usually incubate on rock. Compared to incubation substrate, egg elongation plays a minor role in determining thickness across the Alcidae (Table 5).

Across tribes, the *Alcini* tended to have relatively thick shells for their size, whereas the *Fraterculini* had relatively thin shells. This is likely because the *Alcini* usually incubate their egg on hard substrates such as rock or pebbles, and therefore require enhanced egg strength at the equator. In contrast, the *Fraterculini* tend to nest on softer soil, vegetation, or feathers in burrows, so do not require a particularly thick equator. It is possible that the differences between tribes also relate to the shape of the eggs that they lay, with the *Alcini* typically laying more elongate and asymmetric eggs (with the exception of the little auk) than the *Fraterculini* (Birkhead *et al.* 2019; Fig. S1 & S7). It is worth noting that the *Alcini* seem to have particularly thick shells, especially at the equator of their eggs, compared to the other Alcidae, and this tribe may even be driving the steeper slope of the regression relationship between adult mass and effective thickness at the equator (shown in Fig. 5 & 7). Therefore, the *Alcini* may have even thicker shells than expected given their body mass than our main analyses initially suggest.

Our findings support the suggestions by Uspenski (1958), Belopol'skiĭ (1961), Williams *et al.* (1982), Boersma *et al.* (2004), Pirie-Hay and Bond (2014) and Birkhead *et al.* (2017a) that bird species that nest on hard substrates should have relatively thicker shells than expected for the egg or incubating bird's size. Our study takes this idea further, showing that heavy species that lay elongate eggs and incubate on hard substrates have an

effective eggshell thickness that is higher specifically at the equator – the location where the parent's brood patch makes contact with the egg and where the egg makes contact with the substrate. Although we find evidence of slight increases to thickness at the blunt and pointed end of eggs, the effects are smaller, suggesting these regions do not need to be as strong, probably because they are less likely to be in contact with the incubating parent and/or incubation substrate.

One exception to this could be *Uria sp.* guillemot eggs, which are laid pointed end first (Birkhead 2016) so the egg may need extra reinforcement to ensure it doesn't break when it makes contact with the hard rock ledge upon laying. We found evidence that the pointed end of the common guillemot egg is significantly thicker than the blunt end, but not in all cases (see Results, Fig. 4 & Table 2). The pointed shape may also confer additional strength at this end of the egg (Lazarus *et al.* 2012). The pattern of shell thickness along common guillemot eggs suggests that the equator, as well as the area just below the equator leading to the pointed end, are the thickest regions, followed by the pointed end, tip and shoulder of the egg, with the blunt end being thinnest (Fig. 4 & S6). Shell thickness in the region that rarely, if ever, makes contact with the rock or bird – the blunt end – primarily scales as we would expect with the parent's mass, which may facilitate pipping and hatching despite the rest of the eggshell being so thick (Birkhead *et al.* 2017a). However, changes to the shell's structure may weaken much of the shell in time for hatching. The tips of the mammillary bodies at the equator and pointed end are dissolved leading to the weak attachment of the organic membranes and the true shell making much of the shell brittle (Bond *et al.* 1988a, b; Carnarius *et al.* 1996; Castilla *et al.* 2007; Karlsson & Lilja 2008; Chien *et al.* 2009; Orłowski & Hałupka 2015; Orłowski *et al.* 2016; Rosenberger *et al.* 2017; Athanasiadou *et al.* 2018). Additionally, as cracks initially form on the inner surface, the shell probably breaks more easily from the inside than the outside, even when the shell is thick (Tyler 1969b; Bond *et al.* 1986; Bond *et al.* 1988a, b; Carnarius *et al.* 1996; Bain *et al.* 2006; Hahn *et al.* 2017). Thus having a thin blunt end may not be a specific (or essential) adaptation for hatching.

Why do we find variation in the thickness of the equator (both relatively and absolutely) between little auks, razorbills and the two *Uria sp.* all of which tend to nest on bare rock or pebbles? The reason for this is not entirely clear from our data, but likely relates to the

combined influence of (i) the incubating bird's weight, (ii) incubation site selection, and (iii) egg elongation. Although relative differences in thickness between the blunt end and equator can be difficult to interpret (see Supplementary Materials), little auk eggs seem to have a relatively smaller difference between equator and blunt region thickness (8%, ~15μm) compared to razorbill (18%, ~50μm), common guillemot (29%, ~110μm) and Brünnich's guillemot (31%, ~100μm) eggs. The smaller difference in little auk eggs may be explained by the fact they are small birds that lay relatively rotund eggs (compared to the other *Alcini*; Fig. S1 & S7) and usually incubate on pebbles. In contrast, *Uria sp.* guillemots are large birds that lay elongate eggs and usually incubate on rock. The razorbill represents an intermediate trait set, being reasonably large and laying a somewhat elongate egg, but showing flexibility in nest site selection (e.g. enclosed locations including crevices, burrows or under boulders, or open ledges where it may make a rudimentary nest, the abandoned nest of another species, bare rock, soil or vegetation; Johnsgard 1987; Olsthoorn & Nelson 1990; Tschanz 1990; Gaston & Jones 1998; Hipfner & Dussureault 2001). It is also possible that the thicker equator of the two *Uria sp*. species may be linked to the fact that they breed at very high densities where it is likely neighbouring birds will land on, walk over and fight each other, increasing the risk of damage to the egg (Pirie-hay & Bond 2014; Birkhead *et al.* 2017a).

One species outside of the *Alcini* also possessed a significantly thicker equator compared to the blunt end of its egg: the ancient murrelet. This species incubates its two eggs in a burrow lined with vegetation, which is not consistent with the idea that equatorial eggshell thickness is solely an adaptation for incubation on hard substrates. However, the ancient murrelet lays relatively large and elongate eggs for its body size. Increased egg size may therefore be driving increased thickness at the equator (as we found in common guillemot eggs), and/or increased thickness at the equator may be necessary to compensate for structural weakness associated with egg shape (Maurer *et al.* 2012).

It is unclear precisely how the effective thickness values presented here translate into differences in actual egg strength in nature. However, using equations presented in Ar *et al.* (1979) it is possible to predict the point at which an egg yields (breaks) based on the total thickness of an eggshell. Using this method, we found a similar pattern to that presented in Ar *et al.* (1979) and discussed in Birchard and Deeming (2009), that as

parent body mass increases, the safety factor (yield force divided by bird mass minus 1) decreases. Despite this, across all species eggs tended to be over-engineered i.e. they could withstand a greater mass than that of the incubating parent (approximately at least 2x the bird's mass; Table 6). However, the safety factor at the equator rose for the two heaviest species, the common and Brünnich's guillemot, especially relative to the slightly smaller tufted puffin or razorbill. Furthermore, the safety factor at the equator of the *Uria sp*. eggs is greater than at the blunt end, ensuring that the region that is primarily in contact with the rock substrate and brood patch can withstand greater forces before it breaks compared to the blunt end. In the common guillemot, this is 7 – 8x the mass of the incubating adult, compared to only 4 – 5x at the blunt end. This ensures *Uria sp.* guillemots putatively weaker, more elongate eggs can withstand increased forces incurred from the (i) hard incubation substrate and/or (ii) activity of neighbouring birds in their dense breeding colonies, compared to eggs incubated by razorbills and members of the *Fraterculini.* It is important to note that even though the *Fraterculini* lay relative thin shelled eggs for their body weight, the predicted yielding force at the equator was still 2.9 – 3.9x the weight of the incubating adult, indicating that their eggs are still strong enough to withstand the forces exerted upon them during contact incubation.

Is eggshell thickness adaptive for reasons unrelated to egg strength?

It is possible that our strength-based view of shell thickness ignores the importance of other selection pressures. Below we highlight three relevant alternative hypotheses and discuss why they are unlikely to explain our results presented here.

(1) Uspenski (1958) suggested that eggs incubated on rock without a nest may benefit from a thicker eggshell to provide greater thermal insulation, minimising heat loss. However, eggshell thickness is not related to how effective the shell surface is in emitting thermal radiation (termed thermal emissivity; Björn *et al.* 2012; Jiménez-Muñoz & Sobrino 2012; Björn *et al.* 2016). Studies that suggest shell thickness relates to heat retention (e.g. Yang *et al.* 2018) are anecdotal and do not show a direct relationship between eggshell thickness and thermal properties. In some cases, the parent's anatomy, physiology and incubation behaviour may be important in ensuring eggs do not chill. *Uria sp.* guillemots have one centrally placed brood patch typically 80 – 90mm by 40mm in

Table 6. Predicted mass required to break Alcid eggs based on their total shell thickness (species means) measured using microCT.

Species	Bird mass (kg)	Total eggshell thickness (µm)			Yield force at blunt end (kg)[1]	Safety factor at blunt end[2]	Yield force at equator (kg)[1]	Safety factor at equator[2]	Yield force at pointed end (kg)[1]	Safety factor at pointed end[2]
		Blunt	Equator	Point						
Ancient murrelet	0.21	259	284	283	1.06	4.02	1.28	5.04	1.27	5
Atlantic puffin	0.56	299	319	335	1.42	1.56	1.62	1.91	1.79	2.22
Black guillemot	0.44	346	351	380	1.91	3.35	1.97	3.48	2.31	4.26
Brünnich's guillemot	0.96	490	591	574	3.86	3.04	5.64	4.91	5.32	4.57
Cassin's auklet	0.18	239	263	269	0.9	4.04	1.1	5.11	1.15	5.4
Common guillemot[3]	0.99	559	688	638	5.04	4.07	7.67	6.72	6.58	5.63
Crested auklet	0.26	346	361	391	1.91	6.35	2.08	7.01	2.45	8.42
Horned puffin	0.57	347	365	377	1.92	2.35	2.13	2.71	2.27	2.96
Japanese murrelet	0.19	250	261	260	0.99	4.29	1.08	4.78	1.07	4.73
Least auklet	0.09	207	224	235	0.68	7	0.79	8.38	0.87	9.34
Little auk	0.17	283	315	315	1.27	6.39	1.58	8.18	1.58	8.18
Parakeet auklet	0.28	300	321	338	1.43	4.05	1.64	4.79	1.82	5.43

Table continued on next page

Species	Bird mass (kg)	Total eggshell thickness (µm)			Yield force at blunt end (kg)[1]	Safety factor at blunt end	Yield force at equator (kg)[1]	Safety factor at equator	Yield force at pointed end (kg)[1]	Safety factor at pointed end
		Blunt	Equator	Point						
Razorbill	0.72	401	461	486	2.57	2.59	3.41	3.76	3.8	4.3
Rhino auklet	0.51	311	354	342	1.54	2.03	2	2.94	1.87	2.67
Scripps' murrelet	0.20	271	289	287	1.17	4.94	1.33	5.76	1.31	5.67
Tufted puffin	0.77	422	424	448	2.85	2.69	2.88	2.72	3.22	3.16
Whiskered auklet	0.11	255	267	281	1.03	8.04	1.13	8.92	1.25	10

[1] Equation used to predict yield force is $1{,}718L^{2.022}$ where L is total shell thickness in centimetres (cm). Equation from Ar *et al.* (1979).
[2] Safety factor is (yield force/adult mass) - 1.
[3] Yield force, blunt: 4.30; equator: 6.77; point: 6.09. Safety factor, blunt: 4.33; equator: 6.82, point: 6.13 based on thickness values for all 55 common guillemot eggs studied here.

size that reaches temperatures of 41.5 degrees Celsius, and they incubate their egg constantly throughout incubation, rarely leaving their egg unattended to cool down unlike other auk species (Uspenski 1958; Gaston & Jones 1998). This likely ensures the egg, and embryo within it, remains warm mitigating any thermal costs incurred by incubating an egg on bare rock without an insulative nest.

(2) Thicker eggshells are unlikely to be an adaptation to withstand microbial contamination in species incubating in unsanitary conditions, as suggested for the common guillemot in Hauber *et al.* (2019). A number of other behavioural and egg adaptations (e.g. shell accessory materials or albumen) protect the embryo from faecal material and microbes effectively without necessarily interfering with the general functioning of the shell or making the shell more costly to produce by increasing the amount of calcium required to produce a thicker eggshell (Board & Fuller 1994; D'Alba & Shawkey 2015; D'Alba *et al.* 2017; Jackson *et al.* 2018; Chapter 4; Chen *et al.* 2019). In our study, three species with significantly thicker equator regions (little auk, razorbill and ancient murrelet) tend to incubate their eggs in relatively clean conditions and some species that nest in mud burrows (e.g. the puffins) – a potentially unsanitary environment – laid eggs with relatively thin shells for their body size. Anecdotal evidence from thin-shelled megapode eggs incubated in mounds of rotting vegetation further refutes this hypothesis, as the shell's surface – and not the thickness of the shell – defends against microbes (D'alba *et al.* 2014).

(3) Possessing a thin blunt end may aid in gas exchange (Maurer *et al.* 2012). Yet, despite previous theoretical suggestions, evidence indicates that eggshell thickness may not limit the diffusion of gases across the eggshell (Simkiss 1986; Rahn & Paganelli 1990; Clark *et al.* 2010; Portugal *et al.* 2010; Maurer *et al.* 2012; Portugal *et al.* 2014; Jackson *et al.* 2018; Chapter 4). In fact, Portugal *et al.* (2014) found a positive relationship between eggshell thickness at the equator and eggshell gas conductance across 151 British breeding bird species which directly contradicts the theoretical assumption that thicker shells impose any restriction on gas conductance. Instead, the total number of pores within the shell and how they are distributed may be more important in regulating water and carbon dioxide loss, and consequently oxygen gain (Ar & Rahn 1985; Rokitka & Rahn 1987; Rahn & Paganelli 1990; Jackson *et al.* 2018; Chapter 4), so possessing a

thin blunt end compared to the rest of the egg may have limited benefits for gas exchange (Maurer *et al.* 2012). Furthermore, as blunt end thickness is generally consistent with what is expected for the adult's mass, the blunt end does not appear to be particularly thin, instead in some cases, the rest of the eggshell is particularly thick.

Conclusion

We have shown that both egg size and shape are important in determining within species variation in effective eggshell thickness in the common guillemot, a species with extraordinary variation in egg morphology. Further to this, we have shown across species, variation in effective eggshell thickness is strongly related to the body mass of the incubating parent, as well as to the hardness of the incubation substrate, with how elongate their egg is playing a relatively minor role. We propose that a thicker shell, particularly at the equator, has evolved in larger species that incubate their eggs on rock in order to strengthen the egg during contact incubation, when physical forces exerted from both the incubating parent and the incubation substrate increase the likelihood of the eggshell cracking.

Acknowledgements

We thank all the researchers, their field crews and research assistants who supplied eggshells or helped with the process of getting them imported into the UK including Nora Rojek, Mark Hipfner, Aevar Peterson, Mark Harris, Hallvard Strøm, Akiko Shoji, Kuniko Otsuki, Andrew Power, Ian O'Connor, David Mazurkiewicz, Linnea Hall and René Corado. Jamie Thompson for collecting and imaging the common guillemot egg samples from Skomer Island to obtain data on their shape and size, and Marie Attard and Jamie Thompson for helpful discussions over the course of this study. The Wildlife Trust of South and West Wales Trust for permission to work on Skomer Island NNR, and the Natural Resources Wales (NRW) for licences to take eggs for scientific purposes. We also thank the Skelet.AL lab for use of their microCT scanner.

Competing interests

No competing interests declared.

Author contributions

The study was conceived by D.J., T.R.B. and N.H. D.J. collected and analysed the data; C.R.C. provided advice and assistance on performing and interpreting phylogenetic analyses. D.J. wrote the initial draft; N.H., T.R.B. and C.R.C. commented on the initial draft and revised the manuscript.

Funding

The study was funded by a grant from the Leverhulme Trust (to T.R.B.) and a University of Sheffield Scholarship (to D.J.). N.H. was supported by a Patrick & Irwin-Packington Fellowship from the University of Sheffield and a Royal Society Dorothy Hodgkin Fellowship.

Supplementary information

Supplementary information available in Appendix A3.

References

Ar, A., Paganelli, C. V., Reeves, R. B., Greene, D. G. and Rahn, H., (1974). The Avian Egg: Water Vapor Conductance, Shell Thickness, and Functional Pore Area. *The Condor*. **76**(2), 153–158.

Ar, A. and Rahn, H., (1985). Pores in avian eggshells: Gas conductance, gas exchange and embryonic growth rate. *Respiration Physiology.* **61**(1), 1–20.

Ar, A., Rahn, H. and Paganelli, C. V., (1979). The Avian Egg: Mass and Strength. *The Condor.* **81**(4), 331–337.

Athanasiadou, D., Jiang, W., Goldbaum, D., Saleem, A., Basu, K., Pacella, M. S., Böhm, C. F., Chromik, R. R., Hincke, M. T., Rodríguez-Navarro, A. B., Vali, H., Wolf, S. E., Gray, J. J., Bui, K. H. and McKee, M. D., (2018). Nanostructure, osteopontin, and mechanical properties of calcitic avian eggshell. *Science Advances.* **4**(3), eaar3219.

Bain, M. M., (1991). A reinterpretation of eggshell strength. In: *Egg and Eggshell Quality* (Ed. Solomon, S. E.). Aylesbury, UK: Wolfe Publishing Limited. pp.131 -145.

Bain, M. M., (1992). Eggshell strength: A relationship between the mechanism of failure and the ultrastructural organisation of the mammillary layer. *British Poultry Science.* **33**(2), 303-319.

Bain, M. M., (2005). Recent advances in the assessment of eggshell quality and their future application. *World's Poultry Science Journal.* **61**(2), 268–277.

Bain, M. M., MacLeod, N., Thomson, R. and Hancock, A. J., (2006). Microcracks in eggs. *Poultry Science*. **85**(11), 2001-2008.

Barnett, D. M., Kumpula, B. L., Petryk, R. L., Robinson, N. A., Renema, R. A. and Robinson, F. E., (2004). Hatchability and early chick growth potential of broiler breeder eggs with hairline cracks. *The Journal of Applied Poultry Research.* **13**(1), 65-70.

Barta, Z., & Székely, T., (1997). The Optimal Shape of Avian Eggs. *Functional Ecology.* **11**(5), 656-662.

Belopol'skiĭ, L. O., (1957, translated from Russian 1961). *ecology of sea colony birds of the barents sea*. Jerusalem: Israel Program for Scientific Translations.

Biggins, J. D., Thompson, J. E. and Birkhead, T. R., (2018). Accurately quantifying the shape of birds' eggs. *Ecology and Evolution*. **8**(19), 9728-9738.

Bignert, A., Litzen, K., Odsjo, T., Olsson, M., Persson, W. and Reutergårdh, L., (1995). Time-related factors influence the concentrations of sDDT, PCBs and shell parameters in eggs of Baltic guillemot (*Uria aalge*), 1861–1989. *Environmental pollution*. *89*(1), 27-36.

Birchard, G. F. and Deeming, D. C., (2009). Avian eggshell thickness: scaling and maximum body mass in birds. *Journal of Zoology.* **279**(1), 95–101.

Birkhead, T. R., (1993). *Great Auk Islands*. London, UK: Poyser.

Birkhead, T. R., (2016). *The Most Perfect Thing: the Inside (and Outside) of a Bird's Egg.* London, UK: Bloomsbury.

Birkhead, T. R., Thompson, J. E. and Biggins, J. D., (2017b). Egg shape in the Common Guillemot *Uria aalge* and Brunnich's Guillemot *U. lomvia*: not a rolling matter? *Journal of Ornithology*. **158**(3), 679-685.

Birkhead, T. R., Thompson, J. E., Biggins, J. D. and Montgomerie, R., (2019). The evolution of egg shape in birds: selection during the incubation period. *Ibis*. **161**(3), 605-618.

Birkhead, T. R., Thompson, J. E., Jackson, D. and Biggins, J. D., (2017a). The point of a Guillemot's egg. *Ibis.* **159**(2), 255-265.

Birkhead, T. R., Thompson, J. E. and Montgomerie, R., (2018). The pyriform egg of the Common Murre (*Uria aalge*) is more stable on sloping surfaces. *The Auk*. **135**(4), 1020-1032.

Björn, L. O., Bengtson, S. A., Li, S., Hecker, C., Ullah, S., Roos, A. and Nilsson, A. M., (2016). Thermal emissivity of avian eggshells. *Journal of Thermal Biology*. **57**, 1-5.

Björn, L. O., Uvdal, P. and Li, S., (2012). Ecological importance of the thermal emissivity of avian eggshells. *Journal of Theoretical Biology*. **301**(21), 62-66.

Board, R. G., (1982). Properties of avian egg shells and their adaptive value. *Biological Reviews.* **57**(1), 1–28.

Board, R. G. and Fuller, R., (1994). *Microbiology of the Avian Egg.* London,UK: Chapman and Hall.

Boersma, P. D., Rebstock, G. A. and Stokes, D. L., (2004). Why Penguin Eggshells are Thick. *The Auk*. **21**(1), 148-155.

Bond, G. M., Board, R. G. and Scott, V. D., (1988a). A comparative study of changes in the structure of avian eggshells during incubation. *Zoological Journal of the Linnean Society.* **92**(2), 105–113.

Bond, G. M., Board, R. G. and Scott, V. D., (1988b). An account of the hatching strategies of birds. *Biological Reviews*. **63**(3), 395-415.

Bond, G. M., Scott, V. D. and Board, R. G., (1986). Correlation of mechanical properties of avian eggshells with hatching strategies. *Journal of Zoology*. **209**(2), 225-237.

Carnarius, K. M., Conrad, K. M., Mast, M. G. and MacNeil, J. H., (1996). Relationship of Eggshell Ultrastructure and Shell Strength to the Soundness of Shell Eggs. *Poultry science*. **75**(5), 656–663.

Castilla, A. M., Herrel, A., Díaz, G. and Francesch A., (2007). Developmental stage affects eggshell-breaking strength in two ground-nesting birds: the partridge (*Alectoris rufa*) and the quail (*Coturnix japonica*). *Journal of Experimental Zoology Part A: Ecological Genetics and Physiology.* **307A**(8), 471–477.

Castilla, A. M., Herrel, A., Van Dongen, S., Furio, N. and Negro, J. J., (2009). Determinants of eggshell strength in endangered raptors. *Journal of Experimental Zoology Part A: Ecological Genetics and Physiology*. **311**(4), 303-311.

Chen, X., Li, X., He, Z., Hou, Z., Xu, G., Yang, N. and Zheng, J., (2019). Comparative study of eggshell antibacterial effectivity in precocial and altricial birds using *Escherichia coli*. *PLoS ONE*. **14**(7), e0220054.

Chien, Y. C., Hincke, M. T. and McKee, M. D., (2009). Ultrastructure of avian eggshell during resorption following egg fertilization. *Journal of Structural Biology.* **168**(3), 527–538.

Clark., M. E., Boonstra, T. A., Reed, W. L. and Gastecki, M. L., (2010). Intraclutch Variation in Egg Conductance Facilitates Hatching Synchrony of Canada Geese. *The Condor*. **122**(3), 447-454.

D'Alba, L., Jones, D. N., Badawy, H. T., Eliason, C. M. and Shawkey, M. D., (2014). Antimicrobial properties of a nanostructured eggshell from a compost-nesting bird. *The Journal of Experimental Biology*. **217**(7), 1116-1121.

D'Alba, L. and Shawkey, M. D., (2015). Mechanisms of antimicrobial defense in avian eggs. *Journal of Ornithology*. **156**(1), 399-408.

D'Alba, L., Torres, R., Waterhouse, G. I. N., Eliason, C., Hauber, M. E. and Shawkey, M. D., (2017). What Does the Eggshell Cuticle Do? A Functional Comparison of Avian Eggshell Cuticles. *Physiological and Biochemical Zoology.* **90**(5), 588-599.

Deeming, D. C., (2018). Effect of composition on shape of bird eggs. *Journal of Avian Biology*. **49**(1), jav-01528.

del Hoyo, J., Elliott, A., Sargatal, J., Christie, D. A. and Kirwan, G., (eds.) (2019). *Handbook of the Birds of the World Alive*. Barcelona, Spain: Lynx Edicions. (retrieved from http://www.hbw.com/ on [29/1/2019])

Gaston, A. J. and Jones, I. L., (1998). *Bird Families of the World series: The Auks.* Oxford, UK: Oxford University Press.

Hahn, E. N., Sherman, V. R., Pissarenko, A., Rohrbach, S. D., Fernandes, D. J. and Meyers, M. A., (2017). Nature's technical ceramic: the avian eggshell. *Journal of the Royal Society Interface.* **14**(126), 20160804.

Hargitai, R., Moskát, C., Bán, M., Gil, D., López-Rull, I. and Solymos, E., (2010). Eggshell characteristics and yolk composition in the common cuckoo *Cuculus canorus*: are they adapted to brood parasitism? *Journal of Avian Biology*. **41**(2), 177-185.

Hargitai, R., Mateo, R. and Török, J., (2011). Shell thickness and pore density in relation to shell colouration, female characteristics, and environmental factors in the Collared Flycatcher *Ficedula albicollis*. *Journal of Ornithology*. **152**(3), 579-588.

Hauber, M. E., Bond, A. L., Kouwenberg, A. L., Robertson, G. J., Hansen, E. S., Holford, M., Dainson, M., Luro, A. and Dale, J., (2019). The chemical basis of a signal of individual identity: shell pigment concentrations track the unique appearance of Common Murre eggs. *Journal of the Royal Society Interface.* **16**(153), 20190115.

Hipfner, J. M. and Dussureault, J., (2001). The Occurrence, Size, and Composition of Razorbill Nest Structures. *The Wilson Journal of Ornithology*. **113**(4), 445-449.

Ho, L. S. T. and Ané, C., (2014). A Linear-Time Algorithm for Gaussian and Non-Gaussian Trait Evolution Models. *Systematic Biology.* **63**(3), 397-408.

Hothorn, T., Bretz, F. and Westfall, P., (2008). Simultaneous Inference in General Parametric Models. *Biometrical Journal.* **50**(3), 346-363.

Igic, B., Braganza, K., Hyland, M. M., Silyn-Roberts, H., Cassey, P., Grim, T., Rutila, J., Moskát, C., and Hauber, M. E., (2011). Alternative mechanisms of increased eggshell hardness of avian brood parasites relative to host species. *Journal of The Royal Society Interface*. **8**(64), 1654-1664.

Ives, A. R., (2019). R^2s for correlated data: phylogenetic models, LMMs, and GLMMs. *Systematic Biology.* **68**(2), 234-251.

Jackson, D., Thompson, J. E., Hemmings, N. and Birkhead, T. R., (2018). Common guillemot (*Uria aalge*) eggs are not self-cleaning. *The Journal of Experimental Biology*. **221**(23), jeb188466.

Jagannath, A., Shore, R. F., Walker, L. A., Ferns, P. N. and Gosler, A. G., (2008). Eggshell pigmentation indicates pesticide contamination. *Journal of Applied Ecology*. **45**(1), 133-140.

Jiménez-Muñoz, J. C. and Sobrino, J. A., (2012). Comment on “Ecological importance of the thermal emissivity of avian eggshells”. *Journal of Theoretical Biology*. **304**, 304-307.

Johnsgard, P. A., (1987). Diving Birds of North America: Species Accounts – Auks (Alcidae) In: *Diving Birds of North America, by Paul Johnsgard.* 11. Lincoln, Nebraska, USA: University of Nebraska Press.

Karlsson, O. and Lilja, C., (2008). Eggshell structure, mode of development and growth rate in birds. *Zoology.* **111**(6), 494-502.

Khabisi, M. M., Salahi, A. and Mousavi, S. N., (2012). The influence of egg shell crack types on hatchability and chick quality. *Turkish Journal of Veterinary and Animal Sciences*. **36**(3), 289-295.

Lawrence, M. A., (2016). ez: Easy Analysis and Visualization of Factorial Experiments. R package version 4.4-0. https://CRAN.R-project.org/package=ez

Lazarus, A., Florijn, H. C. B. and Reis, P. M., (2012). Geometry-Induced Rigidity in Nonspherical Pressurized Elastic Shells. *Physical review letters*. **109**(14), 144301.

López-Rull, I., Miksik, I., and Gil, D., (2008). Egg pigmentation reflects female and egg quality in the spotless starling *Sturnus unicolor*. *Behavioral Ecology and Sociobiology*. **62**(12), 1877-1884.

Macleod, N., Bain, M. M. and Hancock, J. W., (2006). The mechanics and mechanisms of failure of hens' eggs. *International Journal of Fracture*. **142**(1-2), 29-41.

Mallory, M. L. and Weatherhead, P. J., (1990). Effects of nest parasitism and nest location on eggshell strength in waterfowl. *The Condor*. **92**(4), 1031-1039.

Maurer, G., Portugal, S. J. and Cassey, P., (2012). A comparison of indices and measured values of eggshell thickness of different shell regions using museum eggs of 230 European bird species. *Ibis.* **154**(4), 714–724.

O'Hanlon, N. J., Alonso, S., Miller, J. A. O., Mcgill, R. A. R. and Nager, R. G., (2019). Landscape-mediated variation in diet is associated with egg size and maculation in a generalist forager. *Ibis*. https://doi.org/10.1111/ibi.12739

Olsthoorn, J. C. M. and Nelson, J. B., (1990). The availability of breeding sites for some British seabirds. *Bird Study*. **37**(3), 145-164.

Orłowski, G. and Hałupka, L., (2015). Embryonic eggshell thickness erosion: A literature survey re-assessing embryo-induced eggshell thinning in birds. *Environmental Pollution.* **205**, 218–224.

Orłowski, G., Hałupka, L., Klimczuk, E. and Sztwiertnia, H., (2016). Shell thinning due to embryo development in eggs of a small passerine bird. *Journal of Ornithology.* **157**(2), 565-572.

Picman, J., (1989). Mechanism of increased puncture resistance of eggs of Brown-headed Cowbirds. *The Auk.* **106**(4), 577–583.

Pinheiro, J., Bates, D., DebRoy, S., Sarkar, D., R Core Team, (2018). nlme: Linear and Nonlinear Mixed Effects Models. R package version 3.1-137, https://CRAN.R-project.org/package=nlme

Pirie-Hay, D. and Bond, A. L., (2014). Thickness of Common Murre (*Uria aalge*) eggshells in Atlantic Canada. *The Canadian Field-Naturalist.* **128**(1), 72–76.

Portugal, S. J., Maurer, G. and Cassey, P., (2010). Eggshell Permeability: A Standard Technique for Determining Interspecific Rates of Water Vapor Conductance. *Physiological and Biochemical Zoology.* **83**(6), 1023–1031.

Portugal, S. J., Maurer, G., Thomas, G. H., Hauber, M. E., Grim, T. and Cassey, P., (2014a). Nesting behaviour influences species-specific gas exchange across avian eggshells. *The Journal of Experimental Biology.* **217**(18), 3326–3332.

R Core Team, (2018). R: A language and environment for statistical computing. R Foundation for Statistical Computing, Vienna, Austria. https://www.R-project.org/

Rahn, H. and Paganelli, C. V., (1989). Shell Mass, Thickness and Density of Avian Eggs Derived from the Tables of Schönwetter. *Journal of Ornithology.* **130**(1), 59–68.

Rahn, H. and Paganelli, C. V., (1990). Gas fluxes in avian eggs: Driving forces and the pathway for exchange. *Comparative Biochemistry and Physiology Part A: Physiology*. **95**(1), 1-15.

Rahn, H., Paganelli, C. V. and Ar, A., (1975). Relation of Avian Egg Weight to Body Weight. *The Auk.* **92**(4), 750–765.

Rayan, G. N. and Badri, F. B. A., (2017). Impact of star crack eggshell type and layer breeder age on eggshell traits, embryonic mortality, hatchability and chick quality. *Egyptian Poultry Science Journal.* **37**(1), 185-197.

Rokitka, M. A. and Rahn, H., (1987). Regional differences in shell conductance and pore density of avian eggs. *Respiration Physiology.* **68**(3), 371–376.

Romanoff, A. L. and Romanoff, A. J., (1949). *The avian egg*. New York, USA: Wiley.

Rosenberger, J., Deeming, D. C., Łukaszewicz, E. and Kowalczyk, A., (2017). Changes of eggshell characteristics during embryo development in Western Capercaillie (*Tetrao urogallus*). *Avian Biology Research.* **10**(2), 92-97.

Schönwetter, M., (1960–1992). *Handbuch der Oologie*. Berlin, Germany: Akademie Verlag.

Simkiss, K., (1986). Eggshell conductance—Fick's or Stefan's law? *Respiration physiology*. **65**(2), 213-222.

Smart, I. H. M., (1991). Egg shape in birds. In: *Egg Incubation: Its Effects on Embryonic Development in Birds and Reptiles* (eds. D. C. Deeming and M. W. J. Ferguson). Cambridge, UK: Cambridge University Press. pp. 101-116.

Smith, N. A., (2016). Evolution of body mass in the Pan-Alcidae (Aves, Charadriiformes): the effects of combining neontological and paleontological data. *Paleobiology*. **42**(1), 8-26.

Smith, N. A. and Clarke, J. A., (2015). Systematics and evolution of the Pan-Alcidae (Aves, Charadriiformes). *Journal of Avian Biology*. **46**(2), 125-140.

Solomon, S. E., (2010). The eggshell: strength, structure and function. *British Poultry Science.* **51**(sup1), 52-59.

Solomon S. E., Bain M. M., Cranstoun S. and Nascimento V., (1994). Hen's egg shell structure and function. In: *Microbiology of the Avian Egg* (eds. Board, R. G. and Fuller, R.). London, UK: Chapman and Hall. pp. 1-24.

Spottiswoode, C. N., (2010). The evolution of host-specific variation in cuckoo eggshell strength. *Journal of Evolutionary Biology.* **23**(8), 1792–1799.

Spottiswoode, C. N. and Colebrook-Robjent, J. F., (2007). Egg puncturing by the brood parasitic Greater Honeyguide and potential host counteradaptations. *Behavioral Ecology*. **18**(4), 792-799.

Tschanz, B., (1990). Adaptations for Breeding in Atlantic Alcids. *Netherlands Journal of Zoology.* **40**(4), 688–710.

Tyler, C., (1969a). Avian Egg Shells: Their Structure and Characteristics. *International Review of General and Experimental Zoology.* **4**, 81-130.

Tyler, C., (1969b). The snapping strength of the egg shells of various orders of birds. *Journal of Zoology.* **159**(1), 65–77.

Uspenski, S. M., (1958). *The Bird Bazaars of Novaya Zemlya.* Canada, Ottawa: Department of Northern Affairs and Natural Resources, Canadian Wildlife Service (translated from Russian).

Weidinger, K., (1996). Egg variability and hatching success in the Cape petrel *Daption capense* at Nelson Island, South Shetland Islands, Antarctica. *Journal of Zoology*. **239**(4), 755-768.

Weir, J. T. and Mursleen, S., (2013). Diversity-dependent cladogenesis and trait evolution in the adaptive radiation of the auks (Aves: Alcidae). *Evolution*. **67**(2), 403-416.

Williams, A. J., Siegfried, W. R. and Cooper, J., (1982). Egg composition and hatchling precocity in seabirds. *Ibis.* **124**(4), 456–470.

Yang, C., Huang, Q., Wang, L., Du, W. G., Liang, W. and Møller, A. P., (2018). Keeping eggs warm: thermal and developmental advantages for parasitic cuckoos of laying unusually thick-shelled eggs. *The Science of Nature*. **105**(1-2), 10.

Chapter 3:

Does the distribution of pores along a bird’s egg matter?

Does the distribution of pores along a bird's egg matter?

Duncan Jackson[1*], Nicola Hemmings[1] and Timothy R. Birkhead[1]

[1]*Department of Animal & Plant Sciences, University of Sheffield, Sheffield, S10 2TN, UK*

*Corresponding author. Email: djackson3@sheffield.ac.uk

Key words

X-ray micro-computed tomography, Gas exchange, Incubation period, Eggshell thickness, Auks, Alcidae.

Abstract

The unequal distribution of gas exchange pores along the common guillemot's (*Uria aalge*) eggshell is striking, with the blunt end of the egg having twice the density of pores than the equator and pointed end. It has been hypothesised that this uneven distribution of pores may allow the guillemot embryo to maintain adequate gas exchange across the eggshell despite it becoming soiled during incubation in dirty environments. We used X-ray micro-computed tomography to examine eggshell microstructure both within the common guillemot and across 17 Alcid species, to investigate how and why pore distributions vary. We show that variation in pore density across common guillemot eggs is largely independent of egg shape and size, but relates to eggshell thickness, with thicker regions of shell containing fewer pores. We also show that a higher density of pores at the blunt end of the egg is not a ubiquitous feature of Alcid eggshells. High pore density at the blunt end of the egg is not more common in Alcids that incubate in dirty conditions, or in precocial species. Instead, variation across species in pore distributions may in part relate to variation in thickness along the shell. Increased eggshell thickness within a particular region of an egg potentially restricts the number of pores that can form in an eggshell, thus leading to low pore density in such regions (e.g. at the equator and pointed end). In such eggs, high pore densities may be required at the blunt end to compensate for low overall pore density, ensuring the total number of pores in an egg is optimal for gas exchange during incubation. Finally, across Alcid species we found that larger eggs contain a higher number of pores but, contrary to common assumption, incubation period is unrelated to total pore number.

Introduction

A key function of a bird's eggshell is to regulate gas exchange to the developing embryo, ensuring the embryo gets enough oxygen while preventing too much water loss (Romanoff & Romanoff 1949; Tyler 1969; Rahn *et al.* 1979; Board 1982). Gases travel through pore channels in the calcium carbonate shell and thus the total number of pores in an eggshell determines the rate at which gases can enter or exit the egg (Ar & Rahn 1985; Rahn & Pagnelli 1990).

The number of pores in the shell (and the resulting gas conductance) is primarily driven by the need for eggs to lose water – typically 10 – 22% of their initial mass – throughout incubation, which is essential for normal embryo growth and hatching (Ar & Rahn 1980; Board 1982; Rahn & Paganelli 1990; Ar 1991; Ar & Deeming 2009). Eggs that are large, and/or incubated (i) for relatively short periods of time, (ii) at lower altitudes, (iii) in wet, humid environments, or (iv) in relatively enclosed nests like burrows, tend to have more porous eggshells to ensure enough water is lost during incubation (Ar *et al*. 1974; Rahn *et al.* 1974; Packard *et al.* 1977; Rahn *et al.* 1977; Rahn *et al.* 1979; Carey 1980; Sotherland *et al.* 1980; Board 1982; Rahn *et al.* 1982; Davis *et al.* 1984; Tullett 1984; Ar & Rahn 1985; Davis & Ackerman 1985; Carey *et al.* 1987; Arad *et al.* 1988; Guerra *et al.* 1988; Carey *et al.* 1990; Rahn & Paganelli 1990; Monge *et al.* 2000; Baggot *et al.* 2003; Portugal *et al.* 2014a). However, while the adaptive function of total pore numbers is well understood, the causes of variation in pore distribution along the eggshell is less clear.

Unequal pore distributions along the eggshell were first observed in domestic chicken (*Gallus gallus domesticus*) eggs by Rizzo (1899) who showed that the average pore density declined from the blunt to the pointed end of the egg (cited in Romanoff & Romanoff 1949). Since then, few studies have assessed the adaptive significance of unequal pore distributions in bird eggs. Rokitka and Rahn (1987) studied six species across four orders and reported what was assumed to be a universal pattern; eggs have more pores at the blunt end than at the equator or pointed end. Other studies, however, observed equal numbers of pores along eggs of some species, and greater density of

pores at the equator or pointed end in others (Tullett 1975; Kern *et al.* 1992; Massaro & Davis 2005).

The common guillemot's (*Uria aalge*) egg has a strikingly unequal distribution of gas exchange pores, with the blunt end typically having approximately twice the density of pores than the equator and pointed end. Birkhead *et al.* (2017) suggested that high blunt end porosity may allow common guillemots to incubate their pyriform (elongate, asymmetric and pointed at one end) egg on wet and dirty cliff ledges, allowing adequate gas exchange across the eggshell even when the rest of the egg is soiled during incubation.

Smart (1991) hypothesised that an asymmetrically pointed egg might be adaptive for precocial species to facilitate accelerated neural development by creating a specialised respiratory site at the blunt end of the egg. Egg shape and/or unequal pore density distributions may therefore be associated with developmental mode across species. Smart's (1991) idea was that the blunt end of an asymmetrically pointed egg has a larger surface area relative to the rest of the egg, and since he assumed that all bird eggs have a higher pore density at the blunt end (Rokitka & Rahn 1987), this increased area would lead to a greater number of pores in this region compared to more spherical or symmetrical eggs. However, a specialized respiratory site could also be achieved without a change to overall egg shape, simply by having a higher density of pores in the blunt region.

Variation in shell thickness along the egg could also influence pore density distributions, explaining the unequal pore distributions we see across common guillemot eggshells. Thicker shells tend to have a lower pore density perhaps as a consequence of how the shell forms (Tullett & Board 1977; Tyler & Fowler 1978). Pore formation is an imperfect process, relying on fluid flowing into the egg ("plumping") to keep gaps open between the calcite crystals during shell growth (Tyler & Simkiss 1959; Tullett 1975; Tullett & Board 1977). Having a thicker shell at the equator of the egg (as the common guillemot does; Maurer *et al.* 2012; Birkhead *et al.* 2017; Chapter 2) may restrict porosity in that region by reducing the number of pores that remain open during eggshell growth. Greater numbers of pores may therefore need to form at the relatively thin blunt end to compensate.

Common guillemot eggs may have high blunt end pore densities to satisfy the gas exchange demands of their reasonably large egg. Tullett and Board (1977) suggested that as eggs increase in size, their shells become thicker and pore density decreases, despite larger eggs containing more pores in total. Greater total pore numbers in large eggs are likely achieved through increased shell surface area, but unequal pore distributions could also be important. Increased pore density in a single region of the eggshell could serve to increase the total number of pores in an egg without requiring an increase in pore density across the entire shell.

Here, we measure pore distributions along Alcid eggs using X-ray micro-computed tomography (microCT) to assess whether eggs possess a high density of pores at the blunt end. We then investigate whether regional variation in the density of pores is related to (i) precocialty, (ii) the risk of surface contamination from debris, (iii) regional variation in eggshell thickness, and (iv) egg size and/or shape, with the aim of understanding why some eggs, such as the common guillemot's, have a considerably greater density of pores at the blunt end compared to other regions. Given the large variation in egg shape and size between Alcids, and the fact that *Uria sp.* guillemots lay the largest, most elongate, asymmetric and pointed eggs of all the Alcids (Birkhead *et al.* 2019), we explored if pore densities were associated with egg size and/or shape. Finally, using new and improved methods for calculating total pore number which incorporate regional variation in pore density, we re-assess the relationships previously explored by Zimmerman and Hipfner (2007) between total pore numbers, egg size, and incubation period.

Materials and Methods

Samples and scanning

Egg shape, size, pore density and effective shell thickness (the distance from the point of fusion of mammillary bodies to the outer surface of the shell) was measured for 15 – 17 Alcid species (16 species n = 1 – 5 eggs per species, and 55 common guillemot eggs; see Chapter 2 for sample details). Five common guillemot eggs collected in 2018 were randomly selected for use in the comparative analysis before they were scanned.

Effective shell thickness measures were obtained from microCT scans performed in a Bruker Skyscan 1172 (see Chapter 2 for details). We were specifically interested in the effective shell thickness because this is where pore channels are located; the thickness of other layers such as the shell membranes or mammillary layer are unlikely to influence pore formation in any meaningful way. Species-specific data on incubation period and developmental mode was obtained primarily from del Hoyo *et al.* (2019), but also from Gaston and Jones (1998). When a range of days was provided we used the median value to the nearest half day in analyses (e.g. 32 – 33 days; a value of 32.5 was used). For developmental mode, we classified species as semi-precocial, intermediate (*Uria sp*. guillemots and razorbills, *Alca torda*) or fully precocial as per Starck and Ricklefs (1998).

Measuring pore density

MicroCT is a non-destructive, three-dimensional imaging technique that can be used to visualise and measure pores in avian eggshells (Riley *et al.* 2014; Willoughby *et al.* 2016; Birkhead *et al.* 2017; Jackson *et al.* 2018; Chapter 4). It requires minimal sample preparation and is likely more reliable and accurate than common methods used to count pores that rely on damaging chemical treatments to enlarge pore channels to permit dyes or light to penetrate them (see Board 1982; Boersma & Rebstock 2009; Stein & Badyaev 2011; Appendix A2 for limitations of historical methods). MicroCT image stacks for each eggshell were loaded into CTVox (version 3.0, Bruker micro-CT, Kontich, Belgium) to produce 3-D volumetric reconstructions of the eggshell fragment. The number of pores was counted and divided by fragment area (~ 25 – 35mm^2 – measured in ImageJ; Schneider *et al.* 2012) to obtain pore density (see Birkhead *et al.* 2017). To compensate for curvature of the eggshell fragments a benzier curve line measurement tool was used to measure each side of the fragment. If the eggshell fragment's shape was highly irregular, we directly measured the area using a polygon tool. Using data collected in Birkhead *et al.* (2017) where three fragments were sampled from each region (blunt, equator and pointed end) of five common guillemot and five razorbill eggs, the repeatability of this sampling technique is moderate to high (common guillemot eggs: r = 0.96, razorbill eggs: r = 0.23, both species: r = 0.61). We did not measure pore size because (a) our scanning resolution (4µm) may have led to inaccurate measurements, particularly in thinner shells where pores are generally smaller (D.J. Pers. Obs.), and (b)

the importance of pore size for regulating gas conductance across species is unclear (Jackson *et al.* 2018; Chapter 4). We therefore focused on pore density, pore distribution along eggs and predicted total pore numbers.

We assessed how pore distribution varied along the length of 10 common guillemot eggs by sampling a transect of approximately adjacent fragments (where possible) from the blunt end to the tip of the pointed end (see Fig. S2 in Chapter 2). We then assessed how pore density varied in relation to egg shape, size and effective shell thickness across all common guillemot eggs (n = 55 eggs, see Chapter 2 for details on egg shape and size acquisition). Finally, we assessed how pore distributions vary between Alcids, and if pore density at different regions of the egg relates to egg size, asymmetry, elongation or developmental mode.

Total pore number calculations

Previously, total pore numbers for an egg have been calculated by either (1) sampling random locations to provide an average pore density for an egg which is multiplied by eggshell surface area (e.g. Ar & Rahn 1985), (2) assuming pore density at each region (blunt, equator and point) represents approximately one third of the egg's surface area (e.g. Zimmerman & Hipfner 2007) or (3) giving double the weighting to the equator region as it likely represents a larger proportion of the surface area than either pole (e.g. Hoyt *et al.* 1979). It is unlikely that these calculations satisfactorily account for variation in pore density along an egg. Instead, they probably overemphasise the importance of pore density in one area and underestimate it in another, especially when pores are unequally distributed along an egg. We therefore need to know how much of the eggshell should be attributed to each region to ensure that blunt end pore densities represent the correct proportion of the shell.

We estimated the area at the blunt half of the egg using the general formula for a spheroid that has small relative error (maximum ±1.061%; see Xu *et al.* 2009):

$$SA = 4\pi\left[1/3\left(a^p b^p + a^p c^p + b^p c^p\right)\right]^{1/p}$$

Where SA is the surface area, p is a constant that approximately equals 1.6075 (see Xu *et al.* 2009), a is the distance from the maximum breadth to the blunt end of the egg and b & c is half the maximum breadth of the egg.

The resultant surface area was divided by 2 to approximate the surface area at the blunt end only. This method of measuring the blunt end includes some of the equatorial region, so we allocated 25% of this area as “true blunt end” based on data from 10 guillemot eggs, in which the shoulder of the egg did not possess as many pores as the blunt end (see Results). If pore densities were equal at the shoulder and blunt end, then a 50% (or even slightly higher) weighting would be more suitable, whereas if the area occupied by high blunt end pore densities was even smaller, 10% may be appropriate. We present results based on the other weighting scenarios (25% termed “realistic” calculation, 50% “moderate” and 10% “conservative”) for completeness. For weighting the equator and pointed end, we took the remaining eggshell surface area (calculated by subtracting the “true blunt end” area from the total surface area of the egg; see Birkhead *et al.* 2017 & Biggins *et al.* 2018) and attributed 25% to the pointed end and 75% to the equator. We multiplied surface areas by regional pore density values and summed the predicted number of pores at each region to obtain a total pore number for each egg. It is likely that the appropriate calculation for total pore number is dependent on the precise nature of how pores are distributed along an egg, and thus may be species-specific. Since we only have detailed information on the pore distributions for common guillemot eggs, we used equations in our study that are representative for this species.

Statistical analysis

All statistical analyses were performed in R version 3.5.1 (R Core Team 2018). A mixture of paired t-tests and repeated measures ANOVAs were used to determine differences in pore density between pairs of common guillemot eggs that differed in shape or size. Spearman’s rank correlations were used to assess the effect of egg volume and egg shape on pore density at each region for all the eggs scanned (n = 55). Spearman’s rank correlations and repeated measures correlations (Bakdash & Marusich 2017) were used to assess the relationship between effective eggshell thickness and pore density in common guillemot eggs. To analyse differences in pore density between regions of Alcid

eggs, we took three measures per egg and assessed variation within eggs using a repeated measures ANOVA to control for egg identity. The ezANOVA function in the ez package (Lawrence 2016) was used to assess sphericity with Mauchly's test and perform Greenhouse-Geisser corrections where needed. For significant ANOVAs we explored which regions differed using post-hoc tests with Tukey contrasts performed on linear mixed effects models that controlled for egg identity using the nlme (Pinheiro *et al.* 2018) and multcomp (Hothorn *et al.* 2008) packages. Some Japanese murrelet eggshell fragments may have been from different eggs so a standard one-way ANOVA was performed instead of a repeated measures ANOVA for this species. Differences in pore density between species were analysed using a MANOVA followed by one-way ANOVAs with post-hoc Tukey tests and are presented in the Supplementary Materials.

We tested how pore density at each region of the egg related to egg shape, size and developmental mode, and how the total number of pores per egg related to egg size and incubation period, with phylogenetic linear regression models that control for phylogenetic relatedness using Pagel's lambda model (Ho & Ané 2014). We downloaded the extant Alcidae phylogenetic tree available from Weir and Mursleen (2013) and pruned it to leave only the species represented in our dataset. R^2 values for full models, including phylogenetic effects and partial R^2 values associated with individual predictors were calculated using the "R2.lik" function in the R package 'rr2' (Ives 2019). Two species (whiskered auklet *Aethia pygmaea* and Japanese murrelet *Synthliboramphus wumizisume*) were dropped from most analyses due to missing data (on egg size and shape). We used the species mean values in our analyses.

Results

Intraspecific patterns in common guillemot eggs

Across 10 common guillemot eggs for which pore density was measured along the entire eggshell, we found the blunt end contained the highest density of pores, approximately twice the density found elsewhere (Fig. 1; Repeated measures ANOVA on natural log transformed pore density; $F_{(5,45)} = 9.68$, $p = 0.0005$; Greenhouse-Geisser corrected p-value due to violation of sphericity assumption; Mauchly's test $p = 0.033$; $\varepsilon = 0.493$,

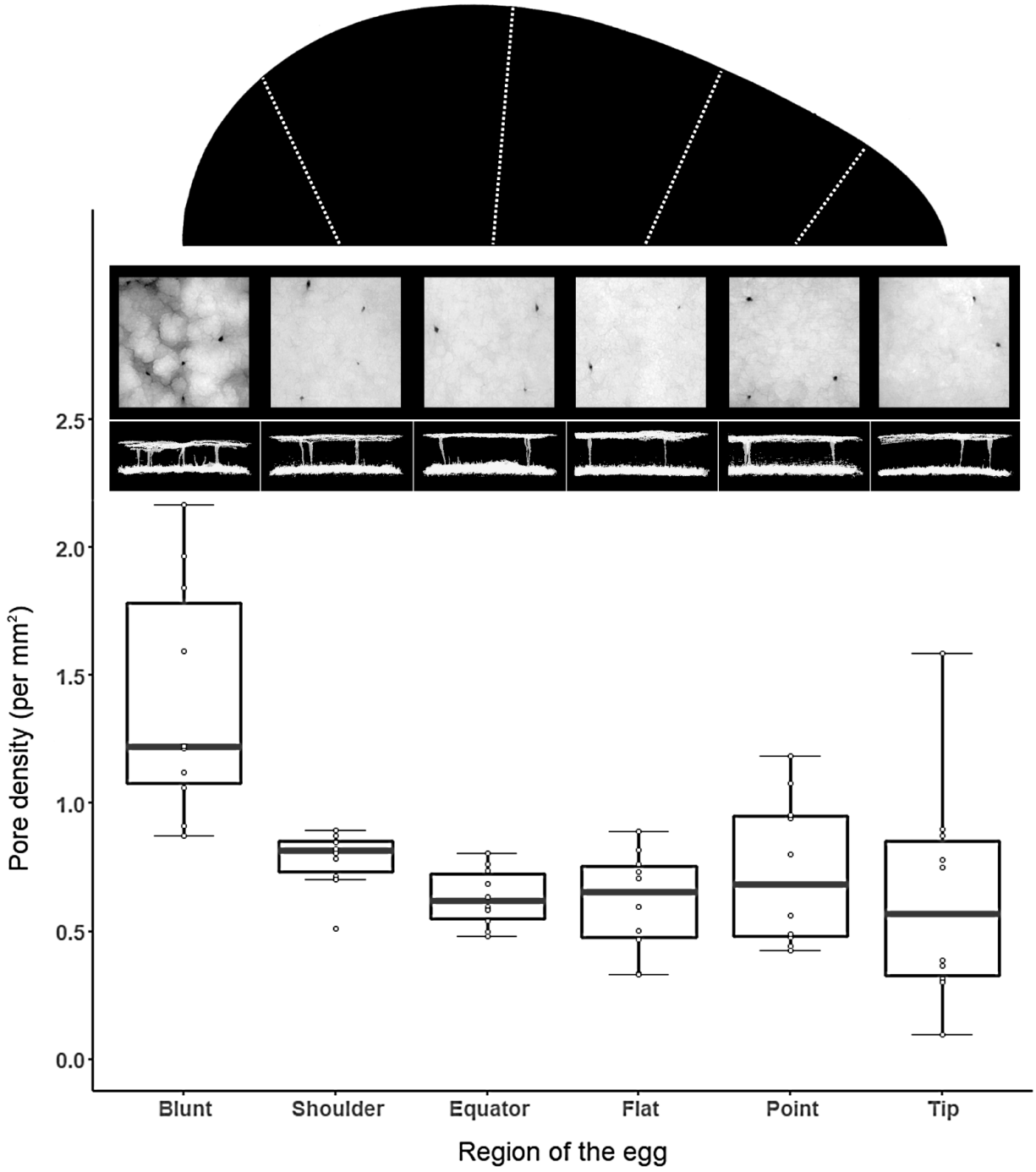

Figure 1. The distribution of pores along ten common guillemot eggs. Above the bars are 4mm^2 areas of eggshells (top – external surface view, below – cross section through the shell where the true shell is transparent to allow visualisation of pore channels through the shell) to demonstrate the difference in the density of pores along one of the eggs studied. The white dashed lines on the egg silhouette mark the approximate sampling locations for the shoulder, equator, flat and pointed regions of the egg

adjusted d.f. = 2.46, 23.18; post-hoc test with Tukey contrasts $p < 0.05$). There were no significant differences between the shoulder, equator, flat, pointed end and tip of the egg ($p > 0.05$). Across all guillemot eggs studied, the blunt end had the most pores (mean ± SD: 1.22 ± 0.369 per mm^2, range: 0.545 – 2.17) followed by the pointed end (mean: 0.751 ± 0.257 per mm^2, range: 0.162 – 1.67) and then the equator (mean: 0.595 ± 0.159 per mm^2, range: 0.216 – 1.07; Repeated measures ANOVA on Box-Cox transformed data; $F_{(2,108)} = 94.4$, $p < 0.0001$ all regions different, post-hoc test with Tukey contrasts $p < 0.05$).

Based on correlations across all common guillemot eggs (n = 55), pore density at all regions was largely independent of the egg shape and size (Table S1 & S2). There was a negative correlation between elongation at the blunt end and pore density at the pointed end across all guillemot eggs ($r_s = -0.281$, $p = 0.038$, n = 55), but this was not supported by our pairwise comparisons of eggs matched for size and most shape parameters (Table S1 – S3). Relatively elongate eggs were found to have fewer pores at the equator of their shell when controlling for egg size by pair-matching (mean difference = -0.102 pores per mm^2, $t = -7.00$, $p = 0.002$; Table S3), but there was no correlation between elongation and equatorial pore density across all 55 common guillemot eggs sampled (Table S1).

Pore density declined with increased shell thickness both across our sample of common guillemot eggshell fragments (n = 165; Fig. 2) and within individual eggs (repeated measures correlation performed on Box-Cox transformed pore density while controlling for egg identity: $r_{rm}(109) = -0.707$, 95% CI [-0.790, -0.598], $p < 0.0001$). Within individual regions, shell thickness was negatively correlated with pore density at the blunt end only ($r_s = -0.281$, $p = 0.038$, n = 55; Fig. 2). After controlling for differences across regions, between eggs there was a slight trend for thicker eggshells to contain fewer pores, but this was not significant (repeated measures correlation performed on Box-Cox transformed pore density controlling for regional variation: $r_{rm}(161) = -0.140$, 95% CI [-0.289, 0.015], $p = 0.074$).

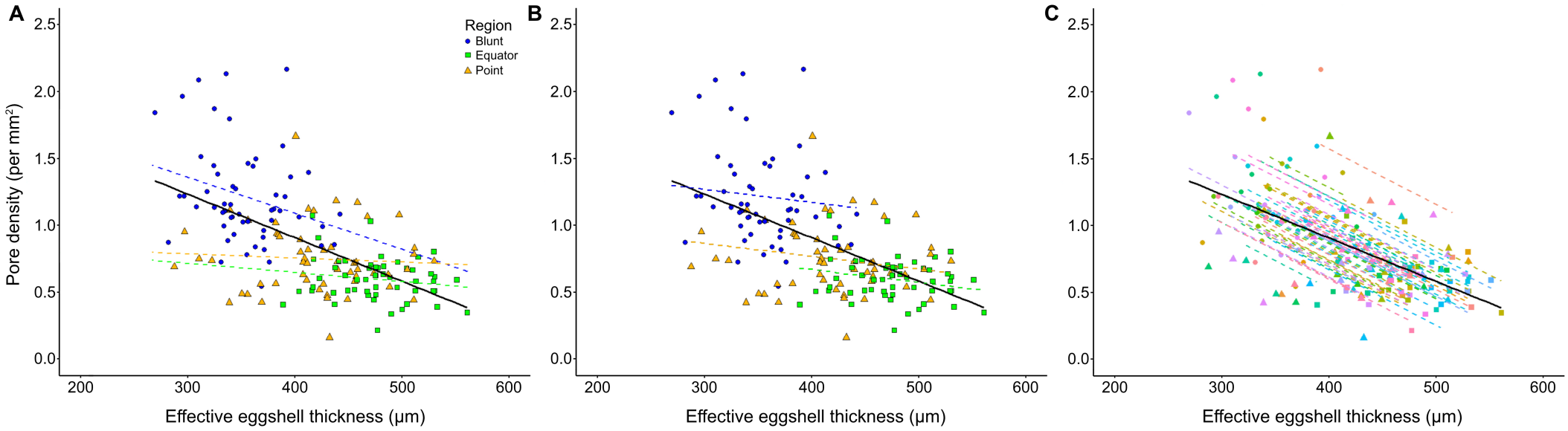

Figure 2. The relationship between eggshell thickness and pore density across 55 common guillemot eggs. The black line is the line of best fit for all fragments, whereas the coloured lines are the lines of best fit for a region (A & B) or an individual egg (C). All lines of best fit are for the raw, untransformed data. (A) Spearman's rank correlations for each shell region (blue is blunt: r_s = - 0.281, p = 0.038, n = 55, green is equator: r_s = - 0.116, p = 0.397, n = 55 and orange is point: r_s = - 0.069, p =0.617, n = 55) and the overall correlation between pore density and effective eggshell thickness (all fragments and all regions: r_s = - 0.593, p < 0.001, n = 165). (B) Repeated measures correlation controlling for egg region showing the correlation between effective eggshell thickness and pore density across eggs (three coloured lines). (C) Repeated measures correlation controlling for egg identity showing the correlation between effective eggshell thickness and pore density within eggs (multiple coloured lines).

Pore density distributions across the Alcids

Within eggs, only Brünnich's guillemot (*Uria Lomvia*) common guillemot, and razorbill eggs had a higher density of pores at the blunt end compared to the equator and pointed end (Table 1). Little auk (*Alle alle*) and ancient murrelet (*Synthliboramphus antiquus*) eggs had a lower density of pores at the blunt end compared to the equator and pointed end, black guillemot (*Cepphus grylle*) eggs had a lower density of pores at the pointed end compared to the blunt end and equator (Table 1), and none of the other species (n = 11) showed any significant differences in pore densities along the egg.

In models where either egg asymmetry or egg volume were included as a single explanatory variable alongside phylogeny, both factors were found to be significantly and positively associated with blunt end pore density (Fig. 3; Table S4). In a maximal model where both were included, egg asymmetry remained significantly related to pore density at the blunt end (lambda = 0.510; estimate = 8.16, t = 2.55, p = 0.025), but egg volume was not (estimate = 0.0008, t = 0.283, p = 0.782). At the equator and pointed end of the eggs, neither egg asymmetry, elongation or volume were significantly related to pore density (Table S4).

In a model including only developmental mode and phylogeny, species with an intermediate developmental mode (n = 3) had a higher density of pores at the blunt end of their eggs than semi- (n = 11; estimate = - 0.655, t = - 4.87, p = 0.0002) and fully precocial species (n = 3; estimate = - 0.484, t = - 4.52, p = 0.0004) after accounting for phylogeny (full model R^2 = 0.661, lambda < 0.001). There was no difference between fully and semi-precocial species (estimate = 0.171, t = 1.59, p = 0.133). When asymmetry and developmental mode were both included as explanatory variables in a phylogenetically controlled linear model with blunt end pore density, neither variable remained significant (lambda < 0.001, R^2 = 0.707; asymmetry intercept estimate = - 1.34, t = - 0.547, p = 0.595, slope estimate = 4.03, t = - 0.420, p = 0.334; intermediate vs fully precocial; estimate = - 0.420, t = - 1.26, p = 0.234; intermediate vs semi-precocial; estimate = - 0.314, t = - 1.53, p = 0.155; fully vs semi-precocial; estimate = 0.106, t = 0.588, p = 0.569). The AIC value for this complete model was higher (-2.94) than models that

Table 1. Regional pore density (mean ±SD, per mm^2) for the Alcidae

Species	Pore density per mm^2 at the			Pattern*	$F_{(d.f.)}$	p
	Blunt end	Equator	Pointed end			
Unequal pore distribution (significant ANOVA)						
Brünnich's guillemot	1.25 ± 0.25	0.48 ± 0.14	0.60 ± 0.27	**B > P = E**	$16.9_{(2,8)}$	0.001
Common guillemot	1.02 ± 0.099	0.55 ± 0.081	0.62 ± 0.34	**B > P = E**	$8.82_{(2,8)}$	0.009
Razorbill	1.14 ± 0.14	0.61 ± 0.18	0.61 ± 0.28	**B > E = P**	$9.33_{(2,8)}$	0.008
Ancient murrelet	0.38 ± 0.19	0.82 ± 0.16	0.81 ± 0.26	**E = P > B**	$7.09_{(2,8)}$	0.017
Little auk	0.58 ± 0.29	1.11 ± 0.12	1.01 ± 0.34	**E = P > B**	$6.04_{(2,8)}$	0.025
Black guillemot	1.12 ± 0.058	1.08 ± 0.25	0.56 ± 0.07	**B = E > P**	$17.4_{(2,8)}$	0.001
Equal pore distribution (Non-significant ANOVA)						
Atlantic puffin	0.69 ± 0.24	0.91 ± 0.42	0.69 ± 0.35	E = P = B	$0.83_{(2,8)}$	0.47
Cassin's auklet	0.53 ± 0.25	0.98 ± 0.26	0.74 ± 0.26	E = P = B	$3.31_{(2,8)}$	0.09
Crested auklet	0.49 ± 0.29	0.54 ± 0.30	0.72 ± 0.19	P = E = B	$0.46_{(2,4)}$	0.66
Horned puffin	0.50 ± 0.27	0.75 ± 0.37	0.97 ± 0.19	P = E = B	$2.23_{(2,6)}$	0.19
Japanese murrelet	0.64 ± 0.27	0.71 ± 0.39	0.79 ± 0.39	P = E = B	$0.23_{(2,12)}$	0.80
Least auklet	0.60 ± 0.20	0.71 ± 0.30	0.63 ± 0.15	E = P = B	$0.29_{(2,6)}$	0.76
Parakeet auklet	0.76 ± 0.62	1.04 ± 0.31	0.84 ± 0.28	E = P = B	$0.35_{(2,4)}$	0.73
Rhinoceros auklet	0.52 ± 0.28	0.96 ± 0.27	0.73 ± 0.24	E = P = B	$4.09_{(2,8)}$	0.06
Scripps' murrelet	0.46 ± 0.19	0.61 ± 0.14	0.42 ± 0.18	E = B = P	$1.46_{(2,8)}$	0.29
Tufted puffin	0.72 ± 0.15	0.71 ± 0.15	0.88 ± 0.14	P = B = E	$2.04_{(2,8)}$	0.19
Whiskered auklet	0.69 ± 0.16	0.68 ± 0.15	0.55 ± 0.026	B = E = P	$1.04_{(2,6)}$	0.41

*B = blunt end, E = equator and P = pointed end. Bold patterns indicate significant differences based on significant repeated measures ANOVA and post-hoc testing with Tukey contrasts (> or < indicates $p < 0.05$).

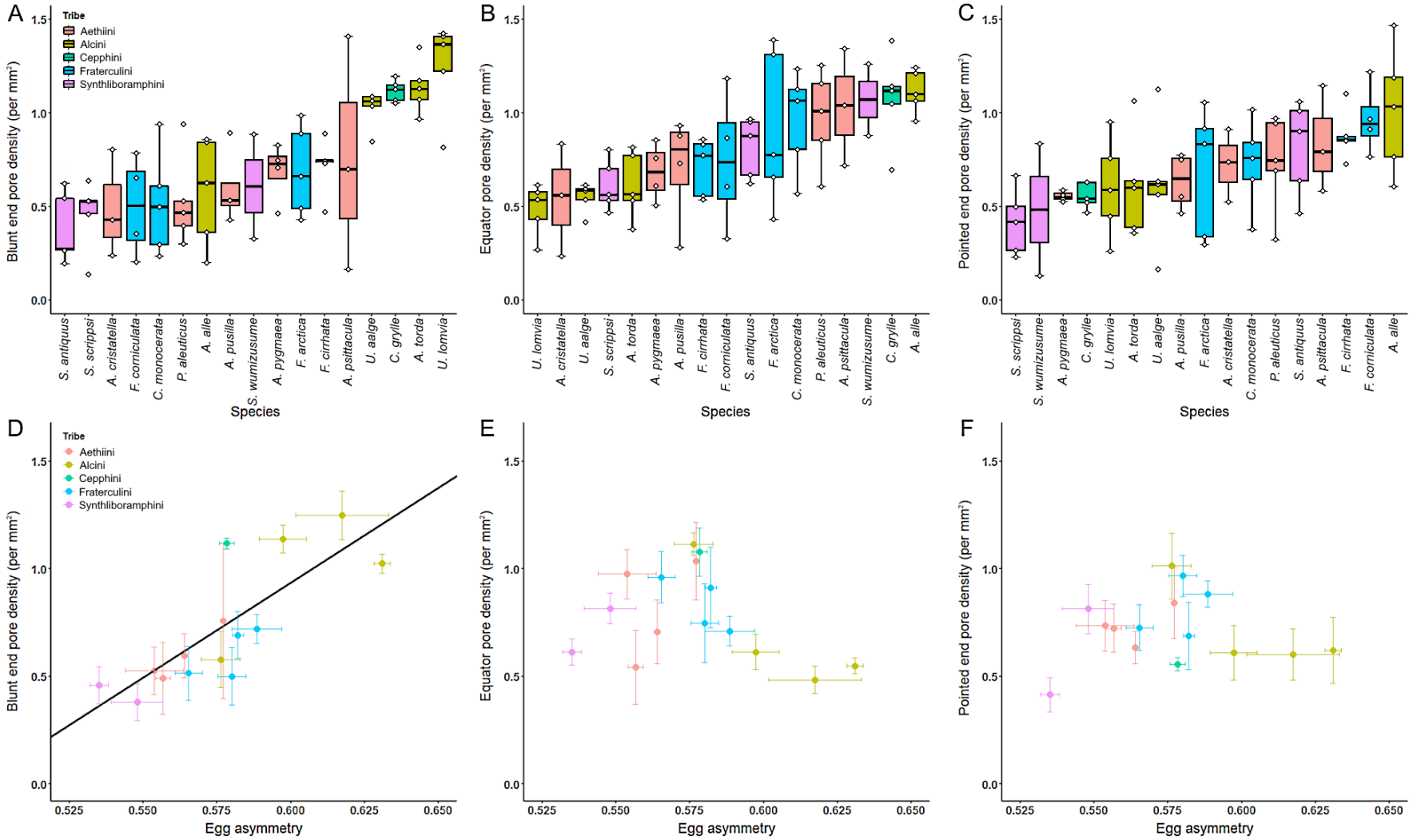

Figure 3. Species variation in pore density and the relationships between egg asymmetry and pore density. Species differences (top row; A-C, ranked from low to high values) can be found in the Supplementary Materials. (D) More asymmetric eggs have a higher density of pores at the blunt end of their shell than more symmetric eggs (pore density = 8.84*asymmetry - 4.37, lambda = 0.378, R^2 = 0.652, asymmetry partial R^2 = 0.604, phylogeny partial R^2 = 0.023). There is no relationship between asymmetry and pore density at the equator (E) or pointed end (F) see Table S4 for statistics. Means plotted with standard error bars on D – F.

included either egg asymmetry (-4.37) or developmental mode (-3.61), although not by more than 2 units, providing only weak evidence that the models including a single explanatory variable fit the data better than this maximal model.

Alcid species with an intermediate developmental mode had a lower density of pores at the equator compared to semi-precocial species after controlling for phylogeny (full model R^2 = 0.330, lambda < 0.001, estimate = - 0.312, t = - 2.61, p = 0.021). There was no difference between fully and semi-precocial species (estimate = 0.027, t = 0.225, p = 0.825), nor those with fully or intermediate developmental modes (estimate = - 0.285, t = - 1.90, p = 0.078). There were no significant differences in pore density at the pointed end of eggs in relation to developmental mode (lambda < 0.001; intermediate vs fully precocial; estimate = - 0.039, t = - 0.316, p = 0.757; intermediate vs semi-precocial; estimate = 0.146, t = 1.47, p = 0.165; fully vs semi-precocial; estimate = 0.185, t = 1.86, p = 0.084).

The total number of pores in an egg

We found that the region of particularly high pore density at the blunt end of common guillemot eggs represents only a relatively small proportion of the total surface area of the shell (Fig. 1). Since previous approaches to calculating total pore number are likely to overestimate the shell surface area for which blunt end pore densities are relevant (see Materials and Methods), they therefore lead to an (a) overestimate of total pore number in species with relatively higher pore densities at the blunt end (e.g. common guillemot), and (b) underestimate of total pore number in species with low pore densities at the blunt end (e.g. ancient murrelet; Fig. 4). If whole eggshells are not available and surface area values can only be approximated from egg length and breadth or values in the literature, we suggest using the following equation to limit inaccuracies caused by variation in pore density distributions across species:

((Blunt PD x 6[equator PD] x 1.5[pointed PD]) / 8.5) x SA

Where PD is pore density per mm^2 and SA is surface area in mm^2. This equation provides estimates that are approximately equivalent to our “realistic” approach (see Materials and Methods) of calculating total pore number directly from regional pore density measures

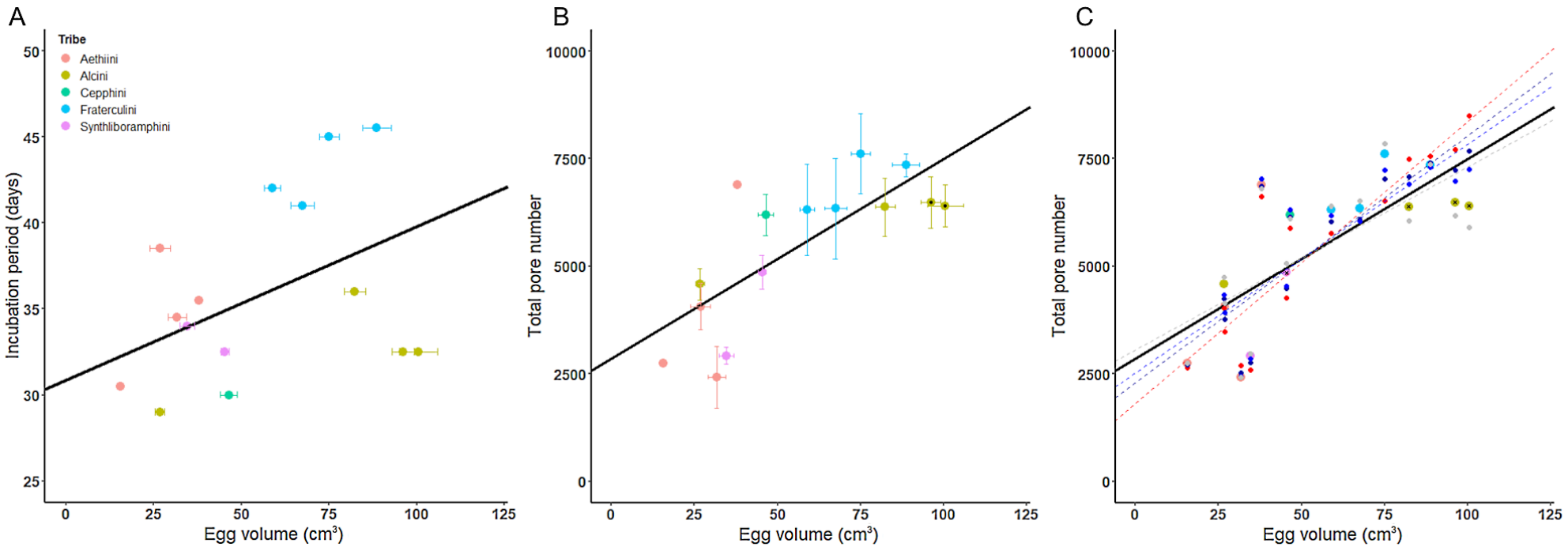

Figure 4. Relationships between egg volume and incubation period (A) or total pore number (B & C). (A) Incubation period = 0.089*egg volume + 30.9, t_{slope} = 2.23, $t_{intercept}$ = 10.8, p_{slope} = 0.044, $p_{intercept}$ < 0.0001; R^2 = 0.644; lambda = 1. (B) Egg volume and total pore number, means plotted with error bars (SE). Total pore number = 46.5*egg volume + 2852, t_{slope} = 4.09, $t_{intercept}$ = 4.07, $p_{slope\ \&\ intercept}$ = 0.001; R^2 = 0.564; lambda < 0.001. Note how the two *Uria sp.* fall below the regression line (green points with black dot) despite being among the largest eggs. (C) Species means and regression relationships for the different ways to estimate total pore number. Red, equal weight to pore density measures at each region. Dark blue, twice the weight to the equator pore density measures. Blue, moderate. Black, realistic. Grey, conservative. See Table S5 for statistics. Note how the traditional calculations (red and dark blue) potentially overestimate pore numbers for some species (e.g. *Uria sp.* and *Alca torda* – three green points marked with X) yet underestimate for others (e.g. *S. antiquus* – pink point marked with X).

and should therefore adequately predict total pore number regardless of whether pore distributions are equal or unequal (see Supplementary Materials for alternatives).

In the Alcidae, larger eggs are typically incubated for longer than small eggs (Fig. 4), but this relationship appears to be driven by phylogeny (lambda = 1, phylogeny partial R^2 = 0.582, volume partial R^2 = 0.227). Regardless of the calculation used to estimate the total number of pores in an egg, larger eggs had a greater total pore number than smaller eggs (Fig. 4; Table S5). Egg volume was significantly associated with total pore number regardless of the weighting used for calculating pore number (see Materials and Methods), but the amount of variation explained by egg volume differed between models from 48% (conservative total pore number prediction) to 81% (equal weighting to pore density at each region; Fig. 4; Table S5). After accounting for egg volume and phylogeny, incubation period was unrelated to total pore number across the Alcidae (realistic calculation: incubation period estimate = 80.5, t = 1.29, p = 0.222; see Table S6).

Discussion

Here we demonstrate that, contrary to a traditional assumption based on studies of chicken eggs and then propagated by Rokitka and Rahn (1987), high pore density at the blunt end of the shell is not a ubiquitous feature of bird eggs. We find unequal pore distributions in the eggs of 6 out of 17 Alcid species and only 3 of these exhibit a greater density of pores at the blunt end of their eggs. Our findings are more consistent with Tullett's (1975) suggestion that pore distributions vary between species, based on non-systematic observations of several unrelated species' eggshells. Here, using reliable microCT imaging techniques to accurately count pores (Riley *et al.* 2014; Willoughby *et al.* 2016; Birkhead *et al.* 2017; Jackson *et al.* 2018; Chapter 4), we demonstrate this to be true. Indeed, given that measured gas conductance values (probably driven by pore density; Rokitka & Rahn 1987; Booth 1989; Balkan *et al.* 2006; Jackson *et al.* 2018; Chapter 4) are often lower at the blunt end than at the equator or pointed end of many species' eggs (Portugal *et al.* 2014a), fewer pores at the blunt end (or approximately equal pore numbers across the egg) may be more prevalent across birds than high blunt end pore densities. Currently, it remains unclear why the distribution of pores varies along

the eggs of different species, and particularly why some species typically lay eggs that have a higher density of pores at the blunt end, but we discuss some possibilities below.

It has been suggested that high blunt end pore densities may be beneficial in eggs that are incubated in dirty environments (Birkhead *et al.* 2017). While two species of guillemot (*Uria sp.*) studied here possess higher blunt end pore densities and tend to incubate their eggs in dirty environments, razorbill eggs also have high blunt end pore densities, but they incubate their eggs in cleaner conditions (Birkhead 2016; Birkhead *et al.* 2017). Furthermore, burrow nesting puffins typically incubate their egg on damp soil – which could block gas exchange pores – yet their eggs do not possess a greater number of pores at the blunt end. We therefore find little convincing evidence that unequal pore distributions along an egg relate specifically to the risk of eggshell surface contamination by debris. *Uria sp*. also appear to have slightly lower total pore numbers than expected based on their egg volume (Fig. 4), so we find little support for the hypothesis that these guillemot species have higher than expected pore numbers to facilitate breeding on wet dirty cliff ledges (Belopol'skiĭ 1961). The presence of protective shell accessory material on common guillemot eggs is probably a more important adaptation to breeding in dirty environments (Jackson *et al.* 2018; Chapter 4).

We also find little evidence to support our hypothesis that high blunt end pore densities are associated with a precocial developmental mode. *Uria sp*. and razorbills have an intermediate development mode between semi- and fully precocial (Starck & Ricklefs 1998), and exhibit the highest pore densities at the blunt end of their eggs of all the auks, while *Synthliboramphus* murrelets are fully precocial, yet do not possess such a high blunt end pore density. Contrary to the hypothesis of Smart (1991), murrelet eggs are reasonably symmetrical and typically have lower pore density at the blunt end compared to the rest of the egg, or approximately equal pore distributions (Fig. 3; Table 1). In fact, even if a species lays asymmetric eggs, this shape typically results in lower relative surface area at the blunt end compared to the pointed end (Fig. S1), contrary to Smart's (1991) suggestion.

The lack of a link between high blunt end pore density and a precocial developmental mode is perhaps unsurprising considering how oxygen reaches the developing embryo.

Oxygen travels through the chorioallantoic membranes that interface with the eggshell membranes around the entire internal surface of the egg – not just at the blunt end via the air-cell (Rahn *et al.* 1979; Reizis *et al.* 2005; Maina 2017). An increase in the total amount of oxygen reaching the eggshell membranes would be more effectively achieved by increasing the total number of pores across the entire eggshell and not by only altering the pore distribution. Modifying the chorioallantoic membranes may also be important in facilitating increased oxygen consumption since they impose a large resistance to oxygen uptake (Rahn *et al.* 1979; Tazawa 1980; Wagner-Amos & Seymor 2002; Wagner-Amos & Seymor 2003; Reizis *et al.* 2005; Ar & Deeming 2009; Maina 2017).

Pore density constraints

Our findings suggest that in *Uria sp.* guillemot and razorbill eggs, pore density at the equator and pointed end is typically lower than what may be expected based on values for other Alcids (Fig. 3; Table 1; Appendix A4). Constraints on pore density due to, for example, regional variation in shell thickness, may be driving unequal pore distributions along these species' eggs.

Within common guillemot eggs, thicker regions of shell typically contain a lower density of pores than thin shells (Fig. 2). As pore formation is probably an imperfect process relying on fluid flowing through the shell to maintain gaps in the calcite crystal columns during shell growth, forming a thicker region of eggshell could increase the likelihood that calcite crystals fuse together, blocking pores and preventing these channels from traversing the entire shell (Tyler & Simkiss 1959; Tullett 1975; Tullett & Board 1977; Tyler & Fowler 1978; Board & Scott 1980; Tullett 1984). Alternatively, another aspect of shell formation may regulate both shell thickness and pore formation leading to thicker shells containing fewer pores (e.g. mammillary body or "cone" density; Tullett 1975; Tullett & Board 1977; Tyler & Fowler 1978). *Uria sp*. guillemot and razorbill eggs have thicker shells at the equatorial region compared to the blunt end, providing increased strength at the region of the egg in contact with the bird's brood patch and substrate during incubation (Birkhead *et al.* 2017; Chapter 2). Regional shell thickening in these species' eggs may limit the number of pores that form at the equator and to some extent, at the pointed end. As a consequence, the thinner-shelled blunt end may contain a higher density of pores to

compensate for lower pore densities along most of the eggshell, ensuring near optimal total pore numbers.

Evidence from other species, including the mute swan (*Cygnus olor;* Booth 1989), and peking duck (*Anas platyrhynchos domesticus*; Balkan *et al.* 2006; El-Hanoun & Mossad 2008) supports the idea that variation in eggshell thickness along an egg may constrain pore formation, because their eggshells have a relatively thick equator with fewer pores than the thinner shelled blunt end. However, not all species follow this pattern. The equator of ancient murrelet and little auk eggshells is thicker yet has more pores than at the thinner shelled blunt end. Shell thickness may not impose such a constraint on pore formation in little auk or ancient murrelet eggs as their overall shell thickness and regional differences are considerably lower than in *Uria sp*. or razorbill eggs (Chapter 2).

Although intraspecific comparisons of common guillemot eggs suggest that pore density is not primarily driven by egg shape or size, across the Alcids, more asymmetric eggs tend to have a higher pore density at the blunt end (Table S1). This interspecific relationship between egg shape and blunt end pore density is most likely driven by *Uria sp.* guillemots and razorbills that lay the most asymmetric eggs out of the Alcids (Fig. 3; Birkhead *et al.* 2019) with high blunt end pore densities for reasons potentially unrelated to egg shape. Importantly, when both developmental mode and egg asymmetry are included in a model with pore density, neither are significantly related to blunt end pore density, suggesting high blunt end pore densities are not really associated with either egg asymmetry or an intermediate developmental mode in the Alcids. However, it remains possible that egg shape drives some variation in pore distributions across bird species, perhaps due to how egg shape influences surface area at the blunt end (Fig. S1). It would be interesting to compare across taxa with modern techniques, such as microCT, to establish if unequal pore distributions occur in species that lay (a) symmetric or asymmetric eggs and/or (b) thick-shelled eggs with regional variation in shell thickness.

Egg size, incubation period and total pore number

Here, we find that the distribution of pores along some Alcid species' eggs is non-uniform, and that accounting for this variation in predictions of total pore number is important.

Using our new method for predicting total pore numbers from regional pore density measures, we find that total pore number in Alcid eggs is positively related to egg volume (Fig. 4). This contrasts the findings of Zimmerman and Hipfner (2007), who found no significant relationship between total pore number (predicted from regional pore density counts using the methods of Tyler (1965) and estimated eggshell surface area using Smart's (1991) formula) and egg size (mass). This difference is likely to be due to methodological differences. MicroCT is superior to older methods used to count pores (see Materials and Methods), and accordingly we find our pore density (and total pore number) measures to be consistently higher than values reported in Zimmerman and Hipfner (2007) (Table S7).

Our finding that total pore number increases with egg size is in agreement with patterns reported across other birds (Ar & Rahn 1985). In many pelagic seabirds and other birds, egg size and incubation period are related to total pore number and measured gas conductance, with species that have large eggs and/or relatively short incubation periods having greater pore numbers and thus higher rates of gas conductance (Rahn & Ar 1974; Rahn *et al.* 1976; Ar & Rahn 1980; Tullett 1984; Ar & Rahn 1985). Eggs that are incubated for prolonged time periods are usually less porous than expected for their size to maintain water balance by ensuring water is not lost too rapidly during incubation (Roudybush *et al.* 1980; Vleck & Kenagy 1980; Whittow 1980; Grant *et al.* 1982; Whittow *et al.* 1982; Ricklefs 1984; Tullett 1984; Ar & Rahn 1985; Rahn & Paganelli 1990). As incubation period and total eggshell pore number are unrelated across Alcids, it is unclear whether this requirement is essential in all species with prolonged incubation periods.

There are several reasons why we may not see a relationship between incubation period and total pore number in the Alcids. First, total pore number may be lower than expected in some species due to constraints on pore density (Fig. 4). Second, other elements of eggshell structure may also regulate water loss from eggs (e.g. shell accessory materials; Deeming 1987; D'Alba *et al.* 2017 or pore area; Grant *et al.* 1982 but see Jackson *et al.* 2018; Chapter 4). Third, the humidity of the air surrounding the egg(s) varies due to nest type and location, and total pore number may vary accordingly, masking differences attributable to incubation period (Vleck *et al.* 1983; Deeming 2011; Portugal *et al.* 2014a).

Fourth, water loss from an egg may be regulated by parental behaviours (e.g. altering egg temperature or providing ventilation; Rahn *et al.* 1976; Grant *et al.* 1982; Rahn 1991). Fifth, rates of water vapour conductance may increase over incubation due to embryonic heat production and potentially due to changes in the shell's structure (Booth & Seymour 1987; Booth 1989; Booth & Rahn 1990; Thompson & Goldie 1990; Packard 1994; Baggot *et al.* 2003; Balkan *et al.* 2006). Finally, water balance may be regulated by the embryo instead of by the shell (Simkiss 1980a, b; Carey 1986).

Zimmerman and Hipfner (2007) suggested that eggshell gas conductance drives variation in incubation period in the Alcids, based on calculated porosity across 7 species (see also Hipfner *et al.* 2010). However, given that (1) incubation period and total pore number is unrelated across 15 Alcids studied here, (2) total pore number is likely a better predictor of gas conductance than calculated porosity (Jackson *et al.* 2018; Chapter 4), and (3) many studies have found no evidence that increased eggshell porosity or conductance relates to quicker embryo development rates (i.e. shorter incubation periods) in other bird species (Boersma & Rebstock 2009; Portugal *et al.* 2014b; Bowers *et al.* 2015; McClelland *et al.* 2019; but see Massaro & Davis 2004; Massaro & Davis 2005; Clark *et al.* 2010), it seems probable that incubation period is not normally driven by increased oxygen concentrations supplied by high eggshell pore numbers. Oxygen may not even be a limiting factor in birds with prolonged incubation periods, since these species typically have low metabolic rates, with oxygen consumption only peaking in the latter stages of development when behavioural adaptations, such as pipping several days before hatch, can satisfy the chick's oxygen requirements (Ackerman *et al.* 1980; Vleck & Kenagy 1980; Whittow 1980; Tullett 1984; Rahn & Paganelli 1990; Vleck & Vleck 1996). Indeed, any adaptive modification of eggshell porosity is likely in response to incubation period, rather than a driver of incubation duration (Ricklefs 1984).

As both egg size and total pore number do not drive incubation duration across the Alcids (Fig. 4), we suggest that egg temperature – due to behavioural, morphological and physiological parental traits, including egg neglect and attentiveness (Vleck & Kenagy 1980; Boersma 1982; Astheimer 1991; Martin 2002; Martin *et al.* 2007; Zimmerman & Hipfner 2007) – may be a crucial factor driving incubation period in this family.

Conclusion

Here we show that pore distributions vary considerably across bird eggs, and contrary to previous assumption, high blunt end porosity is not necessarily the rule. Although the precise reason(s) for variable pore density distributions remains unclear, we provide evidence that regional increases in eggshell thickness may limit pore density in the equatorial and/or pointed regions of the egg. We suggest that, in some species, this possibly leads to increased pore density at the thinner blunt end, a compensatory mechanism which ensures the total number of eggshell pores remains optimal for water loss and respiratory gas exchange over the entirety of incubation.

Acknowledgements

We thank all the researchers, their field crews and research assistants who supplied eggshells or helped with the process of getting them imported into the UK including Nora Rojek, Mark Hipfner, Aevar Peterson, Mark Harris, Hallvard Strøm, Akiko Shoji, Kuniko Otsuki, Andrew Power, Ian O'Connor, David Mazurkiewicz, Linnea Hall and René Corado. Jamie Thompson for collecting and imaging the common guillemot egg samples from Skomer Island to obtain data on their shape and size, and Marie Attard and Jamie Thompson for helpful discussions over the course of this study. The Wildlife Trust of South and West Wales Trust for permission to work on Skomer Island NNR, and the Natural Resources Wales (NRW) for licences to take eggs for scientific purposes. We also thank the Skelet.AL lab for use of their microCT scanner.

Competing interests

No competing interests declared.

Author contributions

The study was conceived by D.J., T.R.B. and N.H. D.J. collected and analysed the data. D.J. wrote the initial draft; N.H. and T.R.B. commented on the initial draft and revised the manuscript.

Funding

The study was funded by a grant from the Leverhulme Trust (to T.R.B.) and a University of Sheffield Scholarship (to D.J.). N.H. was supported by a Patrick & Irwin-Packington Fellowship from the University of Sheffield and a Royal Society Dorothy Hodgkin Fellowship.

Supplementary information

Supplementary information available in Appendix A4.

References

Ackerman, R. A., Whittow, G. C., Paganelli, C. V. and Pettit, T. N., (1980). Oxygen consumption, gas exchange, and growth of embryonic wedge-tailed shearwaters (*Puffinus pacificus chlororhynchus*). *Physiological Zoology*. **53**(2), 210-221.

Ar, A., (1991). Roles of water in avian eggs. In: *Egg Incubation: Its effect on embryonic development in birds and reptiles* (eds. Deeming, D. C. and Ferguson, M. W. J.). Cambridge, UK: Cambridge University Press. pp. 229- 244.

Ar, A. and Deeming, D. C., (2009). Roles of water and gas exchange in determining hatchability success. *Avian Biology Research*. **2**(1/2), 61–66.

Ar, A., Paganelli, C. V., Reeves, R. B., Greene, D. G. and Rahn, H., (1974). The Avian Egg: Water Vapor Conductance, Shell Thickness, and Functional Pore Area. *The Condor*. **76**(2), 153–158.

Ar, A. and Rahn, H., (1980). Water in the avian egg overall budget of incubation. *American Zoologist.* **20**(2), 373-384.

Ar, A. and Rahn, H., (1985). Pores in avian eggshells: Gas conductance, gas exchange and embryonic growth rate. *Respiration Physiology.* **61**(1), 1–20.

Arad, Z., Gavrieli-Levin, I. and Marder, J., (1988). Adaptation of the pigeon egg to incubation in dry hot environments. *Physiological Zoology.* **61**(4), 293-300.

Astheimer, L. B., (1991). Embryo metabolism and egg neglect in Cassin's Auklets. *The Condor.* **93**(3), 486-495.

Baggott, G. K., Deeming, D. C., Hémon, S. and Paillat, P., (2003). Relationships between eggshell pigmentation, ultrastructure and water vapour conductance in the Houbara bustard (*Chlamydotis undulata macqueenii*). In: *Proceedings of the World Association of Wildlife Veterinarians Wildlife Sessions at the 27th World Veterinary Congress, Tunisia, 26th September 2002* (eds. Scullion, F. T. and Bailey, T. A.). Northern Ireland: World Association of Wildlife Veterinarians. pp. 85 – 88.

Bakdash, J. Z. and Marusich, L. R., (2017). Repeated measures correlation. *Frontiers in psychology*. **8**, 456.

Balkan, M., Karakaş, R. and Biricik, M., (2006). Changes in eggshell thickness, shell conductance and pore density during incubation in the Peking Duck (*Anas platyrhynchos f. dom.*). *Ornis Fennica.* **83**(3), 117.

Belopol'skiĭ, L. O., (1957, translated from Russian 1961). *ecology of sea colony birds of the barents sea*. Jerusalem: Israel Program for Scientific Translations.

Birkhead, T. R., (2016). *The Most Perfect Thing: the Inside (and Outside) of a Bird's Egg.* London, UK: Bloomsbury.

Birkhead, T. R., Thompson, J. E., Biggins, J. D. and Montgomerie, R., (2019). The evolution of egg shape in birds: selection during the incubation period. *Ibis*. **161**(3), 605-618.

Birkhead, T. R., Thompson, J. E., Jackson, D. and Biggins, J. D., (2017). The point of a Guillemot's egg. *Ibis.* **159**(2), 255-265.

Board, R. G., (1982). Properties of avian egg shells and their adaptive value. *Biological Reviews.* **57**(1), 1–28.

Board, R. G. and Scott, V. D., (1980). Porosity of the avian eggshell. *American Zoologist.* **20**(2), 339-349.

Boersma, P. D., (1982). Why some birds take so long to hatch. *The American Naturalist.* **120**(6), 733-750.

Boersma, P. D. and Rebstock, G. A., (2009). Magellanic Penguin eggshell pores: does number matter? *Ibis.* **151**(3), 535-540.

Booth, D. T. and Seymour, R. S., (1987). Effect of eggshell thinning on water vapor conductance of Malleefowl eggs. *The Condor.* **89**(3), 453-459.

Booth, D. T., (1989). Regional changes in shell thickness, shell conductance, and pore structure during incubation in eggs of the Mute Swan. *Physiological Zoology.* **62**(2), 607-620.

Booth, D. T. and Rahn, H., (1990). Factors modifying rate of water loss from birds' eggs during incubation. *Physiological Zoology*. **63**(4), 697-709.

Bowers, E. K., White, A., Lang, A., Podgorski, L., Thompson, C. F., Sakaluk, S. K., Jaeckle, W. B. and Harper, R. G., (2015). Eggshell porosity covaries with egg size among female House Wrens (*Troglodytes aedon*), but is unrelated to incubation onset and egg-laying order within clutches. *Canadian Journal of Zoology*. **93**(6), 421-425.

Carey, C., (1980). Adaptation of the avian egg to high altitude. *American Zoologist*. **20**(2), 449-459.

Carey, C., (1986). Tolerance of variation in eggshell conductance, water loss, and water content by red-winged blackbird embryos. *Physiological Zoology*. **59**(1), 109-122.

Carey, C., Leon-Velarde, F., Castro, G. and Monge, C., (1987). Shell conductance, daily water loss and water content of Andean Gull and Puna Ibis eggs. *The Journal of Experimental Zoology. Supplement*. **1**, 247-252.

Carey, C., Leon-Velarde, F. and Monge, C., (1990). Eggshell conductance and other physical characteristics of avian eggs laid in the Peruvian Andes. *The Condor.* **92**(3), 790-793.

Clark., M. E., Boonstra, T. A., Reed, W. L. and Gastecki, M. L., (2010). Intraclutch Variation in Egg Conductance Facilitates Hatching Synchrony of Canada Geese. *The Condor*. **122**(3), 447-454.

D'Alba, L., Torres, R., Waterhouse, G. I. N., Eliason, C., Hauber, M. E. and Shawkey, M. D., (2017). What Does the Eggshell Cuticle Do? A Functional Comparison of Avian Eggshell Cuticles. *Physiological and Biochemical Zoology.* **90**(5), 588-599.

Davis, T. A. and Ackerman, R. A., (1985). Adaptations of black tern (*Chlidonias niger*) eggs for water loss in a moist nest. *The Auk.* **102**(3), 640-643.

Davis, T. A., Platter-Reiger, M. F. and Ackerman, R. A., (1984). Incubation water loss by pied-billed grebe eggs: adaptation to a hot, wet nest. *Physiological Zoology*. **57**(4), 384-391.

del Hoyo, J., Elliott, A., Sargatal, J., Christie, D. A. and Kirwan, G., (eds.) (2019). *Handbook of the Birds of the World Alive*. Barcelona, Spain: Lynx Edicions. (retrieved from http://www.hbw.com/ on [29/1/2019])

Deeming, D. C., (1987). Effect of cuticle removal on the water vapour conductance of egg shells of several species of domestic bird. *British Poultry Science*. **28**(2), 231-237.

Deeming, D. C., (2011). Importance of nest type on the regulation of humidity in bird nests. *Avian Biology Research.* **4**(1), 23-31.

El-Hanoun, A. M. and Mossad, N. A., (2008). Hatchability improvement of Peking duck eggs by controlling water evaporation rate from the egg shell. *Egyptian Poultry Science.* **28**, 767-784.

Gaston, A. J. and Jones, I. L., (1998). *Bird Families of the World series: The Auks.* Oxford, UK: Oxford University Press.

Grant, G. S., Pettit, T. N., Rahn, H., Whittow, G. C. and Paganelli, C. V., (1982). Water loss from Laysan and Black-footed Albatross eggs. *Physiological Zoology.* **55**(4), 405-414.

Guerra, C. G., Aguilar, R. E. and Fitzpatrick, L. C., (1988). Water vapor conductance in gray gulls (*Larus modestus*) eggs: adaptation to desert nesting. *Colonial Waterbirds.* **11**(1), 107-109.

Hipfner, J. M., Gorman, K. B., Vos, R. A. and Joy, J. B., (2010). Evolution of embryonic developmental period in the marine bird families Alcidae and Spheniscidae: roles for nutrition and predation? *BMC Evolutionary Biology*. **10**, 179.

Ho, L. S. T. and Ané, C., (2014). A Linear-Time Algorithm for Gaussian and Non-Gaussian Trait Evolution Models. *Systematic Biology.* **63**(3), 397-408.

Hothorn, T., Bretz, F. and Westfall, P., (2008). Simultaneous Inference in General Parametric Models. *Biometrical Journal.* **50**(3), 346-363.

Hoyt, D. F., Board, R. G., Rahn, H. and Paganelli, C. V., (1979). The eggs of the Anatidae: conductance, pore structure, and metabolism. *Physiological Zoology.* **52**(4), 438-450.

Ives, A. R., (2019). R^2s for correlated data: phylogenetic models, LMMs, and GLMMs. *Systematic Biology.* **68**(2), 234-251.

Jackson, D., Thompson, J. E., Hemmings, N. and Birkhead, T. R., (2018). Common guillemot (*Uria aalge*) eggs are not self-cleaning. *The Journal of Experimental Biology*. **221**(23), jeb188466.

Kern, M. D., Cowie, R. J. and Yeager, M., (1992). Water loss, conductance, and structure of eggs of pied flycatchers during egg laying and incubation. *Physiological Zoology.* **65**(6), 1162-1187.

Lawrence, M. A., (2016). ez: Easy Analysis and Visualization of Factorial Experiments. R package version 4.4-0. https://CRAN.R-project.org/package=ez

Maina, J. N., (2017). Structure and Function of the Shell and the Chorioallantoic Membrane of the Avian Egg: Embryonic Respiration. In: *The Biology of the Avian Respiratory System* (eds. Maina, J.). Springer, Cham. pp. 219-247.

Martin, T. E., (2002). A new view of avian life-history evolution tested on an incubation paradox. *Proceedings of the Royal Society of London. Series B: Biological Sciences.* **269**(1488), 309-316.

Martin, T. E., Auer, S. K., Bassar, R. D., Niklison, A. M. and Lloyd, P., (2007). Geographic variation in avian incubation periods and parental influences on embryonic temperature. *Evolution: International Journal of Organic Evolution.* **61**(11), 2558-2569.

Massaro, M. and Davis, L. S., (2004). The influence of laying date and maternal age on eggshell thickness and pore density in yellow-eyed penguins. *The Condor*. **106**(3), 496-505.

Massaro, M. and Davis, L. S., (2005). Differences in egg size, shell thickness, pore density, pore diameter and water vapour conductance between first and second eggs of Snares Penguins Eudyptes robustus and their influence on hatching asynchrony. *Ibis.* **147**(2), 251-258.

Maurer, G., Portugal, S. J. and Cassey, P., (2012). A comparison of indices and measured values of eggshell thickness of different shell regions using museum eggs of 230 European bird species. *Ibis.* **154**(4), 714–724.

McClelland, S. C., Jamie, G. A., Waters, K., Caldas, L., Spottiswoode, C. N. and Portugal, S. J., (2019). Convergent evolution of reduced eggshell conductance in avian brood parasites. *Philosophical Transactions of the Royal Society B: Biological Sciences*. **374**(1769), 20180194.

Monge, C. C., Ostojic, H., Aguilar, R. and Cifuentes, V., (2000). Reduced oxygen diffusion across the shell of Gray gull (*Larus modestus*) eggs. *Biological research.* **33**(3–4), 209–214.

Packard, M. J., (1994). Mobilization of shell calcium by the chick chorioallantoic membrane in vitro. *The Journal of Experimental Biology.* **190**, 141–153.

Packard, G. C., Sotherland, P. R. and Packard, M. J., (1977). Adaptive reduction in permeability of avian eggshells to water vapour at high altitudes. *Nature.* **266**, 255-256.

Pinheiro, J., Bates, D., DebRoy, S., Sarkar, D., R Core Team, (2018). nlme: Linear and Nonlinear Mixed Effects Models. R package version 3.1-137, https://CRAN.R-project.org/package=nlme

Portugal, S. J., Hauber, M. E., Maurer, G., Stokke, B. G., Grim, T. and Cassey, P., (2014b). Rapid development of brood-parasitic cuckoo embryos cannot be explained by increased gas exchange through the eggshell. *Journal of Zoology.* **293**(4), 219-226.

Portugal, S. J., Maurer, G., Thomas, G. H., Hauber, M. E., Grim, T. and Cassey, P., (2014a). Nesting behaviour influences species-specific gas exchange across avian eggshells. *The Journal of Experimental Biology.* **217**(18), 3326–3332.

R Core Team, (2018). R: A language and environment for statistical computing. R Foundation for Statistical Computing, Vienna, Austria. https://www.R-project.org/

Rahn, H., (1991). Why birds lay eggs. In: *Egg Incubation: Its effect on embryonic development in birds and reptiles* (eds. Deeming, D. C. and Ferguson, M. W. J.). Cambridge, UK: Cambridge University Press. pp. 345-360.

Rahn, H. and Ar, A., (1974). The avian egg: incubation time and water loss. *The Condor.* **76**(2), 147-152.

Rahn, H., Ar, A. and Paganelli, C. V., (1979). How bird eggs breathe. *Scientific American.* **240**(2), 46-55.

Rahn, H., Carey, C., Balmas, K., Bhatia, B. and Paganelli, C., (1977). Reduction of pore area of the avian eggshell as an adaptation to altitude. *Proceedings of the National Academy of Sciences.* **74**(7), 3095-3098.

Rahn, H., Ledoux, T., Paganelli, C. V. and Smith, A. H., (1982). Changes in eggshell conductance after transfer of hens from an altitude of 3,800 to 1,200m. *Journal of Applied Physiology*. **53**(6), 1429-1431.

Rahn, H., Paganelli, C. V. and Ar, A., (1974). The avian egg: air-cell gas tension, metabolism and incubation time. *Respiration physiology*. **22**(3), 297-309.

Rahn, H., Paganelli, C. V., Nisbet, I. C. T. and Whittow, G. C., (1976). Regulation of Incubation Water Loss in Eggs of Seven Species of Terns. *Physiological Zoology*. **49**(2), 245-259.

Rahn, H. and Paganelli, C. V., (1990). Gas fluxes in avian eggs: Driving forces and the pathway for exchange. *Comparative Biochemistry and Physiology Part A: Physiology*. **95**(1), 1-15.

Reizis, A., Hammel, I. and Ar, A., (2005). Regional and developmental variations of blood vessel morphometry in the chick embryo chorioallantoic membrane. *The Journal of Experimental Biology.* **208**(13), 2483–2488.

Ricklefs, R. E., (1984). Prolonged incubation in pelagic seabirds: a comment on Boersma's paper. *The American Naturalist.* **123**(5), 710-720.

Riley, A., Sturrock, C. J., Mooney, S. J. and Luck, M. R., (2014). Quantification of eggshell microstructure using X-ray micro computed tomography. *British poultry science.* **55**(3), 311–320.

Rokitka, M. A. and Rahn, H., (1987). Regional differences in shell conductance and pore density of avian eggs. *Respiration Physiology.* **68**(3), 371–376.

Romanoff, A. L. and Romanoff, A. J., (1949). *The Avian Egg*. New York, USA: Wiley.

Roudybush, T., Hoffman, L. and Rahn, H., (1980). Conductance, pore geometry, and water loss of eggs of Cassin's Auklet. *The Condor.* **82**(1), 105-106.

Schneider, C. A., Rasband, W. S. and Eliceiri, K. W., (2012). NIH Image to ImageJ: 25 years of image analysis. *Nature Methods.* **9**, 671-675.

Simkiss, K., (1980a). Eggshell porosity and the water metabolism of the chick embryo. *Journal of Zoology.* **192**(1), 1-8.

Simkiss, K., (1980b). Water and ionic fluxes inside the egg. *American Zoologist*. **20**(2), 385-393.

Smart, I., (1991). Egg shape in birds. In: *Egg Incubation: Its effect on embryonic development in birds and reptiles* (eds. Deeming, D. C. and Ferguson, M. W. J.). Cambridge, UK: Cambridge University Press. pp. 101–116.

Sotherland, P. R., Packard, G. C., Taigen, T. L. and Boardman, T. J., (1980). An altitudinal cline in conductance of cliff swallow (*Petrochelidon pyrrhonota*) eggs to water vapor. *The Auk.* **97**(1), 177-185.

Starck, J. M. and Ricklefs, R. E., (1998). Patterns of development: the altricial–precocial spectrum. In: *Avian Growth and Development* (eds. Starck, J. M. and Ricklefs, R. E.). Oxford, UK: Oxford University Press. pp. 3–30.

Stein, L. R. and Badyaev, A. V., (2011). Evolution of eggshell structure during rapid range expansion in a passerine bird. *Functional ecology*. **25**(6), 1215-1222.

Tazawa, H., (1980). Oxygen and CO2 exchange and acid-base regulation in the avian embryo. *American Zoologist.* **20**(2), 395-404.

Thompson, M. B. and Goldie, K. N., (1990). Conductance and Structure of Eggs of Adelie Penguins, *Pygoscelis adeliae*, and Its Implications for Incubation. *The Condor*. **92**(2), 304–312.

Tullett, S. G., (1975). Regulation of avian eggshell porosity. *Journal of Zoology.* **177**(3), 339–348.

Tullett, S. G., (1984). The porosity of avian eggshells. *Comparative Biochemistry and Physiology Part A: Physiology.* **78**(1), 5-13.

Tullett, S. G. and Board, R. G., (1977). Determinants of avian eggshell porosity. *Journal of Zoology.* **183**(2), 203-211.

Tyler, C., (1965). A study of the egg shells of the Sphenisciformes. *Proceedings of the Zoological Society of London.* **147**(1), 1-19.

Tyler, C., (1969). Avian Egg Shells: Their Structure and Characteristics. *International Review of General and Experimental Zoology.* **4**, 81-130.

Tyler, C. and Fowler, S., (1978). The distribution of organic cores, cones, cone junctions and pores in the egg shells of wild birds. *Journal of Zoology.* **186**(1), 1-14.

Tyler, C. and Simkiss, K., (1959). A study of the egg shells of ratite birds. *Proceedings of the Zoological Society of London*. **133**(2), 201-243.

Vleck, C. M. and Kenagy, G. J., (1980). Embryonic metabolism of the fork-tailed storm petrel: physiological patterns during prolonged and interrupted incubation. *Physiological Zoology*. **53**(1), 32-42.

Vleck, C. M. and Vleck, D., (1996). Embryonic energetics. In: *Avian energetics and nutritional ecology* (eds. Carey, C.). Boston, USA: Springer. pp. 417-454.

Vleck, C. M., Vleck, D., Rahn, H. and Paganelli, C. V., (1983). Nest microclimate, water-vapor conductance, and water loss in heron and tern eggs. *The Auk*. **100**(1), 76-83.

Wagner-Amos, K. and Seymour, R. S., (2002). Effect of regional changes to shell conductance on oxygen consumption and growth of chicken embryos. *Respiration Physiology.* **129**(3), 385-395.

Wagner-Amos, K. and Seymour, R. S., (2003). Effect of local shell conductance on the vascularisation of the chicken chorioallantoic membrane. *Respiratory Physiology & Neurobiology*. **134**(2), 155-167.

Weir, J. T. and Mursleen, S., (2013). Diversity-dependent cladogenesis and trait evolution in the adaptive radiation of the auks (Aves: Alcidae). *Evolution*. **67**(2), 403-416.

Willoughby, B., Steyn, L., Bam, L., Olivier, A. J., Devey, R. and Maina, J. N., (2016). Micro-Focus X-Ray Tomography Study of the Microstructure and Morphometry of the Eggshell of Ostriches (*Struthio Camerus*). *The Anatomical Record.* **299**(8), 1015-1026.

Whittow, G. C., (1980). Physiological and ecological correlates of prolonged incubation in sea birds. *American Zoologist*. **20**(2), 427-436.

Whittow, G. C., Ackerman, R. A., Paganelli, C. V. and Pettit, T. N., (1982). Pre-pipping water loss from the eggs of the Wedge-tailed Shearwater. *Comparative Biochemistry and Physiology Part A: Physiology*. **72**(1), 29-34.

Xu, D., Cui, J., Bansal, R., Hao, X., Liu, J., Chen, W. and Peterson, B. S., (2009). The ellipsoidal area ratio: an alternative anisotropy index for diffusion tensor imaging. *Magnetic Resonance Imaging*. **27**(3), 311-323.

Zimmermann, K. and Hipfner, J. M., (2007). Egg size, Eggshell Porosity, and Incubation Period in the Marine Bird Family Alcidae. *The Auk.* **124**(1), 307-315.

Chapter 4:

Common guillemot (*Uria aalge*) eggs are not self-cleaning

Common guillemot (*Uria aalge*) eggs are not self-cleaning

Duncan Jackson[1*], Jamie E. Thompson[1], Nicola Hemmings[1], Timothy R. Birkhead[1]

[1]*Department of Animal & Plant Sciences, University of Sheffield, Sheffield, S10 2TN, UK*

*Corresponding author
Email: djackson3@sheffield.ac.uk

Published in The Journal of Experimental Biology.

Article first posted online on the 15 October 2018. Access the most recent version at:

http://jeb.biologists.org/lookup/doi/10.1242/jeb.188466

Movies 1-3 referenced in this chapter can be viewed in the online published version of this manuscript at the above URL.

Key words

Common murre, Faeces, Eggshell, Gas conductance, Incubation, Embryo development

Abstract

Birds are arguably the most evolutionarily successful extant vertebrate taxon, in part because of their ability to reproduce in virtually all terrestrial habitats. Common guillemots (*Uria aalge*) incubate their single egg in an unusual and harsh environment; on exposed cliff ledges, without a nest, and in close proximity to conspecifics. As a consequence, the surface of guillemot eggshells is frequently contaminated with faeces, dirt, water and other detritus, which may impede gas exchange or facilitate microbial infection of the developing embryo. Despite this, guillemot chicks survive incubation and hatch from eggs heavily covered with debris. To establish how guillemot eggs cope with external debris, we tested three hypotheses: (1) contamination by debris does not reduce gas exchange efficacy of the eggshell to a degree that may impede normal embryo development; (2) the guillemot eggshell surface is self-cleaning; and, (3) shell accessory material (SAM) prevents debris from blocking pores, allowing relatively unrestricted gas diffusion across the eggshell. We showed that natural debris reduces the conductance of gases across the guillemot eggshell by blocking gas exchange pores. Despite this problem, we found no evidence that guillemot eggshells are self-cleaning, but instead showed that the presence of SAM on the eggshell surface largely prevents pore blockages from occurring. Our results demonstrate that SAM is a crucial feature of the eggshell surface in a species with eggs that are frequently in contact with debris, acting to minimise pore blockages and thus ensure a sufficient rate of gas diffusion for embryo development.

Introduction

Birds breed in virtually all terrestrial habitats, from deserts to polar regions, and even in wet environments (Deeming 2002). This flexibility in breeding ecology (specifically, in habitat use) can be attributed to the fact that birds lay hard-shelled, desiccation-resistant eggs in a nest (or other incubation site) that is generally attended by one or both parents (Deeming 2002). A consequence of laying eggs into a nest, which is then attended by a parent, is that the microclimate eggs are incubated in, and the conditions the avian embryo experiences during development, are largely independent of the wider environment (Rahn *et al.* 1983; Ar 1991; Rahn 1991; Deeming & Mainwaring 2016). In some species, however, bird eggs are exposed to extreme and potentially detrimental conditions due to the lack of a nest, limitations of incubation sites, or parental behaviours (Board 1982).

The common guillemot (*Uria aalge;* Pontoppidan 1763) breeds colonially on exposed and rocky cliff ledges which minimises predation of their eggs and chicks from terrestrial animals (Nettleship & Birkhead 1985). To reduce the risk of losing eggs or chicks to aerial predators, guillemots also breed at very high densities (typically, 20 pairs per m^2) (Birkhead 1977; Birkhead 1993). One consequence of high density breeding is that colonies become 'unhygienic', with faecal material accumulating on the sea cliffs and breeding ledges. Contrary to previous suggestions (e.g. D'Alba *et al*. 2017), guillemot breeding sites are not usually dry, but are periodically wetted by rain leading to the formation of dirty puddles on the breeding ledges (Fig. S1; T.R.B. Pers. Obs.). Since guillemots do not build a nest and instead incubate their single egg directly on bare rock ledges, their eggs are frequently exposed to a slurry of faeces, dirt, other detritus and water (henceforth, 'debris') during incubation (Tschanz 1990; Birkhead 2016; Birkhead *et al.* 2017). Contamination of the eggshell by debris is almost inevitable as guillemots typically incubate their eggs between their legs (rarely with the egg entirely on top of their feet), and usually with the lower surface of the egg in direct contact with the substrate (Fig. S1; Manuwal *et al.* 2001; Birkhead *et al.* 2018).

Wet debris on the eggshell is likely to have a detrimental effect on embryonic survival since it may enter and block the gas exchange pores in the eggshell, reducing the gas exchange efficacy and also facilitate microbial invasion via the pore canals (Board 1982). Both of these effects could compromise embryonic development through reduced water loss, carbon dioxide retention leading to hypercapnia (enhanced carbon dioxide in the embryo's blood), asphyxiation or infection, and ultimately result in embryo mortality (Board & Fuller 1994; Ar & Deeming 2009). Despite these potential risks, guillemot eggs covered with debris are known to hatch successfully (T.R.B. Pers. Obs.), suggesting that either (a) the debris that guillemot eggs are exposed to is relatively benign and does not compromise embryo survival, and/or (b) guillemot eggs possess adaptations to cope with the impact of debris.

Guillemot eggs could be unaffected by extensive debris cover if, due to intrinsic properties of the debris, it does not reduce the gas exchange efficacy of the shell. Coating either part of the blunt or pointed end of a chicken (*Gallus gallus domesticus*) egg with a man-made impermeable material (epoxy cement) has been shown to increase embryo mortality and levels of hatching failure (Tazawa *et al.* 1971). However, natural debris that adheres to the eggshell comes from a variety of sources and may include faecal material (which varies in its composition depending on the bird's diet e.g. guillemot's faeces contains small fish bones), dirt, sand, small stones, dust, feathers and vegetation. It is therefore likely to vary in gas permeability depending on its composition, and consequently may not have the same negative effects on embryo survival as impermeable cement.

Verbeek (1984) found that the water loss and hatching success of glaucous gull (*Larus glaucescens*) eggs were reduced when they were coated with gull faeces, but not when the eggs were coated with cormorant (*Phalacrocorax auritus, P. pelagicus*) faeces. This result is likely due to differences in the composition of faeces between species, and therefore the ability of gases to diffuse through. As a result, Verbeek (1984) suggested that birds that direct their faeces away from the nest site during incubation (like glaucous gulls) produce faeces that would inhibit gas exchange if it covered their egg(s); defecating away from the incubation site may therefore have evolved in response to the negative impact of faeces on embryo development. Birds producing faeces that has little effect on

eggshell conductance or hatching success may not be under the same selection to defecate away from their eggs or those of their neighbours in colonial breeding species. If Verbeek (1984) is correct, one might predict that guillemot faeces has little impact on gas exchange efficiency of the eggshell, since guillemots can not deliberately defecate away from their colony because they breed at such high densities. In fact, although they propel their faeces away from themselves, they regularly propel their faeces onto neighbouring birds and their eggs. In addition to faecal material, the debris on guillemot breeding ledges can include bones, stones, feathers, vegetation and soil, and thus may be porous and permeable to gases, allowing the relatively unrestricted diffusion of gases through it. However, if debris penetrates and blocks the gas exchange pores, it may still impede gas exchange by reducing the number of functional pores (open channels that allow the passage of gases through them) in the eggshell.

If guillemot eggs are affected by debris, one potential way they might cope is through 'self-cleaning' to remove contaminants, as suggested by Steven Portugal and his team (https://phys.org/news/2013-07-unique-shell-guillemot-eggs-edge.html). Despite being widely covered by the media, including The Guardian (https://www.theguardian.com/science/small-world/2013/jul/18/nanotech-roundup-cosmetic-fix-micro-batteries), National Geographic (https://www.nationalgeographic.com/science/phenomena/2013/07/04/scientist-spills-water-discovers-self-cleaning-bird-egg/) and the BBC (article no longer available online), this work remains unpublished (media reports were based on a conference presentation).

For a surface to be self-cleaning it must possess three properties; (i) high water repellency (known as super-hydrophobicity), with a stationary water contact angle of ~150°, (ii) low adhesion of extraneous debris to the eggshell surface and hence (iii) effortless removal of water and debris from the eggshell when water droplets make contact with its surface (Genzer & Marmur 2008; Ensikat *et al.* 2011; Yuan & Lee 2013). According to the unpublished findings (see above), the surface structure of guillemot eggshells makes them super-hydrophobic and consequently, self-cleaning. If true, debris should simply leave the surface of the guillemot’s eggshell every time water makes contact with the shell. The idea that guillemot eggs are self-cleaning seems biologically implausible since most guillemot eggshells remain contaminated with debris during the

incubation period (Birkhead 2016; Birkhead *et al.* 2017), but the hypothesis has yet to be empirically tested.

If the guillemot eggshell is not self-cleaning then the shell accessory material (SAM) on the surface of the eggshell could limit the impact of debris by preventing pore blockages (Board 1982). Here, we use Board and Scott's (1980) more general terminology: 'shell accessory material' (henceforth, SAM), rather than 'cuticle' (implying organic material) or 'cover' (implying inorganic material) as SAM is semantically more appropriate (Board *et al.* 1977). SAM is the outermost substance that sits on the exterior surface of the eggshell and can provide a variety of benefits including waterproofing (Board & Halls 1973a, b; Sparks & Board 1984), microbial defence (Wellman-Labadie *et al.* 2008; Ishikawa *et al.* 2010; D'Alba *et al*. 2014; Gole *et al.* 2014a, b), desiccation resistance (Deeming 1987; Thompson & Goldie 1990), aesthetic properties such as gloss (Igic *et al.* 2015), UV reflectance (Fecheyr-Lippens *et al*. 2015), colouration and patterning (Lang & Wells 1987; Samiullah & Roberts 2014) and, as a consequence, protection from harmful wavelengths of light (Maurer *et al.* 2015; Lahti & Ardia 2016). SAM may also provide increased shell strength (Tyler 1969; Portugal *et al.* 2018). This wide range of properties may be attributable to the composite nature of SAM, as well as its varied thickness and composition in different species (Mikhailov 1997). Despite the variability that exists in SAM, D'Alba *et al.* (2017) showed that SAM may possess some universal functions including modulating UV reflectance and providing a barrier against microbes across seven bird species studied. However, it is not clear whether SAM can also provide a barrier to debris. More specifically, whether or not SAM can prevent debris from entering pores and blocking them.

Board and Perrott (1982) provided circumstantial, observational evidence that SAM may prevent pore blockages by debris in naturally incubated guinea fowl (*Numidia meleagris)* eggs. However, no manipulations of eggshell structure were performed to explicitly test the hypothesis that SAM prevents pore blockages. The adaptive role of SAM in the common guillemot's egg is not clear (but see D'Alba *et al.* 2017 for suggestions). It is therefore unknown if SAM mitigates the negative costs of debris on the guillemot eggshell by, for example, preventing pores from becoming blocked.

The aim of the present study was to establish how common guillemot embryos survive incubation in eggs with large amounts of debris on their shell surface, by testing the following three hypotheses: (1) the properties of natural debris are such that contamination of the eggshell does not reduce the gas exchange efficacy of the shell; (2) the guillemot eggshell is self-cleaning; and (3) shell accessory material prevents pore blockages by debris, which in turn ensures sufficient gas exchange is permitted across the eggshell for embryonic development.

Materials and methods

Eggshell and debris sampling

Fresh eggs were collected in 2013 – 16 under licence from Skomer Island, Wales, UK. All eggs were drained of their contents before being washed in distilled water and allowed to air dry at room temperature before storage. A hand-held rotary saw (DREMEL Multi) was used to cut fragments (~1 cm^2) from the eggshells for use in the experiments detailed below. Where possible, fragments were cut from areas of the eggshell that appeared to be clean and the fragments were then rinsed in distilled water and allowed to air dry. No soap or chemicals were used in the cleaning process as they can damage the surface of the shell and SAM (D.J. Pers. Obs.). Natural debris was opportunistically collected directly into sterile Eppendorf tubes from guillemot breeding ledges in 2014 – 17. Debris was stored dry or semi-dry and rehydrated prior to use in experiments. All debris was used within one year of collection, typically sooner within 1 – 2 months.

Effect of debris on eggshell gas conductance

Fragments from the blunt end (see Birkhead *et al.* 2017 for sampling location) of each egg were carefully fixed to individual custom glass vials with an aperture diameter of ~0.3 – 0.5cm using cyanoacrylate glue (Loctite, USA), so that the inside of the eggshell membrane was fixed to the glass vial, and left to dry for 24 hours. The seal between the eggshell and the glass vial was checked before any excess shell around the edge of the glass vial was removed with a hand-held rotary saw. Finally, a further layer of super glue was applied to the circumference of the eggshell fragment and glass vial and left to dry.

Each fragment underwent two treatments, a "clean trial" followed by a "dirty trial". Before clean trials, eggshell fragments were carefully cleaned on the outer surface using a fine paintbrush to remove any dust and debris. For dirty trials, rehydrated natural debris (1g of natural debris mixed with 300µl of distiller water) was applied to the outer eggshell surface of fragments using a paintbrush until they were evenly coated and no eggshell surface was visible.

A Bruker Alpha Fourier-transform infrared (FTIR) Spectrometer fitted with an Alpha-T module cell at a resolution of 0.8cm^{-1} was used to record the spectra of gases within the glass vials. Sample scan and background scan times were set to 32 scans, the result spectrum was set to 'Absorbance', and the resulting spectrum was saved from the 360-7000cm^{-1} range. All spectra were baseline corrected using an independent background scan of laboratory air that was recorded before each series of measurements. To record the spectra readings, a glass vial with an eggshell fragment fixed to the top, was placed on to the extended finger of a gas cell (calcium fluoride windows, a 7cm path length and one gas-tight 'Youngs' valve) and sealed using a petroleum-based jelly. To create the carbon dioxide rich environment inside the gas cell, small pieces of dry ice were initially placed into the cell before the attachment of the glass vial. To avoid a build-up of pressure while the dry ice sublimed, the gas-tight tap was opened slightly and the gas cell attached to a gas bubbler. Once the dry ice had completely sublimed and no further bubbles were observed inside the gas bubbler, the gas-tight tap was closed, and the gas bubbler removed. Immediately after this, the gas cell was positioned onto the Alpha-T cell sample holder on the Bruker Alpha FTIR and an absorbance spectrum was recorded and saved. Another spectrum was recorded and saved 1 hour later to determine how much carbon dioxide had diffused through the shell within this time frame.

To quantify the rate constant of eggshell carbon dioxide gas diffusion for each fragment (henceforth, carbon dioxide conductance), integral measurements were taken within a range that is know to correspond to several CO_2 absorption bands (range set between 3482.5 and 3763.15 cm^{-1}) from the initial spectra and the spectra after 1 hour for each individual sample (see https://webbook.nist.gov/chemistry/). Integral values were standardised so that the initial value was 100. The carbon dioxide conductance was calculated by subtracting the standardised integral after 1 hour from the standardised

initial integral.

The method described above was chosen over other methods to measure eggshell conductance of eggshell fragments (e.g. Portugal *et al.* 2010) for two main reasons. Firstly, it directly measures the amount of carbon dioxide gas lost through the eggshell rather than predicting gas loss from measured mass loss. This potentially provides more precise measurements as the precision of weighing scales can be more limiting than the FTIR Spectrometer (J.E.T. Pers. Obs.), as well as providing more accurate data because gas loss is directly measured rather than predicted from mass loss. Secondly, and crucially, this method allowed us to repeat each trial on the same fragments when they were clean and dirty without damaging the fragment or the vessel the sample was attached onto, which would not be possible using Portugal *et al.'s* (2010) approach. Even though we were measuring the change in carbon dioxide loss, water vapour, oxygen and carbon dioxide conductance are all linked (Rahn & Paganelli 1990; Ar & Deeming 2009) so all gases are likely to be affected in a similar way and, therefore, any restrictions on carbon dioxide conductance can theoretically be more broadly applied to any gas crossing the shell.

After the gas conductance of dirty fragments was measured, we cut the eggshell fragment off the glass vial and used X-ray micro computed tomography (microCT) to assess the extent to which eggshell pores were blocked by debris. Because the eggshell fragment needed to be cut off the glass vial for microCT scanning, we could not scan the eggshell fragments in between clean and dirty treatments, only once the gas conductance experiment was over and the eggshell fragment was dirty. Eggshell fragments were scanned in a Bruker Skyscan 1172 set to 100kV electron acceleration energy and 90uA current, with the sample 45.7mm from the X-ray source with a 1.0mm aluminium filter; and the camera 218mm away from the source. Camera resolution was set at 1048 x 2000 pixels, and a pixel size of 4.87μm. We used the same settings for each scan, collecting a total of 513 projection images over a 180° rotation using a rotation step size of 0.4° and a detector exposure of 885ms integrated over three averaged images resulting in a total scan time of 38 minutes. One eggshell fragment was scanned during each session. Projection images were reconstructed in NRecon software (version 1.6.10.2) after which image analysis was performed in CT analyser (CTAn, version

1.14.41), CTVox (version 3.0) and CT volume (CTVol, version 2.2.3.0; all the above software was provided by Bruker micro-CT, Kontich, Belgium). Reconstruction parameters used were: dynamic image range; minimum attenuation coefficient = 0.0025, maximum = 0.05, level 2 asymmetrical boxcar smoothing, ring artefact correction = 12, beam hardening correction of 20% and auto misalignment compensation. Resultant images were saved as 8-bit bitmaps.

Two 3D models – one for the shell and another for the debris – were created for each shell fragment by segmenting the images in CTAn. Shell models were created by initially resizing the data-set by a factor 2 with averaging in 3D on, before using automatic (Otsu's method) thresholding to segment the images, followed by low level despeckling of white and black pixels in 2D space (< 10 pixels). The 3D model was then created using an adaptive rendering algorithm with smoothing on, a locality value of 1, a tolerance of 0.05 and then saved as a .ctm file. Debris models were created by initially resizing the data-set by a factor of 2 with averaging in 3D off, before manually thresholding for debris to segment the images, followed by low level despeckling of white (< 2 pixels) and black (< 10 pixels) pixels in 2D space (< 10 pixels). Again, the 3D model was then created using an adaptive rendering algorithm with smoothing on, a locality value of 1, a tolerance of 0.05 and saved as a .ctm file. Both models were loaded into CTVol, aligned, and pore channels were visually inspected to see if they were blocked by debris (Fig. S2). Owing to the image processing protocols followed, we could detect air spaces (and blockages) no smaller than 10μm, so our method may have overestimated the number of blocked pores since any pores with small air spaces within the debris blockage would have been undetectable at the resolution limit. This measure is therefore a proxy of the level of pore blockages within an eggshell fragment, rather than an absolute value. This methodology may introduce a bias if different types of debris are studied, but in each of our experiments debris was used from a single sample collected from the field, removing this issue. Only blockages inside the pore channel were counted, and not blockages at the surface of the pores, because the thresholding parameters used to identify debris could not distinguish between debris and the shell membranes, and potentially SAM on the shell surface.

The number of blocked pores was divided by the total number of pores to provide an estimate of the proportion of blocked pores per fragment. The thickness of debris on the surface of the shell (above each pore), and the length of each pore channel was measured in CTAn using the line measurement tool and averaged for each eggshell fragment. The thickness of the true shell (the calcium carbonate layers of the eggshell, excluding the organic membranes) was also measured at 10 locations using the line measurement tool and averaged for each fragment (see Birkhead *et al.* 2017).

Self-cleaning eggs

Using a method similar to Vorobyev and Guo (2015), we tested the most important property of self-cleaning surfaces; whether water droplets and debris readily leave the guillemot eggshell surface together. Ten freshly collected guillemot eggshells, and five museum samples were used in this study. Fragments were taken from the equator of each eggshell (see Birkhead *et al.* 2017), and two fragments per eggshell were studied per treatment. An eggshell fragment was attached to a stand tilted at 8° and dust from a household vacuum cleaner (as used in Vorobyev & Guo 2015), was applied to the shell's surface. In a series of 15 – 20 droplets, 400µl of water was dripped on to the fragment and the shell was examined by eye. If the eggshell fragment contained a puddle of water carrying floating or stationary dust then the surface was deemed to not be self-cleaning, as water and debris still remained on the surface (see Introduction for definition of self-cleaning). If the surface did not contain any floating dust particles or any water, then the surface was classified as self-cleaning (Vorobyev & Guo 2015). To validate this simple self-cleaning test, we repeated this trial using the following known self-cleaning materials; the fresh, young leaves of cauliflower (*Brassica oleracea var. botrytis*), broccoli (*Brassica oleracea var. italica*) and collard (spring) greens (*Brassica oleracea var. viridis*). After the dust trial on *Brassica* leaves, very little or no water remained on the surface of the leaves as it bounced off the samples removing debris with it (Movie 1), therefore validating the use of this simple self-cleaning test to determine if guillemot eggshells are self-cleaning. Self-cleaning tests were repeated using wet debris (a vial containing 2.5ml of semi-dry natural debris was diluted with 100µl of distilled water) and debris that had been allowed to dry onto the shell to assess if guillemot eggshell is self-cleaning against natural debris it would encounter during incubation.

After the self-cleaning experiment was conducted, eggshell fragments were washed in excess water and allowed to dry, to mimic a heavy rain shower and followed by natural drying. Eggshell fragments were then qualitatively assessed (yes, or no) – by eye, using a macro lens on a digital camera, and by microscope – to establish whether any debris remained on the shell surface.

Shell accessory material and pore blockages

To test the role of shell accessory material in preventing pore blockages by debris, we chemically manipulated eggshell fragments to remove shell accessory materials from the eggshell. Two pieces of shell (~1cm^2) were cut from the equator of five fresh eggs (see Birkhead *et al.* 2017 for sampling location). One fragment acted as a control, and was washed in distilled water only, whereas the other fragment was first treated with thick household bleach (containing sodium hydroxide and hypochlorite) to remove organic shell accessory material (see Fig. S3), and then also washed in distilled water. Both sodium hydroxide and sodium hypochlorite – key components of bleach – have been used to remove organic shell accessory material from the surface of the shell in previous studies (Tullett *et al.* 1976; Deeming 1987). Following the cleaning treatments, debris was carefully added to the surface of each shell fragment by squeezing a paintbrush loaded with wet debris (1g of natural debris mixed with 300µl of water) with forceps. The debris was allowed to air dry for at least 24 hours.

Eggshell fragments were scanned in a Bruker Skyscan 1172 using similar settings as detailed above, except that in this case a pixel size of 4µm was used, thus the sample was 48.7mm from the X-ray source with a 1.0mm aluminium filter, and the camera was 283mm away from the source. We collected 499 projection images each with an exposure time of 1475ms, leading to a scan time of 49min. These settings provided higher resolution data compared to those used above. A larger pixel size had to be used to scan the fragments used in the gas conductance trials to ensure that all of the eggshell over the aperture of the glass vial (i.e. the area of eggshell exposed and available for gases to diffuse through) was scanned, whereas there was not the same limitation here.

Two 3D models were created per shell fragment (one for the shell and another for the debris) in CTAn by thresholding for each material (automatically for the shell using Otsu's method and manually for debris). Model creation parameters were the same as those discussed earlier except that shell models were created by initially resizing the data set by a factor of 2 with averaging in 3D off. To account for differences in pore numbers between pairs of fragments, only the first fifteen pores that could be visualised by re-slicing the z-stack of reconstructed images were selected to assess pore blockages. The models were then loaded into CTVol, and pore channels were visually inspected to see if they were blocked by the debris model (Fig. S2). As explained above, this measure provides a proxy rather than the absolute number of blocked pores. However, since we were able to use a higher scanning (and model) resolution in this experiment, detection of pore blockages and air spaces in between debris should have a limit of ~8μm.

Statistical analysis

All statistical analyses were performed in R version 3.3.1 (R Development Core Team 2016). We used a paired t-test to test whether the presence of debris on the eggshell influenced carbon dioxide conductance. We used Pearson's product moment correlations to establish whether a correlation existed between the clean eggshell carbon dioxide (CO_2) conductance and (a) the number of pores in an eggshell fragment or (b) the length of those pores (measured both directly and by using the proxy of shell thickness). Pearson's product moment correlations were also used to establish whether a correlation existed between the relative change in CO_2 loss between clean and dirty fragments and the proportion of pores blocked in an eggshell fragment, or the thickness of the debris on the surface of the shell. Finally, paired t-tests were performed to assess whether SAM on the surface of guillemot eggshells limits the number of pores that are blocked by wet debris when it is applied to the outer surface of the shell.

Results

Effect of debris on eggshell gas conductance

The rate of gas exchange for clean eggshell fragments was positively correlated with the number of pores present in an eggshell fragment ($r = 0.733$, $p = 0.016$, $n = 10$), but not with either the mean length of pores ($r = 0.045$, $p = 0.902$, $n = 10$), nor the mean true shell thickness ($r = -0.185$, $p = 0.610$, $n = 10$). After debris was applied to the eggshell, carbon dioxide conductance significantly decreased ($t = 3.02$, d.f. = 9, $p = 0.014$; Fig. 1). The relative reduction in carbon dioxide conductance of the eggshell after the application of debris was negatively correlated with the proportion of pores in the eggshell that were blocked ($r = -0.821$, $p = 0.004$, $n = 10$), with fragments possessing a greater proportion of blocked pores showing a greater reduction in carbon dioxide conductance compared to when the fragments were clean (Fig. 2). The reduction in carbon dioxide conductance was not related to the average thickness of the debris on the eggshell above each pore (absolute difference in CO_2 conductance: $r = -0.160$, $p = 0.66$, $n = 10$; relative difference: $r = -0.21$, $p = 0.56$, $n = 10$).

Self-cleaning eggs

None of the common guillemot eggshell fragments studied here demonstrated any self-cleaning ability against dust. All fragments were covered in a puddle of water containing dust at the end of the trial, which is characteristic of materials that are not super-hydrophobic and not self-cleaning (Movie 2; Vorobyev & Guo 2015). None of the guillemot eggshell fragments demonstrated any self-cleaning ability against either wet or dry natural debris (Fig. 3; Movie 3). It was possible to remove some debris – but not all – by washing the eggshell with water, but a large volume of water had to be applied and debris removal appeared to depend on water volume and/or pressure. This is not necessarily biologically relevant with respect to the circumstances in which guillemots breed because even when it is raining, it is unlikely that a large volume of pressurised clean water will make contact with the eggshell surface all at once. Instead, it is more likely that dirty water and wet debris from the cliff ledges will come into contact with the egg. Even after excessive washing, fragments were not completely clean, with small

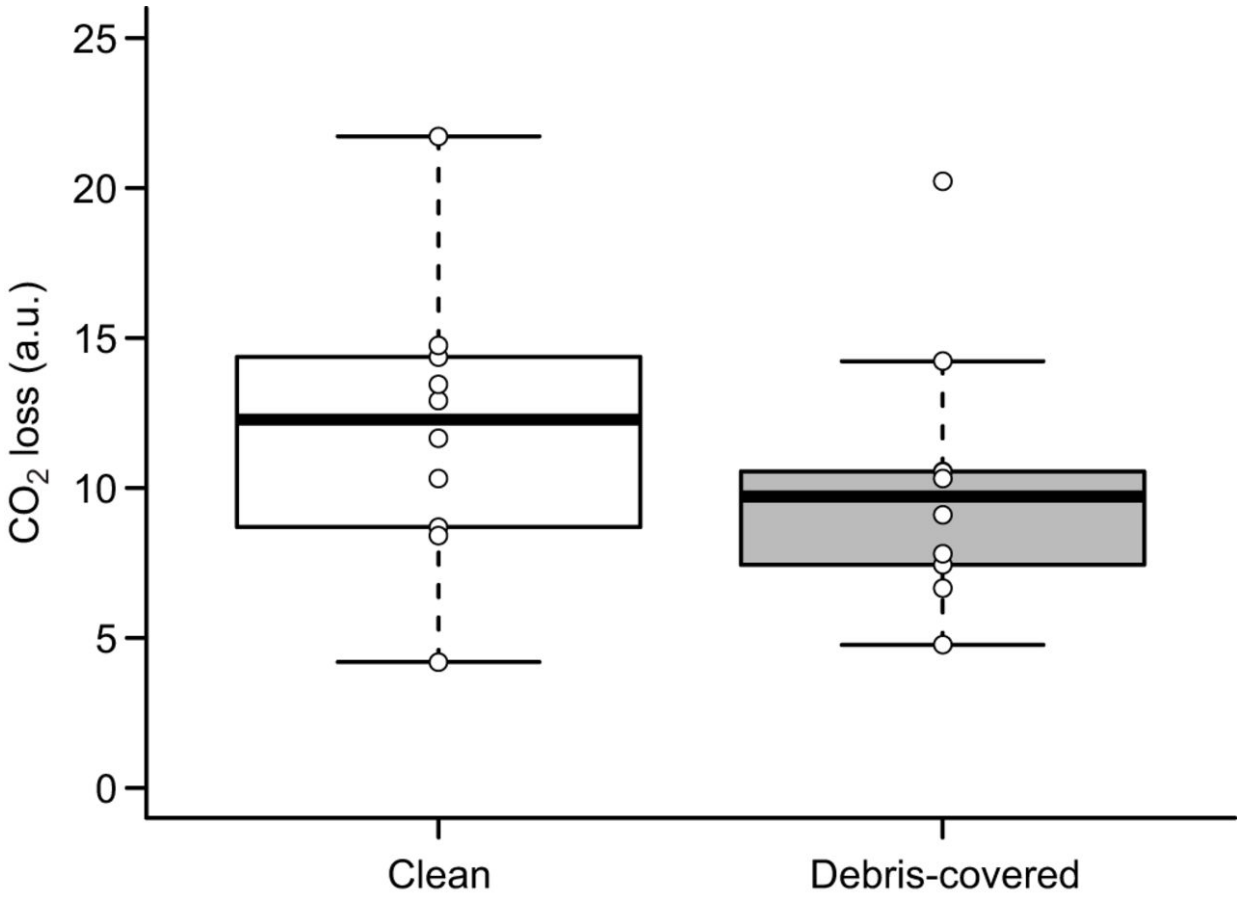

Figure 1. The effect of debris on carbon dioxide loss through common guillemot eggshell. The rate of carbon dioxide loss significantly decreased after the application of natural debris onto the eggshell (paired t-test: t = 3.02, d.f. = 9, p = 0.0144, n = 10). Boxes are the interquartile range, black line within the box is the median, the whiskers show the highest and lowest values and the circles are the individual data points. a.u., arbitrary units.

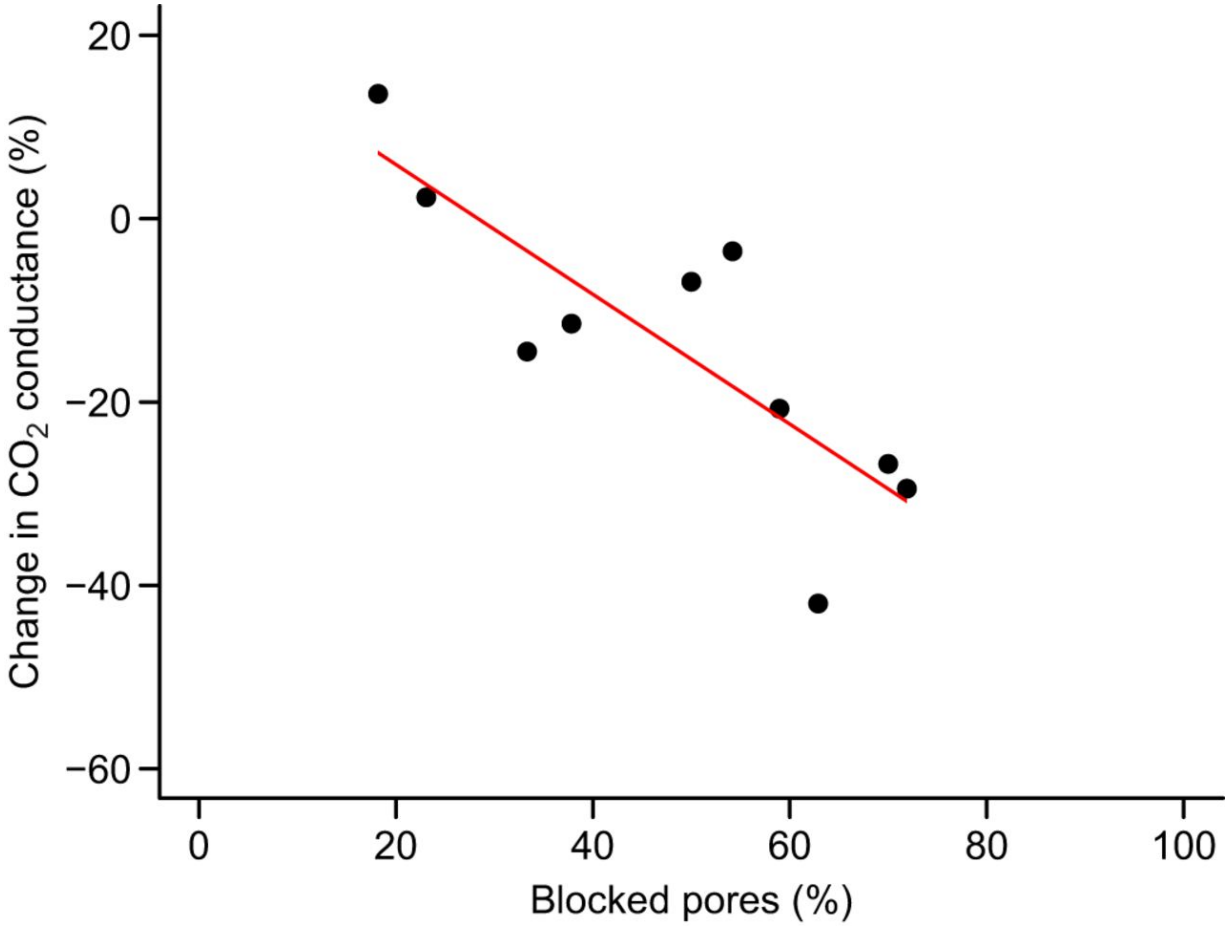

Figure 2. The effect of blocked pores on carbon dioxide conductance through guillemot eggshell. The relative reduction in carbon dioxide conductance of the eggshell after the application of debris was negatively correlated with the proportion of pores in the eggshell that are blocked (Pearson's product moment correlation: r = -0.821, p = 0.004, n = 10). Change in carbon dioxide conductance was calculated as: ([dirty gas conductance - clean gas conductance] / clean gas conductance) x 100. The red line is the line of best fit.

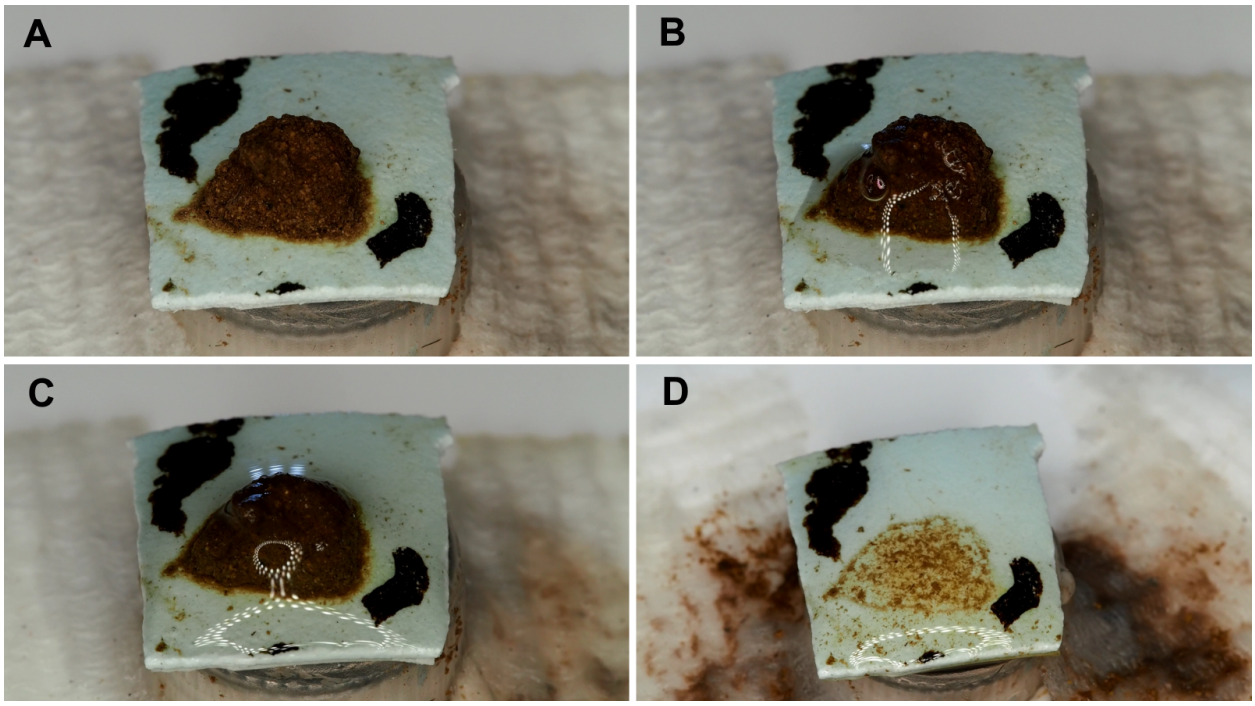

Figure 3. A self-cleaning trial involving debris dried onto guillemot eggshells. (A) An eggshell fragment with debris on the surface, (B) the same fragment after the first drop of water has fallen onto the shell surface. (C) At the end of the trial water and debris remained on the eggshell surface illustrating that the sample is not self-cleaning. (D) After the trial, excess clean water was used to wash off the debris. Even after this cleaning, debris remained on the eggshell surface as stains or remnants. The large patch in the centre of the eggshell fragment is the debris; the two smaller dark patches either side are pigment on the eggshell surface. Eggshell sample is ~1cm^2.

amounts of debris and staining remaining (Fig. 3 & 4).

Shell accessory material and pore blockages

The removal of SAM from eggshell fragments resulted in a significant increase in the proportion of pores that were blocked after the experimental application of natural debris to the shell surface, compared to control fragments where SAM was still present ($t = 4.74$, $d.f. = 4$, $p = 0.009$; Fig. 5).

Discussion

Our results show that debris contaminating the surface of guillemot eggshells during incubation reduces the gas exchange efficacy of the eggshell, and the eggshell is not self-cleaning to help resolve this problem. Instead, the full impact of debris on the gas exchange efficacy of eggshell is minimised by shell accessory material (SAM). SAM protects pores, reducing the number that are blocked by debris, which in turn minimises the reduction in eggshell gas conductance caused by debris on the eggshell.

The drivers of eggshell gas conductance

Our data suggest that pore number is the primary driver of gas conductance in guillemot eggshell fragments. This is contrary to the predictions of Zimmerman and Hipfner (2007) who suggest that shell thickness (i.e. pore length) and pore size are the key drivers of porosity and therefore gas conductance in common guillemot eggs. The fact that pore length (shell thickness) does not drive eggshell gas conductance is consistent with ideas initially presented by Ar and Rahn (1985) and Rahn and Paganelli (1990), as well as in the discussions of Portugal *et al.* (2010) and Maurer *et al.* (2012), which allude to the fact that shell thickness is not a determinant of water vapour conductance. In the present study, we were unable to use microCT to scan clean fragments that were used in our gas conductance trials (see Materials and Methods for further details), so we cannot explicitly link pore size to eggshell conductance. However, evidence from other studies suggests that the role of pore size is likely to be minor compared to that of pore number or density (Ar & Rahn 1985; Simkiss 1986; Rokitka & Rahn 1987; Rahn & Paganelli 1990; Table 1).

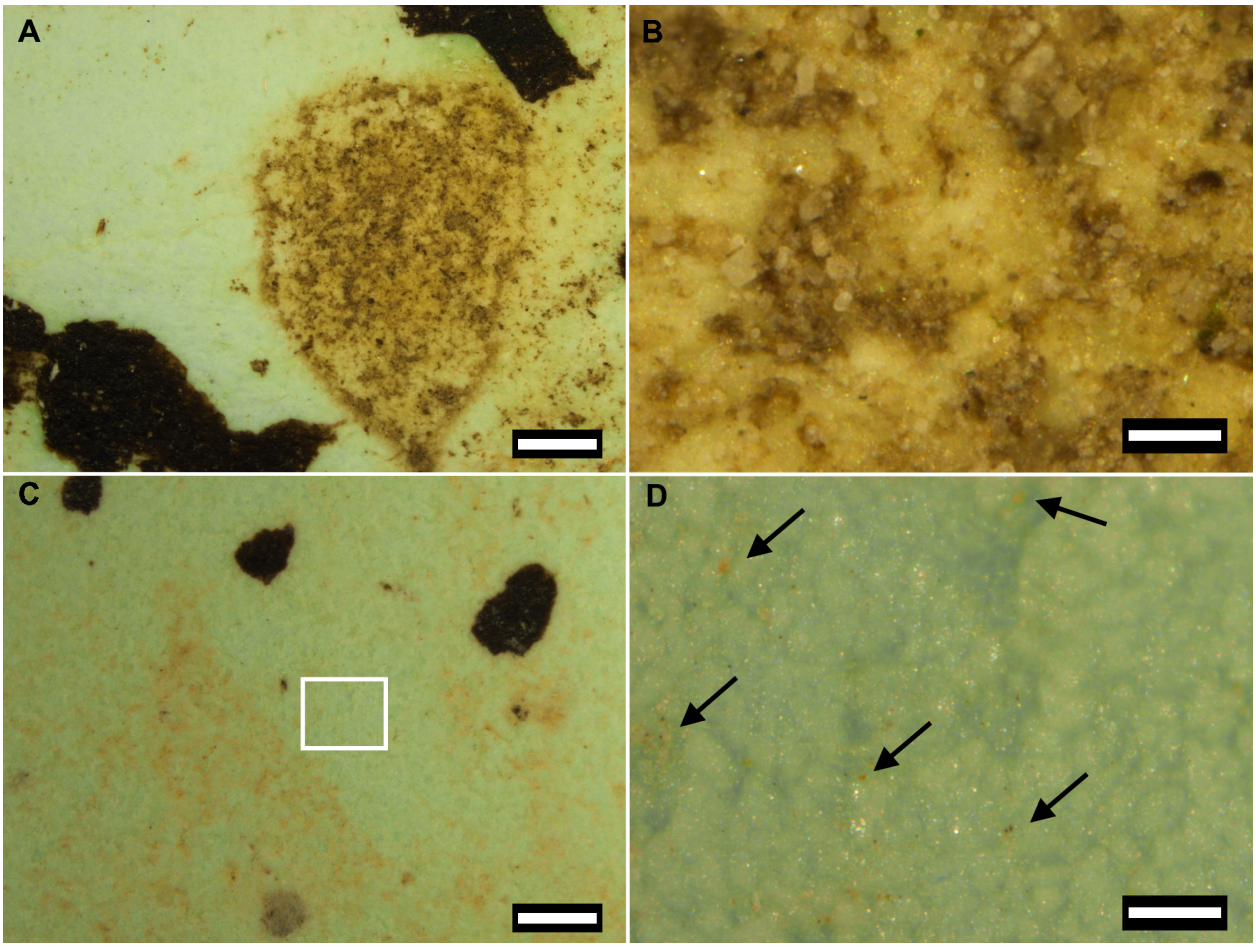

Figure 4. Natural debris on common guillemot shells. (A, B) Stereoscopic microscopy images showing the remnants of debris remaining on a guillemot fragment after washing with excess water. (C, D) Stereoscopic microscopy images showing natural debris on common guillemot eggshell. The unmanipulated piece of guillemot eggshell in C shows natural debris staining, but also a patch that, to the naked eye, looks clean. The rectangle marks the "clean" area shown in (D). There are in fact small particles of debris on the shell surface, a few of which are marked with arrows. Debris is light brown; darker brown/black patches in these images are eggshell pigment. Scale bars: 1000μm (A, C) and 100μm (B, D).

Figure 5. Removal of shell accessory material increases the number of pores blocked by natural debris. The proportion of pores blocked by debris significantly increased after the removal of shell accessory material using bleach (paired t-test: t = 4.74, d.f. = 4, p = 0.00904, n = 5). Boxes are the interquartile range, black line within the box is the median, the whiskers show the highest and lowest values, and the circles are the individual data points.

Table 1. Linear regression relationships between measured or calculated eggshell parameters and observed gas conductance in the eggs of 21 species of Anatidae.

Parameter	Calculation	Adjusted R^2	Regression equation	p-value	Source
Total pore circumference[1] (μm)	2 x π x pore radius x pores per egg	0.633	y = 0.0153x + 5.35	< 0.0001	Re-calculated from Hoyt *et al.*'s (1979) data using Simkiss's (1986) formula
Calculated gas conductance[2] (mg Day^{-1} $Torr^{-1}$)	(2.24 x pore area x pores per egg) / shell thickness	0.371	y = 0.575x + 9.41	0.00202	Calculated by Hoyt *et al.* (1979)
Total pore area (μm^2)	Measured pore area x pores per egg	0.485	y = 0.0079x + 9.63	0.000271	Calculated from data in Hoyt *et al.* (1979)
Pores per egg[3]	Calculated from surface area and measured pore density	0.624	y = 0.00157x + 2.52	< 0.0001	Data from Hoyt *et al.* (1979)
Shell thickness (mm)	Measured directly from shell	0.267	y = 56.7x - 3.32	0.00968	Data from Hoyt *et al.* (1979)
Pore area (μm^2)	Average measured area of a pore	0.00479	y = 0.0143x + 14.5	0.308	Data from Hoyt *et al.* (1979)

The total number of pores per egg (R^2 = 0.624) and the total pore circumference (R^2 = 0.633) explain more variation in observed gas conductance than does calculated gas conductance using the traditional calculation (R^2 = 0.371), highlighting an issue with the assumption that pore area and shell thickness are determinants of gas conductance. The fact that total pore area per egg (R^2 = 0.485) explains less variation than the total number of pores per egg, and that pore area is not significantly associated with gas conductance, suggests that pore area does not drive eggshell gas conductance.

[1] Based on Stefan's law of diffusion.

[2] Constant x total pore area x $pore\ length^{-1}$ (based on Fick's law of diffusion).

[3] It is worth noting that Ar and Rahn's (1985) regression analysis of pore number against eggshell gas conductance on eggs from 134 different species had an R^2 value of 0.89.

If pore number is the main driver of gas conductance across the eggshell, then predictions made using the calculations based on the traditional theoretical formulae presented in Ar *et al.* (1974) and Ar and Rahn (1985), based on Fick's law of diffusion, may be incorrect as they erroneously include terms for pore length (shell thickness) and pore area. Previous research has suggested that calculated versus measured conductance values are not consistent; in fact, measured values can be three times lower than calculated values (Tøien *et al.* 1988). Inclusion of pore size and pore length (shell thickness) could be one reason for this discrepancy, alongside a lack of consideration of the effects of (1) SAM (Tøien *et al.* 1988; Thompson & Goldie 1990), (2) convective and diffusive resistance (Tøien *et al.* 1988), and (3) internal heat changes due to the metabolic rate of the developing embryo. In addition, historical methods used to study shell thickness and porosity were imprecise, unreliable and inaccurate. For example, pore size was likely overestimated in previous studies because the minimum cross-sectional dimensions (e.g. area or radius) could not always be measured as they are within the pore channel, and therefore measures from the inner surface of the shell were used instead under the presumption that these dimensions were the limiting dimensions (see Birkhead *et al.* 2017). Furthermore, shell thickness measures are not always the same as pore length (see Supplementary Material, datasets 1 & 2). Further investigation into the drivers of eggshell gas conductance is needed, particularly with the advent of more precise and accurate methods for measuring eggshell parameters and gas conductance. Gaining a better understanding of what drives eggshell conductance is particularly important because predicted gas conductance values are used in a variety of ways, including for inferring the nesting conditions of extinct birds and dinosaurs (e.g. Deeming 2006; Deeming & Reynolds 2016) and drawing comparative conclusions about species' developmental biology (e.g. Jaeckle *et al.* 2012).

The role of shell accessory materials in protecting pores

Our finding that eggshell gas conductance is driven by pore number is important because it means that any blockages within pores impose a serious restriction on gas exchange through reducing the number of functional pores (i.e. unblocked, complete pores that gases can diffuse through) available for gas exchange. Our results show that blockage of pores by debris has a direct effect on the gas exchange efficacy of the eggshell, as was

previously suggested by Board (1982) and Board and Perrott (1982). In a previous study, we suggested that the pyriform shape of common guillemot eggs, and the distribution of pores across the eggshell, may help to minimise the effects of eggshell contamination on the developing embryo (Birkhead *et al.* 2017). The orientation of the guillemot's pyriform egg during incubation is such that the blunt end of the egg (where porosity is highest) generally does not come into contact with the substrate, so most debris is concentrated on the pointed end of the egg where porosity is low. This potentially minimises the overall number of pores that become blocked and maximises the number of functional pores available for gas exchange. However, debris on the elongated, pointed end of the egg could still lead to a large reduction in overall eggshell gas exchange, and, despite the egg's shape, debris is still sometimes seen on the blunt end. We show here that SAM prevents pores becoming blocked by debris, a finding consistent with Board and Perrott's (1982) observations that nesting debris penetrates pores and may reduce the total area of eggshell available for gases to diffuse through. SAM could therefore minimise the negative effects of debris covering the eggshell surface by minimising the number of pores that become blocked.

How SAM prevents pore blockages is not clear. One possibility is that the SAM acts as a physical barrier to the penetration of debris, as seemed to be the case for helmeted guinea fowl eggs (Board & Perrott 1982). Alternatively, SAM may provide water resistance to the eggshell, which prevents aqueous debris from entering eggshell pores (Board 1981). Either way, if SAM is removed or damaged, the pores become vulnerable to blockages. Natural cracking of SAM can occur due to dehydration, and cracks could leave pores vulnerable, which may explain why some of the untreated eggshell fragments we studied to assess the impact of debris on eggshell conductance had a large proportion of blocked pores (Fig. S4). Some eggshells also had poor quality SAM or a patchy SAM coverage meaning pores were uncovered and left vulnerable (Fig. S3), and in addition, our limited imaging and blockage detection resolution may have led us to consistently overestimate the proportion of blocked pores (see Materials and Methods). Although this would not invalidate our overall findings, it could explain the unexpectedly high proportion of blocked pores found in untreated eggshells when debris was added onto the surface of the shell. Whether SAM plays the same role on the eggs of other species that are directly exposed to debris (e.g. the blue footed booby, *Sula nebouxii;*

Mayani-Parás *et al.* 2015), remains to be tested.

Guillemot eggs are not self-cleaning

Despite suggestions of previous researchers, we found no evidence that the guillemot eggshell surface is self-cleaning. Common guillemot eggshells lack the three important properties which would make them self-cleaning. (1) They are not super-hydrophobic. Reported water contact angles are lower than 150°. For example, Portugal and colleagues reported values of approximately 120° (Portugal, S. as reported by Yong 2013 in http://phenomena.nationalgeographic.com/2013/07/04/scientist-spills-water-discovers-selfcleaning-bird-egg/) while D'Alba *et al.* (2017) reported values of just over 90°. The latter is potentially lower due to eggshell treatment with 70% alcohol in that study. (2) Debris strongly adheres to the guillemot eggshell surface (see Fig. 3 in Birkhead *et al.* 2017). Our self-cleaning trials corroborate observations that debris cannot easily be washed off most guillemot eggshells. Instead scrubbing or wiping with excess amounts of clean water is required to remove debris, and this is still often unsuccessful, implying that debris has high adhesion with the shell (J.E.T. and D.J. Pers. Obs.). It is worth noting that even apparently clean sections of naturally incubated eggs usually contain staining or particles of debris when viewed at high magnification, illustrating that debris does indeed adhere to the eggshell surface (Fig. 4). (3) Consequently, natural debris on the guillemot eggshell surface does not readily leave when water makes contact with it and the eggshell (Fig. 3; Movie 3).

The fact that guillemot eggshells do not possess self-cleaning properties becomes intuitive when we consider how debris interacts with the eggshell surface. A single application of wet debris can not only cover the eggshell surface, but also cause pore blockages that reduce the ability of gases to pass through the shell. A self-cleaning surface on its own would thus be insufficient to maintain adequate gas exchange across the eggshell, unless there was also a unique mechanism to un-block pore channels. Given that SAM prevents pore blockages, and that the presence of debris does not appear to limit the ability of gases to diffuse across the eggshell, there would be little selection on guillemot eggshell structure for self-cleaning properties in the context of eggshell conductance.

Instead of evolving self-cleaning eggs, guillemots may avoid the problem of their eggs becoming excessively covered in debris during incubation via an altogether different mechanism: egg turning. Egg turning is the process where incubating parents turn their eggs around along the longitudinal axis, which is important for normal embryonic development and subsequent hatching (Deeming & Reynolds 2016). Turning may physically remove debris via abrasion and limit an excessive build-up of material on the surface of the shell (Board & Scott 1980; Board 1982; Board *et al.* 1984), which could affect embryo development by reducing gas conductance, increasing the risk of embryonic infection or interfering with contact incubation and thermoregulation. Anecdotal observations suggest that incubation and egg turning limits the build-up of material on common guillemot eggs, as abandoned, un-incubated eggs soon become completely covered in debris (T.R.B. Pers. Obs; see Fig S1 for an example). Furthermore, Verbeek (1984) suggested that abrasion of faecal material from the surface of glaucous gull eggs may have partially restored their hatching success, although this was not based on direct experimental evidence. However, guillemot eggs that are partially or largely covered with debris still tend to hatch (T.R.B. Pers. Obs.), indicating that complete debris removal is not essential for normal embryo development in this species.

Conclusion

The findings of the present study suggest that the effect of debris contaminating the surface of common guillemot eggs is minimised by the presence of SAM, which reduces the number of pores that become blocked. This, in combination with the fact that the pyriform shape of the guillemot egg minimises the amount of debris that covers the highly porous blunt end of the egg (Birkhead *et al.* 2017), ensures that a high proportion of pores remain functional during incubation and guillemot eggs are able to maintain efficient gas exchange despite being covered in debris. The ability of SAM to minimise pore blockages by debris, rather than the egg's shape or pore distribution, is presumably crucial when eggs are heavily covered with debris. It seems likely that the presence of functional SAM, rather than solely the egg's shape, allows guillemot eggs to maintain gas exchange despite being covered in debris throughout the 32 day long incubation period, allowing the embryo to develop normally.

Acknowledgements

We thank the Skelet.AL lab for use of their microCT scanner; Thomas W. Smith and Dr Michael Hippler in the Department of Chemistry at the University of Sheffield for their guidance and assistance in conducting the gas conductance experiments using FTIR, the Wildlife Trust of South and West Wales Trust for permission to work on Skomer Island NNR, and the Natural Resources Wales (NRW) for licences to take eggs for scientific purposes. We also thank Professor Ben Hatchwell and the referees for comments on the manuscript.

Competing interests

No competing interests declared.

Author contributions

T.R.B. conceived the study, D.J., J.E.T., N.H. and T.R.B. conceived and planned the experiments. D.J. and J.E.T. carried out the experiments. D.J. and J.E.T. analysed the data. D.J. took the lead in writing the manuscript with support and input from T.R.B., N.H. and J.E.T.

Funding

This work was funded by a grant from the Leverhulme Trust to T.R.B. and a University of Sheffield Postgraduate Scholarship to D.J. N.H. was supported by a Patrick & Irwin-Packington Fellowship from the University of Sheffield and a Royal Society Dorothy Hodgkin Fellowship.

Data availability

Data are available in the supplementary material (Datasets 1 & 2).

Supplementary information

Supplementary information available online at:
http://jeb.biologists.org/lookup/doi/10.1242/jeb.188466.supplemental (see Appendix A5).

References

Ar, A., (1991). Roles of water in avian eggs. In: *Egg Incubation: Its effect on embryonic development in birds and reptiles* (eds. Deeming, D. C. and Ferguson, M. W. J.). Cambridge, UK: Cambridge University Press. pp. 229- 244.

Ar, A. and Deeming, D. C., (2009). Roles of water and gas exchange in determining hatchability success. *Avian Biology Research*. **2**(1/2), 61–66.

Ar, A., Paganelli, C. V., Reeves, R. B., Greene, D. G. and Rahn, H., (1974). The Avian Egg: Water Vapor Conductance, Shell Thickness, and Functional Pore Area. *The Condor*. **76**(2), 153–158.

Ar, A. and Rahn, H., (1985). Pores in avian eggshells: Gas conductance, gas exchange and embryonic growth rate. *Respiration Physiology.* **61**(1), 1–20.

Birkhead, T. R., (1977). The Effect of Habitat and Density on Breeding Success in the Common Guillemot (*Uria aalge)*. *The Journal of Animal Ecology.* **46**(3), 751-764.

Birkhead, T. R., (1993). *Great Auk Islands*. London, UK: Poyser.

Birkhead, T. R., (2016). *The Most Perfect Thing: the Inside (and Outside) of a Bird's Egg.* London, UK: Bloomsbury.

Birkhead, T. R., Thompson, J. E., Jackson, D. and Biggins, J. D., (2017). The point of a Guillemot's egg. *Ibis.* **159**(2), 255-265.

Birkhead, T. R., Thompson, J. E. and Montgomerie, R., (2018). The pyriform egg of the Common Murre (*Uria aalge*) is more stable on sloping surfaces. *The Auk*. **135**(4), 1020-1032.

Board, R. G., (1981). The microstructure of avian eggshells, adaptive significance and practical implications in aviculture. *Wildfowl.* **32**, 132–136.

Board, R. G., (1982). Properties of avian egg shells and their adaptive value. *Biological Reviews.* **57**(1), 1–28.

Board, R. G. and Fuller, R., (1994). *Microbiology of the Avian Egg.* London, UK: Chapman and Hall.

Board, R. G. and Halls, N. A., (1973a). The cuticle: A barrier to liquid and particle penetration of the shell of the hen's egg. *British Poultry Science.* **14**(1), 69-97.

Board, R. G. and Halls, N. A., (1973b). Water uptake by eggs of mallards and guinea fowl. *British Poultry Science.* **14**(3), 311-314.

Board, R. G. and Perrott, H. R., (1982). The fine structure of the outer surface of the incubated eggshells of the Helmeted guinea fowl (*Numidia meleagris*). *The Journal of Zoology.* **196**(4), 445–451.

Board, R. G., Perrott, H. R., Love, G. and Scott, V. D., (1984). The phosphate- rich cover on the eggshells of grebes (Aves: Podicipitiformes). *Journal of Zoology.* **203**(3), 329–343.

Board, R. G. and Scott, V. D., (1980) Porosity of the Avian Eggshell. *American Zoologist.* **20**, 339-349.

Board, R. G., Tullett, S. G. and Perrott, H. R., (1977). An arbitrary classification of the pore systems in avian eggs. *Journal of Zoology.* **182**(2), 251–265.

D'Alba, L., Jones, D. N., Badawy, H. T., Eliason, C. M. and Shawkey, M. D., (2014). Antimicrobial properties of a nanostructured eggshell from a compost-nesting bird. *The Journal of Experimental Biology*. **217**(7), 1116-1121.

D'Alba, L., Torres, R., Waterhouse, G. I. N., Eliason, C., Hauber, M. E. and Shawkey, M. D., (2017). What Does the Eggshell Cuticle Do? A Functional Comparison of Avian Eggshell Cuticles. *Physiological and Biochemical Zoology.* **90**(5), 588-599.

Deeming, D. C., (1987). Effect of cuticle removal on the water vapour conductance of egg shells of several species of domestic bird. *British Poultry Science*. **28**(2), 231-237.

Deeming, D. C., (2002). *Avian Incubation: Behaviour, Environment and Evolution.* Oxford, UK: Oxford University Press.

Deeming, D. C., (2006). Ultrastructural and functional morphology of eggshells supports idea that dinosaur eggs were incubated buried in a substrate. *Paleontology.* **49**(1), 171-185.

Deeming, D. C. and Mainwaring, M. C., (2016). Functional properties of nests. In *Nests, eggs and incubation: new ideas about avian reproduction* (eds. Deeming, D. C. and Reynolds, S. J.). Oxford, UK: Oxford University Press. pp 29-49.

Deeming, D. C. and Reynolds, S. J. (2016). *Nests, eggs and incubation: new ideas about avian reproduction.* Oxford, UK: Oxford University Press.

Ensikat, H. J., Ditsche-Kuru, P., Neinhuis, C. and Barthlott, W., (2011). Superhydrophobicity in perfection: the outstanding properties of the lotus leaf. *Beilstein Journal of Nanotechnology.* **2,** 152–61.

Fecheyr-Lippens, D. C., Igic, B., D'Alba, L., Hanley, D., Verdes, A., Holford, M., Waterhouse, G. I. N., Grim, T., Hauber, M. E. and Shawkey, M. D., (2015). The cuticle modulates ultraviolet reflectance of avian eggshells. *Biology Open.* **4**(7), 753-759.

Genzer, J. and Marmur, A., (2008). Biological and Synthetic Self- Cleaning Surfaces. *MRS bulletin.* **33**(8), 742– 746.

Gole, V. C., Chousalkar, K. K., Roberts, J. R., Sexton, M., May, D., Tan, J. and Kiermeier, A., (2014a). Effect of Egg Washing and Correlation between Eggshell Characteristics and Egg Penetration by Various *Salmonella* Typhimurium Strains. *PLoS ONE.* **9**(3), e90987.

Gole, V. C., Roberts, J. R., Sexton, M., May, D., Kiermeier, A. and Chousalkar, K. K., (2014b). Effect of egg washing and correlation between cuticle and egg penetration by various *Salmonella* strains. *International Journal of Food Microbiology.* **182-183**, 18–25.

Hoyt, D. F., Board, R. G., Rahn, H. and Paganelli, C. V., (1979). The Eggs of the Anatidae: Conductance, Pore structure, and Metabolism. *Physiological Zoology***. 52**(4), 438-450.

Igic, B., Fecheyr-Lippens, D., Xiao, M., Chan, A., Hanley, D., Brennan, P. R. L., Grim, T., Waterhouse, G. I. N., Hauber, M. E. and Shawkey, M. D., (2015). A nanostructural basis for gloss of avian eggshells. *Journal of The Royal Society Interface.* **12**(103), 20141210.

Ishikawa, S. I., Suzuki, K., Fukuda, E., Arihara, K., Yamamoto, Y., Mukai, T. and Itoh, M., (2010). Photodynamic antimicrobial activity of avian eggshell pigments. *FEBS letters.* **584**(4), 770-774.

Jaeckle, W. B., Kiefer, M., Childs, B., Harper, R. G., Rivers, J. W., and Peer, B. D., (2012). Comparison of eggshell porosity and estimated gas flux between the brown-headed cowbird and two common hosts. *Journal of Avian Biology*. **43**(6)**,** 486-490.

Lahti, D. C. and Ardia, D. R., (2016). Shedding Light on Bird Egg Color: Pigment as Parasol and the Dark Car Effect. *The American Naturalist.* **187,** 547–563.

Lang, M. R. and Wells, J. W., (1987). A Review of eggshell pigmentation. *World's Poultry Science Journal.* **43**(3), 238–246.

Manuwal, D. A., Carter, H. R., Zimmerman, T. S. and Orthmeyer, D. L., (2001). *Biology and conservation of the common murre in California, Oregon, Washington, and British Columbia. Vol. 1. Natural history and population trends*. US Geological Survey Biological Resources Division Information and Technology Report USGS/BRD/ITR-2000-0012. Washington, DC, USA.

Maurer, G., Portugal, S. J. and Cassey, P., (2012). A comparison of indices and measured values of eggshell thickness of different shell regions using museum eggs of 230 European bird species. *Ibis.* **154**(4), 714–724.

Maurer, G., Portugal, S. J., Hauber, M. E., Mikšík, I., Russell, D. G. D. and Cassey, P., (2015). First light for avian embryos: eggshell thickness and pigmentation mediate variation in development and UV exposure in wild bird eggs. *Functional Ecology.* **29**(2), 209–218.

Mayani-Parás, F., Kilner, R. M., Stoddard, M. C., Rodríguez, C. and Drummond, H., (2015). Behaviorally Induced Camouflage: A New Mechanism of Avian Egg Protection. *The American Naturalist.* **186**(4), E91–E97.

Mikhailov, K. E., (1997). *Avian eggshells: an atlas of scanning electron micrographs.* Hertfordshire, UK: British Ornithologists' Club Occasional Publications 3.

Nettleship, D. N. and Birkhead, T. R., (1985). *The Atlantic Alcidae: the evolution, distribution and biology of the auks inhabiting the Atlantic Ocean and adjacent water areas*. London, UK: Academic Press Inc.

Portugal, S. J., Bowen, J. and Riehl, C., (2018). A rare mineral, vaterite, acts as a shock absorber in the eggshell of a communally nesting bird. *Ibis.* **160**(1), 173-178.

Portugal, S. J., Maurer, G. and Cassey, P., (2010). Eggshell Permeability: A Standard Technique for Determining Interspecific Rates of Water Vapor Conductance. *Physiological and Biochemical Zoology.* **83**(6), 1023–1031.

R Development Core Team, (2016). R: A Language and Environment for Statistical Computing. Vienna: R Foundation for Statistical Computing. Available at: http://www.R-project.org/

Rahn, H., (1991). Why birds lay eggs. In: *Egg Incubation: Its effect on embryonic development in birds and reptiles* (Ed. Deeming, D. C. and Ferguson, M. W. J.). Cambridge, UK: Cambridge University Press. pp. 345-360.

Rahn, H., Krog, J. and Mehlum, F., (1983). Microclimate of the nest and egg water loss of the Eider *Somateria mollissima* and other waterfowl in Spitsbergen. *Polar Research.* **1**(2), 171–183.

Rahn, H. and Paganelli, C. V., (1990). Gas fluxes in avian eggs: Driving forces and the pathway for exchange. *Comparative Biochemistry and Physiology Part A: Physiology*. **95**(1), 1-15.

Rokitka, M. A. and Rahn, H., (1987). Regional differences in shell conductance and pore density of avian eggs. *Respiration Physiology.* **68**(3), 371–376.

Samiullah, S. and Roberts, J. R., (2014). The eggshell cuticle of the laying hen. *World's Poultry Science Journal*. **70**(4), 693-708.

Simkiss, K., (1986). Eggshell conductance—Fick's or Stefan's law? *Respiration physiology*. **65**(2), 213-222.

Sparks, N. H. C. and Board, R. G., (1984). Cuticle, shell porosity and water uptake through hens' eggshells. *British Poultry Science.* **25**(2), 267-276.

Tazawa, H., Mikami, T. and Yoshimoto, C., (1971). Effect of reducing the shell area on the respiratory properties of chicken embryonic blood. *Respiration Physiology.* **13**(3), 352–360.

Thompson, M. B. and Goldie, K. N., (1990). Conductance and Structure of Eggs of Adelie Penguins, *Pygoscelis adeliae*, and Its Implications for Incubation. *The Condor*. **92**(2), 304–312.

Tøien, Ø., Paganelli, C. V., Rahn, H. and Johnson, R. R., (1988). Diffusive resistance of avian eggshell pores. *Respiration Physiology.* **74**(3), 345–354.

Tschanz, B., (1990). Adaptations for Breeding in Atlantic Alcids. *Netherlands Journal of Zoology.* **40**(4), 688–710.

Tullett, S. G., Board, R. G., Love, G., Perrott, H. R. and Scott, V. D., (1976). Vaterite Deposition During Eggshell Formation in the Cormorant, Gannet and Shag, and in 'Shell-less' Eggs of the Domestic Fowl. *Acta Zoologica.* **57**(2), 79-87.

Tyler, C., (1969). The snapping strength of the egg shells of various orders of birds. *Journal of Zoology.* **159**(1), 65–77.

Verbeek, N. A. M., (1984). The Effects of Adult Fecal Material on Egg Hatchability in Glaucous-Winged Gulls (*Larus glaucescens*). *The Auk.* **101**(4), 824–829.

Vorobyev, A. Y. and Guo, C., (2015). Multifunctional surfaces produced by femtosecond laser pulses. *Journal of Applied Physics.* **17**, 033103.

Wellman-Labadie, O., Picman, J. and Hincke, M. T., (2008). Antimicrobial activity of the Anseriform outer eggshell and cuticle. *Comparative Biochemistry and Physiology Part B: Biochemistry and Molecular Biology.* **149**(4), 640–649.

Yuan, Y. and Lee, T. R., (2013). Contact angle and wetting properties. In: *Surface Science Techniques* (Ed. Bracco, G. and Holst, B.). Heidelberg Berlin, Germany: Springer. pp 3-34.

Zimmermann, K. and Hipfner, J. M., (2007). Egg Size, Eggshell Porosity, and Incubation Period in the Marine Bird Family Alcidae. *The Auk.* **124**(1), 307–315.

Chapter 5:

Dark blue-green common guillemot eggshells have rougher surfaces than white eggshells

Dark blue-green common guillemot eggshells have rougher surfaces than white eggshells

Duncan Jackson[1*], Nicola Hemmings[1] and Timothy R. Birkhead[1]

[1]*Department of Animal & Plant Sciences, University of Sheffield, Sheffield, S10 2TN, UK*

*Corresponding author. Email: djackson3@sheffield.ac.uk

Key words

Structural colour, Pigment, X-ray micro-computed tomography, Eggshell thickness, Microstructure, Incubation.

Abstract

Despite much recent interest in avian eggshell traits, eggshell surface microstructure has rarely been studied. The common guillemot (*Uria aalge*) represents an exception: eggshells of this species have a surface made up of peaks and troughs which has received considerable attention. It was initially hypothesised that this surface roughness conferred self-cleaning properties to the egg through increasing hydrophobicity, but this has since been disproved. It remains unclear why laying an egg with a rough shell surface would be beneficial. Eggshell surface structure may influence the egg's visual appearance, altering UV reflectance or gloss. Eggshell microstructure may also contribute to egg colour by influencing how light is absorbed or reflected. Here, we use X-ray micro-computed tomography and optical microscopy to investigate how eggshell colour relates to surface structure and eggshell thickness in the common guillemot, a species with remarkable variation in egg colouration. We reveal considerable variation in eggshell surface topography both within and between guillemot eggs, with darker coloured eggs tending to have a rougher shell surface than paler eggs, and dark patches of pigment pattern within the shell surface layers often being associated with areas of localised roughness. We find that within an individual egg, thicker regions of the shell (usually the equator) have the greatest surface roughness and are darker. Between eggs, thicker shells typically have greater surface roughness, however, there is no association between colour and shell thickness. Finally, we find consistent patterns of surface roughness along guillemot eggs, with the equator – the region that primarily interacts with the incubation substrate and bird's brood patch – tending to be roughest. We discuss the implications of our results for the adaptive significance of eggshell surface structure in birds.

Introduction

The avian eggshell is a remarkable bio-ceramic that ensures the developing embryo is protected in a wide range of environments (Board 1982; Deeming 2002; Deeming & Reynolds 2016). The eggshell is broadly made up of three components: the organic membranes on the inner surface of the shell, the calcium carbonate shell itself, and a layer of shell accessory materials that coat the shell's surface (Board & Scott 1980; Sparks 1994). While the shell accessory materials are relatively well studied (see D'Alba *et al.* 2017; Jackson *et al.* 2018; Chapter 4), little is known about how and why the underlying shell surface varies within and between species.

To date, there have been few detailed observations of avian eggshell surface microstructure. The few studies that do exist provide a qualitative assessment only (e.g. Harrison 1966; Mikhailov 1997) and/or comment on apparent species-specific structures such as holes in the shell surface called pits or crypts (Becking 1975; Kern *et al.* 1992; Martín-Vivaldi *et al.* 2014; Fecheyr-Lippens *et al.* 2015), or surface protrusions, such as nodes (Grellet-Tinner *et al.* 2017), cones (S. Portugal, unpublished https://phys.org/news/2013-07-unique-shell-guillemot-eggs-edge.html & https://www.nationalgeographic.com/science/phenomena/2013/07/04/scientist-spills-water-discovers-self-cleaning-bird-egg/), granulations (Tyler & Simkiss 1959), ridges (Harrison 1966), domes (Board & Tullett 1975; Tullett 1984) and pimples or peaks (Birkhead 2016). The lack of detailed intraspecific and comparative studies of eggshell microstructure leave a gap in our understanding of how surface structure varies both within and between species.

One important aspect of the calcium carbonate shell's surface is its roughness. Roughness can be quantified in various ways (see Materials and Methods), but it is essentially a measure of surface texture complexity resulting from morphological variation in surface structure. Rough shell surfaces are likely caused by non-uniform termination of eggshell growth which results in unequal calcium carbonate crystal column heights and an irregular (not flat) surface (Tyler 1969). Becking (1975) noted that the outer most crystalline layer of the calcium carbonate shell (the vertical crystal layer) is not uniform, and instead polygonal fields of differently oriented crystals create patterns that result in

characteristic differences in eggshell surface texture between avian families. Such differences in surface texture and roughness may be ecologically adaptive. In other biological materials, rough surfaces are known to influence water repellency (hydrophobicity) or adhesion properties (Genzer & Marmur 2008), and can even trap air over a shell surface allowing gas exchange to be maintained when reptile eggs are wet (specifically, *Caiman latirostris;* Cedillo-Leal *et al.* 2017). Any adaptive significance of avian eggshell roughness currently remains unknown.

Surface roughness could play a role in structural colour in bird eggs. Eggshell colour is broadly comprised of two elements: (1) the base (or background) colour of the shell and (2) the pigment patterns that exist in or on top of the shell surface often referred to as speckling, streaking, marking, pencilling, spottiness or maculation. Despite variation in eggshell colour and pattern being well documented across bird species, it remains unclear exactly how the final colour of an egg is produced. Two main classes of pigments, porphyrins (specifically, protoporphyrin IX) and biliverdins, are related to egg colouration in birds (Kennedy & Vevers 1976; Mikšík *et al.* 1996; Gorchein *et al.* 2009). Both pigments relate to base eggshell colour, with biliverdin producing blue-green tones and protoporphyrin responsible for red-yellow-brown-black tones (Harrison 1966; Kennedy & Vevers 1976). Their interactions with each other, and with the eggshell matrix, can produce many different colours (Sparks 2011; Hanley *et al.* 2015). Since pigment patterns (i.e. lines, blotches etc) on many species' eggs are dark rusty brown, protoporphyrin presumably plays a more prominent role in eggshell patterning, however biliverdin may also be involved (Kennedy & Vevers 1976; Sparks 2011; Brulez *et al.* 2014; Hauber *et al.* 2019). Although these pigments could explain a wide range of variation in egg colour seen in nature (Cassey *et al.* 2010; Igic *et al.* 2011; Hanley *et al.* 2015), the concentration of these pigments found within eggshells does not always fully explain all the variation in egg base colour and patterning observed within (Butler & Waite 2016; Hauber *et al.* 2019) and between species (Brulez *et al.* 2016). Some eggs that are the same colour have even been found to contain different amounts of pigment (Dainson *et al.* 2018).

The fact that measured pigment concentrations do not fully explain egg colour may be due to two key reasons. First, although pigment is distributed throughout the eggshell (Tyler 1964; Harrison 1966; Tyler 1969; Mikhailov 1997), it is likely only the pigment found

in the surface layers of the shell that contribute to its external base colour as well as potentially to pattern colour. However, studies of eggshell pigments typically sample the entire thickness of the shell, not just the surface layers, so data obtained may not reflect the true external colour of the shell (e.g. Brulez *et al.* 2014; Brulez *et al.* 2016). Second, the nano- and microstructural roughness of the eggshell surface may also play an important role in eggshell appearance and colour, by influencing how light is absorbed, transmitted and reflected by the surface. A rough surface, for example, may absorb light more readily than a smooth surface, resulting in a darker colouration.

Surface roughness and egg colour are likely to be influenced by the shell accessory materials, which are present on the eggs of many (but not all) bird species and cover the surface of the crystalline shell (Board & Scott 1980; Board 1982; Sparks 1994; Mikhailov 1997; Igic *et al.* 2015). Shell accessory materials vary in thickness, form, and surface coverage and contain a range of chemical compounds which form an inorganic cover, organic cuticle, or composite organic layer that contains inorganic elements, such as “cuticular spheres” (Board & Scott 1980; Board 1982; Sparks 1994; Kusuida *et al.* 2011; D’Alba *et al.* 2014; D’Alba *et al.* 2016). As a result, shell accessory materials can have a range of protective and regulatory roles (see D’Alba *et al.* 2017; Jackson *et al.* 2018; Chapter 4 for examples) and can also alter egg aesthetics (Lang & Wells 1987; Sparks 1994; Deeming 2011; Sparks 2011).

Shell accessory materials may contain white inorganic compounds, such as vaterite – a polymorph of calcium carbonate (Harrison 1966; Tullett *et al.* 1976; Riehl 2010; Portugal *et al.* 2018; Hauber *et al.* 2018) – or calcium phosphate (Board 1981) as well as pigments (Sparks 1994; Deeming 2011; Samiullah & Roberts 2013; Samiullah & Roberts 2014), all of which may alter base egg colouration and/or the colour of any patterning. Shell accessory materials form a thin (and sometimes translucent) layer and therefore could also influence colour through thin-film interference (Richards & Deeming 2001). Shell accessory materials may also act to smooth the shell, altering an egg’s appearance by influencing how glossy, and potentially iridescent, it is (Igic *et al.* 2015), and affecting its UV reflectance (Fecheyr-Lippens *et al.* 2015; D’Alba *et al.* 2017). Both shell accessory materials and the roughness of the underlying crystalline shell surface may therefore influence an eggshell’s base colour through structural mechanisms in addition to

pigments present in the shell and/or shell accessory materials. Any patterns are then determined by patches of pigment typically distinct from the eggshell base colouration found within the outer surface of the calcium carbonate shell and/or in/on the shell accessory material layer (Harrison 1966; Sparks 1994; Sparks 2011).

Here, we use optical microscopy and X-ray micro-computed tomography (microCT) to examine whether eggshell surface microstructure is related to egg colouration and shell thickness in the common guillemot, a species known for its rough shell surface and large variation in egg colouration (Tschanz 1990; Birkhead 2016). It was initially hypothesised that this surface roughness conferred self-cleaning properties to the guillemot's egg, but this has since been disproved (Jackson *et al.* 2018; Chapter 4). Egg base colour and patterning in the common guillemot is partially driven by pigment composition and concentration, but eggshell microstructure may also contribute to an egg's perceived colour (Hauber *et al.* 2019). We also assess how surface structure varies along the egg, predicting that because the equatorial region of the egg is frequently in contact with the abrasive incubation substrate, this region will have the greatest surface roughness potentially to minimize abrasion and wear.

Materials and Methods

Samples

We used a total sample of 55 common guillemot eggs collected under licence from Skomer Island, UK (2014 – 2018) and Ireland (2017 – 2018; see Chapter 2 & Appendix A3 for further details). We chose to study freshly collected eggshells instead of historical museum samples because it is often unclear how they have previously been cleaned. Chemicals and abrasive scrubbing methods historically used to clean eggs in collections can damage the shell surface, either by removing shell accessory material and pigment, or damaging/removing/flattening any surface texture (Kennard 1921; Prynne 1963; Hill 2008; Portugal *et al.* 2010). Damage can also occur due to excessive handling of eggshell specimens (Becking 1975). Although guillemot eggs were initially selected from a larger sample to represent a spectrum of shapes and sizes for Chapter 2, they were not selected according to their colour or shell surface structure and the sample used here

should therefore be considered reasonably random with respect to these traits. Egg shape (elongation, asymmetry, and tapering at the pointed end) and size (volume, cm^3) of the eggs were measured using the methods of Biggins *et al.* (2018) in Chapter 2. Eggs were emptied of their contents and rinsed with distilled water and stored in low humidity conditions to minimise fungal growth. Fragments of approximately 0.5 – 1 cm^2 were cut from the blunt, equator and pointed regions of eggshells (See Fig. S4 in Chapter 2) using a hand-held rotary saw. Fragments were not washed before microCT scanning to avoid cracking caused by drying of the rehydrated membrane (D.J. Pers. Obs.).

MicroCT scanning and shell thickness measurement

Eggshell fragments were scanned in a Bruker Skyscan 1172 set to 49kV electron acceleration energy and 179uA current (for further details see Chapter 2). To obtain effective eggshell thickness, shell fragment image stacks (reconstructed microCT data) were loaded into CT analyser (CTAn, version 1.14.41; Bruker micro-CT, Kontich, Belgium) and the thickness from the point of fusion of the mammillary bodies to the outer exterior surface of the shell was measured using the line measurement tool at 10 locations throughout the shell. An average value for each eggshell fragment was used for analysis (data from Chapter 2). We also measured the thickness of the mammillary layer as the distance from the point of fusion of the mammillary bodies to the tip of the mammillary body on the interior surface of the shell at 10 locations. An average value for each eggshell fragment was used for analysis.

Creating and measuring height maps

The advantage of using microCT to analyse the structure and roughness of the calcium carbonate shell's surface is that it does not require chemical or physical removal of any shell accessory material, which would likely damage the eggshell surface, as other common surface analysis methods do (e.g. scanning electron microscopy, extended depth of field microscopy, light interferometry or contact profilometers such as atomic force microscopy or a stylus profilometer). Instead, the shell accessory materials can be removed from reconstructed microCT images using image processing and segmentation techniques.

We developed a simple workflow to create height maps where the grey (or colour) scale represents the height (Z dimension) of surface structures, from regions of interest of reconstructed microCT image stacks. Images were loaded into ImageJ (Schneider *et al.* 2012) and 1mm^2 areas were selected using the specify selection tool on orthogonal views of the eggshell fragment. The selected eggshell area was levelled as much as possible by rotating the data in all dimensions in ImageJ. We avoided sampling especially rough areas of shell that appeared to be unrepresentative of the fragment's surface as a whole (see Results), and where possible, excluded gas exchange pores from the sampling area as their size (X – Y dimensions) and depth (Z dimension) can create biases in roughness measures. We also avoided areas with excessive debris (such as dense fish bones) on the shell that could not be removed during segmentation of the surface of the shell or through digital image noise removal (i.e. de-speckling and outlier removal in ImageJ). The 1mm^2 stack was shortened to contain only images that covered the surface.

We segmented the surface from the rest of the eggshell and the surrounding low density materials (e.g. polystyrene and/or air) using manual thresholds in ImageJ (i.e. by selecting grey scale pixel values that represented only the shell surface). This allowed us to produce a binary stack of images that represented the outer surface of the crystalline shell only, as any shell accessory material or debris on the surface was excluded during the segmentation process. The resultant binary image stack was used to create a height map using the z-project function (average intensity option) in ImageJ. Because the stack contained only binary images (e.g. each pixel was white or black) a single image output was produced by the z-project function where the highest point on the surface was white and the lowest point was black with pixels of intermediate height values occupying an intermediary grey scale value depending on their height. The height map image underwent two rounds of despeckle in ImageJ to remove any significant digital noise in the image before being saved as a TIFF file.

Height maps were loaded into Gwyddion (Nečas & Klapetek 2012) and manually resized so that the length and width equalled 1mm and Z height was the resolution (4µm) multiplied by the number of images in the stack followed by subtracting 1 to level the data to zero. In Gwyddion, we removed polynomial background (value of 3 in both degrees) and levelled the data by mean plane subtraction to remove bias caused by curvature or

tilt of the eggshell. The minimum data value was shifted to zero before the statistical quantities tool was used to obtain roughness parameters over the entire area. Although multiple roughness parameters were recorded, one particular parameter was our main variable of interest; the surface area of the shell. Since all fragments were 1mm^2, values above 1mm^2 indicated that the surface was not flat or smooth but had texture and structure. The higher the surface area value, the rougher a surface is. This parameter is more useful than mean surface roughness (Sa) in assessing eggshell surface structure because the surface area encapsulates variation in all three (X, Y and Z) dimensions, whereas mean surface roughness (Sa) is primarily a measure of variation in the Z-height profile of a surface. Unlike Ra, the arithmetical mean deviation of the assessed profile, Sa is calculated over an entire 3D surface rather than over a single 2D height profile. Here, when we discuss “roughness” we are referring to variation in surface area unless specified otherwise. We also recorded the maximum height of the surface, peak height, and pit depth as well as values for skewness and kurtosis of the surfaces. Skewness (Ssk) is a measure of the degree of bias in the roughness shape and indicates whether a surface is primarily made up of peaks (> 0) or valleys (< 0). Kurtosis (Sku) is a measure of how sharp the roughness (height) profile is and indicates if the surface has any inordinately high peaks or deep valleys (> 3).

We qualitatively assessed variation in surface structure and roughness within eggshell fragments using 3D volumetric reconstructions in CTVox (version 3.0; Bruker micro-CT, Kontich, Belgium). In addition to microCT, we used optical microscopy to qualitatively assess the influence shell accessory materials had on the final surface texture of the eggshell and to further assess causes of variation in surface structure within eggshell fragments. Eggshell fragments were optically imaged on a Nikon SMZ25 stereoscopic microscope using fixed lighting (goose neck lights clamped in a bespoke mount). Where possible, eggshell fragments were manually levelled prior to imaging to limit the influence of curvature on the resulting images.

Measuring eggshell colour

Common guillemot eggshell fragments were imaged on a grey card under standardised lighting (4600K, 100% power using a Viltrox LED light panel) using an Olympus OM-D

Em-5 with an Olympus 60mm macro lens. ISO 200, F14 and manual white balance (4600k) were used with a flexible shutter speed to allow for any potential variation in lighting due to changes in the battery level of the LED light source. RAW images were opened in Adobe Photoshop CC 2018 and the white balance and exposure were corrected using the grey card, ensuring an RGB value of 128, 128, 128 was obtained close to the areas of the eggshell that would be measured. Due to the position of the light source and curvature of the eggshell, lighting was sometimes unavoidably uneven over the fragments, therefore we deliberately measured a transect along the central portion of the shell (horizontally) where the lighting was even. Using the eyedropper tool (with a radius of 5 pixels) in Adobe Photoshop, 10 areas of eggshell were measured using the L*a*b* colour scale. We avoided dark pigment, dirt, stains, damage and specular (gloss) highlights, and shadows to achieve a representative set of measurements of the eggshell's base colouration. We averaged 10 measurements to obtain a mean value for L* (lightness; 100 white, 0 black), a* (negative values green, positive values red/magenta) and b* (negative values blue, positive values yellow) for each eggshell fragment.

Statistical analysis

All statistical analyses performed in R version 3.5.1 (R Core Team 2018). Due to concerns over the presence of potential outliers in our data, and in some cases violations of bivariate normality, Spearman's rank correlations were performed to investigate the relationships between eggshell thickness, colour and surface structure across all common guillemot eggshell fragments and egg regions. Repeated measures correlations (Rmcorr package; Bakdash & Marusich 2017) were used to assess correlations within eggs (controlling for egg identity) and between eggs (controlling for regional variation in egg traits). Mixed effects (lme4 package; Bates *et al.* 2015) and generalized linear models are presented in the supplementary materials to complement correlations. Repeated measures ANOVAs with egg identity as a factor were used to assess regional variation in egg colour and surface texture in common guillemot eggs. To explore which regions differed, post-hoc tests using Tukey contrasts were performed on linear mixed effects models that controlled for egg identity using the nlme (Pinheiro *et al.* 2018) and multcomp (Hothorn *et al.* 2008) packages. Eggs (or eggshell fragments) that were deemed too dirty to accurately measure colour were removed from analyses.

Results

Within egg variation in eggshell surface structure and colour

Surface topography, and thus roughness, was not uniform along individual common guillemot eggshells. The shell of common guillemot eggs is thickest at the equator (Birkhead *et al.* 2017; Chapter 2), and we found this region to also possess the roughest surface (higher surface area) and darkest colouration compared to the blunt and pointed ends (Table 1; Fig. 1). We also found that along an egg, darker and/or bluer areas of shell were typically thicker and that thicker and/or darker shells were rougher (Table 2).

Surface structure varied even within eggshell fragments (Fig. S1), some areas with pigment pattern (i.e. black/grey/brown patches) were especially rough and more frequently possessed small protruding peaks compared to other areas with base colouration only (e.g. blue/green/white/beige; Fig. 2 & S2). Some pigment patches that contribute to patterning also appeared “sunken” into the shell surface and were lower than the surrounding surface texture (Fig. 2 & S1). Rougher areas appeared to be associated with patches of pigment pattern that occur within the surface layers of the calcium carbonate shell, rather than on top of the shell or within/on top of the main shell accessory material layer (Fig. 2 & S1 – S4). Pigment patches within the shell often appear paler than pigment pattern within/on top of the shell accessory material layer, probably because white calcium carbonate crystals cover and obscure the former pigment patches (Fig. 2, S2 & S3).

Between egg variation in eggshell surface structure, effective thickness and colour

Surface topography between common guillemot eggshells varied considerably, ranging from surfaces that were relatively smooth and flat, to those that were rough with structures of varying widths, shapes, and heights (Fig. 3). Variation in the crystalline shell surface area correlated with all three colour measures (significantly with L*, a*, and approaching significance for b*; Table 3), thus darker (negative L*), greener (negative a*) and perhaps bluer (negative b*) eggshell fragments tended to be rougher (Fig. 4). After

Table 1. Regional variation in common guillemot eggshell colour and surface structure.

Variable	Region of the egg (mean ± SD)			Pattern[1]	F (d.f.)	p (*adjusted)
	Blunt	Equator	Point			
L* (lightness)	74.7 ± 10.3	73.1 ± 10.1	76.6 ± 8.6	**P > B > E**	$15.0_{(2,82)}$	< 0.001 (< 0.001)
a*	-5.25 ± 4.51	-5.78 ± 4.70	-5.55 ± 4.55	B = E = P	$2.24_{(2,82)}$	0.113
b*	3.97 ± 4.13	3.19 ± 5.11	3.45 ± 4.43	**B > E, P = E, B = P**	$3.19_{(2,82)}$	0.047
Surface area (mm^2) (Box-Cox transformed data)	1.24 ± 0.14	1.30 ± 0.18	1.21 ± 0.12	**E > P, E > B, B = P**	$19.3_{(2,108)}$	< 0.001
Mean roughness, Sa (µm) (ln transformed data)	5.56 ± 2.08	5.91 ± 1.90	5.51 ± 1.65	E = B = P	$2.71_{(2,108)}$	0.071
Residual surface area (mm)	-0.0025 ± 0.0294	0.0141 ± 0.0281	-0.0116 ± 0.0299	**E > B > P**	$26.8_{(2,108)}$	< 0.001
Skew	-0.423 ± 0.281	-0.487 ± 0.222	-0.468 ± 0.266	B = P = E	$1.33_{(2,108)}$	0.269
Kurtosis, Sku (Box-Cox transformed data)	3.75 ± 0.87	3.51 ± 0.47	3.56 ± 0.73	B = P = E	$1.42_{(2,108)}$	0.245
Max height (µm) (Box-Cox transformed)	60.0 ± 29.8	57.1 ± 17.0	54.2 ± 17.2	B = E = P	$1.12_{(2,108)}$	0.329
Max peak height (µm) (Box-Cox transformed)	23.8 ± 11.2	22.8 ± 6.0	21.9 ± 6.5	B = E = P	$0.72_{(2,108)}$	0.487
Max pit depth (µm) (Box-Cox transformed)	36.1 ± 20.9	34.3 ± 12.4	32.3 ± 12.3	B = E = P	$1.14_{(2,108)}$	0.325

n = 55 eggs except for colour (L*, a*, b*) where n = 42 (dirty eggs excluded). Some variables were transformed to reduce skew and normalise their distribution.

[1] B = blunt end, E = equator and P = pointed end. Bold patterns are significant; > or < indicate $p < 0.05$ (post-hoc tests with Tukey contrasts).

*adjusted p-values (Greenhouse-Geisser) if sphericity assumption not met using the ezANOVA function in the ez package (Lawrence 2016).

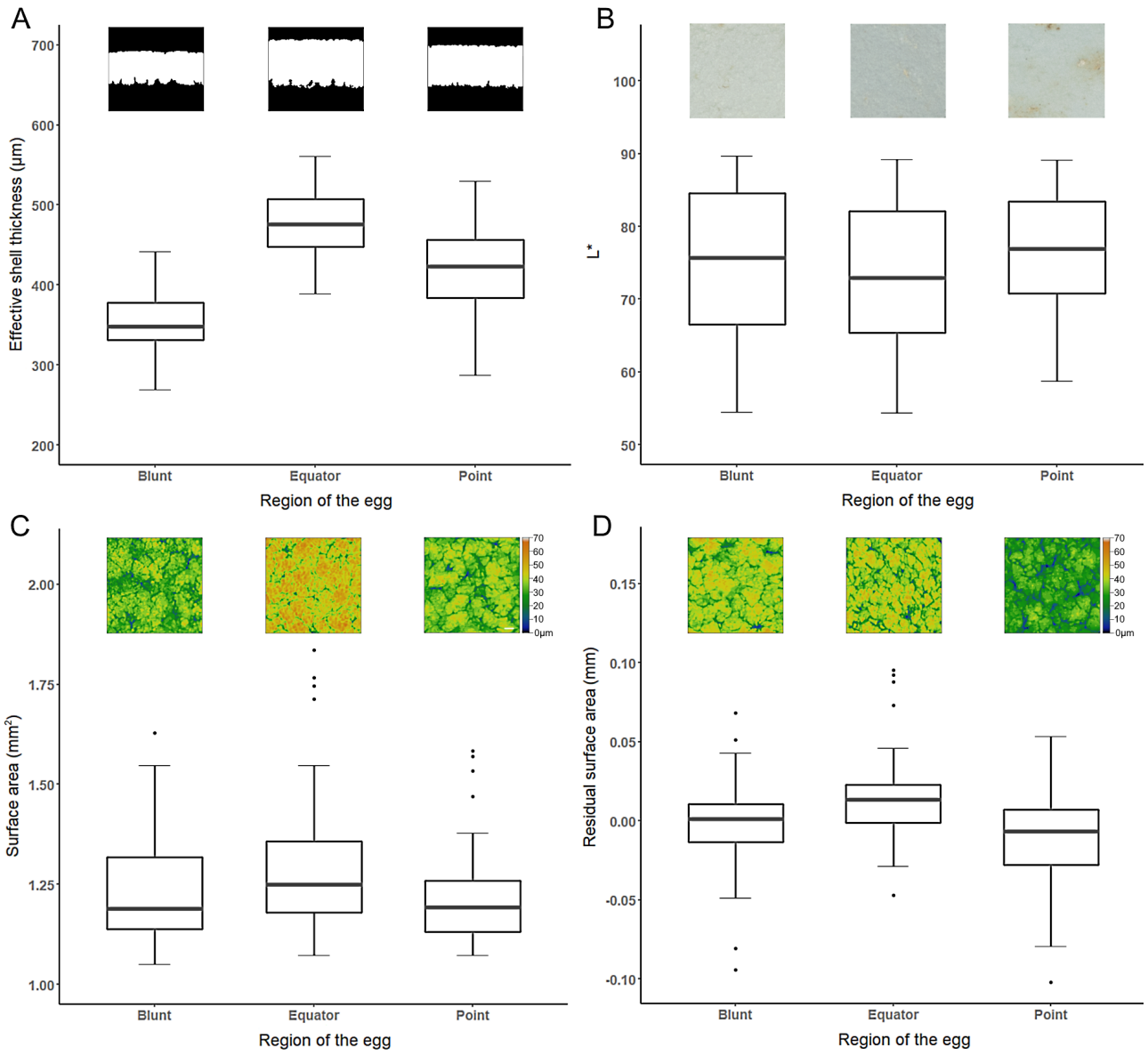

Figure 1. Regional variation in effective eggshell thickness (A), colour (L* scale – lightness, B), and surface structure complexity – actual surface area (C) and residual surface area (D) (see Results). Significant differences and statistics can be found in Chapter 2 (effective thickness) and Table 1. Each set of images above each box plot were selected to represent the median differences between each region in a single egg. Height maps are 1mm^2, scale bar = 100µm and eggshell thickness images are 1mm in length. Images illustrating colour variation on the L* graph are from the same egg and not to scale.

Table 2. Repeated measures correlations between egg colour (L*,a*,b*), effective thickness and surface roughness within eggs after controlling for egg identity.

Variable	Effective thickness (μm)			L*			a*			b*		
	R_{rm}	CI	p	R_{rm}	CI	p	R_{rm}	CI	p	R_{rm}	CI	p
L^*_1	**-0.228**	**-0.431, 0.036**	**0.035**		-							
a*	-0.143	-0.318, 0.054	0.191	**0.403**	**0.125, 0.620**	**< 0.001**		-				
b*	**-0.238**	**-0.432, -0.024**	**0.028**	**0.249**	**0.010, 0.456**	**0.022**	**0.480**	**0.296, 0.654**	**< 0.001**		-	
Surface area (mm^2)$_1$	**0.325**	**0.126, 0.536**	**0.002**	**-0.345**	**-0.537, -0.154**	**0.001**	0.146	-0.069, 0.383	0.182	-0.032	-0.263, 0.226	0.772
Mean roughness, Sa (μm)$_1$	0.145	-0.074, 0.400	0.186	-0.163	-0.367, 0.038	0.136	0.198	-0.002, 0.411	0.069	-0.054	-0.280, 0.174	0.624
Residual surface area (mm)	**0.424**	**0.240, 0.563**	**< 0.001**	**-0.288**	**-0.483, -0.121**	**0.008**	0.008	-0.179, 0.161	0.939	-0.030	-0.204, -0.266	0.785

CI = bootstrapped confidence interval (1000 reps). d.f. = 83. n = 42 eggs, 1 fragment per region. Bold indicates significant correlation.
$_1$ Box-Cox transformed surface area and surface roughness to reduce skew and normalise the distribution (and L* for correlation with effective thickness only).

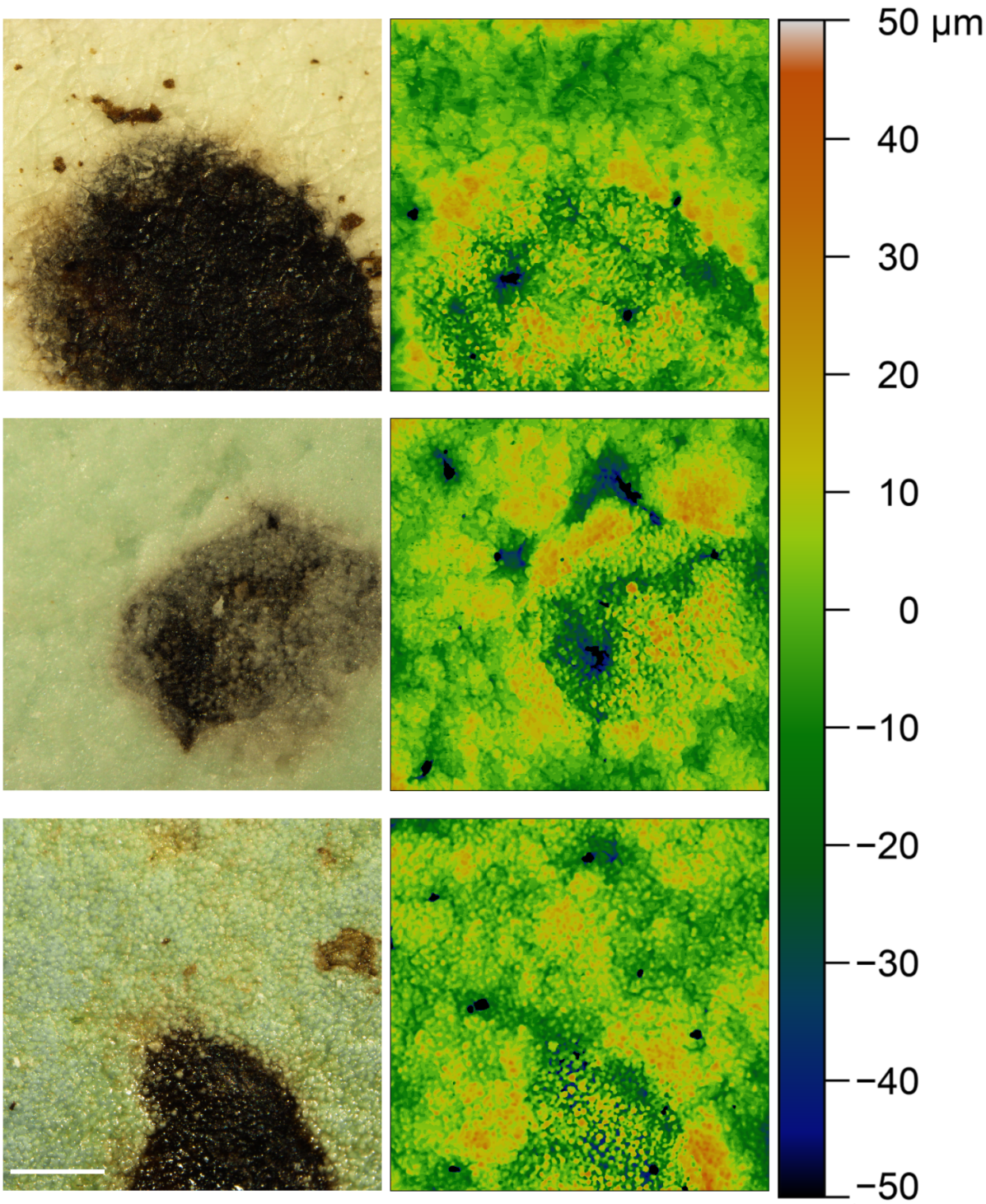

Figure 2. Variation in surface structure within common guillemot eggshell fragments. Note that the especially rough areas of each height map (right) correspond to the dark black-brown pigment patches on the optical images (left). The second set of images down illustrates that it is the pigment in the surface layers of the shell that is associated with these extra rough areas, but the other two sets show that pigment may be added on top of these especially rough areas. The dark black or blue dots on the height maps are gas exchange pores. Each image is 4mm^2. Scale bar = 500µm.

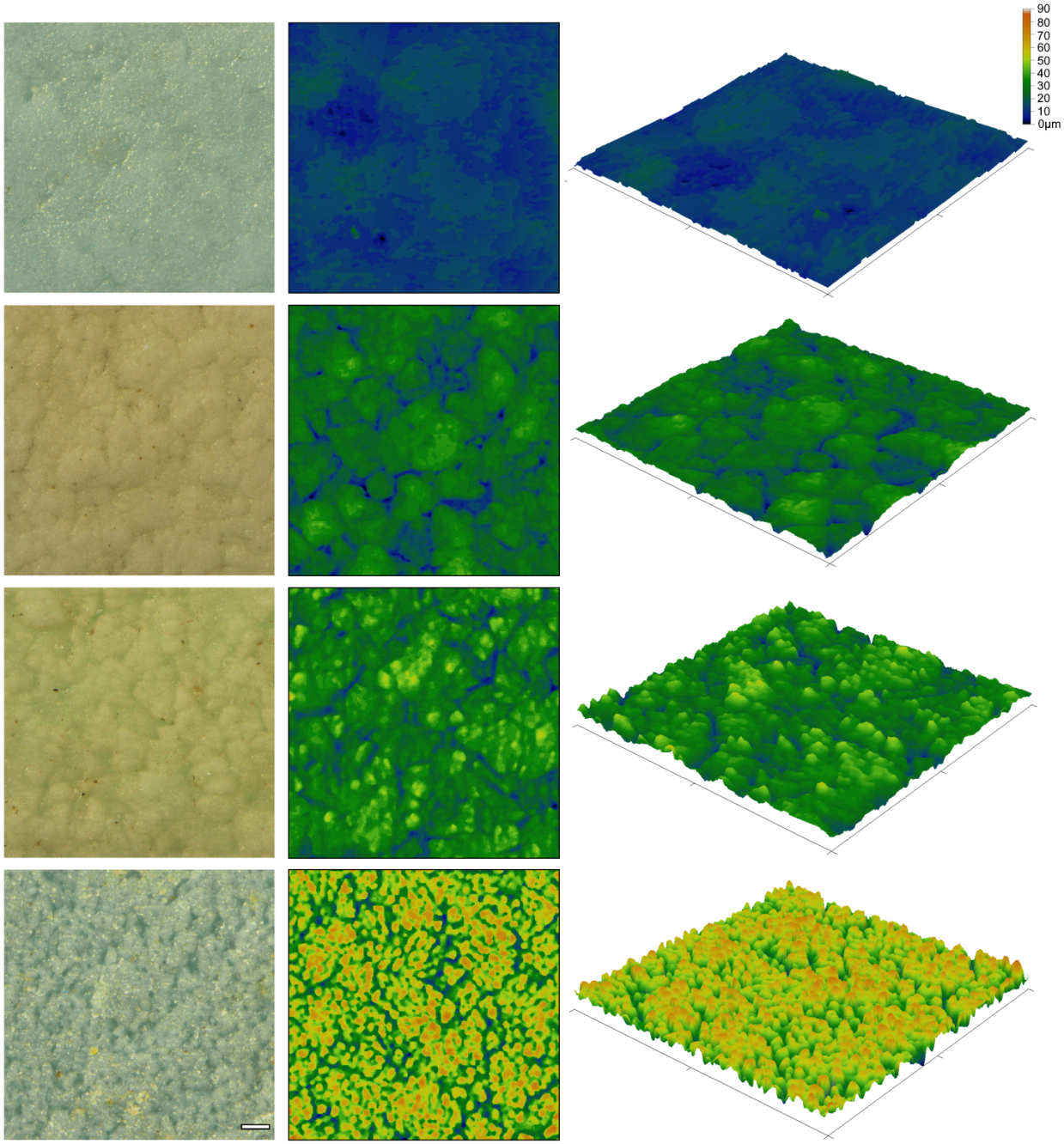

Figure 3. Variation in the surface structure of common guillemot (*Uria aalge*) eggshells. Left images taken on an optical microscope, middle are height maps produced from microCT data and the right column are the corresponding 3D models. Scale bar = 100µm. Each square image is 1mm^2.

Table 3. Spearman's rank correlations between guillemot eggshell traits (colour, thickness and surface structure) across eggshell fragments.

Variable	Effective thickness (µm)	L*	a*	b*	Surface area (mm^2)	Surface roughness, Sa (µm)	Residual surface area (mm)	Skew	Kurtosis, Sku	Max height (µm)	Max peak height (µm)
L*	*-0.094*	-									
a*	*-0.084*	**0.903**	-								
b*	*-0.053*	**0.785**	**0.834**	-							
Surface area (mm^2)	**0.339**	**-0.303**	-0.195	*-0.156[1], 0.063*	-						
Mean roughness, Sa (µm)	**0.321**	-0.182	*-0.124*	*-0.050*	**0.885**	-					
Residual surface area (mm)	*0.151[1] 0.073*	**-0.298**	-0.194	**-0.290**	**0.388**	*-0.002*	-				
Skew	-0.171	*-0.157[1], 0.062*	*-0.157[1], 0.062*	-0.178	*-0.159[1], 0.058*	*-0.165[1], 0.050*	*0.023*	-			
Kurtosis, Sku	*-0.025*	*0.162[1], 0.055*	0.194	*0.118*	*-0.063*	*-0.060*	*-0.097*	**-0.693**	-		
Max height (µm)	0.257	*-0.139*	*-0.070*	*-0.043*	**0.831**	**0.932**	*0.009*	-0.261	0.193	-	
Max peak height (µm)	0.253	-0.178	*-0.105*	*-0.070*	**0.812**	**0.899**	*0.030*	*0.060*	*-0.057*	**0.898**	-
Max pit depth (µm)	0.241	*-0.086*	*-0.038*	*-0.015*	**0.748**	**0.850**	*-0.025*	**-0.464**	**0.350**	**0.951**	**0.730**

Correlations performed on subset of fragments excluding dirty fragments (n = 142 fragments from 52 eggs). *n.s. $p > 0.05$*, $p < 0.05$, $p < 0.01$, **$p < 0.001$**.
[1] $0.1 > p > 0.05$, r_s and p-value reported.

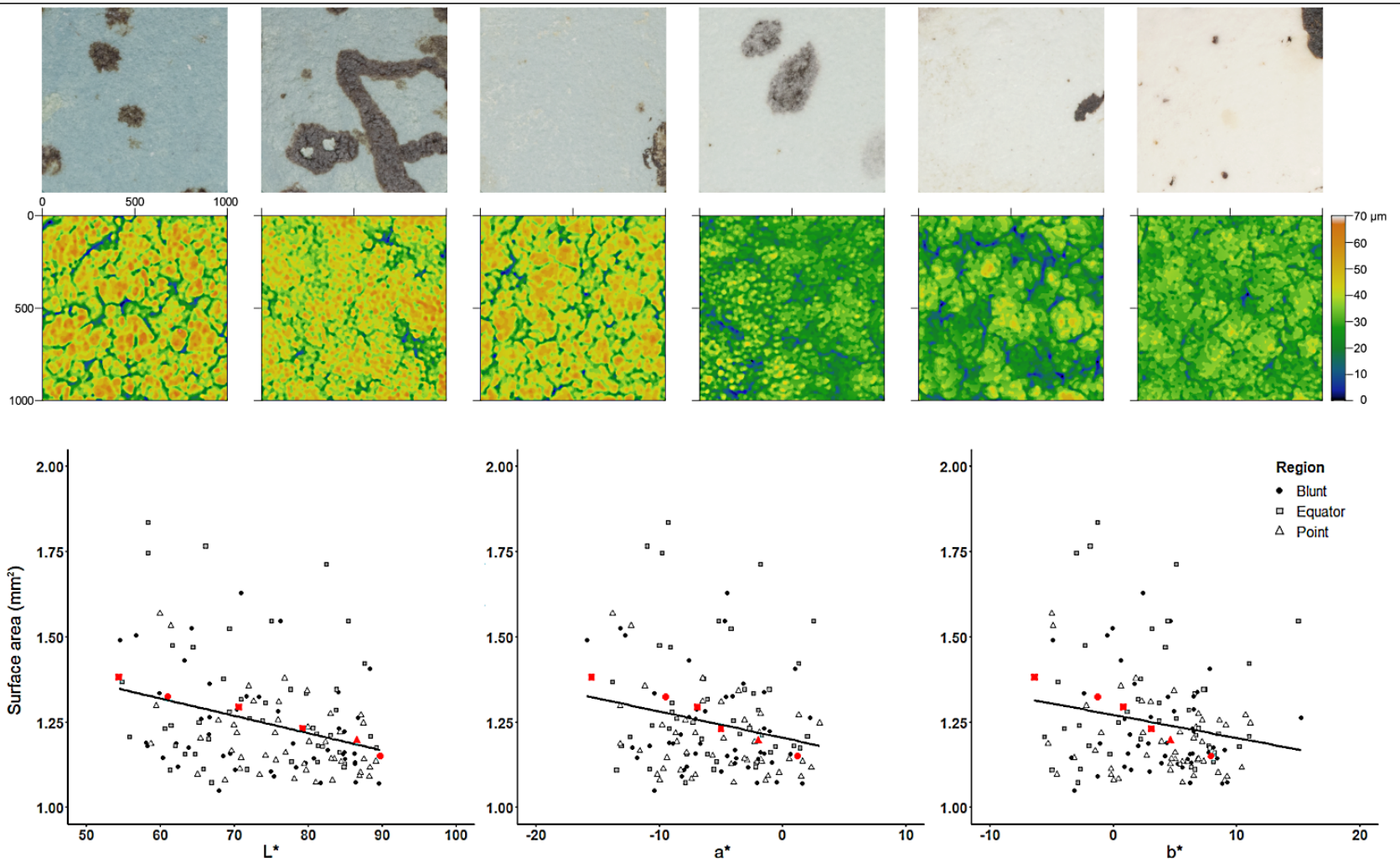

Figure 4. The relationship between shell colour and surface roughness (surface area). Treating each fragment as an independent measure, Spearman's rank correlations showed L* and a* are negatively correlated with surface area (and b* approached significance; Table 3). Optical images and their corresponding height maps were selected to best match the line of best fit for the relationships between all three colour parameters and surface area, and are marked on the graphs with red points. Priority was given to match the line of best fit between L* and surface area (the strongest correlation). The colour images at the top are not to scale. Height maps are all 1mm^2. Black lines indicate lines of best fit for all eggshell fragments (n = 142).

controlling for regional variation, darker eggs typically possessed a more complex surface structure with a greater surface area than paler eggs (Table 4). There was a trend for greener eggs to possess rougher surfaces with higher surface areas however this relationship only approached significance (Table 4). The three colour parameters measured in this study are all highly correlated with each other (Tables 2 – 4), but based on correlations presented in Tables 2 – 4, L* (lightness) appears to be most strongly related to surface area.

Across common guillemot eggshells, shell surface structure height made up 5 – 51% of the effective shell thickness, with a median value of 12%. In real terms, this means surface structures range from 25μm to 193μm in maximum height, with a median value of 54μm. Surface structure area was significantly positively correlated with the effective thickness of the shell (across fragments; Table 3, within eggs; Table 2, between eggs controlling for region; Table 4), potentially because shell thickness positively correlates with the absolute maximum height of surface structures and variation in the height profile of the surface ("mean roughness", Sa; Tables 2 – 4; Fig. S5). To examine this relationship further, we accounted for variation in the height of the shell's surface profile by analysing the residuals of the relationship between mean roughness (Sa) with the square root of shell surface area, obtaining a parameter that may better represent variation in the X and Y dimensions, after accounting for variation in the Z-height of a surface. Using this approach, we still found significant relationships between residual shell surface area and shell colour (Tables 2 – 4; Fig. S6). The effective thickness of the shell was not significantly correlated with residual shell surface area between eggs (Table 4). None of the colour parameters correlated with effective eggshell or mammillary layer thickness across our sample of common guillemot eggs (Tables 4 & S1 – 3).

Due to the existence of regional variation in eggshell surface roughness and colour (Table 1), we also tested for correlations between shell surface area and colour within each region of the eggs. At the blunt end of common guillemot eggs, rougher surfaces tended to be darker in colour, and after accounting for variation in the height of the surface (Sa), bluer eggs tended to be rougher with a greater residual shell surface area (Table S4). At the equator of common guillemot eggs, thicker eggshells were typically rougher (Table S5). Lastly, at the pointed end of common guillemot eggs, thicker and darker coloured

Table 4. Repeated measures correlations between egg colour (L*, a*, b*), effective thickness and surface roughness between eggs controlling for regional differences.

Variable	Effective thickness (μm)			L*			a*			b*		
	R_{rm}	CI	p	R_{rm}	CI	p	R_{rm}	CI	p	R_{rm}	CI	p
L*	-0.020	-0.226, 0.109	0.824		-							
a*	-0.025	-0.223, 0.114	0.785	**0.906**	**0.858, 0.929**	**< 0.001**		-				
b*	0.032	-0.185, 0.135	0.728	**0.833**	**0.764, 0.877**	**< 0.001**	**0.856**	**0.782, 0.910**	**< 0.001**		-	
Surface area (mm^2)$_1$	**0.329**	**0.144, 0.452**	**< 0.001**	**-0.254**	**-0.427, -0.116**	**0.004**	-0.171	-0.346, 0.010	0.057	-0.087	-0.282, 0.110	0.339
Mean roughness, Sa (μm)$_1$	**0.396**	**0.151, 0.438**	**< 0.001**	-0.153	-0.332, -0.003	0.089	-0.091	-0.290, 0.078	0.316	0.030	-0.181, 0.218	0.742
Residual surface area (mm)	-0.138	-0.054, 0.229	0.127	**-0.252**	**-0.426, -0.105**	**0.005**	**-0.218**	**-0.365, -0.049**	**0.015**	**-0.305**	**-0.465, -0.142**	**< 0.001**

CI = bootstrapped confidence interval (1000 reps). d.f. = 122, n = 42 eggs, 1 fragment per region. Bold indicates significant correlation.
$_1$ Box-Cox transformed surface area and surface roughness to reduce skew and normalise the distribution.

eggshells tended to be rougher (Table S6). After accounting for variation in the height of the surface (Sa), darker, and/or bluer, and/or greener eggs tended to have more complex surface structure with greater residual shell surface area (Table S6). When looking at a single region of an egg, variation in surface structure therefore appears to relate to colouration at the blunt and pointed end of eggs and eggshell thickness at the equator and pointed end.

Finally, we assessed the importance of both eggshell thickness and colour on surface roughness by including effective shell thickness and all colour parameters in a single mixed effects multiple linear regression model that controlled for regional differences in surface area and egg identity. This revealed that effective thickness and L* were significantly related to shell surface area, with thicker-shelled and darker coloured eggs being rougher (Table S7). Using a generalized linear mixed model controlling for egg region, only b* was significantly negatively related to residual surface area, indicating that bluer eggshells have a more complex surface structure in the X and Y dimensions (Table S8).

Is variation in eggshell surface structure and colour related to egg shape and size?

We found little evidence that the shape and size of common guillemot eggs related to their surface structure (specifically, surface area), with egg volume and egg shape not significantly relating to surface area at any region of the eggs (Table S9). Egg size and shape was also largely independent of egg colour, except that smaller eggs tended to have a higher L* value, i.e. they were lighter in colour, at their blunt end ($r = -0.352$, $n = 42$, $p = 0.022$; see Tables S10 – 12).

The influence of shell accessory material on roughness and colour

Qualitative observations supported the idea shell accessory materials (including any overlying superficial pigmentation) influence the roughness of the shell surface. Shell accessory materials altered surface micro-topography primarily by smoothing the shell surface, but cracks in the shell accessory material layer could also cause increased roughness (although the latter may result from dehydration of shell accessory materials

during eggshell storage; Fig. 2, 3 & 5). Shell accessory materials also appeared to influence egg colour, since areas without any shell accessory material were often a different colour to the rest of the eggshell (Fig. 5). This is particularly evident for green eggs, where areas of shell with shell accessory material were smoother (at the micro-scale) and appeared green or yellow, while areas where it is absent were rougher and appear more blue or white (Fig. 5).

Discussion

We have shown that the surface topography of common guillemot eggshells varies considerably, and this variation is associated with both eggshell colour and effective shell thickness. Thicker and/or darker eggshells tend to have a rougher surface, with a higher surface area, than thinner and/or paler coloured eggshells, and bluer eggs also have a more complex surface structure. These relationships between shell thickness, colour and roughness were also detectable within individual eggs. The shell accessory material layer also appears to play an important role in egg colouration in the common guillemot, especially in producing green/yellow colours.

Why does eggshell colour relate to surface roughness?

Egg pigment was typically concentrated in the surface layers of the common guillemot's eggshell (Fig. S3 & S4) but could also be found throughout the shell (as is also the case in some other bird species; Tyler 1964; Harrison 1966; Tyler 1969; Mikhailov 1997). It is possible that calcium carbonate crystal growth is influenced by pigment molecules, leading to variation in crystal form, and how crystal columns end at the shell's outer surface which then presumably determines the surface topography and the resulting roughness. Consistent with this idea, we found patches of particularly rough eggshell to be associated with dark pigment patterns (typically, black or brown patches) within the surface of the shell. Proteins and chemicals found in the shell surface layers and shell accessory materials are thought to regulate shell growth, crystal texture and form (Tullett *et al.* 1976; Dominguez-vera *et al.* 2000; Nys *et al.* 2004; Hernández-Hernández *et al.* 2008; Hincke *et al.* 2010; Rodríguez-Navarro *et al.* 2015); since pigment is secreted in these outer layers, its ability to affect crystal growth is a very plausible possibility.

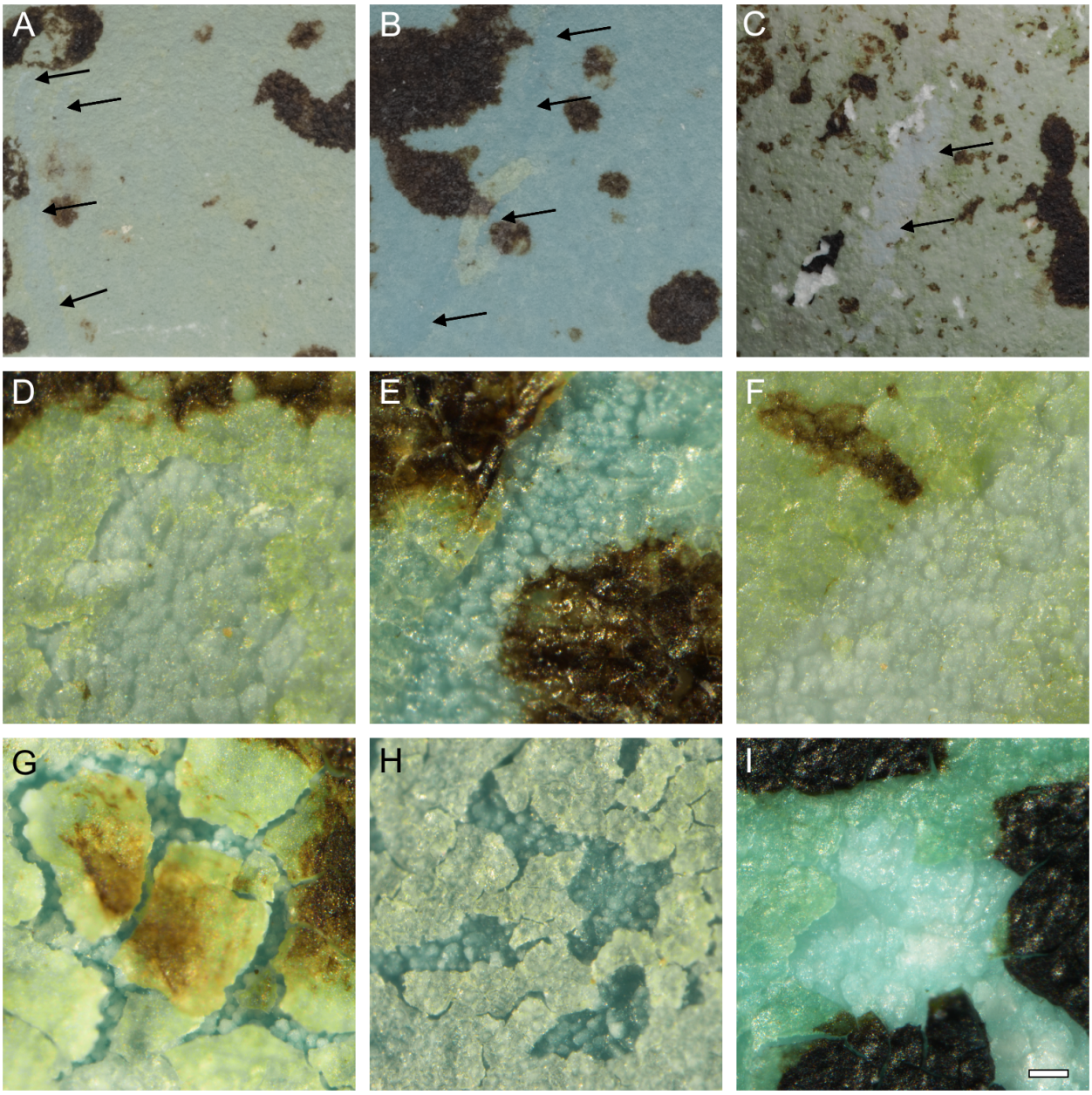

Figure 5. Examples of the influence of shell accessory material on shell surface roughness and colour. Top: images of eggshells to illustrate the affect shell accessory material can have on eggshell colour. A and B are colour calibrated images, C is an egg not used to quantify colour and the image is not colour calibrated. Instead, dynamic lighting was used to illustrate more clearly the colour difference seen by the human eye under natural lighting. (A) Along the left side a strip of blue colour can be seen (indicated by arrows) whereas the rest of the egg is more green or yellow in colour. (B) Along the egg (indicated by arrows) a darker blue colour can be seen whereas the rest of the egg is paler. (C) A pale blue patch of colour can be seen whereas the rest of the egg is more yellow or green in colour. These patches of colour are associated with regions of the egg where shell accessory material is absent (D – F). The areas where the shell accessory material is present also appear smoother than those where it is absent. This is illustrated by the bottom three images (G – I) from three different eggs where shell accessory material on the surface has cracked showing the surface underneath, note again the difference in surface roughness and colouration. Scale bar = 100μm. Top three colour images are not to scale.

Surface microstructure may also influence eggshell colour via structural mechanisms. Rougher eggshell surfaces may absorb more light than smooth surfaces, resulting in darker base colouration. Shell accessory materials may also affect colour by containing pigments or via thin-film interference effects (Sparks 1994; Richards & Deeming 2001; Deeming 2011; Sparks 2011; Samiullah & Roberts 2013). Alternatively, shell accessory materials may adhere less strongly to a smooth shell surface than a rough one, so smooth eggs could appear paler because pigment and/or other shell accessory materials wear off more easily. Precisely how the shell accessory material layer alters the eggshell's base colour remains unclear and warrants further investigation.

Blue-green egg colouration may reflect female and/or egg quality in some bird species (Moreno & Osorno 2003). If creating a rougher shell is costly due to some aspect of the shell formation process, but confers benefits to the egg and developing embryo, then rougher eggs may be more frequently produced by high quality females. If egg colour co-varies with roughness (e.g. due to any structural colour effects or because pigment influences surface formation), then this would form an indirect link between female/egg quality and egg colour. However, evidence that blue-green eggs are higher quality is mixed across species, with several studies finding evidence against this hypothesis (Kilner 2006; Cassey *et al.* 2008; López-Rull *et al.* 2008; Reynolds *et al.* 2009; Cherry & Gosler 2010; Hargitai *et al.* 2011; Honza *et al.* 2011; Butler & Waite 2016). Moreover, in our study, although larger eggs tended to be darker in colour at the blunt end only, we did not find bluer and/or greener common guillemot eggs to be thicker-shelled or larger, both of which may be indicators of female and/or egg quality (Hargitai *et al.* 2011; Krist 2011). It therefore seems unlikely that covariation in eggshell colour and roughness relates specifically to egg quality.

Whatever the explanation for the relationship between shell surface structure and colour in common guillemot eggs, our results highlight the importance of considering the role of shell accessory materials and the underlying eggshell surface structure when assessing variation in eggshell colouration. The influence of surface structure and shell accessory materials on colour may explain why the full range of colour variation exhibited across bird eggs is not solely explained by variation in the concentrations of two commonly recognised eggshell pigments (e.g. Brulez *et al.* 2016; Dainson *et al.* 2018; Hauber *et al.*

2019). Alternatively, sampling and methodological limitations could be responsible. To date, studies have typically analysed pigment concentration throughout the entire thickness of the shell, which includes layers of shell that may be a completely different colour to that which is seen from the outside (Fig. S3 & S4; Harrison 1966; also see Brulez *et al.* 2014). Using techniques like Raman spectroscopy to study the surface of the shell and the pigments in it may avoid this methodological issue in future studies (Thomas *et al.* 2015; Wiemann *et al*. 2018). Our observations highlight the importance of focusing on both the microstructure and pigment content of the external eggshell surface and shell accessory materials when assessing the drivers of variation in eggshell base colour and pigment patterning within and between bird species.

Egg colour, pigmentation and shell thickness

We found no relationship between external base eggshell colouration and eggshell thickness in common guillemot eggs. Although our results are consistent with those of Pirie-Hay and Bond (2014), they disagree with those of Hauber *et al.* (2019). This discrepancy may be explained by a number of methodological differences. First, Hauber *et al.* (2019) used a colour scale that aimed to reflect how birds perceive visual information, rather than the human visible spectrum. It is unclear which colour scale is more appropriate when investigating relationships between colour and shell thickness. Second, it is unclear if Hauber *et al.* (2019) appropriately accounted for regional variation in eggshell traits, as we did here; for example, the blunt end of guillemot eggs tends to be both highly maculated (i.e. possesses many dense dark pigment patches) and thin-shelled relative to the equator and point (Birkhead *et al.* 2017; Chapter 2), and base shell colouration also tends to vary between egg regions. Third, Hauber *et al.* (2019) did not account for variation in shell thickness driven by egg size and shape (Tables S1 & S2; Chapter 2).

Previous studies of other species' eggs have not found a relationship between eggshell thickness and base colour (e.g. Jagannath *et al.* 2008; López-Rull *et al.* 2008; Hargitai *et al.* 2010; Hargitai *et al.* 2011; but see Butler & Waite 2016), yet some have found relationships between shell thickness and eggshell patterning (Gosler *et al.* 2005; Jagannath *et al.* 2008; Maruer *et al.* 2011; Bulla *et al.* 2012). Consistent with this, we

show pigment patterns (i.e. black/brown patches) within the shell's surface crystal layers correspond with areas of eggshell that have slightly lower ("sunken") surfaces (Fig. 2). Indeed, this effect may in part explain the negative relationship between eggshell thickness and maculation density found by Hauber *et al.* (2019) in common guillemot eggs. It is plausible that the connection between eggshell pigment patches and thin shells in some species is not because dark protoporphyrin pigment is specifically needed to enhance shell strength (as suggested by Gosler *et al.* 2005; Jagannath *et al.* 2008; Gosler *et al.* 2011) but because the secretion of pigment within certain layers of the shell disrupts calcium carbonate crystal growth, resulting in locally thinner regions of shell. This is consistent with suggestions in Maurer *et al.* (2011) that shell thinning is a consequence of pigment pattern due to protoporphyrin pigment and calcium competing for the same deposition pathway. Pigmentation lying on top of the shell (or the shell accessory material layer), on the other hand, leads to locally thicker regions of eggshell through the addition of extra material onto the shell (Orłowski *et al.* 2017; Rosenberger *et al*. 2019).

Variability in shell surface structure

Our analyses revealed guillemot eggshell surface texture was extremely variable, from smooth and flat to possessing large mound-like structures or even having small protruding peaks and deep troughs. Preliminary qualitative comparisons across the Alcid family suggest that shell surface structure within common guillemots may be as variable as it is across other species (Fig. S7). We also found that the micro-roughness of the underlying crystalline shell surface was often smoothed by the presence of shell accessory materials on the shell surface (but see D'Alba *et al.* 2017 for variation in nano-roughness). Formation of an irregular surface probably depends on chemical or protein control during shell formation. The eggshell develops over numerous hours (typically ~ 20 in chickens, *Gallus gallus domesticus*) in the uterus, regulated by proteins and other chemicals (Nys *et al.* 2004; Hincke *et al.* 2010; Rodriguez-Navarro *et al.* 2015). Termination of shell growth is likely initiated by chemical compounds such as magnesium, potassium, and phosphorus (Tullett *et al.* 1976; Fraser *et al.* 1999), and proteins (Nys *et al.* 2004) that are secreted to control and inhibit crystal growth. If these compounds do not halt crystal growth instantaneously, an irregular surface structure may form.

Within and between common guillemot eggs, effective shell thickness was related to shell surface area. This highlights the importance of accounting for shell thickness in any future comparative analyses of eggshell surface structure. Thicker eggshells are likely rougher for two reasons. First, rougher surfaces are typified by increases in surface structure height which will also contribute to effective eggshell thickness. Secondly, the proportion of the effective thickness layer that is made up by the shell surface can be similar across both thick and thin shells, but in thick shells this proportion would translate into a larger absolute surface structure height resulting in greater roughness measures.

It is plausible that some variation in surface topography and roughness observed here within the common guillemot (and across auks; Fig S7) is non-adaptive and simply the result of eggshell formation. As discussed, the termination of shell growth is likely an imprecise and imperfect process as it relies on the secretion of substances to inhibit crystal growth, therefore it is likely this process results in the shell surface forming in an irregular manner. Variation in shell thickness within and between eggs likely also contributes to variation in roughness formation, with thicker shells becoming inherently rougher. Finally, any pigment secreted within the shell's surface may interfere with crystal growth or termination further leading to variation in surface topography and contributing to the formation of a rough surface.

Is surface roughness ecologically adaptive?

A final important finding of our study was the fact that common guillemot eggs were significantly rougher at their equator than their blunt and pointed end. These differences may be explained in part by variation in eggshell thickness and colouration along common guillemot eggs, but it is also possible that regional variation in surface roughness is ecologically adaptive. The equator is the region of the egg that interacts directly with both the incubation substrate and the brood patch of the incubating bird. Possessing a rough equatorial surface may therefore be beneficial in resisting or tolerating physical wear from abrasive rock or the brood patch, especially during egg turning (Board & Perrott 1982), and chemical damage from organic acids in faeces or dirt (Grellet-Tinner *et al.* 2017). Surface roughness may also allow the shell accessory material layer to adhere more strongly to the shell, protecting it from being worn off, as

can happen just after egg-laying when the shell accessory materials are fragile (Harrison 1966; Board & Sparks 1991; Sparks 1994; Birkhead 2016) and throughout incubation (Becking 1975; Board & Perrott 1982; Rahn & Hammel 1982; Thompson & Goldie 1990; Baggot *et al.* 2003), especially if the surface is wet (Tyler 1965). This in turn would allow shell accessory materials to remain on the egg throughout incubation to defend the egg and embryo against microbes (D'Alba *et al.* 2017), water (D. Jackson, Unpublished Data) and debris (Jackson *et al.* 2018; Chapter 4). This putative requirement for a rougher shell at the equator may explain why we found no relationship between egg colour and surface roughness across the equator of guillemot eggs, despite finding associations between colour and surface structure across other regions and within eggs.

Conclusion

In summary, we have shown that eggshell base colour, patches of pigment pattern in the shell's surface and shell thickness is related to eggshell surface structure in the common guillemot, and these patterns can be seen not only across, but within individual eggs. Future investigations of the ecological significance of eggshell surface structure need to consider the underlying crystalline surface, any shell accessory materials, and how they interact. The shell accessory material is likely to play a crucial role in interactions between the eggshell surface and external incubation environment, as well as contributing to egg colour.

Acknowledgements

We thank Andrew Power and Ian O'Connor for providing common guillemot eggshell samples collected in Ireland. We also thank Jamie Thompson for collecting and imaging the common guillemot egg samples from Skomer Island to obtain data on their shape and size, and for helpful discussions over the course of this study. The Wildlife Trust of South and West Wales Trust for permission to work on Skomer Island NNR, and the Natural Resources Wales (NRW) for licences to take eggs for scientific purposes. Finally, we thank the Skelet.AL lab for use of their microCT scanner.

Competing interests

No competing interests declared.

Author contributions

The study was conceived by D.J., T.R.B. and N.H. D.J. collected and analysed the data. D.J. wrote the initial draft; N.H. and T.R.B. commented on the initial draft and revised the manuscript.

Funding

The study was funded by a grant from the Leverhulme Trust (to T.R.B.) and a University of Sheffield Scholarship (to D.J.). N.H. was supported by a Patrick & Irwin-Packington Fellowship from the University of Sheffield and a Royal Society Dorothy Hodgkin Fellowship.

Supplementary information

Supplementary information available in Appendix A6.

References

Baggott, G. K., Deeming, D. C., Hémon, S. and Paillat, P., (2003). Relationships between eggshell pigmentation, ultrastructure and water vapour conductance in the Houbara bustard (*Chlamydotis undulata macqueenii*). In: *Proceedings of the World Association of Wildlife Veterinarians Wildlife Sessions at the 27th World Veterinary Congress, Tunisia, 26th September 2002* (eds. Scullion, F.T. and Bailey, T.A.). Northern Ireland: World Association of Wildlife Veterinarians. pp. 85 – 88.

Bakdash, J. Z. and Marusich, L. R., (2017). Repeated measures correlation. *Frontiers in psychology*. **8**, 456.

Bates, D., Maechler, M., Bolker, B. and Walker, S., (2015). Fitting Linear Mixed-Effects Models Using lme4. *Journal of Statistical Software.* **67**(1), 1-48.

Becking, J. H., (1975). The Ultrastructure of the Avian Eggshell. *Ibis.* **117**(2), 143–151.

Biggins, J. D., Thompson, J. E. and Birkhead, T. R., (2018). Accurately quantifying the shape of birds' eggs. *Ecology and Evolution*. **8**(19), 9728-9738.

Birkhead, T. R., (2016). *The Most Perfect Thing: the Inside (and Outside) of a Bird's Egg.* London, UK: Bloomsbury.

Birkhead, T. R., Thompson, J. E., Jackson, D. and Biggins, J. D., (2017). The point of a Guillemot's egg. *Ibis.* **159**(2), 255-265.

Board, R. G., (1981). The microstructure of avian eggshells, adaptive significance and practical implications in aviculture. *Wildfowl*. **32**, 132-136.

Board, R. G., (1982). Properties of avian egg shells and their adaptive value. *Biological Reviews.* **57**(1), 1–28.

Board, R. G. and Perrott, H. R., (1982). The fine structure of the outer surface of the incubated eggshells of the Helmeted guinea fowl (*Numidia meleagris*). *The Journal of Zoology.* **196**(4), 445–451.

Board, R. G. and Scott, V. D., (1980). Porosity of the Avian Eggshell. *American Zoologist.* **20**(2), 339-349.

Board, R. G. and Sparks, N. H. C., (1991). Shell structure and formation in avian eggs. In: *Egg Incubation: Its effect on embryonic development in birds and reptiles* (eds. Deeming, D. C. and Ferguson, M. W. J.). Cambridge, UK: Cambridge University Press. pp. 71-86.

Board, R. G. and Tullett, S. G., (1975). The pore arrangement in the emu (*Dromaius novaehollandiae*) eggshell as shown by plastic models. *Journal of Microscopy*. **103**(2), 281-284.

Brulez, K., Cassey, P., Meeson, A., Mikšík, I., Webber, S. L., Gosler, A. G. and Reynolds, S. J., (2014). Eggshell spot scoring methods cannot be used as a reliable proxy to determine pigment quantity. *Journal of Avian Biology*. **45**(1), 94-102.

Brulez, K., Mikšík, I., Cooney, C. R., Hauber, M. E., Lovell, P. G., Maurer, G., Portugal, S. J., Russell, D., Reynolds, S. J. and Cassey, P., (2016). Eggshell pigment composition covaries with phylogeny but not with life history or with nesting ecology traits of British passerines. *Ecology and Evolution*. **6**(6), 1637-1645.

Bulla, M., Šálek, M., and Gosler, A. G., (2012). Eggshell spotting does not predict male incubation but marks thinner areas of a shorebird's shells. *The Auk*. **129**(1), 26-35.

Butler, M. W. and Waite, H. S., (2016). Eggshell biliverdin concentration does not sufficiently predict eggshell coloration. *Journal of Avian Biology*. **47**(4), 491-499.

Cassey, P., Ewen, J. G., Blackburn, T. M., Hauber, M. E., Vorobyev, M. and Marshall, N. J., (2008). Eggshell colour does not predict measures of maternal investment in eggs of Turdus thrushes. *Naturwissenschaften*. **95**(8), 713-721.

Cassey, P., Portugal, S. J., Ewen J. G., Boulton, R. L., Hauber, M. E. and Blackburn T. M., (2010). Variability in eggshell colour: a comparative study of museum eggshells. *PLoS ONE.* **5**(8), e12054.

Cedillo-Leal, C., Simoncini, M. S., Leiva, P. M., Larriera, A., Lang, J. W. and Pina, C. I., (2017). Eggshell structure in *Caiman latirostris* eggs improves embryo survival during nest inundation. *Proceedings of the Royal Society B: Biological Sciences*. **284**(1854), 20162675.

Cherry, M. I. and Gosler, A. G., (2010). Avian eggshell coloration: new perspectives on adaptive explanations. *Biological Journal of the Linnean Society*. **100**(4), 753-762.

Dainson, M., Mark, M., Hossain, M., Yoo, B., Holford, M., McNeil, S., Riehl, C. and Hauber, M. E., (2018). How to make a mimic? Brood parasitic Striped Cuckoo eggs match host shell color but not pigment concentration. *Journal of Chemical Ecology*. **44**(10), 940– 946.

D'Alba, L., Jones, D. N., Badawy, H. T., Eliason, C. M. and Shawkey, M. D., (2014). Antimicrobial properties of a nanostructured eggshell from a compost-nesting bird. *The Journal of Experimental Biology*. **217**(7), 1116-1121.

D'Alba, L., Maia, R., Hauber, M. E. and Shawkey, M. D., (2016). The evolution of eggshell cuticle in relation to nesting ecology. *Proceedings of the Royal Society B: Biological Sciences*. **283**(1836), 20160687.

D'Alba, L., Torres, R., Waterhouse, G. I. N., Eliason, C., Hauber, M. E. and Shawkey, M. D., (2017). What Does the Eggshell Cuticle Do? A Functional Comparison of Avian Eggshell Cuticles. *Physiological and Biochemical Zoology.* **90**(5), 588-599.

Deeming, D. C., (2002). *Avian Incubation: Behaviour, Environment and Evolution.* Oxford, UK: Oxford University Press.

Deeming, D. C., (2011). A Review of the Relationship between Eggshell Colour and Water Vapour Conductance. *Avian Biology Research.* **4**(4), 224–230.

Deeming, D. C. and Reynolds, S. J., (2016). *Nests, eggs and incubation: new ideas about avian reproduction.* Oxford, UK: Oxford University Press.

Dominguez-Vera, J. M., Gautron, J., Garcia-Ruiz, J. M. and Nys, Y., (2000). The Effect of Avian Uterine Fluid on the Growth Behavior of Calcite Crystals. *Poultry Science*. **79**(6), 901-907.

Fecheyr-Lippens, D. C., Igic, B., D'Alba, L., Hanley, D., Verdes, A., Holford, M., Waterhouse, G. I. N., Grim, T., Hauber, M. E. and Shawkey, M. D., (2015). The cuticle modulates ultraviolet reflectance of avian eggshells. *Biology Open.* **4**(7), 753-759.

Fraser, A. C., Bain, M. M. and Solomon, S. E., (1999) Transmission electron microscopy of the vertical crystal layer and cuticle of the eggshell of the domestic fowl. *British Poultry Science.* **40**(5), 626–631.

Genzer, J. and Marmur, A., (2008). Biological and synthetic self-cleaning surfaces. *MRS Bulletin*. **33**(8), 742-746.

Gorchein, A., Lim, C. K. and Cassey, P., (2009). Extraction and analysis of colourful eggshell pigments using HPLC and HPLC/electrospray ionization tandem mass spectrometry. *Biomedical Chromatography*. **23**(6), 602-606.

Gosler, A. G., Connor, O. R. and Bonser, R. H., (2011). Protoporphyrin and eggshell strength: preliminary findings from a passerine bird. *Avian Biology Research*. **4**(4), 214-223.

Gosler, A. G., Higham, J. P. and Reynolds, S. J., (2005). Why are birds' eggs speckled? *Ecology Letters*. **8**(10), 1105-1113.

Grellet-Tinner, G., Lindsay, S. and Thompson, M. B., (2017). The biomechanical, chemical and physiological adaptations of the eggs of two Australian megapodes to their nesting strategies and their implications for extinct titanosaur dinosaurs. *Journal of Microscopy.* **267**(2), 237-249.

Hanley, D., Grim, T., Cassey, P. and Hauber, M. E., (2015). Not so colourful after all: eggshell pigments constrain avian eggshell colour space. *Biology letters*. **11**(5), 20150087.

Hargitai, R., Moskát, C., Bán, M., Gil, D., López-Rull, I. and Solymos, E., (2010). Eggshell characteristics and yolk composition in the common cuckoo *Cuculus canorus*: are they adapted to brood parasitism? *Journal of Avian Biology*. **41**(2), 177-185.

Hargitai, R., Mateo, R. and Török, J., (2011). Shell thickness and pore density in relation to shell colouration, female characteristics, and environmental factors in the Collared Flycatcher *Ficedula albicollis*. *Journal of Ornithology*. **152**(3), 579-588.

Harrison, C. J. O., (1966). Variation in the distribution of pigment within the shell structure of birds' eggs. *Journal of Zoology*. **148**(4), 526-539.

Hauber, M. E., Bond, A. L., Kouwenberg, A. L., Robertson, G. J., Hansen, E. S., Holford, M., Dainson, M., Luro, A. and Dale, J., (2019). The chemical basis of a signal of individual identity: shell pigment concentrations track the unique appearance of Common Murre eggs. *Journal of the Royal Society Interface.* **16**(153), 20190115.

Hauber, M. E., Dainson, M., Baldassarre, D. T., Hossain, M., Holford, M. and Riehl, C., (2018). The perceptual and chemical bases of egg discrimination in communally nesting greater anis *Crotophaga major*. *Journal of Avian Biology*. **49**(8), e01776.

Hernández-Hernández, A., Gómez-Morales, J., Rodríguez-Navarro, A. B., Gautron, J., Nys, Y. and García-Ruiz, J. M., (2008). Identification of some active proteins in the process of hen eggshell formation. *Crystal Growth and Design*. **8**(12), 4330-4339.

Hill, S., (2008) Conservation of the “Great Bass Rock” diorama - an ICON internship at Ipswich Museum. *Natural Sciences Collections Association (NatSCA) News.* **14**, 20–25.

Hincke, M. T., Nys, Y. and Gautron, J., (2010). The role of matrix proteins in eggshell formation. *The Journal of Poultry Science.* **47**(3), 208-219.

Honza, M., Požgayová, M., Procházka, P. and Cherry, M. I., (2011). Blue-green eggshell coloration is not a sexually selected signal of female quality in an open-nesting polygynous passerine. *Naturwissenschaften*. **98**(6), 493.

Hothorn, T., Bretz, F. and Westfall, P., (2008). Simultaneous Inference in General Parametric Models. *Biometrical Journal.* **50**(3), 346-363.

Igic, B., Cassey, P., Grim, T., Greenwood, D. R., Moskat, C., Rutila, J. and Hauber, M. E., (2011). A shared chemical basis of avian host–parasite egg colour mimicry. *Proceedings of the Royal Society B: Biological Sciences*. **279**(1731), 1068-1076.

Igic, B., Fecheyr-Lippens, D., Xiao, M., Chan, A., Hanley, D., Brennan, P. R. L., Grim, T., Waterhouse, G. I. N., Hauber, M. E. and Shawkey, M. D., (2015). A nanostructural basis for gloss of avian eggshells. *Journal of The Royal Society Interface.* **12**(103), 20141210.

Jackson, D., Thompson, J. E., Hemmings, N. and Birkhead, T. R., (2018). Common guillemot (*Uria aalge*) eggs are not self-cleaning. *The Journal of Experimental Biology*. **221**(23), jeb188466.

Jagannath, A., Shore, R. F., Walker, L. A., Ferns, P. N. and Gosler, A. G., (2008). Eggshell pigmentation indicates pesticide contamination. *Journal of Applied Ecology*. **45**(1), 133-140.

Kennard, F. H., (1921) Moulds and Bacteria on Egg collections. *The Auk.* **38**(3), 345–356.

Kennedy, G. Y. and Vevers, H. G., (1976). A survey of avian eggshell pigments. *Comparative Biochemistry and Physiology Part B: Comparative Biochemistry*. **55**(1), 117-123.

Kern, M. D., Cowie, R. J. and Yeager, M., (1992). Water and Structure of Eggs Loss, Conductance, of Pied Flycatchers during Egg Laying and Incubation. *Physiological Zoology.* **65**(6), 1162–1187.

Kilner, R. M., (2006). The evolution of egg colour and patterning in birds. *Biological Reviews.* **81**(3), 383–406.

Krist, M., (2011). Egg size and offspring quality: a meta-analysis in birds. *Biological Reviews*. **86**(3), 692-716.

Kusuida, S., Iwasawa, A., Doi, O., Ohya, Y. and Yoshizaki, N., (2011). Diversity of the Cuticle Layer of Avian Eggshells. *Japan Poultry Science.* **48**(2), 119–124.

Lang, M. R. and Wells, J. W., (1987). A Review of Eggshell Pigmentation. *World's Poultry Science Journal.* **43**(3), 238–246.

López-Rull, I., Miksik, I., and Gil, D., (2008). Egg pigmentation reflects female and egg quality in the spotless starling *Sturnus unicolor*. *Behavioral Ecology and Sociobiology*. **62**(12), 1877-1884.

Martín-Vivaldi, M., Soler, J. J., Peralta-Sánchez, J. M., Arco, L., Martín-Platero, A. M., Martínez-Bueno, M., Ruiz-Rodríguez, M. and Valdivia, E., (2014). Special structures of hoopoe eggshells enhance the adhesion of symbiont-carrying uropygial secretion that increase hatching success. *Journal of Animal Ecology*. **83**(6), 1289-1301.

Maurer, G., Portugal, S. J., Mikšík, I. and Cassey, P., (2011). Speckles of cryptic black-headed gull eggs show no mechanical or conductance structural function. *Journal of Zoology*. **285**(3), 194-204.

Mikhailov, K. E., (1997). *Avian eggshells: an atlas of scanning electron micrographs.* Hertfordshire, UK: British Ornithologists' Club Occasional Publications 3.

Mikšík, I., Holáň, V. and Deyl, Z., (1996). Avian eggshell pigments and their variability. *Comparative Biochemistry and Physiology Part B: Biochemistry and Molecular Biology*. **113**(3), 607-612.

Moreno, J. and Osorno, J. L., (2003). Avian egg colour and sexual selection: does eggshell pigmentation reflect female condition and genetic quality? *Ecology Letters*. **6**(9), 803-806.

Nečas, D. and Klapetek, P., (2012). Gwyddion: an open-source software for SPM data analysis. *Central European Journal of Physics.* **10**(1), 181-188.

Nys, Y., Gautron, J., Garcia-Ruiz, J. M. and Hincke, M. T., (2004). Avian eggshell mineralization: biochemical and functional characterization of matrix proteins. *Comptes Rendus Palevol*. **3**(6-7), 549-562.

Orłowski, G., Pokorny, P., Dobicki, W., Łukaszewicz, E. and Kowalczyk, A., (2017). Speckled and plain regions of avian eggshells differ in maternal deposition of calcium and metals: A hitherto overlooked chemical aspect of egg maculation. *The Auk.* **134**(3), 721-731.

Pinheiro, J., Bates, D., DebRoy, S., Sarkar, D., R Core Team, (2018). nlme: Linear and Nonlinear Mixed Effects Models. R package version 3.1-137, https://CRAN.R-project.org/package=nlme

Pirie-Hay, D. and Bond, A. L., (2014). Thickness of Common Murre (*Uria aalge*) eggshells in Atlantic Canada. *The Canadian Field-Naturalist.* **128**(1), 72–76.

Portugal, S. J., Bowen, J. and Riehl, C., (2018). A rare mineral, vaterite, acts as a shock absorber in the eggshell of a communally nesting bird. *Ibis.* **160**(1), 173-178.

Portugal, S. J., Cooper, H. J., Zampronio, C. G., Wallace, L. L. and Cassey, P., (2010) Can museum egg specimens be used for proteomic analyses? *Proteome science.* **8**, 40.

Prynne, M., (1963). *Egg-shells*. London, UK: Barrie & Rockliff.

R Core Team, (2018). R: A language and environment for statistical computing. R Foundation for Statistical Computing, Vienna, Austria. https://www.R-project.org/

Rahn, H. and Hammel, H. T., (1982). Incubation water loss, shell conductance, and pore dimensions in Adelie penguin eggs. *Polar Biology*. **1**(2), 91-97.

Reynolds, S. J., Martin, G. R. and Cassey, P., (2009). Is sexual selection blurring the functional significance of eggshell coloration hypotheses? *Animal Behaviour*. **78**, 209-215.

Richards, P. D. G. and Deeming, D. C., (2001). Correlation between shell colour and ultrastructure in pheasant eggs. *British Poultry Science*. **42**(3), 338-343.

Riehl, C., (2010). A simple rule reduces costs of extragroup parasitism in a communally breeding bird. *Current Biology*. **20**(20), 1830-1833.

Rodríguez-Navarro, A. B., Marie, P., Nys, Y., Hincke, M. T. and Gautron, J., (2015). Amorphous calcium carbonate controls avian eggshell mineralization: a new paradigm for understanding rapid eggshell calcification. *Journal of Structural Biology*. **190**(3), 291-303.

Rosenberger, J., Łukaszewicz, E., Kowalczyk, A. and Rzońca, Z., (2018). Capercaillie (*Tetrao urogallus*) eggshell pigmentation, maculation and thickness. *Ornis Fennica*. **95**(4), 160-170.

Samiullah, S. and Roberts, J. R., (2013). The location of protoporphyrin in the eggshell of brown-shelled eggs. *Poultry science*. **92**(10), 2783-2788.

Samiullah, S. and Roberts, J. R., (2014). The eggshell cuticle of the laying hen. *World's Poultry Science Journal*. **70**(4), 693-708.

Schneider, C. A., Rasband, W. S. and Eliceiri, K. W., (2012). NIH Image to ImageJ: 25 years of image analysis. *Nature Methods.* **9**, 671-675.

Sparks, N. H. C., (1994). Shell accessory materials: structure and function. In: *Microbiology of the Avian Egg* (eds. Board, R. G. and Fuller, R.). London, UK: Chapman and Hall. pp. 25-42.

Sparks, N. H. C., (2011). Eggshell pigments–from formation to deposition. *Avian Biology Research*. **4**(4), 162-167.

Thomas, D. B., Hauber, M. E., Hanley, D., Waterhouse, G. I., Fraser, S. and Gordon, K. C., (2015). Analysing avian eggshell pigments with Raman spectroscopy. *The Journal of Experimental Biology*. **218**(17), 2670-2674.

Thompson, M. B. and Goldie, K. N., (1990). Conductance and Structure of Eggs of Adelie Penguins, *Pygoscelis adeliae*, and Its Implications for Incubation. *The Condor*. **92**(2), 304–312.

Tschanz, B., (1990). Adaptations for Breeding in Atlantic Alcids. *Netherlands Journal of Zoology.* **40**(4), 688–710.

Tullett, S. G., (1984). The porosity of avian eggshells. *Comparative Biochemistry and Physiology Part A: Physiology.* **78**(1), 5-13.

Tullett, S. G., Board, R. G., Love, G., Perrott, H. R. and Scott, V. D., (1976). Vaterite Deposition During Eggshell Formation in the Cormorant, Gannet and Shag, and in 'Shell-less' Eggs of the Domestic Fowl. *Acta Zoologica.* **57**(2), 79–87.

Tyler, C., (1964). Wilhelm Von Nathusius 1821-1899 on Avian Eggshells: A Translated and Edited Version of His Work. Reading, UK: The University of Reading

Tyler, C., (1965). A study of the egg shells of the Sphenisciformes. *Proceedings of the Zoological Society of London.* **147**(1), 1-19.

Tyler, C., (1969). Avian Egg Shells: Their Structure and Characteristics. *International Review of General and Experimental Zoology.* **4**, 81-130.

Tyler, C. and Simkiss, K., (1959). A study of the egg shells of ratite birds. *Proceedings of the Zoological Society of London*. **133**(2), 201-243.

Wiemann, J., Yang, T. R. and Norell, M. A., (2018). Dinosaur egg colour had a single evolutionary origin. *Nature*. **563**(7732), 555-558.

Chapter 6:

General Discussion

Thesis overview and new insights

The aim of this thesis was to understand how eggshell microstructure, and particularly variation in microstructure along an egg, is adaptive in birds. I focused primarily on the common guillemot, a species that incubates its egg in a harsh environment without a nest. I then contrasted the common guillemot against its relatives in the Alcidae that incubate their egg(s) in a range of conditions due to varying degrees of nest structure.

In chapter 2, I showed that the eggshells of several Alcid species, especially members of the *Alcini*, are thickest and therefore likely strongest at the equator of the egg. I hypothesised that the most likely function of enhanced shell thickness at the equator is to withstand the weight of large, heavy parent birds during contact incubation. I also found that across Alcid species, birds that incubate their egg(s) on rock and those that lay elongate eggs (which are likely inherently weak due to their shape) have thicker eggshells at the equator than expected for the adult's body mass. This probably confers additional strength to minimize the risk of egg breakage. However, within the common guillemot, I found a contrasting relationship between egg shape – notably elongation – and shell thickness, with more elongate, asymmetric and pointed eggshells being thinner in certain regions. This suggests a potential individual cost associated with laying more extreme shaped eggs.

In chapter 3, I found evidence to support the hypothesis that, as a consequence of variation in regional shell thickness along the egg (Chapter 2), fewer pores form at the thicker-shelled equatorial region of the egg, and more pores form at the thinner-shelled blunt end in order to meet the egg's gas exchange demands. I also found that the total number of pores in an eggshell relates to absolute egg size across the Alcids, but not incubation period.

In chapter 4, I show that the layer of shell accessory material on the surface of common guillemot eggs protects pores by preventing blockage. Gas exchange pores are a weakness in the eggshell's structure into which foreign material may enter, potentially blocking a pore channel or passing into the egg (Board 1982). My data suggest that the

shell accessory material physically prevents such debris from entering and blocking pores.

Finally, in chapter 5, I explored variation in eggshell surface microstructure within the common guillemot, showing that the surface of the calcium carbonate shell is highly variable – potentially as varied as it is between Alcids. I found the equator of the common guillemot eggshell to be rougher than either end of the egg. A rougher eggshell surface may help the shell accessory material to adhere to the eggshell, ensuring it protects the pores over the course of incubation. This would be particularly beneficial at the equator of the egg, since this is the region in contact with the parent and substrate during incubation and is therefore most likely to be abraded. I also found that surface roughness related to eggshell thickness and colour, with darker coloured eggshells tending to be rougher. One hypothesis to explain this result is that pigment influences surface structure formation, and this was supported by my observation that localised patches of surface roughness were associated with dark patches of pigment pattern within the surface layers of the shell. Rougher shell surfaces may also influence the colour of common guillemot eggshell by absorbing and reflecting light differently to smooth surfaces.

Questioning assumptions

In this thesis I question a range of historical and more recent assumptions about the adaptive significance of eggshell microstructure in birds. Here, I summarise the most important of these and the implications for our understanding of how the eggshell functions. I also compare and contrast my findings with those in the literature, aiming to identify which historical assumptions about bird eggs we should carefully consider and question, essentially indicating where a “one size fits all” approach is invalid.

Assumption 1: Eggshell thickness is driven by egg size across species.

It has been traditionally assumed that egg size (specifically, initial egg mass) drives variation in eggshell thickness across birds. However, because contact incubation is likely to exert a much greater force upon the eggshell than any internal hydrostatic pressure within the egg, the mass of the incubating parent is likely to be the primary selective

pressure acting on shell thickness (or strength) (Birchard & Deeming 2009). Due to the positive correlation between adult mass and egg size across birds (and possibly limitations of thickness measures available in the literature; Maurer *et al.* 2010), some previous studies have been unable to distinguish whether egg size or adult mass is the primary determinant of variation in shell thickness (Birchard & Deeming 2009). In this thesis, I show that eggshell thickness is positively related to egg size within the common guillemot (Chapter 2), but across the Alcidae, parental body mass is the more important driver of variation in shell thickness.

Assumption 2: Bird eggs have more pores at the blunt end than at any other region.

For over 100 years, researchers have assumed bird's eggs have the highest density of pores at the blunt end, based on the distribution of pores in chicken eggs first observed by Rizzo (1899 cited in Romanoff & Romanoff 1949). This assumption was further propagated by Rokitka and Rahn (1987) who reported high blunt end pore densities for an additional 6 species. To this day, many researchers still assume that all bird eggs have the highest density of pores at the blunt end (e.g. Smart 1991; Duursma *et al*. 2018), despite the fact that other studies (e.g. Tullett 1975) have observed a range of pore distributions across different species' eggs, and species-specific studies have provided mixed evidence (e.g. Booth 1989; Kern *et al.* 1992; Massaro & Davis 2005; Balkan *et al.* 2006). In this thesis I show conclusively that high blunt end pore densities are not a ubiquitous feature of bird eggs: only 3 of 17 Alcid species studied have a significantly higher density of pores at the blunt end compared to the equator and pointed end.

Assumption 3: Fick's law of diffusion determines eggshell gas conductance.

For around fifty years, gas conductance across the eggshell has been assumed to follow Fick's law of diffusion, with the rate of gas exchange being determined by an eggshell's permeability and the gas tension difference across the shell (Wangensteen & Rahn 1970). Wangensteen *et al.* (1970) and Ar *et al.* (1974) assumed that eggshell permeability was determined by (1) the total number of pores in an egg, (2) the area of each pore and (3) pore length, measured as eggshell thickness. This framework has since been used to

estimate eggshell porosity or gas conductance (e.g. Zimmerman & Hipfner 2007) or to calculate eggshell characteristics from measured rates of daily egg water loss (see Kern *et al.* 1992). However, evidence suggests Fick's law of diffusion may not adequately explain measured eggshell gas conductance (e.g. Simkiss 1986; Deeming 1987; Tøien *et al.* 1988; Jackson *et al.* 2018). Indeed, Portugal *et al.* (2014) found a positive relationship between eggshell thickness at the equator and eggshell gas conductance across 151 British breeding bird species which directly contradicts the theoretical assumption that thicker shells impose any restriction on gas conductance, as thicker shells showed higher rates of gas conductance than thinner shells.

In chapter 4, I show that pore number, but not shell thickness, is related to carbon dioxide conductance. Furthermore, through re-examination of data on duck (Anatidae) eggs from Hoyt *et al.* (1979), I show that total pore number explains more variation in measured gas conductance than calculated gas conductance or total pore area does. Based on our findings across common guillemot and duck eggs, and the strong relationship between total pore number and measured gas conductance presented in Ar and Rahn (1985), total pore number appears to be the most important component of eggshell microstructure for determining eggshell gas exchange efficacy both within and across bird species. Shell accessory materials present on the surface of the shell may further regulate gas exchange in some species (Deeming 1987; Thompson & Goldie 1990; D'Alba *et al.* 2017) – a consideration neglected by the methods of Ar *et al.* (1974). Despite an absence of evidence in these taxa that shell thickness and pore size regulates eggshell gas conductance, it may not be true in all bird species or families. Although it remains possible that shell thickness and pore size are important in determining gas conductance in some bird species or families, I advise caution is taken when inferring any biological significance from gas conductance values calculated from eggshell parameters using the theoretical methods of Ar *et al.* (1974) until these factors are proven to regulate gas conductance in many taxa. Instead when gas conductance cannot be directly measured, it may be more meaningful to compare the estimated values for the total number of pores in an egg across species to draw more valid comparative conclusions on species' evolutionary ecology, reproductive or developmental biology (see Chapter 3 & 4).

Assumption 4: Species with prolonged incubation periods lay less porous eggs.

It is often assumed that bird species with long incubation periods lay eggs that are less porous than expected for the egg's size to ensure the egg does not lose too much water before the chick is ready to hatch (Rahn & Ar 1974; Rahn *et al.* 1976; Ar & Rahn 1980; Roudybush *et al.* 1980; Vleck & Kenagy 1980; Whittow 1980; Grant *et al.* 1982; Whittow *et al.* 1982; Ricklefs 1984; Tullett 1984; Ar & Rahn 1985; Rahn & Paganelli 1990). In this thesis, I found no relationship between total pore numbers and incubation period across the Alcids. Possible reasons why I did not find any relationship are discussed in Chapter 3, but most notably I propose adult incubation behaviour (e.g. altering egg temperature or providing ventilation; Rahn *et al.* 1976; Grant *et al.* 1982; Rahn 1991) and/or components of the incubation environment (e.g. humidity or temperature) may influence the rate of water loss over time and/or other aspects of shell structure (e.g. shell accessory materials; Deeming 1987; D'Alba *et al.* 2017) may be important for regulating eggshell gas exchange. It is important to note that the developing embryo may have more control over egg water balance, and be more tolerant to any imbalance (e.g. Simkiss 1980a, b; Carey 1986), than researchers have previously appreciated, meaning that the eggshell may not be as vital in regulating water loss as is often assumed.

Despite evidence in the literature indicating that selection acting on eggshell porosity primarily relates to the need for an egg to lose the optimal amount of water over the incubation period (see Introduction and Chapter 3), it remains possible that oxygen drives some variation in eggshell porosity across a few bird species (e.g. Zimmerman & Hipfner 2007 but see Discussion in Chapter 3). However, if this is true, we would still expect to find the same predicted pattern, that bird species with short incubation periods lay eggs that are more porous than expected for an egg's size to ensure the embryo gets enough oxygen for rapid embryo development (e.g. Zimmerman & Hipfner 2007), so it does not seem like a pertinent explanation for why I found no relationship between total pore numbers and incubation period across the Alcids.

Assumption 5: Common guillemot eggs have (1) a higher density of pores at the blunt end and/or (2) exceptionally porous eggshells to cope with eggshell surface contamination by debris to facilitate breeding on wet, dirty cliff ledges.

(1) In Birkhead *et al.* (2017) we suggested that common guillemot eggs have a higher porosity at the blunt end to cope with surface contamination by debris, with high blunt end porosity primarily driven by an unequal distribution of pores along its egg (also see Jackson *et al.* 2018; Chapter 4). Here, I show that the unequal pore distribution seen in common guillemot eggs is in fact unlikely to be linked to risk of surface contamination. Like *Uria sp.* guillemots, razorbill eggs also tend to have more pores at the blunt end of their egg, but razorbills do not incubate their eggs in extremely dirty conditions like guillemots do. Equally, species that nest in other dirty environments, such as puffins in mud burrows, do not exhibit an unequal pore distribution along their eggs (Chapter 3).

(2) Belopol'skiĭ (1961) suggested that greater eggshell porosity of *Uria sp*. eggs was adaptive, facilitating adequate gas exchange despite the egg becoming coated in a thick layer of faeces during incubation. Contrary to this hypothesis, I show that common guillemot eggs have similar, if not lower, than expected total pore numbers for the size of their egg (Chapter 3). The differences in pore number reported in Belopol'skiĭ (1961), initially from Kaftanovskii (1941), may instead relate to differences in egg size between *Uria sp*., razorbills (*Alca torda*) and black guillemots (*Cepphus grylle).*

Assumption 6: Common guillemot eggs are self-cleaning.

In 2013, it was suggested that common guillemot eggs were self-cleaning and this allowed them to cope with salt and debris from the incubation environment. These claims were based on observations of the guillemot's shell surface structure, which appeared to be similar to the surfaces of many super hydrophobic, self-cleaning plants, including the lotus (*Nelumbo sp.;* S. Portugal, Unpublished Data; see Birkhead 2016). In recent years, the media (see Chapter 4) have propagated this suggestion, despite no evidence in support of the claim being published. In chapter 4, I demonstrate, using a simple test, that common guillemot eggshells are not self-cleaning.

A broader perspective: can we apply our findings in the Alcidae to all birds?

It is undeniable that the Alcids are an unusual family of birds. For example, most Alcids tend to lay a single egg (or in some cases, two) and incubate it in directly on a natural substrate making little to no nest, whereas other birds typically lay multi-egg clutches and incubate them in a precisely constructed protective nest (Gaston & Jones 1998). Due to the auks uniqueness, the patterns found here may be specific to them. However, studying unusual taxa often gives us an unprecedented opportunity to understand adaptation. Firstly, within the auks there is huge diversity in a range of traits that can be exploited which allowed us to robustly test several hypotheses within a single family. Second, looking at species living at the extremes (such as the common guillemot) can prove enlightening as these are the species where selection is presumably acting most strongly, therefore if no evidence to support hypotheses is found in these focal species, it is unlikely that the factor being investigated is important across a wider range of species, especially those where selection pressures would be lower. Last, some species and the environments they live in are rare or unique therefore they may possess specialised adaptations that can only be studied in such species. Consequently, the auks are among some of the only species where such hypotheses can be tested. However, as a consequence of the auks peculiarities, it may be unwise to generalise the patterns found here to all bird species and families. Indeed, it is likely that a “one size fits all” approach is invalid across all bird families with differences in a family’s (or species’) distinguishing characteristics resulting from multiple section pressures acting at variable magnitudes across different taxa.

In this section, I aim to provide a broader perspective on my findings by comparing some of the key findings of this thesis with other published studies, aiming to identify some patterns which appear to be common in other birds. Later, I highlight the areas where further study is needed to gain a greater understanding into the adaptive significance of avian eggshell architecture.

Our finding that eggshell thickness scales with the mass of the incubating parent is inline with findings across other taxa, including falcons (Falconidae; Castilla *et al.* 2009) and across a wider range of bird families (Birchard & Deeming 2009). Furthermore, the fact that more elongate Alcid eggs tended to be thicker shelled at the equator compared to the blunt end is complementary to the results of a study across 230 British breeding bird species by Maurer *et al.* (2012). The fact that auks that tend to incubate their egg on rock have even thicker shells (especially at the equator) than would be expected based on the mass of the adult bird or how elongate their egg is, corroborates earlier data (Uspenski 1958, Belopol'skiĭ 1961, Williams *et al.* 1982, Pirie-Hay & Bond 2014, Birkhead *et al.* 2017a) and suggestions made in other taxa such as penguins (Spheniscidae), petrels (Fulmarine petrels in the Procellariidae, including the Cape petrel *Daption capense*), Gannets (*Morus sp.*) and terns (*Sterna sp*.; Williams *et al.* 1982; Weidinger 1996; Boersma *et al.* 2004).

It is important to note that these differences in auk eggshells (primarily the effective shell thickness) translated to larger species that lay more elongate eggs on harder substrates (i.e. rock), having a larger safety factor associated with their shell (calculated according to Ar *et al.* 1979) than species that laid less elongate eggs on softer substrates (e.g. puffins; Chapter 2). Even so, all species had a safety factor value which indicated that their eggs could withstand at least twice the weight of an incubating adult on the egg, and thus all Alcid eggs appear to be "over-engineered", as seems to be the case for most other species of bird, apart from those that are exceptionally large such as ostriches (*Struthio sp.*; Ar *et al.* 1979; Birchard & Deeming 2009).

In chapter 3, we suggested that unequal pore distributions may be found in *Uria sp.* guillemot and razorbill eggs because their shell is thicker at the equator and pointed end than at the blunt end, and as a result, fewer pores form at these thicker regions leading to more pores being required at the thinner shelled blunt end to compensate. Anecdotal evidence from other species (e.g. the mute swan *Cygnus olor;* Booth 1989, and peking duck *Anas platyrhynchos domesticus*; Balkan *et al.* 2006; El-Hanoun & Mossad 2008) suggests that this could also be the case in other taxa. However, even within the Alcids, two species that had relatively thick equators compared to the blunt end did not have more pores at the blunt end of their eggs compared to the equator, therefore not all

species with shell thickening at the equator may also have unequal pore distributions (see Chapter 3). Having greater numbers of pores at the blunt end compensates for the fact that razorbill and *Uria sp.* guillemot eggs have fewer pores than we expect at the equator and pointed end, therefore the total number of pores in their egg is in line with what we expect for the size of their egg. The fact that total pore number scales with egg size is a pattern that appears to exist across numerous bird species (see Ar & Rahn 1985; Rahn & Pagnelli 1990).

In chapter 4, we show that shell accessory material on the common guillemot's egg protects eggshell pores by preventing debris from blocking them, allowing optimal gas conductance despite eggs becoming covered in debris during the incubation period. This finding corroborates the observations of Board and Perrott (1982) in guinea fowl (*Numidia meleagris)* eggs and is consistent with the theory and evidence that shell accessory material protects the egg from both nesting debris and water (Board 1981; Board 1982; Board & Fuller 1994; Sparks 1994).

I found evidence to suggest that an egg's base colour may be determined by shell surface structure (Chapter 5). Previous studies in pheasants (*Phasianus colchinus*; Richards & Deeming 2001), chickens (*Gallus gallus domesticus*; Samiullah & Roberts 2013; Samiullah & Roberts 2014) and a wider range of species (e.g. Harrison 1966; Lang & Wells 1987; Sparks 1994; Deeming 2011; Sparks 2011) have highlighted the importance of the shell accessory material in contributing to egg colour and other aspects of an egg's appearance (e.g. gloss or iridescence in tinamou eggs; Igic *et al.* 2015 or UV reflectance; Fecheyr-Lippens *et al.* 2015; D'Alba *et al.* 2017), so our findings complement previous research. However, to our knowledge, our data is the first empirical support for the suggestion that the underlying crystal structure of the eggshell may determine an egg's colour, although previous studies have suggested this may be the case (e.g. Hanley *et al.* 2015; Brulez *et al.* 2016).

Interestingly, we found no evidence that eggshell colour relates to eggshell thickness (Chapter 5). This is complementary to the findings of Pirie-Hay and Bond (2014), but in disagreement with relationships found by Hauber *et al.* (2019) in the common guillemot (see Chapter 5 for greater discussion). Suggestions have been made in other taxa, for

example pheasants, that base eggshell colour putatively relates to eggshell thickness (Richards & Deeming 2001) and Butler and Waite (2016) found that in European starling (*Sturnus vulgaris*) eggs eggshell thickness correlated with several colour metrics. Yet in Eurasian sparrowhawk (*Accipiter nisus;* Jagannath *et al.* 2008), spotless starling (*Sturnus unicolor*; López-Rull *et al.* 2008), common cuckoo (*Cuculus canorus*; Hargitai *et al.* 2010), and collared flycatcher (*Ficedula albicollis*; Hargitai *et al.* 2011) eggs, base egg colour is unrelated to eggshell colour. These findings highlight that any relationship between eggshell colour and shell thickness is probably not universal across all bird families, species or even populations.

The utility of microCT in studying eggshell microstructure

As discussed in the chapter 1, traditional methods used to study eggshell microstructure have several limitations (Appendix A2). In this thesis, I further demonstrate the advantages of using microCT to gain precise and accurate measures of eggshell microstructure specifically, shell thickness (Chapters 2 – 5), pore density (Chapters 3 & 4), pore size (Chapter 4) and surface structure (Chapter 5). Preliminary investigations suggest that additional structural measurements (including quantification of the mammillary bodies) can also be obtained from microCT scans.

Due to the non-destructive nature of microCT, eggshell fragments can be scanned before or after their use in experiments to gain a range of structural measurements without damaging the sample. This increases the utility of microCT compared to methods previously used to measure shell microstructure. In chapter 4 I demonstrate this by scanning the exposed area of shell fragments mounted over the aperture of glass vials. These fragments were also used for carbon dioxide conductance measurements using a Bruker Alpha FTIR Spectrometer, which allowed us to assess the aspects of eggshell microstructure that determine the rate of carbon dioxide loss through the shell, and to scan the shell after the application of debris to quantify the proportion of blocked pores.

One further advantage of microCT is that whole eggshells can be scanned. A recent development of this imaging technique, made possible by a collaboration between myself, colleagues at Sheffield University, and members of the Natural History Museum in

London, has also allowed the scanning of large, fragile, intact eggshells at high resolution (Russell *et al.* 2018; Birkhead *et al.* 2020). My own preliminary investigations also indicate that small eggs, such as those laid by the zebra finch, *Taeniopygia guttata,* can be scanned whole at a sufficient resolution to allow measurement of eggshell microstructure, including quantification of every pore, allowing assessment of how they are distributed over the entire shell surface. Such applications of microCT may allow future research projects to investigate several important questions about eggshell microstructure.

Future directions

Although this thesis has answered several important questions about the structure and function of the avian eggshell, it has also raised many more. Furthermore, as the auks (and especially the common guillemot) are a peculiar taxa, it is important to determine which of our findings are relevant to a wider range of bird species and families, and therefore generalisable. Here, I suggest some directions for future research, which I feel will provide additional insight into the adaptive significance of avian eggshell structure.

Exploring shell thickness variation

Shell thickness is likely an important proxy for shell strength (Ar *et al.* 1979; Bain 2005). Localised crack resistance is expected to be reflected in the thickness of the outer shell layers (termed “effective thickness”; see Chapter 2), because cracks typically originate within the mammillary layer at the point where mammillary bodies fuse together, before propagating through the rest of the shell (Bain 1991; Bain 1992; Solomon *et al.* 1994; Carnarius *et al.* 1996; Bain 2005; Bain *et al.* 2006; Macleod *et al.* 2006; Solomon 2010; Hahn *et al.* 2017). Our results demonstrate that multiple factors are responsible for regional variation in effective shell thickness along an egg. It would be interesting to investigate whether the same factors – adult mass, egg elongation and incubation substrate – found here to be driving shell thickness at the equator of Alcidae eggs, also drive regional variation in eggshell thickness in other taxa. Studies focusing on other families within the Charadriiformes or Sphenisciformes (specifically penguins, Spheniscidae) are likely to be enlightening, as these groups exhibit large variation in egg

shape, adult mass and incubation substrate due to variation in nest type or incubation strategy (e.g. Birkhead *et al.* 2019).

In chapter 2, I found no significant relationship between shell thickness and clutch size, despite the suggestion by Birchard and Deeming (2009) that shell thickness increases with decreasing clutch size. However, the number of species in our dataset that lay more than one egg was small. Studying other taxa with greater interspecific variation in clutch size could help us assess whether clutch size is an important driver of shell thickness variation across birds. If it is, it may confound relationships we expect to see with other factors, such as incubation substrate and egg elongation, because as clutch size increases, the force applied to each egg decreases. This may be one reason why Maurer *et al.* (2012) found that passerine eggs tended to have uniform shell thickness. The equator of eggs in multi-egg clutches may not need to be enhanced if (1) the bird is relatively small and light (as many passerines are), or (2) the weight applied to each egg is low due to the size of the clutch.

The role that the mammillary layer and organic shell and egg membrane thickness have in egg strength remains unclear. The form, structure and irregular distribution of the mammillary bodies, as well as their integration with the membranes, appears to contribute to eggshell strength by reducing the propensity for cracks to propagate through the shell (Bain 1992; Bain *et al*. 2006; Macleod *et al.* 2006; Solomon 2010). However, the absolute thickness of the mammillary bodies seems less important for egg strength (Tyler 1969; Carnarius *et al.* 1996). It may even be advantageous for an eggshell to possess relatively short mammillary bodies that fuse early during eggshell formation, because this would facilitate increased effective shell thickness (for a shell of a given total thickness) and ensure the shell is relatively strong (Bain 1992; Solomon *et al.* 1994; Bain 2005; Macleod *et al.* 2006; Solomon 2010; but see Dunn et *al.* 2012). The ratio of calcified shell to organic membranes, and/or the thickness of the membranes, may contribute to eggshell toughness and how flexible or brittle the shell is, but this idea seemingly remains untested (Bond *et al.* 1986; Bond *et al.* 1988). A greater understanding of the specific eggshell microstructural characteristics of tough and flexible or hard and brittle eggshells across all bird species is still required (Board & Sparks 1991). Empirical testing of eggshells using modern techniques along with precise measurement of shell

microstructure using microCT, would also help clarify the importance of the different layers of the shell in providing strength to the egg. Furthermore, by utilising techniques to analyse the crystal structure of the shell (e.g. Dunn et *al.* 2012; Soler *et al.* 2019), surface microstructure (Chapter 5), nanostructure (e.g. Portugal *et al.* 2018) and hardness (e.g. Portugal *et al.* 2018), and the overall shape of the egg (e.g. Bain 2005; Biggins *et al.* 2018) greater insight could be gained into which macro-, micro- and nanoscale factors determine global and localised egg strength.

Further testing of eggshell thermal properties (e.g. Björn *et al.* 2012; Jiménez-Muñoz & Sobrino 2012; Björn *et al.* 2016) could also confirm whether the eggshell can indeed provide any thermal insulation, as has been claimed by some anecdotal studies (e.g. Yang *et al.* 2018a). A combination of comparative studies of eggshell thickness and empirical tests of the properties that may vary with changing eggshell thickness will help clarify the adaptive significance of eggshell thickness variation across bird eggs.

Why does the distribution of pores vary along an egg?

Assessing regional pore densities across a wide range of bird species' eggs using microCT would provide us with a better understanding of why the distribution of pores along some species' eggs is unequal. The most efficient way to achieve this is to focus on families with known variation in pore distribution, such as the Anatidae (Tullett 1975; Booth 1989; Balkan *et al.* 2006). Investigating pore density variation in relation to egg shape, specifically asymmetry, and/or regional variation in eggshell thickness would allow researchers to corroborate or dispute the results we found within the Alcidae (Chapter 3). Targeting other families within the Charadriiformes could prove enlightening due to the high variation in egg shape within this family (Stoddard *et al.* 2017).

Drivers of eggshell gas conductance

In chapter 3 and 4, I suggest calculated measures of eggshell porosity or gas conductance may not accurately reflect measured gas conductance, in part because the predictive calculations used may not be appropriate. A comparison of predicted and measured eggshell gas conductance across the Alcidae, using modern techniques (such

as microCT and FTIR spectroscopy – Chapter 4), would be beneficial to assess whether a relationship similar to that found in Zimmerman and Hipfner (2007) and previous larger comparative studies (e.g. Ar & Rahn 1985) exists between egg size, incubation period and gas conductance. A study like this could also clarify the relative importance of total pore numbers, pore size, pore length and shell accessory materials in determining the rate of gas exchange across an eggshell.

Understanding eggshell surface structure

In chapter 5, I found an interesting relationship between eggshell base colour and surface structure. Both true shell surface roughness and the coating shell accessory materials were associated with the surface colour of the egg. Further detailed exploration of these relationships would be beneficial to assess whether a combination of surface structure, shell accessory material and surface level pigment are determining base eggshell colour in the common guillemot, and/or whether the association between pigment and colour is due to pigment influencing crystal formation instead. Surface analysis techniques such as microCT and Raman spectroscopy (Thomas *et al.* 2015; Wiemann *et al*. 2018) may prove useful in such studies. To explore the relative importance of shell accessory materials in producing egg colour, accessory materials could be carefully separated from the shell with EDTA (Samiullah & Roberts 2013) and pigment analysis performed separately for the surface layers of the shell and the liberated shell accessory materials. This may facilitate understanding of whether shell accessory materials alter colour exclusively by containing pigment or also via thin-film interference effects. It would be particularly interesting to see if similar patterns between shell surface structure and egg colour exist in other species, or whether this is a unique phenomenon in the common guillemot.

In chapter 4, we demonstrate that shell accessory material protects pores from debris by preventing it from entering and blocking them, ensuring gas conductance remains optimal despite guillemot eggs becoming covered in debris during incubation. It is worth investigating whether shell accessory material has a similar role in other species that incubate their egg in dirty environments, such as the blue footed booby (*Sula nebouxii;* Mayani-Parás *et al.* 2015). In this thesis, (Chapter 5) I suggested that rougher eggshell surfaces may be beneficial in keeping shell accessory material adhered to the eggshell

and in providing protection from abrasion and wear allowing eggs to be protected from debris, water and microbes throughout incubation. However, rougher eggshell surfaces may not be essential for all birds due to the necessity for shell accessory materials to be removed in the latter stages of embryo development to facilitate increased rates of gas conductance across the eggshells of some species (Rahn & Hammel 1982; Thompson & Goldie 1990; Baggot *et al.* 2003). Such species' eggs probably do not require protection provided by shell accessory materials throughout incubation, thus may possess a relatively smooth shell surface to facilitate the wear and removal of these materials by the required time during incubation. Birds that deliberately, but infrequently, soil their eggs as an anti-predator adaptation (e.g. the common eider, *Somateria mollissima*; McDoughall & Milne 1978) may also have a reasonably smooth shell (D.J. Pers. Obs.) to limit the initial adhesion of faecal material to the shell's surface, allowing it to fall off the egg as a powder upon drying (Kear 1963).

It will be interesting to note whether other species that incubate their eggs in conditions where they are threatened by a combination of water, debris, microbes and physical or chemical abrasion, such as members of the Charadriiformes, also have rough eggshells. My preliminary observations suggest that some wading birds (e.g. Kentish plovers, *Charadrius alexandrinus*, and snowy plovers, *Charadrius nivosus*) also have rough eggshell surfaces. Any benefits of this roughness may be especially important in some wading birds due to their tendency to nest in rough scrapes in soil, sand or shingle/pebbles. Some species of wading birds also perform egg wetting behaviours to help cool their eggs down, and this can introduce dirty liquid water onto their eggs throughout incubation (e.g. Howell 1979; Grant 1982; Amat & Masero 2007; Amat *et al.* 2012). Maintaining a functional shell accessory material layer for the entire duration of incubation may therefore be crucial in such species.

To test whether a rougher surface improves adhesion, wear and abrasion resistance properties, techniques devised by tribologists – scientists and engineers who study interacting surfaces in relative motion – could be utilised to provide enlightening qualitative and quantitative data. The use of a modular universal materials tester which provides a range of precise data on surface interactions between two samples would be particularly advantageous. I undertook preliminary exploratory work with this technique

and found I could successfully simulate “realistic” abrasion an egg may experience in the nesting environment against rock or a softer material. Precise conditions can be specified under this set up, including temperature, moisture, humidity, and the force applied onto the eggshell surface. This technique allows controlled lab simulations that likely represent the abrasion an egg experiences in nature.

Beyond living birds: understanding eggshell microstructure in extinct species

I have used microCT in this thesis to study the eggshells of extant birds to gain a greater understanding into the adaptive significance of avian eggshell architecture (Chapters 2 – 5). Although many different imaging techniques can be applied to the study of eggshell microstructure (see Choi *et al.* 2018 for examples in reptile eggs and Appendix A2), microCT’s non-destructive nature means it can also be used to scan irreplaceable specimens (e.g. great auk, *Pinguinus impennis,* eggshells*;* Russell *et al.* 2018; Birkhead *et al.* 2020) that cannot be studied with other advanced, but destructive, techniques. MicroCT has also been used to study hard-shelled eggs of other taxa, including dinosaurs (Hechenleitner *et al.* 2016). A greater understanding of the adaptive significance of avian and reptilian eggshell microstructure in extant species would allow us to better interpret the adaptive significance of shell structure in extinct species, facilitating reconstruction of their nesting ecology (e.g. Hechenleitner *et al.* 2016; Russell *et al.* 2018; Yang *et al.* 2018b; Birkhead *et al.* 2020).

Concluding remarks

Using microCT has proved illuminating for both qualitative and quantitative analysis of eggshell microstructure. It has aided our understanding of why eggshell microstructure varies at the intra- and interspecific level, as well as along individual eggs. In this thesis, I have shown how some aspects of eggshell structure may help mitigate negative aspects of the incubation environment in the Alcidae – a family of pelagic seabirds that incubate their eggs in a wide range of conditions, often with little in the way of a protective nest structure. I have shown that common guillemot eggs are thicker shelled at the equator, probably to provide increased strength needed for contact incubation on a hard rock substrate. Common guillemot eggs also have a rough shell surface at the equator, probably to help shell accessory materials to adhere strongly to the shell and resist wear or removal during incubation on an abrasive substrate. This shell accessory material layer protects pores against wet debris that would otherwise block eggshell pores preventing gas exchange across the shell. Together, these adaptations mitigate the negative components of the common guillemot's incubation environment and are therefore vital to the function of their eggshell.

References

Amat, J. A. and Masero, J. A., (2007). The functions of belly-soaking in Kentish Plovers *Charadrius alexandrinus*. *Ibis*. **149**(1), 91-97.

Amat, J. A., Monsa, R. and Masero, J. A., (2012). Dual function of egg-covering in the Kentish plover *Charadrius alexandrinus*. *Behaviour.* **149**(8), 881–895.

Ar, A., Paganelli, C. V., Reeves, R. B., Greene, D. G. and Rahn, H., (1974). The Avian Egg: Water Vapor Conductance, Shell Thickness, and Functional Pore Area. *The Condor*. **76**(2), 153–158.

Ar, A. and Rahn, H., (1980). Water in the avian egg overall budget of incubation. *American zoologist.* **20**(2), 373-384.

Ar, A. and Rahn, H., (1985). Pores in avian eggshells: Gas conductance, gas exchange and embryonic growth rate. *Respiration Physiology.* **61**(1), 1–20.

Ar, A., Rahn, H. and Paganelli, C. V., (1979). The Avian Egg: Mass and Strength. *The Condor.* **81**(4), 331–337.

Baggott, G. K., Deeming, D. C., Hémon, S. and Paillat, P., (2003). Relationships between eggshell pigmentation, ultrastructure and water vapour conductance in the Houbara bustard (*Chlamydotis undulata macqueenii*). In: *Proceedings of the World Association of Wildlife Veterinarians Wildlife Sessions at the 27th World Veterinary Congress, Tunisia, 26th September 2002* (eds. Scullion, F.T. and Bailey, T.A.). Northern Ireland: World Association of Wildlife Veterinarians. pp. 85 – 88.

Bain, M. M., (1991). A reinterpretation of eggshell strength. In: *Egg and Eggshell Quality* (Ed. Solomon, S. E.). Aylesbury, UK: Wolfe Publishing Limited. pp.131 -145.

Bain, M. M., (1992). Eggshell strength: A relationship between the mechanism of failure and the ultrastructural organisation of the mammillary layer. *British Poultry Science.* **33**(2), 303-319.

Bain, M. M., (2005). Recent advances in the assessment of eggshell quality and their future application. *World's Poultry Science Journal.* **61**(2), 268–277.

Bain, M. M., MacLeod, N., Thomson, R. and Hancock, A. J., (2006). Microcracks in eggs. *Poultry Science*. **85**(11), 2001-2008.

Balkan, M., Karakaş, R. and Biricik, M., (2006). Changes in eggshell thickness, shell conductance and pore density during incubation in the Peking Duck (*Anas platyrhynchos f. dom.*). *Ornis Fennica.* **83**(3), 117.

Belopol'skiĭ, L. O., (1957, translated from Russian 1961). *ecology of sea colony birds of the barents sea*. Jerusalem: Israel Program for Scientific Translations.

Biggins, J. D., Thompson, J. E. and Birkhead, T. R., (2018). Accurately quantifying the shape of birds' eggs. *Ecology and Evolution*. **8**(19), 9728-9738.

Birchard, G. F. and Deeming, D. C., (2009). Avian eggshell thickness: scaling and maximum body mass in birds. *Journal of Zoology.* **279**(1), 95–101.

Birkhead, T. R., (2016). *The Most Perfect Thing: the Inside (and Outside) of a Bird's Egg.* London, UK: Bloomsbury.

Birkhead, T. R., Russell, D., Garbout, A., Attard, M., Thompson, J. E. and Jackson, D., (2020) New insights from old eggs – the shape and thickness of Great Auk *Pinguinus impennis* eggs. *Ibis.*

Birkhead, T. R., Thompson, J. E., Biggins, J. D. and Montgomerie, R., (2019). The evolution of egg shape in birds: selection during the incubation period. *Ibis*. **161**(3), 605-618.

Birkhead, T. R., Thompson, J. E., Jackson, D. and Biggins, J. D., (2017). The point of a Guillemot's egg. *Ibis.* **159**(2), 255-265.

Björn, L. O., Bengtson, S. A., Li, S., Hecker, C., Ullah, S., Roos, A. and Nilsson, A. M., (2016). Thermal emissivity of avian eggshells. *Journal of Thermal Biology*. **57**, 1-5.

Björn, L. O., Uvdal, P. and Li, S., (2012). Ecological importance of the thermal emissivity of avian eggshells. *Journal of Theoretical Biology*. **301**(21), 62-66.

Board, R. G., (1981). The microstructure of avian eggshells, adaptive significance and practical implications in aviculture. *Wildfowl.* **32**, 132–136.

Board, R. G., (1982). Properties of avian egg shells and their adaptive value. *Biological Reviews.* **57**(1), 1–28.

Board, R. G. and Fuller, R., (1994). *Microbiology of the Avian Egg.* London, UK: Chapman and Hall.

Board, R. G. and Perrott, H. R., (1982). The fine structure of the outer surface of the incubated eggshells of the Helmeted guinea fowl (*Numidia meleagris*). *The Journal of Zoology.* **196**(4), 445–451.

Board, R. G. and Sparks, N. H. C., (1991). Shell structure and formation in avian eggs. In: *Egg Incubation: Its effect on embryonic development in birds and reptiles* (eds. Deeming, D. C. and Ferguson, M. W. J.). Cambridge, UK: Cambridge University Press. pp. 71-86.

Boersma, P. D., Rebstock, G. A. and Stokes, D. L., (2004). Why Penguin Eggshells are Thick. *The Auk*. **21**(1), 148-155.

Bond, G. M., Board, R. G. and Scott, V. D., (1988). A comparative study of changes in the structure of avian eggshells during incubation. *Zoological Journal of the Linnean Society.* **92**(2), 105–113.

Bond, G. M., Scott, V. D. and Board, R. G., (1986). Correlation of mechanical properties of avian eggshells with hatching strategies. *Journal of Zoology*. **209**(2), 225-237.

Booth, D. T., (1989). Regional changes in shell thickness, shell conductance, and pore structure during incubation in eggs of the Mute Swan. *Physiological Zoology.* **62**(2), 607-620.

Brulez, K., Mikšík, I., Cooney, C. R., Hauber, M. E., Lovell, P. G., Maurer, G., Portugal, S. J., Russell, D., Reynolds, S. J. and Cassey, P., (2016). Eggshell pigment composition covaries with phylogeny but not with life history or with nesting ecology traits of British passerines. *Ecology and Evolution*. **6**(6), 1637-1645.

Butler, M. W. and Waite, H. S., (2016). Eggshell biliverdin concentration does not sufficiently predict eggshell coloration. *Journal of Avian Biology*. **47**(4), 491-499.

Carey, C., (1986). Tolerance of variation in eggshell conductance, water loss, and water content by red-winged blackbird embryos. *Physiological Zoology*. **59**(1), 109-122.

Carnarius, K. M., Conrad, K. M., Mast, M. G. and MacNeil, J. H., (1996). Relationship of Eggshell Ultrastructure and Shell Strength to the Soundness of Shell Eggs. *Poultry science*. **75**(5), 656–663.

Castilla, A. M., Herrel, A., Van Dongen, S., Furio, N. and Negro, J. J., (2009). Determinants of eggshell strength in endangered raptors. *Journal of Experimental Zoology Part A: Ecological Genetics and Physiology*. **311**(4), 303-311.

Choi, S., Han, S., Kim, N. H., and Lee, Y. N. (2018). A comparative study of eggshells of Gekkota with morphological, chemical compositional and crystallographic approaches and its evolutionary implications. *PloS one.* **13**(6), e0199496.

D'Alba, L., Torres, R., Waterhouse, G. I. N., Eliason, C., Hauber, M. E. and Shawkey, M. D., (2017). What Does the Eggshell Cuticle Do? A Functional Comparison of Avian Eggshell Cuticles. *Physiological and Biochemical Zoology.* **90**(5), 588-599.

Deeming, D. C., (1987). Effect of cuticle removal on the water vapour conductance of egg shells of several species of domestic bird. *British Poultry Science*. **28**(2), 231-237.

Deeming, D. C., (2011). A Review of the Relationship between Eggshell Colour and Water Vapour Conductance. *Avian Biology Research.* **4**(4), 224–230.

Dunn, I. C., Rodríguez-Navarro, A. B., Mcdade, K., Schmutz, M., Preisinger, R., Waddington, D., Wilson, P. W. and Bain, M. M., (2012). Genetic variation in eggshell crystal size and orientation is large and these traits are correlated with shell thickness and are associated with eggshell matrix protein markers. *Animal Genetics*. **43**(4), 410-418.

Duursma, D. E., Gallagher, R. V., Price, J. J. and Griffith, S. C., (2018). Variation in avian egg shape and nest structure is explained by climatic conditions. *Scientific reports*. **8**(1), 4141.

El-Hanoun, A. M. and Mossad, N. A., (2008). Hatchability improvement of Peking duck eggs by controlling water evaporation rate from the egg shell. *Egyptian Poultry Science.* **28**, 767-784.

Fecheyr-Lippens, D. C., Igic, B., D'Alba, L., Hanley, D., Verdes, A., Holford, M., Waterhouse, G. I. N., Grim, T., Hauber, M. E. and Shawkey, M. D., (2015). The cuticle modulates ultraviolet reflectance of avian eggshells. *Biology Open.* **4**(7), 753-759.

Grant, G. S., (1982). Egg Temperature, Nest Humidity, and Behavioral Thermoregulation in a Hot Environment. *Ornithological Monographs.* **30**, 1–75.

Grant, G. S., Pettit, T. N., Rahn, H., Whittow, G. C. and Paganelli, C. V., (1982). Water loss from Laysan and Black-footed Albatross eggs. *Physiological Zoology.* **55**(4), 405-414.

Hahn, E. N., Sherman, V. R., Pissarenko, A., Rohrbach, S. D., Fernandes, D. J. and Meyers, M. A., (2017). Nature's technical ceramic: the avian eggshell. *Journal of the Royal Society Interface.* **14**(126), 20160804.

Hanley, D., Grim, T., Cassey, P. and Hauber, M. E., (2015). Not so colourful after all: eggshell pigments constrain avian eggshell colour space. *Biology letters*. **11**(5), 20150087.

Hargitai, R., Moskát, C., Bán, M., Gil, D., López-Rull, I. and Solymos, E., (2010). Eggshell characteristics and yolk composition in the common cuckoo *Cuculus canorus*: are they adapted to brood parasitism? *Journal of Avian Biology*. **41**(2), 177-185.

Hargitai, R., Mateo, R. and Török, J., (2011). Shell thickness and pore density in relation to shell colouration, female characteristics, and environmental factors in the Collared Flycatcher *Ficedula albicollis*. *Journal of Ornithology*. **152**(3), 579-588.

Harrison, C. J. O., (1966). Variation in the distribution of pigment within the shell structure of birds' eggs. *Journal of Zoology*. **148**(4), 526-539.

Hauber, M. E., Bond, A. L., Kouwenberg, A. L., Robertson, G. J., Hansen, E. S., Holford, M., Dainson, M., Luro, A. and Dale, J., (2019). The chemical basis of a signal of individual identity: shell pigment concentrations track the unique appearance of Common Murre eggs. *Journal of the Royal Society Interface.* **16**(153), 20190115.

Hechenleitner, E. M., Grellet-Tinner, G., Foley, M., Fiorelli, L. E. and Thompson, M. B., (2016). Micro-CT scan reveals an unexpected high-volume and interconnected pore network in a Cretaceous Sanagasta dinosaur eggshell. *Journal of the Royal Society Interface*. **13**(116), 20160008.

Howell, T. R., (1979). *Breeding biology of the Egyptian Plover, Pluvianus aegyptius. University of California Publications in Zoology Vol. 133.* Berkeley, California, USA: University of California Press.

Hoyt, D. F., Board, R. G., Rahn, H. and Paganelli, C. V., (1979). The Eggs of the Anatidae: Conductance, Pore structure, and Metabolism. *Physiological Zoology*. **52**(4), 438-450.

Igic, B., Fecheyr-Lippens, D., Xiao, M., Chan, A., Hanley, D., Brennan, P. R. L., Grim, T., Waterhouse, G. I. N., Hauber, M. E. and Shawkey, M. D., (2015). A nanostructural basis for gloss of avian eggshells. *Journal of The Royal Society Interface.* **12**(103), 20141210.

Jackson, D., Thompson, J. E., Hemmings, N. and Birkhead, T. R., (2018). Common guillemot (*Uria aalge*) eggs are not self-cleaning. *The Journal of Experimental Biology*. **221**(23), jeb188466.

Jagannath, A., Shore, R. F., Walker, L. A., Ferns, P. N. and Gosler, A. G., (2008). Eggshell pigmentation indicates pesticide contamination. *Journal of Applied Ecology*. **45**(1), 133-140.

Jiménez-Muñoz, J. C. and Sobrino, J. A., (2012). Comment on “Ecological importance of the thermal emissivity of avian eggshells”. *Journal of Theoretical Biology*. **304**, 304-307.

Kear, J., (1963). The production of offensive excreta by nesting wildfowl. *Wildfowl Trust Annual Report.* **14,** 162-4.

Kern, M. D., Cowie, R. J. and Yeager, M., (1992). Water loss, conductance, and structure of eggs of pied flycatchers during egg laying and incubation. *Physiological Zoology.* **65**(6), 1162-1187.

Lang, M. R. and Wells, J. W., (1987). A Review of Eggshell Pigmentation. *World’s Poultry Science Journal.* **43**(3), 238–246.

López-Rull, I., Miksik, I., and Gil, D., (2008). Egg pigmentation reflects female and egg quality in the spotless starling *Sturnus unicolor*. *Behavioral Ecology and Sociobiology*. **62**(12), 1877-1884.

Macleod, N., Bain, M. M. and Hancock, J. W., (2006). The mechanics and mechanisms of failure of hens’ eggs. *International Journal of Fracture*. **142**(1-2), 29-41.

Massaro, M. and Davis, L. S., (2005). Differences in egg size, shell thickness, pore density, pore diameter and water vapour conductance between first and second eggs of Snares Penguins Eudyptes robustus and their influence on hatching asynchrony. *Ibis.* **147**(2), 251-258.

Maurer, G., Portugal, S. J. and Cassey, P., (2012). A comparison of indices and measured values of eggshell thickness of different shell regions using museum eggs of 230 European bird species. *Ibis.* **154**(4), 714–724.

Maurer, G., Russell, D. G. D. and Cassey, P., (2010). Interpreting the Lists and Equations of Egg Dimensions in Schönwetter’s *Handbuch der Oologie*. *The Auk.* **127**(4), 940–947.

Mayani-Parás, F., Kilner, R. M., Stoddard, M. C., Rodríguez, C. and Drummond, H., (2015). Behaviorally Induced Camouflage: A New Mechanism of Avian Egg Protection. *The American Naturalist.* **186**(4), E91–E97.

McDougall, P. and Milne, H., (1978). The anti-predator function of defecation on their own eggs by female Eiders. *Wildfowl*. **29**, 55-59.

Pirie-Hay, D. and Bond, A. L., (2014). Thickness of Common Murre (*Uria aalge*) eggshells in Atlantic Canada. *The Canadian Field-Naturalist.* **128**(1), 72–76.

Portugal, S. J., Bowen, J. and Riehl, C., (2018). A rare mineral, vaterite, acts as a shock absorber in the eggshell of a communally nesting bird. *Ibis.* **160**(1), 173-178.

Portugal, S. J., Maurer, G., Thomas, G. H., Hauber, M. E., Grim, T. and Cassey, P., (2014). Nesting behaviour influences species-specific gas exchange across avian eggshells. *The Journal of Experimental Biology.* **217**(18), 3326–3332.

Rahn, H., (1991). Why birds lay eggs. In: *Egg Incubation: Its effect on embryonic development in birds and reptiles* (eds. Deeming, D. C. and Ferguson, M. W. J.). Cambridge, UK: Cambridge University Press. pp. 345-360.

Rahn, H. and Ar, A., (1974). The avian egg: incubation time and water loss. *The Condor.* **76**(2), 147-152.

Rahn, H. and Hammel, H. T., (1982). Incubation water loss, shell conductance, and pore dimensions in Adelie penguin eggs. *Polar Biology*. **1**(2), 91-97.

Rahn, H. and Paganelli, C. V., (1990). Gas fluxes in avian eggs: Driving forces and the pathway for exchange. *Comparative Biochemistry and Physiology Part A: Physiology*. **95**(1), 1-15.

Rahn, H., Paganelli, C. V., Nisbet, I. C. T. and Whittow, G. C., (1976). Regulation of Incubation Water Loss in Eggs of Seven Species of Terns. *Physiological Zoology*. **49**(2), 245-259.

Richards, P. D. G. and Deeming, D. C., (2001). Correlation between shell colour and ultrastructure in pheasant eggs. *British Poultry Science*. **42**(3), 338-343.

Ricklefs, R. E., (1984). Prolonged incubation in pelagic seabirds: a comment on Boersma's paper. *The American Naturalist.* **123**(5), 710-720.

Rokitka, M. A. and Rahn, H., (1987). Regional differences in shell conductance and pore density of avian eggs. *Respiration Physiology.* **68**(3), 371–376.

Romanoff, A. L. and Romanoff, A. J., (1949). *The avian egg*. New York, USA: Wiley.

Roudybush, T., Hoffman, L. and Rahn, H., (1980). Conductance, pore geometry, and water loss of eggs of Cassin's Auklet. *The Condor.* **82**(1), 105-106.

Russell, D., Bernucci, A., Scott-Murray, A., Jackson, D., Farah, A., Garbout, A. and Birkhead, T., (2018). All Our Eggs In One Basket: Challenges of High Resolution X-Ray Micro-Computed Tomography of Great Auk *Pinguinus impennis* Eggshell. *Biodiversity Information Science and Standards 2.* e25784.

Samiullah, S. and Roberts, J. R., (2013). The location of protoporphyrin in the eggshell of brown-shelled eggs. *Poultry science*. **92**(10), 2783-2788.

Samiullah, S. and Roberts, J. R., (2014). The eggshell cuticle of the laying hen. *World's Poultry Science Journal*. **70**(4), 693-708.

Simkiss, K., (1980a). Eggshell porosity and the water metabolism of the chick embryo. *Journal of Zoology.* **192**(1), 1-8.

Simkiss, K., (1980b). Water and ionic fluxes inside the egg. *American Zoologist*. **20**(2), 385-393.

Simkiss, K., (1986). Eggshell conductance—Fick's or Stefan's law? *Respiration physiology*. **65**(2), 213-222.

Smart, I., (1991). Egg shape in birds. In: *Egg Incubation: Its effect on embryonic development in birds and reptiles* (eds. Deeming, D. C. and Ferguson, M. W. J.). Cambridge, UK: Cambridge University Press. pp. 101–116.

Soler, M., Rodríguez-Navarro, A. B., Pérez-Contreras, T., García-Ruiz, J. M. and José Soler, J., (2019). Great spotted cuckoo eggshell microstructure characteristics can make eggs stronger. *Journal of Avian Biology*. https://doi.org/10.1111/jav.02252

Solomon, S. E., (2010). The eggshell: strength, structure and function. *British Poultry Science.* **51**(sup1), 52-59.

Solomon S. E., Bain M. M., Cranstoun S. and Nascimento V., (1994). Hen's egg shell structure and function. In: *Microbiology of the Avian Egg* (eds. Board, R. G. and Fuller, R.). London, UK: Chapman and Hall. pp. 1-24.

Sparks, N. H. C., (1994). Shell accessory materials: structure and function. In: *Microbiology of the Avian Egg* (eds. Board, R. G. and Fuller, R.). London, UK: Chapman and Hall. pp. 25-42.

Sparks, N. H. C., (2011). Eggshell pigments–from formation to deposition. *Avian Biology Research*. **4**(4), 162-167.

Stoddard, M. C., Yong, E. H., Akkaynak, D., Sheard, C., Tobias, J. A. and Mahadevan, L., (2017). Avian egg shape: Form, function, and evolution. *Science.* **356**(6344), 1249-1254.

Thomas, D. B., Hauber, M. E., Hanley, D., Waterhouse, G. I., Fraser, S. and Gordon, K. C., (2015). Analysing avian eggshell pigments with Raman spectroscopy. *The Journal of Experimental Biology*. **218**(17), 2670-2674.

Thompson, M. B. and Goldie, K. N., (1990). Conductance and Structure of Eggs of Adelie Penguins, *Pygoscelis adeliae*, and Its Implications for Incubation. *The Condor*. **92**(2), 304–312.

Tøien, Ø., Paganelli, C. V., Rahn, H. and Johnson, R. R., (1988). Diffusive resistance of avian eggshell pores. *Respiration Physiology.* **74**(3), 345–354.

Tullett, S. G., (1975). Regulation of avian eggshell porosity. *Journal of Zoology.* **177**(3), 339–348.

Tullett, S. G., (1984). The porosity of avian eggshells. *Comparative Biochemistry and Physiology Part A: Physiology.* **78**(1), 5-13.

Tyler, C., (1969). The snapping strength of the egg shells of various orders of birds. *Journal of Zoology.* **159**(1), 65–77.

Uspenski, S. M., (1958). *The Bird Bazaars of Novaya Zemlya.* Canada, Ottawa: Department of Northern Affairs and Natural Resources, Canadian Wildlife Service (translated from Russian).

Vleck, C. M. and Kenagy, G. J., (1980). Embryonic metabolism of the fork-tailed storm petrel: physiological patterns during prolonged and interrupted incubation. *Physiological Zoology*. **53**(1), 32-42.

Wangensteen, O. D. and Rahn, H., (1970). Respiratory gas exchange by the avian embryo. *Respiration Physiology.* **11**(1), 31-45.

Wangensteen, O. D., Wilson, D. and Rahn, H., (1970). Diffusion of gases across the shell of the hen's egg. *Respiration physiology*. **11**(1), 16-30.

Weidinger, K., (1996). Egg variability and hatching success in the Cape petrel *Daption capense* at Nelson Island, South Shetland Islands, Antarctica. *Journal of Zoology*. **239**(4), 755-768.

Wiemann, J., Yang, T. R. and Norell, M. A., (2018). Dinosaur egg colour had a single evolutionary origin. *Nature*. **563**(7732), 555-558.

Williams, A. J., Siegfried, W. R. and Cooper, J., (1982). Egg composition and hatchling precocity in seabirds. *Ibis.* **124**(4), 456–470.

Whittow, G. C., (1980). Physiological and ecological correlates of prolonged incubation in sea birds. *American Zoologist*. **20**(2), 427-436.

Whittow, G. C., Ackerman, R. A., Paganelli, C. V. and Pettit, T. N., (1982). Pre-pipping water loss from the eggs of the Wedge-tailed Shearwater. *Comparative Biochemistry and Physiology Part A: Physiology*. **72**(1), 29-34.

Yang, C., Huang, Q., Wang, L., Du, W. G., Liang, W. and Møller, A. P., (2018a). Keeping eggs warm: thermal and developmental advantages for parasitic cuckoos of laying unusually thick-shelled eggs. *The Science of Nature*. **105**(1-2), 10.

Yang, T. R., Chen, Y. H., Wiemann, J., Spiering, B. and Sander, P. M., (2018b). Fossil eggshell cuticle elucidates dinosaur nesting ecology. *PeerJ.* **6**, e5144.

Zimmermann, K. and Hipfner, J. M., (2007). Egg Size, Eggshell Porosity, and Incubation Period in the Marine Bird Family Alcidae. *The Auk.* **124**(1), 307–315.

Appendices

Appendix A1:

The point of a Guillemot's egg

Timothy R. Birkhead[1*], Jamie E. Thompson[1], Duncan Jackson[1], John D. Biggins[1]

[1]*Department of Animal & Plant Sciences, University of Sheffield, Sheffield, S10 2TN, UK*
[2]*School of Mathematics and Statistics, University of Sheffield, Sheffield S3 7RH, UK*

*Corresponding author
Email: t.r.birkhead@sheffield.ac.uk

Published in IBIS.

IBIS
BOU international journal of avian science
Ibis (2017), **159**, 255–265 doi: 10.1111/ibi.12458

The point of a Guillemot's egg

TIM R. BIRKHEAD,[1]* JAMIE E. THOMPSON,[1] DUNCAN JACKSON[1] & JOHN D. BIGGINS[2]
[1]*Department of Animal & Plant Sciences, University of Sheffield, Sheffield, UK*
[2]*School of Mathematics and Statistics, University of Sheffield, Sheffield, UK*

The adaptive significance of avian egg shape in birds is poorly understood. The pyriform (pear-like) shape of the Common Guillemot's *Uria aalge* egg has long been considered to be an adaptation to prevent eggs rolling off the bare cliff ledges on which this species breeds. Rolling was thought to be prevented either by the egg spinning like a top, which is not the case, or by rolling in an arc, which it does but with little influence on whether the egg will fall from a ledge. We therefore sought alternative explanations for the pyriform shape of the Common Guillemot's egg. This species breeds in extremely dense colonies, which makes their eggs vulnerable to mechanical damage from conspecifics, and to contamination by debris such as faeces and soil. We present evidence consistent with both these possible explanations. First, the pyriform shape of Common Guillemot eggs means that a higher proportion of the eggshell lies in contact with the substrate and this may minimize the effect of impacts. Resistance to impacts may be further enhanced because their eggshells are especially thick where they are in contact with the substrate. Secondly, Common Guillemot eggs are often heavily contaminated with faecal material and other debris during incubation. Most contamination is on the pointed end of the egg where it is in contact with the substrate; the pyriform shape thus keeps the blunt end of the egg, which has the highest porosity, relatively free of contamination, which in turn may facilitate both gas exchange during incubation and the hatching process, because the chick emerges from the blunt end of the egg.

Keywords: Common Murre *Uria aalge*, egg shape, eggshell thickness, faecal contamination, pyriform, Razorbill *Alca torda*, stress concentration.

The shape of birds' eggs varies considerably, from near-spherical, to oval, elongate, bi-conical and pyriform (Thomson 1964). With few exceptions (e.g. in waders, Andersson 1978), the adaptive significance of avian egg shape is poorly understood. However, the pyriform (pear-shaped) egg of the Common Guillemot *Uria aalge* (hereafter Guillemot) and Brünnich's Guillemot *Uria lomvia* has long been considered an adaptation to reduce the risk of rolling off the narrow, rocky cliff ledges on which these species breed without constructing a nest (MacGillivray 1852, Belopol'skii 1957, Gill 2007).

The first explanation for the Guillemot's pyriform egg shape was that it allowed the egg to spin like a top (on its side) when knocked or blown by the wind (Hewitson 1831). However, the ability of Guillemot eggs to spin was based on empty museum eggshells and is biologically meaningless, and it was later shown that intact Guillemot eggs containing yolk and/or an embryo did not move in this way when knocked. Instead, they tend to roll in an arc (Belopol'skii 1957, Ingold 1980, Birkhead 2016). In contrast, the 'elliptical ovate' (i.e. much less pointed) egg of the Razorbill *Alca torda* rolls in a much wider arc (Kaftanovski 1941, Belopol'skii 1957, Ingold 1980).

Tschanz *et al.* (1969) provided what appeared to be clear-cut evidence that as the shape of Guillemot eggs becomes more pyriform, the tighter the rolling arc becomes and the greater the protection it provides against falling off a ledge. However, Tschanz *et al.*'s (1969) results were

*Corresponding author.
Email: t.r.birkhead@sheffield.ac.uk

derived from model eggs made of plaster, which do not behave in the same way as real eggs (Ingold 1980). Comparing real Guillemot and Razorbill eggs on natural substrates, Ingold (1980) found little difference in their rolling arcs, suggesting that the pyriform shape of the Guillemot's egg provides little or no protection from rolling. Even so, and slightly confusingly, having found that mass as well as shape affected an egg's rolling trajectory, Ingold (1980) concluded that a pyriform shape must still be advantageous for Guillemot eggs, because if they were the same shape as Razorbill eggs (which are smaller and therefore lighter in mass), they would be more likely to roll off the ledge.

The evidence that the Guillemot's pyriform egg shape is an adaptation to facilitate rolling in an arc, thus reducing the risk of rolling off the ledge, is very limited. Moreover, there are several reasons for questioning the assumptions of the rolling-in-an-arc hypothesis: (1) Guillemots often breed on ledges much narrower than the arc described by a rolling egg (Harris & Birkhead 1985, Birkhead & Nettleship 1987); (2) as Guillemots typically incubate facing the cliff wall with the pointed end of their egg directed towards the cliff edge (Tschanz 1968, T.R. Birkhead pers. obs.), a dislodged egg would roll *outwards* towards the cliff edge and thus be more likely to fall; (3) Guillemot eggs vary considerably in shape (Tschanz *et al.* 1969, Birkhead *et al.* 2017), suggesting that there is little stabilizing selection on egg shape; (4) Brünnich's Guillemots produce eggs that are less pyriform-shaped than those of Common Guillemots (Belopol'skii 1957, Harris & Birkhead 1985), despite their breeding on narrower ledges (Birkhead & Nettleship 1987). Ingold (1980) explained this apparent anomaly by invoking the interaction between shape and mass and suggesting that because the eggs of Brünnich's Guillemots were smaller and lighter in mass, they would roll in a smaller arc and thus be less vulnerable to falling than are Common Guillemot eggs. However, a test of this hypothesis comprising a comparison of the shape and mass of Common and Brünnich's Guillemot eggs provided no support for this idea (Birkhead *et al.* 2017).

The eggs of both guillemot species are subject to two selection pressures that have not previously been considered: the risk of physical damage from conspecifics and contamination by debris.

Guillemots typically breed in direct bodily contact with conspecifics at high densities (regularly at around 20 pairs per square metre, but up to 70 pairs per square metre; Birkhead 1993) on both broad and narrow ledges (Birkhead 1977). Incubating birds are frequently jostled by their neighbours during fights and it is not uncommon for birds returning from the sea to land heavily (body mass *c.* 1 kg) directly on top of incubating conspecifics. It has been argued that, all else being equal, a spherical egg will have the greatest resilience to impacts (Smart 1969, Bain 1991). However, no bird lays a completely spherical egg. Moreover, with a spherical egg, the effects of any impact, from above, for example, would be concentrated onto a very small region of the shell where the egg is in contact with the substrate. In engineering terms, this point is referred to as the 'stress concentration' (Pilkey & Pilkey 2008) and is the place on the shell where it is most likely to break. With a pyriform egg, it seems plausible that a greater proportion of the shell lies in contact with the substrate, meaning that the stress of any impact will be spread over a greater surface area, thereby conferring greater eggshell strength.

Guillemots defecate without regard to their neighbours, so that the rocky substrate on which they breed is usually covered with faecal material. Along with any soil already present at the breeding site, faecal material can contaminate the eggs, especially in wet weather. Brünnich's Guillemots breed under similar crowded and 'dirty' conditions, albeit on narrower cliff ledges at lower density (Gaston & Nettleship 1981, Birkhead & Nettleship 1987). Contamination of the eggshell by faeces and other debris can potentially compromise gas exchange and facilitate microbial infection, both of which can be fatal to avian embryos (Board 1982, Verbeek 1984).

Our aim here is to offer two new explanations for the pyriform shape of Guillemot eggs: first, the pyriform egg shape confers physical strength that enables Guillemot eggs to withstand impacts resulting from the vigorous 'rough and tumble' of a dense breeding colony; secondly, the pyriform egg shape reduces the consequences of debris contamination of the egg surface. We provide data in support of each possibility, and offer some suggestions for further study.

METHODS

To obtain measurements of eggshell characteristics we used Guillemot eggs from our field site at

Skomer Island, Wales, UK (under licence). We made some comparisons between the eggshells of Guillemots and Razorbills, the latter also from Skomer and collected under licence; all eggs were from 2014, 2015 and 2016. The Razorbill is closely related to the Guillemot and also breeds colonially on sea cliffs (and often in close proximity to Guillemots), but as isolated pairs and often in rocky cavities where there is little risk of their egg falling (Harris & Birkhead 1985, Smith & Clarke 2015). Ingold's (1980) investigation of the adaptive significance of Guillemot egg shape was based partly on comparisons with Razorbill eggs, which is why we have included data for that species here.

Contact of the eggshell with the substrate

We calculated the 'contact index' (defined below) for Guillemot and Razorbill eggs to quantify the extent to which the eggshell is in contact with the substrate and the extent to which the pyriform shape of the Guillemot egg results in a higher value. A greater area in contact with the substrate would reduce the stress per unit area should there be an impact, particularly from above, and thus reduce the probability of breakage. To obtain a sufficiently large sample of eggs of both Guillemot (n = 83) and Razorbill (n = 79) from the same colony, we used eggshells collected from Bempton, Yorkshire, UK, and held in the Natural History Museum, Tring, UK, for this part of the study.

Typically, an egg's centre of gravity moves towards the pointed end of the egg as incubation proceeds and the air cell increases in size, changing the egg area in contact with the substrate over incubation (Belopol'skii 1957). Because Guillemots incubate in a semi-upright posture, the weight of the bird's body essentially causes the egg to adopt the maximum contact with the substrate (Tschanz 1990, T.R. Birkhead pers. obs.). To account for this, we used the following method to obtain an objective index of the maximum proportion of the egg in contact with the substrate during incubation. Using the outline from an egg silhouette image obtained by photographing each egg against a lightbox, we mathematically captured the shape of an egg from which we could derive the other parameters including the two-dimensional area of the silhouette and the egg surface area, using the methods described by Preston (1953) and Todd and Smart (1984). The formula for the shape was then used to locate the place on the eggshell surface where the profile was flattest. Although the actual profile is a smooth curve with only a tiny point of contact, in reality imperfections in the egg surface and irregularities in the substrate will spread this contact. In the plane that is tangential at the point where the profile is flattest, we calculated the area within 0.2 mm of the egg surface on the assumption that a 0.2-mm tolerance reflects both the flexing of the shell and these imperfections and irregularities. That area in contact with the substrate was then expressed as a percentage of the area of the egg silhouette, so that egg size is not a factor, to give the 'contact index'. We also explored the consequences of tolerances of 0.1 and 0.5 mm to account for the unevenness of the substrate. See Appendix S1 for further methodological details.

Measuring eggshell thickness

Eggshell strength is determined in part by thickness (Romanoff & Romanoff 1949), and as the two *Uria* species have thicker eggshells than those of any other bird laying similarly sized eggs (Schoenwetter 1960–1992, see also Pirie-Hay & Bond 2014), it follows that their eggshells are particularly strong. Our aim was to compare shell thickness in different regions of the eggshell, to establish whether the shell was thickest in the region where it is in contact with the substrate. Different studies have measured eggshell thickness in different ways, but most have assessed the entire thickness of the shell, with or without the shell membrane. According to Bain (2005), however, the measure of thickness that best reflects eggshell strength is the distance between the point of fusion of the palisade columns to the outer edge of the shell accessory material; this measure is referred to as 'effective thickness' (Fig. S2 and Table S1).

Eggshell thickness measures were obtained from 10 Guillemot eggs collected on Skomer Island in 2014 (n = 5), 2015 (n = 3) and 2016 (n = 2). For each egg, 10 measures were taken from the blunt pole, the equator (maximum diameter) and near (but not at) the pointed end of the egg (see Results for details on sampling location) using micro-CT scanning. From these 10 measures, we calculated mean values for several different measures of thickness for each eggshell fragment, obtained as follows.

Fresh eggs were drained of their contents, washed in distilled water and allowed to dry. To obtain shell fragments for measuring, a hand-held rotary saw (DREMEL Multi, Mod. 395 Type 5 Code 83; DREMEL, USA) was used to cut *c.* 1-cm^2 pieces from each of three regions of the egg. Eggshell fragments were scanned in a Bruker Skyscan 1172 using the following settings: scanner set at 100 kV electron acceleration energy and 90 μA current with the sample 48.7 mm from the X-ray source with a 1.0-mm aluminium filter, with the sample 283.349 mm away from the camera. Camera resolution was set at 1048 × 2000 pixels, with a pixel size of 4 μm. We used the same setting for each scan, collecting a total of 1048 projection images using a rotation step size of 0.4° and a detector exposure of 1475 ms integrated over three averaged images resulting in a total scan time of 50 min. Two eggshell fragments were scanned during each session. Projection images were then reconstructed in NRECON software (version 1.6.10.1) before image analysis was performed in CT analyser (CTAN, version 1.14.41), CTVOX (version 3.0; all the above software provided by Bruker micro-CT, Kontich, Belgium) and IMAGEJ (version 1.49p; Schneider *et al.* 2012). Reconstruction parameters were: dynamic image range; minimum attenuation coefficient = 0, maximum = 0.08, level 2 Gaussian smoothing, ring artefact correction = 12, beam hardening correction of 20% and auto misalignment compensation, images saved as 8-bit bitmaps. Shell thickness was measured in CTAN software using the line measurement tool at 10 haphazardly selected locations within each shell fragment.

To test for differences in eggshell thickness between the three regions of the Guillemot eggshell we ran a one-way ANOVA, using repeated measures analysis to control for multiple measures from the same egg. To test for differences in the relative variation in effective eggshell thickness between Guillemot and Razorbill eggs (whose eggs are slightly smaller: Harris & Birkhead 1985), we calculated the ratios between eggshell thickness in different regions of the eggs (blunt/equator, blunt/point and equator/point) of both species.

Measuring debris contamination on the egg surface

We recorded the extent of debris (mainly faeces and soil) contamination of 59 Guillemot and 40 Razorbill eggs on Skomer Island, Wales, in 2016. To standardize the time period available to accumulate debris, we photographed eggs on a single occasion 22–25 days after each species' median laying date (9 May for Guillemots and 12 May for Razorbills; T.R. Birkhead pers. obs.). The eggs of both species were all from the same (mixed) colony where the two species were breeding as close as 15 cm to each other.

Using a life-size image of each egg, we superimposed a grid of 5-mm squares, and recorded whether each egg had any opaque debris (i.e. debris that obscured the ground colour or maculation), to provide an estimate of the proportion of 'dirty' eggs. We also recorded whether each 5-mm square contained any debris, to provide an estimate of the extent (expressed as a percentage) of the total area of the blunt end (i.e. lying above the maximum egg diameter) and the pointed end (below the maximum egg diameter) of each egg that was covered by debris. To check for repeatability (Lessells & Boag 1987, Nakagawa & Schielzeth 2010), 20 Guillemot and Razorbill egg images were scored independently by five different individuals; repeatability was found to be high (blunt end: $F_{19,80} = 62.3$, $r = 0.92$, $P < 0.0001$; pointed end: $F_{19,80} = 43.8$, $r = 0.89$, $P < 0.0001$).

Measuring eggshell porosity

The efficacy of gas exchange between the embryo and outside world is determined by the number and dimensions of the eggshell pores (Ar & Rahn 1985). Gas exchange is likely to be compromised if eggshell pores are blocked with debris (Board 1982).

The limiting dimension for the diffusion of gases is the minimum cross-sectional pore area, that is, the narrowest part of the pore (Tøien *et al.* 1988). Using *c.* 1-cm^2 fragments of eggshell from three different regions of each egg (as above), we calculated eggshell porosity (i.e. total pore area in mm^2) by multiplying the average minimum cross-sectional area of pores by the pore density (pores per mm^2), to give the total functional pore area in 1 mm^2 of eggshell (Ar & Rahn 1985). Our method was similar to that of Riley *et al.* (2014), who also used micro-CT to identify and measure the narrowest cross-sectional pore areas directly. Fragment area and minimum cross-sectional pore area were both measured in IMAGEJ. Pores were measured by re-slicing the reconstructed image stack and taking measurements from orthogonal views, working through 4-μm image slices one at a time from the shell outer

surface to the inner surface until the minimum cross-sectional area of the pore was measured. Ten pores per fragment were haphazardly selected for measurements. Image stacks were then loaded into CTVox to produce 3-D volumetric reconstructions of the eggshell fragment, and the number of pores was counted and then divided by fragment area (mm^2) to obtain pore density.

We determined the repeatability of porosity and shell thickness measures within each region of an egg using three fragments from each region of five Guillemot and five Razorbill eggs (Lessells & Boag 1987, Nakagawa & Schielzeth 2010). Repeatability was very high for effective shell thickness for both species ($r = 0.97$, for both species) and reasonably high for porosity (Guillemot: $r = 0.74$, Razorbill: $r = 0.58$) (Table S2).

To test for differences in porosity between the three regions of the Guillemot eggshell, we ran a one-way ANOVA on log-transformed data, with the repeated measures analysis to control for multiple measures for each egg. Log transformation was necessary to make the Guillemot egg data fulfil the assumptions of the analysis. This was not necessary for the Razorbill egg data.

All data were analysed using the base package R (R Development Core Team 2012). Where two-sample *t*-tests were used, Welch's correction was applied to account for unequal sample sizes and variances and thus provide degrees of freedom that are lower than would otherwise be expected for given samples sizes. Means are expressed ± 1 sd.

RESULTS

Contact of the eggshell with the substrate

The Guillemot's pyriform-shaped egg is characterized by a relatively long, straight surface below the equator towards the point, compared with that of the elliptical-ovate egg of a Razorbill (Fig. 1). The contact index of Guillemot eggs, assuming a tolerance of 0.2 mm, was significantly greater (mean = 2.14 ± 0.32, $n = 83$) than that of Razorbill eggs (mean = 1.81 ± 0.14, $n = 79$) (Welch's two-sample *t*-test: $t = 8.48$, df = 111, $P < 0.001$; Fig. 1). We obtained very similar results with tolerances of 0.1 and 0.5 mm, both of which were highly correlated with the 0.2-mm tolerance measures (Spearman's correlation: $r_s > 0.997$ in both cases). For 83 Guillemot eggs, this contact index is strongly and positively correlated (Spearman's correlation: $r_s = 0.83$, $n = 83$, $P < 0.001$) with the degree of pointedness (i.e. the proportion of overall egg length between the egg's widest point and the more pointed end of the egg). These results are consistent with our hypothesis that the pyriform shape of the Guillemot's egg results in a relatively larger proportion of the egg's surface being in contact with the substrate, potentially reducing the stress per unit area during impacts.

Eggshell thickness

Guillemot eggshells were thinnest (total eggshell thickness including the shell membranes) at the blunt end (536 μm ± 23.8) and thickest at the equator (651 μm ± 28.2) and pointed end (639 μm ± 39.5). This difference in thickness between the blunt end and the other regions was significant ($F_{2,18} = 44.1$, $P < 0.001$; Tukey multiple comparison test: $P < 0.05$). Pirie-Hay and Bond (2014) obtained a similar result with Common Guillemot eggs, as did Uspenski (1958) for

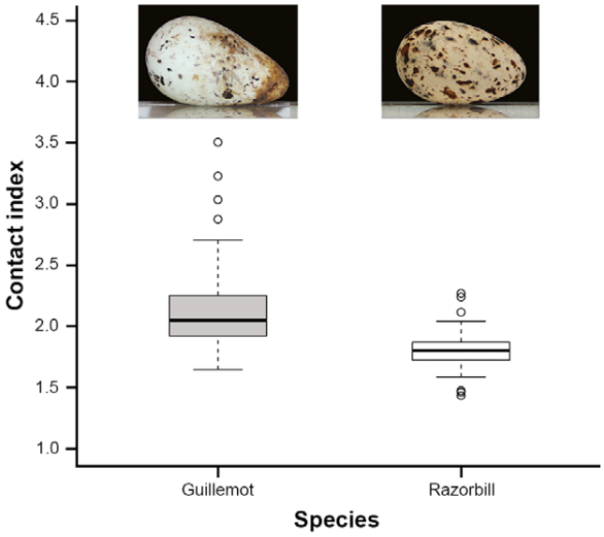

Figure 1. Contact index in Guillemot ($n = 83$) and Razorbill eggs ($n = 79$): museum specimens collected from Bempton Cliffs, Yorkshire, UK. Upper images show profiles of an intact and partly incubated Guillemot egg (left) and Razorbill egg (right), to illustrate the difference in the percentage of eggshell in contact with the substrate. Boxes are the interquartile range, black line within the box is the median, the whiskers show the highest and lowest values and open circles indicate potential outliers. The contact index of Guillemot eggs is significantly greater than that of Razorbill eggs ($P < 0.001$): see text for details. [Colour figure can be viewed at http://onlinelibrary.wiley.com/journal/10.1111/(ISSN)1474-919X]

Brünnich's Guillemot eggs. In terms of effective eggshell thickness (see Methods), the equator was significantly thickest (471 μm ± 23.8), followed closely by the pointed end (432 μm ± 30.6), and the blunt end of eggs was thinnest (362 μm ± 32) ($F_{2,18} = 41.0$, $P < 0.001$; Tukey multiple comparison test: $P < 0.05$). However, effective thickness ratios between different regions of the egg showed that the pattern in shell thickness differs between Guillemot and Razorbill eggs, primarily in the magnitude of difference between the blunt and equator region, but also in the magnitude of difference between the equator and pointed region (Fig. 2).

Debris contamination on the egg surface

Guillemot eggs were significantly more likely to have any visible faecal material and/or soil – measured as opaque contamination – on their surface (56/59, 97%) than were Razorbill eggs (17/40, 43%) ($\chi^2 = 31.2$, df = 1, $P < 0.001$; Fig. 3). In the Guillemot eggs, debris contamination was more frequent on the pointed end of the egg than on the blunt end (paired *t*-test: $t = 7.75$, df = 58, $P < 0.001$), but this was not the case with the Razorbill eggs (paired *t*-test: $t = 0.01$, df = 39, $P = 0.992$) (Fig. 4).

Eggshell porosity

The blunt end of Guillemot eggshells was significantly more porous than other egg regions (one-way ANOVA with repeated measures: $F_{2,8} = 13.5$, $P < 0.001$; Tukey multiple comparison test: $P < 0.05$; Fig. 5). Specifically, the blunt end of a Guillemot egg ($3.21 \times 10^{-4} \pm 1.58 \times 10^{-4}$ mm^2) was significantly more porous than both the equator ($1.24 \times 10^{-4} \pm 7.25 \times 10^{-5}$ mm^2) and the pointed region ($9.68 \times 10^{-5} \pm 4.57 \times 10^{-5}$ mm^2). Although the pattern was similar in Razorbill eggs, it was much less pronounced and not statistically significant (one-way ANOVA with repeated measures: $F_{2,8} = 3.13$, $P = 0.0684$; Fig. 5).

DISCUSSION

Contrary to popular belief, there is almost no evidence that the pyriform shape of Guillemot eggs, and their resulting tendency to roll in an arc, is an

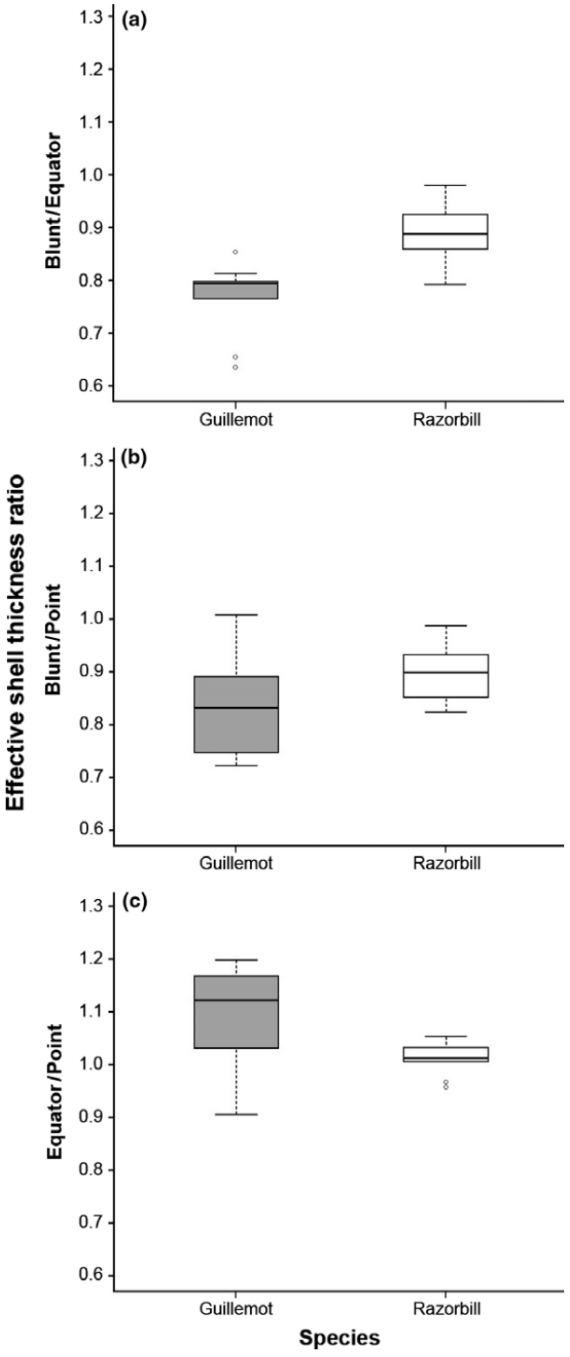

Figure 2. Effective shell thickness ratios between different regions of Guillemot and Razorbill eggs: (a) blunt/equator, (b) blunt/point, (c) equator/point. The Guillemot eggshell blunt/equator ratio (Welch's two-sample *t*-test; $t = 4.38$, df = 17, $P < 0.001$) and equator/point ratio (Welch's two-sample *t*-test; $t = 2.74$, df = 11, $P = 0.02$) are significantly different from that of Razorbill eggshells. There is no significant difference in blunt/point ratio between the two species (Welch's two-sample *t*-test; $t = 1.79$, df = 15, $P = 0.09$). A total of 20 ratios were analysed from 10 Guillemot and 10 Razorbill eggs.

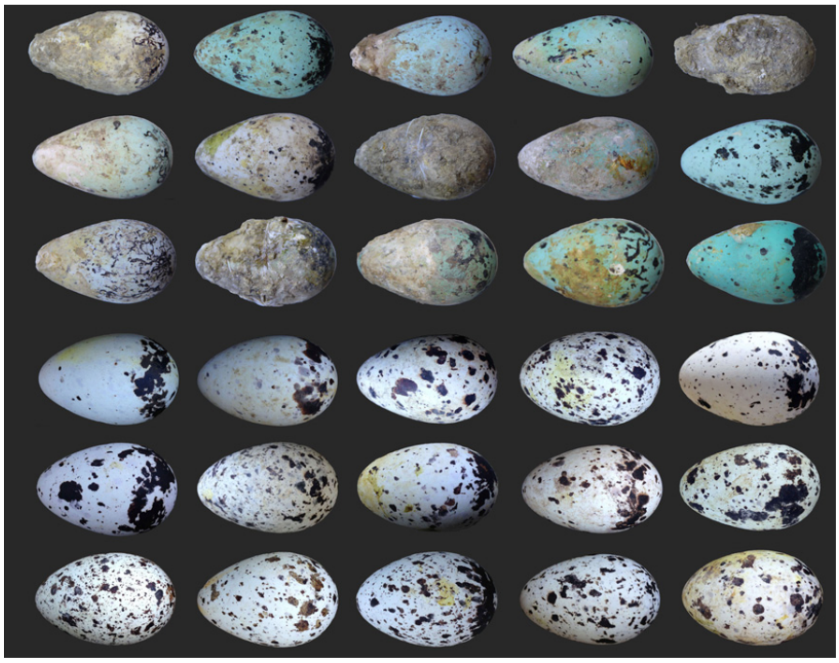

Figure 3. Examples of naturally incubated Guillemot (top three rows) and Razorbill (bottom three rows) eggs (n = 15 each), located haphazardly and photographed on the same ledge at approximately the same stage of incubation on Skomer Island, Wales (see text), to illustrate the extent of debris (both faecal and soil) contamination. The Guillemot eggs are more likely to be encrusted with faecal material and dirt, especially towards the pointed end of the egg. Some Razorbill eggs are contaminated with yellow material that we presume is a thin layer of faecal material, but not especially at the pointed end and none are encrusted in the same way as Guillemot eggs.

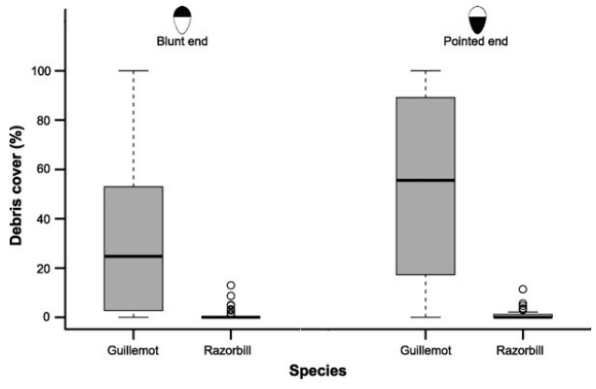

Figure 4. Extent of debris contamination on the eggs of Guillemots (n = 59) and Razorbills (n = 40) photographed part-way through incubation on Skomer Island, Wales (see Fig. 3). Contamination is significantly greater on Guillemot eggs, on both the blunt and the pointed ends, than on Razorbill eggs. Boxes are the interquartile range, black line within the box is the median, the whiskers show the highest and lowest values and open circles indicate potential outliers.

adaptation to reduce the risk of their falling off cliff ledges. We offer two new hypotheses to account for the pyriform shape of Guillemot eggs: that it provides resistance against impacts and protection from faecal and other contamination.

We obtained several results consistent with our first hypothesis that the Guillemot's pyriform egg shape confers strength and resistance against impacts. The pyriform shape of the Guillemot's egg results in a greater proportion of the egg surface area being in contact with the substrate than in the closely related Razorbill, which has less pear-shaped eggs. We propose that having a large proportion of the egg in contact with the substrate minimizes the 'stress concentration', that is, it disperses the consequences of any impact, which in turn reduces the likelihood of breakage resulting from an impact, particularly from above (Pilkey & Pilkey 2008). We suggest that the pyriform shape means that Guillemot eggs are relatively crush-proof in the region where impact is most likely.

As noted by several other authors, the eggshells of the Common Guillemot and Brünnich's Guillemot are, for their size, thicker than those of almost any other bird (Schoenwetter 1960–1992, Pirie-Hay & Bond 2014). We found Guillemot eggshells to be thickest at the equator and the pointed pole

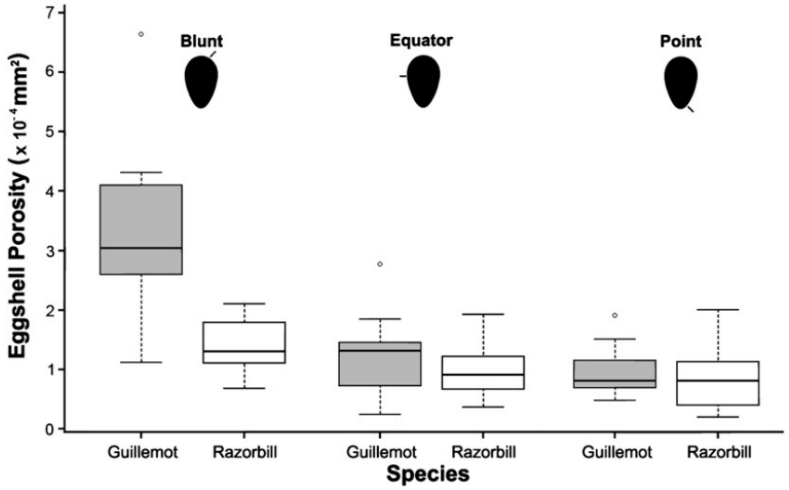

Figure 5. Porosity (total minimum pore area per mm^2) of Guillemot and Razorbill eggshells. The blunt end of Guillemot eggshells was significantly more porous than other egg regions ($P < 0.05$); Razorbill eggs were equally porous in all regions ($P > 0.05$). Boxes are the interquartile range, black line within the box is the median, the whiskers show the highest and lowest values and open circles indicate potential outliers. Ten Guillemot eggs and 10 Razorbill eggs were analysed and a mean value for each eggshell region (blunt, equator and point) was calculated, providing a total of 60 measurements.

(as did Maurer *et al.* 2012), essentially the area that lies in contact with the substrate during incubation. Indeed, as Maurer *et al.* (2012) found, although the blunt pole is thinner than the equator in the eggs of many of the 230 bird species they examined, that difference was most extreme in the Guillemot (also see Fig. 2). Our data show that the greater thickness at the equator is primarily due to an increase in effective shell thickness, rather than an increase in membrane or mammillary layer thickness (Fig. S3). This is also the case for the thickness at the pointed end, although an increase in membrane thickness contributes to the total thickness in this region. As greater shell thickness within a Guillemot egg is due to an increase in effective shell thickness, it is likely that the eggshell strength at the equator and pointed end is enhanced compared with the blunt pole. The blunt pole is less vulnerable to impact and, by being thinner, may enable the chick to emerge more easily from the shell. If it is true that a spherical egg has the greatest resistance to crushing (Smart 1969, Bain 1991), the enhanced shell strength at the equator and pointed end may be necessary to reinforce a potentially weak egg shape resulting from the Guillemot egg's elongation and deviation from a sphere (Maurer *et al.* 2012).

In reality, the minimization of the stress concentration by maximizing contact with the substrate, together with the increased shell thickness in the region of the eggshell where impact is most likely, must work together to create the Guillemot's robust eggshell, but it will require detailed experiments to establish the relative importance of these two features.

We also obtained evidence consistent with our second hypothesis that a pyriform shape provides some protection from debris contamination. In other species, debris contamination of eggshells can be fatal for the embryo, either because the pores in the eggshell become blocked and compromise gas exchange, or because of microbial infection (Verbeek 1984). The pyriform shape of the Guillemot's egg means that the blunt end of the egg is raised above the substrate surface and less likely to be covered in faecal material and/or soil than the pointed end. This may also explain the striking increase in porosity at the blunt end of the egg, which is also the end at which the chick's head is located in the later stages of incubation and from which the chick emerges from the shell (Tschanz 1968).

In a previous study, Zimmermann and Hipfner (2007) found no differences in pore density or pore size between the same three regions of Guillemot eggs as examined here. It seems likely that this discrepancy between their result and ours is a consequence of the methods used to assess porosity. For example, Zimmermann and Hipfner (2007) measured the area at the pore orifice on

the inner surface of the shell, which we found to be on average 545 $\mu m^2 \pm 424$ greater than the minimum pore area measured using micro-CT. Although these two measures are weakly and positively correlated, the scatter is considerable (Fig. S4).

We have not, as yet, tested either hypothesis directly and two remaining questions are whether an elliptical-ovate egg (such as that of a Razorbill) of the same thickness as a Guillemot egg would confer the same degree of protection from impacts, and whether the elliptical-ovate Razorbill egg subjected to the same degree of faecal exposure as Guillemot eggs would suffer greater contamination of its blunt end and, as a result, reduced hatching success.

There are several reasons why the view that the pyriform shape of a Guillemot's egg is an adaptation to prevent rolling has been so pervasive. First, the idea is intuitively appealing, in part because single factor explanations are often preferred. Secondly, the rolling-in-an-arc idea gained traction initially because rolling was seen as a major mortality factor. However, this was a consequence of researchers such as Belopol'skii (1957) and Tuck (1961) using crude study methods (including walking on to the breeding ledges and firing guns at colonies), causing massive disturbance. Thirdly, the experimental results of Tschanz *et al.* (1969) helped perpetuate the rolling-in-an-arc idea, even after Tschanz's student and colleague, Ingold (1980), showed that those experiments were flawed. Finally, it is interesting that, in an overview, Tschanz (1990) agreed with Ingold that the Guillemot egg shape 'confers no greater advantage than a Razorbill egg on a Guillemot ledge (in preventing egg loss via rolling), but brooding behaviour does'.

Under normal circumstances, undisturbed guillemots of both *Uria* species very rarely leave their egg unattended and the risk of rolling is minimal, except during incubation changeovers, or sometimes during bouts of intraspecific aggression (e.g. Birkhead 1977, Gaston & Nettleship 1981, Harris & Wanless 1988). During incubation exchanges, Guillemots minimize the risk of egg-rolling by careful manipulation of the egg with their beak, retaining or sometimes transferring the egg between the tarsi, but also using their drooped wings to prevent the egg from rolling (Tschanz 1990, T.R. Birkhead pers. obs.). In addition, incubating Guillemots routinely accumulate small stones under and around the egg, which although dismissed as 'vestigial nest-building' (Tuck 1961) almost certainly provide additional stability to the egg. In many instances, because Guillemots breed in such close proximity, an egg that rolls away from an incubating bird will, when the colony is undisturbed, roll only as far as an immediate neighbour and be duly recovered. However, in the presence of predators such as Bald Eagles *Haliaeetus leucocephalus*, Red Foxes *Vulpes vulpes*, Arctic Foxes *Vulpes lagopus*, Polar Bears *Ursus maritimus* or humans, all of which can kill an adult Guillemot, it is hardly surprising that adult Guillemots (which are long-lived) look after their own safety and abandon their eggs (e.g. Birkhead & Nettleship 1995): under such circumstances no egg rolling adaptation can ensure the safety of an egg.

In summary, in light of the failure of the rolling-in-an-arc hypothesis to account for the pyriform shape of Guillemot eggs, we offer two new hypotheses: strength, and protection from debris contamination. We are not making a case for either one, and there may well be others (see Ingold 1980, Tschanz 1990). Indeed, it seems likely that the Guillemot's pyriform egg is a compromise between a number of different selection pressures.

We thank Chris Holland, Paul Ingold, Oleksandra Mykhaylyk, Tony Ryan and Craig Sturrock for helpful discussion; Skelet.AL lab for use of their micro-CT scanner; the Wildlife Trust of South and West Wales Trust for permission to work on Skomer Island NNR, Douglas Russell at the Natural History Museum, Tring, for access to eggs, and Nicola Hemmings, Bob Montgomerie and the referees for comments on the manuscript. This work was funded by a grant from the Leverhulme Trust to T.R.B.

REFERENCES

Andersson, M. 1978. Optimal egg shape in waders. *Ornis. Fenn.* **55**: 105–109.

Ar, A. & Rahn, H. 1985. Pores in avian eggshells: gas conductance, gas exchange and embryonic growth rate. *Respir. Physiol.* **61**: 1–20.

Bain, M.M. 1991. A reinterpretation of eggshell strength. In Solomon, S.E. (ed.) *Egg and Eggshell Quality*. Aylesbury: Wolfe Publishing Limited.

Bain, M.M. 2005. Recent advances in the assessment of eggshell quality and their future application. *Worlds Poult. Sci. J.* **61**: 268–277.

Belopol'skii, L.O. 1957. Ecology of Sea Colony Birds of the Barents Sea. Israel Program for Scientific Translations. Jerusalem. (Translated from Russian 1961).

Birkhead, T.R. 1977. The effect of habitat and density on breeding success in the Common Guillemot *Uria aalge*. *J. Anim. Ecol.* **46**: 751–764.

Birkhead, T.R. 1993. *Great Auk Islands*. London: Poyser.

Birkhead, T.R. 2016. *The Most Perfect Thing: the Inside (and Outside) of a Bird's Egg*. London: Bloomsbury.

Birkhead, T.R. & Nettleship, D.N. 1987. Ecological relationships between Common Murres, *Uria aalge* and Thick-billed Murres, *Uria lomvia*, at the Gannet Islands, Labrador. II: breeding success and site characteristics. *Can. J. Zool.* **65**: 1630–1637.

Birkhead, T.R. & Nettleship, D.N. 1995. Arctic fox influence on a seabird community in Labrador: a natural experiment. *Wilson Bull.* **107**: 397–412.

Birkhead, T.R., Thompson, J.E. & Biggins, J.D. 2017. Egg shape in Common *Uria aalge* and Brünnich's Guillemots *U. lomvia*: not a rolling matter. *J. Ornithol.* DOI: 10.1007/s10336-017-1437-8

Board, R.G. 1982. Properties of avian egg shells and their adaptive value. *Biol. Rev. Camb. Philos. Soc.* **57**: 1–28.

Gaston, A.J. & Nettleship, D.N. 1981. *The Thick-billed Murres of Prince Leopold Island*. Ottawa: Canadian Wildlife Service Monographs, No. 6.

Gill, F. 2007. *Ornithology*. New York: Freeman.

Harris, M.P. & Birkhead, T.R. 1985. Breeding ecology of the Atlantic Alcidae. In Nettleship, D.N. & Birkhead, T.R. (eds) *The Atlantic Alcidae*: 155–205. London: Academic Press.

Harris, M.P. & Wanless, S. 1988. The breeding biology of guillemots *Uria aalge* on the Isle of May over a six year period. *Ibis* **130**: 172–192.

Hewitson, W.C. 1831. *British Oology: being Illustrations of the Eggs of British Birds*. Newcastle upon Tyne: Empson.

Ingold, P. 1980. Anpassungen der Eier und des Brutverhaltens von Trottelummen an das Brüten auf felssimen. *Z. Tierpsychol.* **53**: 341–388.

Kaftanovski, Y.M. 1941. Opyt sravnitel'noi kharakteristiki biologii razmnozhenyia nekotorykh chistikovykh. (Studies on comparative characteristics of the reproduction of some murre species). Trudy Gosudarstvennogo Zapovednika 'Sem'Ostrovov'. Glavnoe Upravlenie po Zapovednikam pri SNK RSFSR (Works by the 'Seven Islands' Sanctuary. Main Board of Reserves attached to Council of Comminssars for the RSFSR) **1**: 53072.

Lessells, C.M. & Boag, P.T. 1987. Unrepeatable repeatabilities: a common mistake. *Auk* **104**: 116–121.

MacGillivray, W. 1852. *A History of British Birds*. London: Scott, Webster & Geary.

Maurer, G., Portugal, S.J. & Cassey, P. 2012. A comparison of indices and measured values of eggshell thickness of different shell regions using museum eggs of 230 European bird species. *Ibis* **154**: 714–724.

Nakagawa, S. & Schielzeth, H. 2010. Repeatability for Gaussian and non-Gaussian data: a practical guide for biologists. *Rev. Camb. Philos. Soc.* **85**: 935–956.

Pilkey, W.D. & Pilkey, D.F. 2008. *Peterson's Stress Concentration Factors*. New York: Wiley.

Pirie-Hay, D.W. & Bond, A.L. 2014. Thickness of Common Murre (*Uria aalge*) eggshells in Atlantic Canada. *Can. Field Nat.* **128**: 72–76.

Preston, F.W. 1953. The shapes of birds' eggs. *Auk* **70**: 160–182.

R Development Core Team. 2012. *R: A Language and Environment for Statistical Computing*. Vienna: R Foundation for Statistical Computing. Available at: http://www.R-project.org/

Riley, A., Sturrock, C.J., Mooney, S.J. & Luck, M.R. 2014. Quantification of eggshell microstructure using X-ray micro computed tomography. *Br. Poult. Sci.* **55**: 311–320.

Romanoff, A.J. & Romanoff, A.L. 1949. *The Avian Egg*. New York: Wiley.

Schneider, C.A., Rasband, W.S. & Eliceiri, K.W. 2012. NIH Image to ImageJ: 25 years of image analysis. *Nat. Methods* **9**: 671–675.

Schoenwetter, M. 1960–1992. *Handbuch der Oologie*. Berlin: Akademie Verlag.

Smart, I.H.M. 1969. The method of transformed coordinates applied to deformations produced by the walls of a tubular viscus on a contained body: the avian egg as a model system. *J. Anat.* **104**: 507–518.

Smith, A. & Clarke, J.A. 2015. Systematics and evolution of the Pan-Alcidae (Aves, Charadriiformes). *J. Avian Biol.* **45**: 125–140.

Thomson, A.L. 1964. *A New Dictionary of Birds*. London: Nelson.

Todd, P.H. & Smart, I.H.M. 1984. The shape of birds' eggs. *J. Theor. Biol.* **106**: 239–243.

Tøien, Ø., Paganelli, C.V., Rahn, H. & Johnson, R.R. 1988. Diffusive resistance of avian eggshell pores. *Respir. Physiol.* **74**: 345–354.

Tschanz, B. 1968. *Trottellummen: Die Entstehung der persönlichen Beziehungen zwischen Jungvogel und Eltern*. Berlin: Paul Parey.

Tschanz, B. 1990. Adaptations for breeding in Atlantic Alcids. *Neth. J. Zool.* **40**: 688–710.

Tschanz, B., Ingold, P. & Lengacher, H. 1969. Eiform und Bruterfolg bei Trottellummen. *Ornithol. Beob.* **66**: 25–42.

Tuck, L.M. 1961. *The Murres: their distribution, populations and biology – a study of the genus Uria*. Ottawa: Canadian Wildlife Monograph Series, No. 1.

Uspenski, S.N. 1958. *The Bird Bazaars of Novaya Zemlya*. Ottawa: Department of Northern Affairs and Natural Resources, Canada (translated from Russian).

Verbeek, N.A.M. 1984. The effect of adult fecal material on egg hatchability in Glaucous-winged Gulls (*Larus glaucescens*). *Auk* **101**: 824–829.

Zimmermann, K. & Hipfner, J.M. 2007. Egg size, eggshell porosity, and incubation period in the marine bird family Alcidae. *Auk* **124**: 307–315.

Received 19 May 2016;
revision accepted 6 January 2017.
Associate Editor: Richard Phillips.

SUPPORTING INFORMATION

Additional Supporting Information may be found in the online version of this article:

Appendix S1. Method for calculating the 'contact index'.

Figure S1. Images illustrating how the contact index was calculated.

Table S1. Correlation coefficients between different measures of eggshell thickness.

Table S2. Repeatability values for eggshell thickness and porosity measures calculated according to the methods in Lessells and Boag (1987) and Nakagwa and Schielzeth (2010).

Figure S2. Cross sectional image of a piece of Guillemot eggshell showing the different shell thickness measures, taken using X-ray micro computed tomography.

Figure S3. Differences in effective shell thickness/total shell thickness ratios between the three regions of Guillemot and Razorbill eggs.

Figure S4. Relationship between minimum cross sectional pore area and inner pore orifice area.

Supplementary materials

Supplementary methods for calculating the ‘contact index’

We used the mathematically captured shape of the egg’s silhouette to give an egg profile, and assumed circular cross sections orthogonal to this to give the egg’s overall (three-dimensional) shape. We identified the point on the profile where it was flattest (see main manuscript text), and superimposed a plane that is tangent at this point. Using the (three-dimensional) shape, the points in this plane are within 0.2 mm of the egg are identified (Fig. S1a & b). This is an area in the tangent plane, not an area on the surface of the egg: it is the area of a slice the plane takes out of the egg when it is displaced 0.2 mm into the egg. To account for egg size, this area (‘1’ in Fig. S1c), was expressed as a proportion of the total two-dimensional area of the egg silhouette, which is the maximum area a plane could slice through, to obtain the contact index. The 0.2 mm “tolerance” accounts for both small deformation of the eggshell, and also small irregularities in the eggshell and substrate surfaces. Using tolerances (see text) of 0.1 mm and 0.5 mm provided results that were highly correlated with those for 0.2 mm.

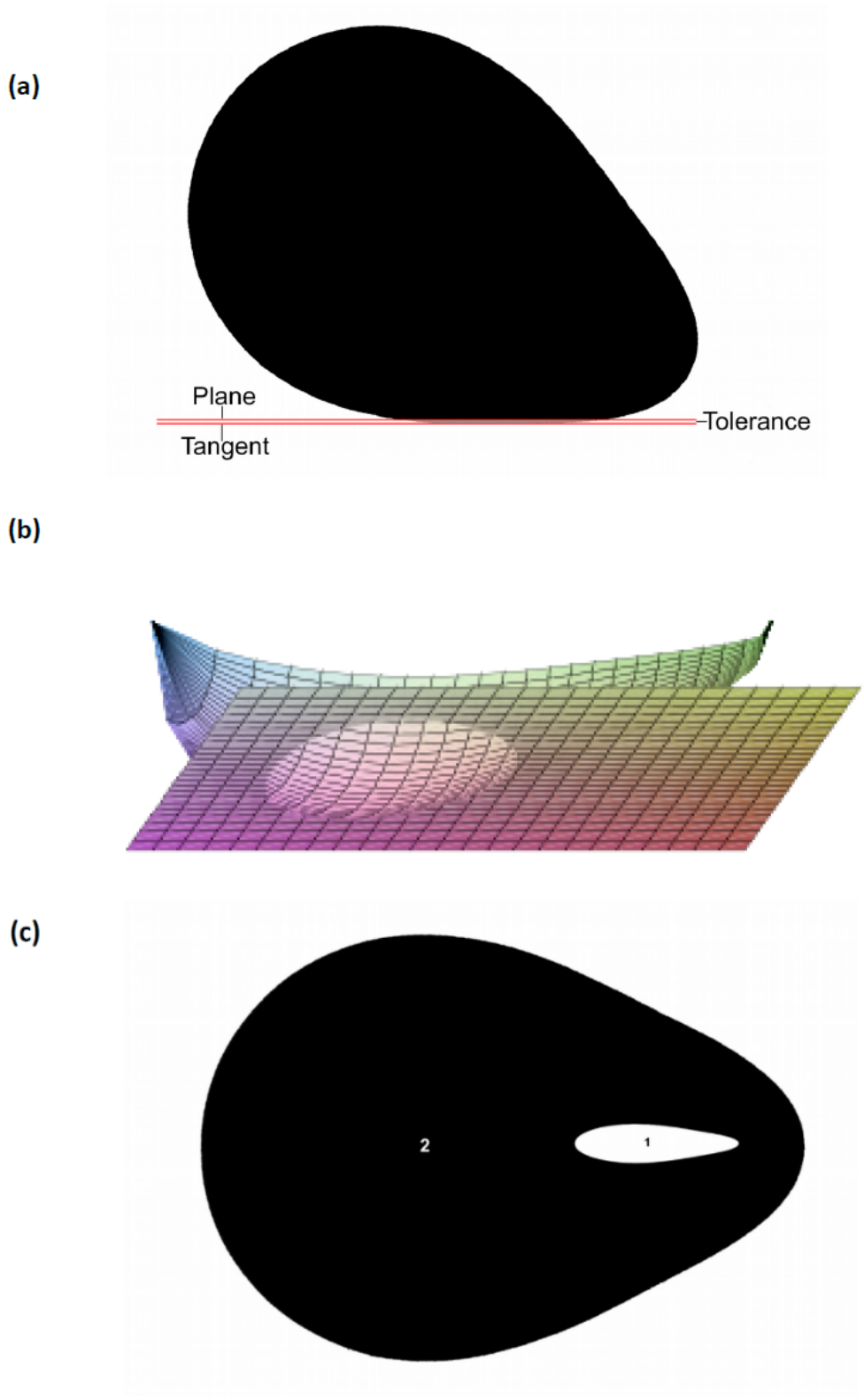

Figure S1. Images illustrating how the contact index was calculated.
(a) Two-dimensional egg silhouette showing the tangent, tolerance and plane.
(b) A three-dimensional model of an egg with a plane cutting through it. The two-dimensional area the plane creates by slicing through the egg is equivalent to our calculated area, not the three-dimensional surface area of the protruding bit of shell.
(c) Two-dimensional egg silhouette showing our calculated area (‘1’) and the two-dimensional area of the egg silhouette (‘2’ + ’1’).

Table S1. Correlation coefficients between different measures of eggshell thickness (μm). Correlation coefficients were calculated using Spearman's rank correlation on 60 measures from twenty eggs — ten Guillemot and ten Razorbill eggs, for which a mean value for each eggshell region (blunt end, equator, and pointed end) was used.

	Shell thickness parameter[1]				
	Total	True shell	Effective	Mammillary	Membrane
Total[2]	-	0.98	0.96	0.65	0.78
True shell[3]	0.98	-	0.98	0.68	0.69
Effective	0.96	0.98	-	0.54	0.65
Mammillary	0.65	0.68	0.54	-	0.48
Membrane	0.78	0.69	0.65	0.48	-

[1] see Figure S2 for visualisation and descriptions of the eggshell thickness parameters discussed in the main manuscript.
[2] Total shell thickness.
[3] True shell thickness is the distance from the tip of the mammillary bodies to the outer surface of the shell, i.e. the calcium carbonate components of the shell, not the shell membranes. This is equivalent to the sum of effective shell thickness and mammillary layer thickness; see Figure S2.
$P < 0.001$ for all correlations.

Table S2. Repeatability values for eggshell thickness (µm) and porosity (x10^{-4} mm^2) measures calculated according to the methods in Lessells & Boag (1987) and Nakagwa & Schielzeth (2010). Three mean shell thickness values and three porosity measures were obtained for each region of five Guillemot and five Razorbill eggs, leading to a total of 90 data points per parameter. Analyses were performed on square root transformed data.

Sample	Total shell thickness[1]		Effective shell thickness[1]		Mammillary layer thickness[1]		Membrane thickness[1]		Porosity[1]	
	r	*F*	*r*	*F*	*r*	*F*	*r*	*F*	*r*	*F*
Guillemot[2]	0.98	191	0.97	107	0.54	4.59	0.87	20.9	0.74	9.40
Razorbill[2]	0.96	82.6	0.97	112	0.63	6.12	0.58	5.23	0.58	5.13
All[3]	0.99	426	0.99	271	0.73	8.92	0.87	20.1	0.72	8.63

[1] see Figure S2 for visualisation and definition of shell thickness parameters.
[2] degrees of freedom for all *F* values (14,30)
[3] degrees of freedom for all *F* values (29,60)
$P < 0.001$ for all *F* values

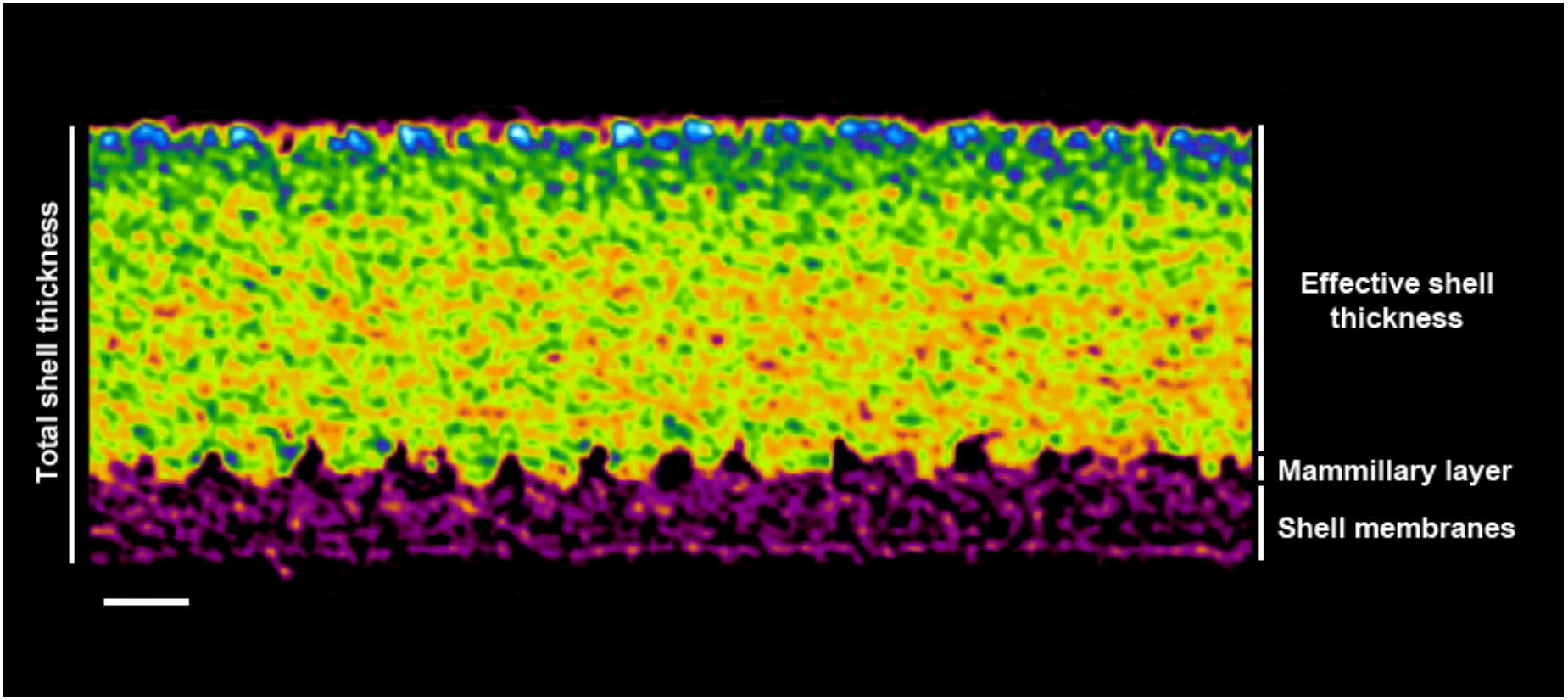

Figure S2. Cross sectional image of a piece of Guillemot eggshell showing the different shell thickness measures, taken using X-ray micro computed tomography. Effective shell thickness is the distance from the point of fusion of the palisade columns to the outer edge of the shell accessory material (see Bain 2005); mammillary layer thickness is the distance from the end of a mammillary body to the point of fusion of the palisade columns, and total shell thickness is the distance from the inner side of the shell membrane to the outer edge of the shell accessory material. Images were false coloured according to grey value to allow better visualisation of the different layers of the eggshell. Scale bar = 100 µm.

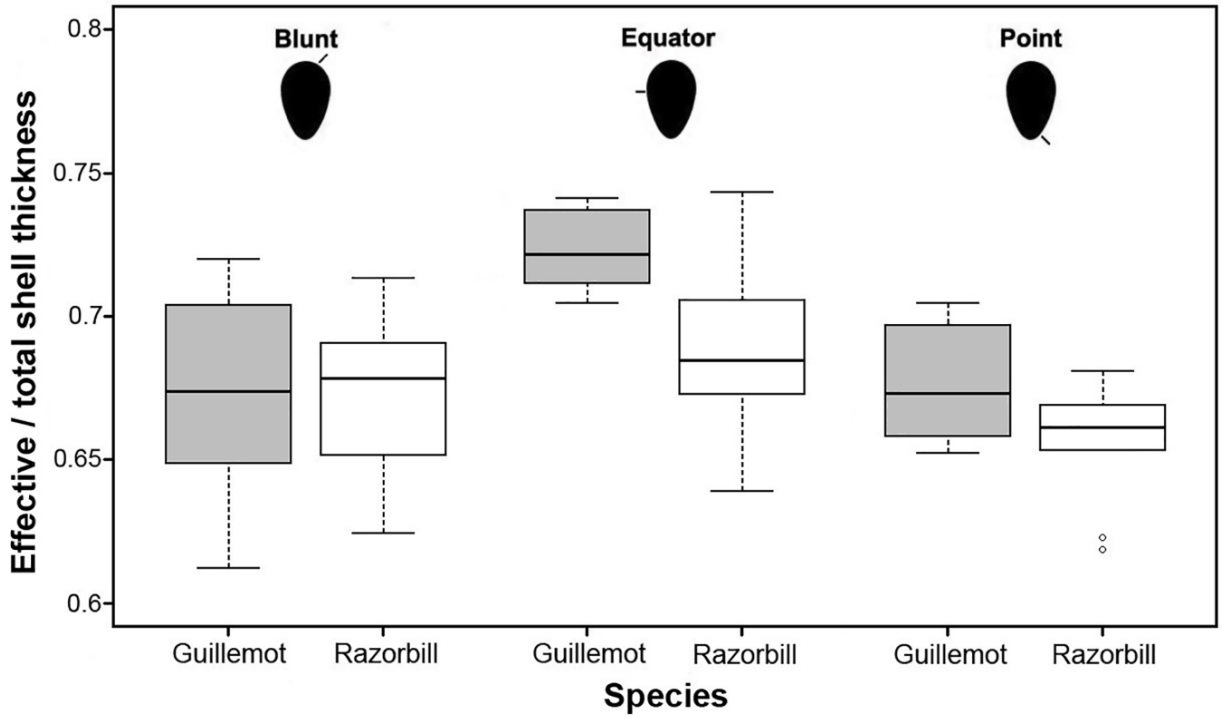

Figure S3. Differences in effective shell thickness/total shell thickness ratios between the three regions of Guillemot and Razorbill eggs. A greater proportion of total shell thickness can be attributed to effective shell thickness at the equator of Guillemot eggs compared to the pointed or blunt end (one-way ANOVA with repeated measures performed on Arcsine square root transformed data: $F_{2,18}$ = 16.7, P < 0.001; Tukey multiple comparison test P < 0.05). Additionally, there are no significant differences in mammillary layer thickness (blunt: 78.3µm ± 13.7µm, equator: 83.1µm ± 6.21µm, point: 90.4µm ± 7.09µm) (one-way ANOVA with repeated measures: $F_{2,18}$ = 3.15, P > 0.05) and the shell membrane is significantly thicker at the pointed end (131µm ± 15.9µm) of the Guillemot egg than at either the equator (114µm ± 10.6µm) or blunt end (110µm ± 10.8µm; one-way ANOVA with repeated measure: $F_{2,18}$ = 12.5, P < 0.001). The increased total eggshell thickness at the equator can therefore be primarily attributed to an increase in effective shell thickness and not an increase in thickness of all the shell layers. Razorbill eggs show a different pattern: a lower proportion of total shell thickness is attributed to effective shell thickness at the pointed end compared to the equator (one-way ANOVA with repeated measures performed on Arcsine square root transformed data: $F_{2,18}$ = 6.80, P < 0.01) (Tukey multiple comparison test P < 0.05). No other differences in effective/ total shell thickness between regions are significant (Tukey multiple comparison test P > 0.05), despite the blunt end (438µm ± 37.1µm) of Razorbill eggs being significantly thinner than the equator (483µm ± 37.6µm) or pointed end (501µm ± 47.3µm) (one-way ANOVA with repeated measures: $F_{2,18}$ = 19.9, P < 0.001; Tukey multiple comparison test P < 0.05), indicating that differences in total shell thickness in Razorbill eggs are driven by differences in the thickness of all shell layers and not primarily by changes in the effective thickness layer, as is the case in Guillemot eggs. Ten Guillemot and ten Razorbill eggs were analysed and an average value for each eggshell region was used in analysis, leading to a total of 60 data points.

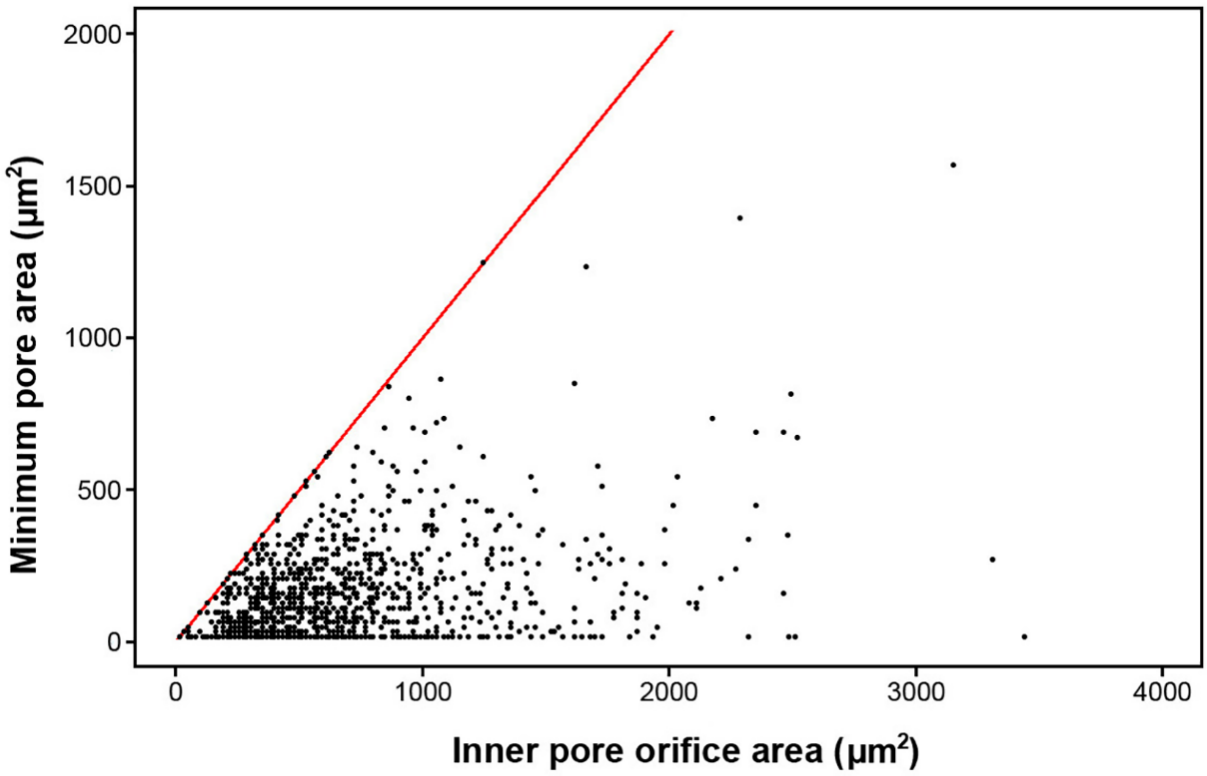

Figure S4. Relationship between minimum cross sectional pore area and inner pore orifice area. Inner pore orifice measures are weakly positively correlated with minimum pore area measures (Spearman's rank correlation, overall dataset: r_s = 0.287, n = 1195, P < 0.0001; Guillemots: r_s = 0.297, n = 595, P < 0.0001; Razorbills: r_s = 0.246, n = 600, P < 0.0001). The red line shows the 1:1 relationship between measures. Most measures lie below this 1:1 line, indicating that inner pore orifice measures are generally larger than minimum pore area measures; for this data, on average, 545µm² ± 424µm² larger. Inner pore orifice measures are therefore not a useful measure of the narrowest part of a pore channel. Ten pores were measured per region (blunt, equator, point) of five Guillemot and five Razorbill eggs and thirty pores per region were measured for another five Guillemot and five Razorbill eggs. Some regions of Guillemot eggs had fewer than 10 pores per region, leading to a total 595 Guillemot pore measurements.

Appendix A2:

Summary table of methods previously used to study eggshell microstructure

Appendix A2

Table 1. Summary of methods previously used to study eggshell microstructure – specifically shell thickness, pore length, size and density.

Parameter	Technique	Fragmentation	Measure	Damaging or destructive?[1]	Examples of limitations	Example(s) of use
Shell thickness	Weighing the whole shell	No	Eggshell thickness index calculated from shell mass and egg dimensions	No	Potentially imprecise, a measure of the amount/density of shell rather than its thickness (Maurer *et al.* 2010 but see Maurer *et al.* 2012). No regional thickness measures. No measures of the thickness of different shell layers.	Schönwetter (1960-1992); Rahn & Pagnelli 1989; Birchard & Deeming 2009; Maurer *et al.* 2010; Maurer *et al.* 2012
	Calipers, micrometer, modified micrometer with a ball bearing on one jaw etc	Yes	Total shell thickness	No	Measurement of mammillary or effective thickness (palisade, vertical crystal layer and any shell accessory material) not possible. Prone to human error in applying (e.g. varying pressure) and reading the instrument, and prone to calibration issues (Santalo 2018). Shell curvature may affect measurements.	Balch & Tyler 1964; Booth 1989; Massero & Davis 2005; Zimmerman & Hipfner 2007; Castilla *et al.* 2010
			True shell thickness	Yes – membranes physically (sometimes with boiling) or chemically removed. Weakens the shell. Can cause cracking and fragmentation		
			Membrane thickness	Yes – shell dissolved (acid or EDTA) to remove membranes, or physically removed when wet.		
	Modified micrometer for measuring whole eggs	No	Total shell thickness	No	Only measures total shell thickness at the equator. See above limitations of micrometers.	Maurer *et al.* 2012

Table continued on next page

Parameter	Technique	Fragmentation	Measure	Damaging or destructive?[1]	Examples of limitations	Example(s) of use
Shell thickness	Hall-effect digital thickness gauge	No. Can measure thickness at any region of blown eggshells.	Total shell thickness True shell thickness	No Yes – membranes removed	Slight overestimates compared to micrometer measures (but highly correlated with micrometer measures).	Santalo 2018
	Scanning electron microscopy (SEM)	Yes	Total, true, effective, palisade, vertical crystal, mammillary layer or membrane thickness	Yes – sputter coated and mounted onto a stub. May require chemical treatment to remove organic matter from shell.	Miss-alignment leads to inaccurate measures. Inaccurate (for mammillary and effective thickness) as assuming point of fusion of mammillary bodies from a 2D cross-section.	Carnarius *et al.* 1996; Igic *et al.* 2010; Dunn *et al.* 2011
	Optical microscopy	Yes	Total, true, effective, mammillary layer or membrane thickness	Not always but likely requires a snapped edge. Yes if sectioning required.	Cross-section alignment issues lead to inaccurate measures. Accuracy issues as measurer assumes the point of fusion of mammillary bodies (limitation of 2D cross-section).	Rodriguez-Navarro *et al*. 2007
Pore length	Any technique to measure shell thickness	See above	Not directly measured. Thickness assumed to equal pore length.	See above	Total or true shell thickness assumed to equal the pore length but may not be true (see Jackson *et al*. 2018).	Ar *et al*. 1974; Ar & Rahn 1985

Table continued on next page

Parameter	Technique	Fragmentation	Measure	Damaging or destructive?[1]	Examples of limitations	Example(s) of use
Pore number or density	Optical microscopy or a slide projector	Usually (half shells can be studied – see Blankespoor 1987)	Pore count per unit area	Yes – requires removal of organic matter and pore enlargement with acid before application of dye or light is shone through the shell.	Counts can be over or underestimates. → reliance on chemical enlargement of pores with varying treatment timings (determined by trial and error) → reliance on dyes or light, but may not penetrate thin pores (Board 1982; Ar & Rahn 1985; Boersma & Rebstock 2009; Stein & Badyaev 2011). Shell curvature leads to difficulties visualising pores (Boersma & Rebstock 2009). Crooked pores not visible when light shone through shell (Boersma & Rebstock 2009). Measurement difficulties due to fragile shell from treatments.	Tullett 1975; Hoyt *et al.* 1979; Ar & Rahn 1985; Blankespoor 1987; Zimmerman & Hipfner 2007; Boersma & Rebstock 2009; Stein & Badyaev 2011
	Optical microscopy	Usually	Pore count per unit area	Yes – requires removal of organic matter and treatment with dye dissolved in alcohol.	Underestimates pore number, dye unable to penetrate thin or “blocked” pores.	Booth 1989
	SEM	Yes	Pore count per unit area	Yes – chemically treated to remove organic matter, sputter coated and mounted.	Inner surface counts may not represent the number of functional pores that fully traverse the shell.	Tullett 1975; Silyn-Roberts 1983a, b
	Plastic or resin pore casts	Yes	Pore count per unit area	Yes – requires resin treatment and dissolving the shell partially to view pores.	Inaccurate, resin may not penetrate thin pores.	Tullett 1975

Table continued on next page

Parameter	Technique	Fragmentation	Measure	Damaging or destructive?[1]	Examples of limitations	Example(s) of use
Pore size	SEM or optical microscopy	Yes	Internal or external pore diameter (or radius) or area.	SEM – sputter coated and glued to mount. Both – chemical removal of membranes or shell accessory material necessary.	Does not reflect true minimum pore area (e.g. Birkhead *et al.* 2017). Internal pore area measures may be collected for incomplete, non-functional pores.	Tullett & Board 1977; Massero & Davis 2005; Zimmerman & Hipfner 2007
	Pore casts (optical microscopy and drawings)	Yes	Pore diameter (or radius)	Yes – shell dissolved to leave pore casts.	Pore casts are fragile and can break at the minimum dimension. Cannot measure pore area directly. Drawings may be inaccurate.	Tyler & Simkiss 1959; Tyler 1965; Tøien *et al*. 1988
	Pore casts (and SEM)	Yes	Pore diameter	Yes – shell dissolved away to produce pore casts. Casts mounted on a stub and likely sputter coated.	Pore casts are fragile and can break at minimum dimension. Cannot measure pore area directly. Miss-alignment of SEM scan (i.e. not completely perpendicular to pore channel) could lead to inaccurate data.	Silyn-Roberts 1983b; Booth & Seymour 1987; Booth 1989

[1]Here I classify a technique as damaging or destructive if the shell fragment has been altered and another structural trait would not be able to be accurately measured from the eggshell fragment. For example, scanning electron microscopy is technically non-destructive and causes minimal damage to a sample, but the process of chemically treating the fragment, coating it and mounting it (often with glue) prior to scanning causes changes to the shell likely restricting the utility of the fragment in further studies.

References

Ar, A., Paganelli, C. V., Reeves, R. B., Greene, D. G. and Rahn, H., (1974). The Avian Egg: Water Vapor Conductance, Shell Thickness, and Functional Pore Area. *The Condor*. **76**(2), 153–158.

Ar, A. and Rahn, H., (1985). Pores in avian eggshells: Gas conductance, gas exchange and embryonic growth rate. *Respiration Physiology.* **61**(1), 1–20.

Balch, D. A. and Tyler, C., (1964). Variation in some shell membrane characteristics over different parts of the same shell. *British Poultry Science*. **5**(3), 201-215.

Birchard, G. F. and Deeming, D. C., (2009). Avian eggshell thickness: scaling and maximum body mass in birds. *Journal of Zoology.* **279**(1), 95–101.

Birkhead, T. R., Thompson, J. E., Jackson, D. and Biggins, J. D., (2017). The point of a Guillemot's egg. *Ibis.* **159**(2), 255-265.

Blankespoor, G. W., (1987). An Improved Procedure for Counting Pores in Avian Eggshells. *The Condor*. **89**(3), 663-665.

Boersma, P. D. and Rebstock, G. A., (2009). Magellanic Penguin eggshell pores: does number matter? *Ibis*. **151**(3), 535-540.

Booth, D. T. and Seymour, R. S., (1987). Effect of Eggshell Thinning on Water Vapor Conductance of Malleefowl Eggs. *The Condor.* **89**(3), 453-459.

Booth, D. T., (1989). Regional Changes in Shell Thickness, Shell Conductance, and Pore Structure during Incubation in Eggs of the Mute Swan. *Physiological Zoology*. **62**(2), 607-620.

Carnarius, K. M., Conrad, K. M., Mast, M. G. and MacNeil, J. H., (1996). Relationship of Eggshell Ultrastructure and Shell Strength to the Soundness of Shell Eggs. *Poultry science*, **75**(5), 656–663.

Castilla, A. M., Van Dongen, S., Herrel, A., Francesch, A., de Aragón, J. M., Malone, J. and Negro, J. J., (2010). Increase in membrane thickness during development compensates for eggshell thinning due to calcium uptake by the embryo in falcons. *Naturwissenschaften*. **97**(2), 143-151.

Dunn, I. C., Rodríguez-Navarro, A. B., Mcdade, K., Schmutz, M., Preisinger, R., Waddington, D., Wilson, P. W. and Bain, M. M., (2012). Genetic variation in eggshell crystal size and orientation is large and these traits are correlated with shell thickness and are associated with eggshell matrix protein markers. *Animal Genetics*. **43**(4), 410-418.

Hoyt, D. F., Board, R. G., Rahn, H. and Paganelli, C. V., (1979). The Eggs of the Anatidae: Conductance, Pore structure, and Metabolism. *Physiological Zoology***. 52**(4), 438-450.

Igic, B., Hauber, M. E., Galbraith, J. A., Grim, T., Dearborn, D. C., Brennan, P. L., Moskát, C., Choudhary, P. K. and Cassey, P., (2010). Comparison of micrometer-and scanning electron microscope-based measurements of avian eggshell thickness. *Journal of Field Ornithology*. **81**(4), 402-410.

Jackson, D., Thompson, J. E., Hemmings, N. and Birkhead, T. R., (2018). Common guillemot (*Uria aalge*) eggs are not self-cleaning. *The Journal of Experimental Biology*. **221**(23), jeb188466.

Massaro, M. and Davis, L. S., (2005). Differences in egg size, shell thickness, pore density, pore diameter and water vapour conductance between first and second eggs of Snares Penguins *Eudyptes robustus* and their influence on hatching asynchrony. *Ibis.* **147**(2), 251-258.

Maurer, G., Russell, D. G. D. and Cassey, P., (2010). Interpreting the Lists and Equations of Egg Dimensions in Schönwetter's *Handbuch der Oologie*. *The Auk.* **127**(4), 940–947.

Maurer, G., Portugal, S. J. and Cassey, P., (2012). A comparison of indices and measured values of eggshell thickness of different shell regions using museum eggs of 230 European bird species. *Ibis.* **154**(4), 714–724.

Rahn, H. and Paganelli, C. V., (1989). Shell Mass, Thickness and Density of Avian Eggs Derived from the Tables of Schönwetter. *Journal of Ornithology.* **130**(1), 59–68.

Rodriguez-Navarro, A. B., Yebra, A., Nys, Y., Jimenez-Lopez, C. and Garcia-Ruiz, J. M., (2007). Analysis of avian eggshell microstructure using X-ray area detectors. *European Journal of Mineralogy*. **19**(3), 391-398.

Santolo, G. M., (2018). A new nondestructive method for measuring eggshell thickness using a non-ferrous material thickness gauge. *The Wilson Journal of Ornithology*. **130**(2), 502-509.

Schönwetter, M., (1960–1992). *Handbuch der Oologie*. Berlin, Germany: Akademie Verlag.

Silyn-Roberts, H., (1983a). BSE Z contrast imaging of uranium stained pores in the avian eggshell. *Journal of Microscopy*. **130**(1), 111-114.

Silyn-Roberts, H., (1983b). The pore geometry and structure of the eggshell of the North Island brown kiwi, *Apteryx australis mantelli*. *Journal of Microscopy*. **130**(1), 23-36.

Stein, L. R. and Badyaev, A. V., (2011). Evolution of eggshell structure during rapid range expansion in a passerine bird. *Functional ecology*. **25**(6), 1215-1222.

Tøien, Ø., Paganelli, C. V., Rahn, H. and Johnson, R. R., (1988). Diffusive resistance of avian eggshell pores. *Respiration Physiology.* **74**(3), 345–354.

Tullett, S. G., (1975). Regulation of avian eggshell porosity. *Journal of Zoology.* **177**(3), 339–348.

Tullett, S. G. and Board, R. G., (1977). Determinants of avian eggshell porosity. *Journal of Zoology.* **183**(2), 203–211.

Tyler, C., (1965). A study of the egg shells of the Sphenisciformes. *Proceedings of the Zoological Society of London.* **147**(1), 1-19.

Tyler, C. and Simkiss, K., (1959). A study of the egg shells of ratite birds. *Proceedings of the Zoological Society of London*. **133**(2), 201-243.

Zimmermann, K. and Hipfner, J. M., (2007). Egg Size, Eggshell Porosity, and Incubation Period in the Marine Bird Family Alcidae. *The Auk.* **124**(1), 307–315.

Appendix A3:

Supplementary materials for Chapter 2

Supplementary methods

Eggshell samples

Common guillemot (*Uria aalge*) eggs used for the intraspecific study on egg size and shape in relation to eggshell thickness were collected from Skomer Island in Wales, 51.7358° N, 5.2964° W (2014 – 2018, n = 43) and Ireland, specifically Great Saltee Island (2017, n = 5), 52.1167° N, 6.6167° W, Lambay Island (2017, n = 5), 53.4909° N, 6.0163° W, and Aughris head, 54.2763° N, -8.7734° W (2018, n = 2) under licence. Alcidae eggs used for our comparative study of effective eggshell thickness were collected from the wild under licence between 2004 – 2018. Where possible, eggs were collected at the onset of incubation but abandoned, de-predated and a few hatched eggs were also used (see below). Common guillemot (n = 5) and razorbill (*Alca torda;* n = 5) eggs were collected from Skomer Island, Wales, UK in 2018. Three Atlantic puffin (*Fratercula arctica*) eggs were collected from the Isle of May, 56.1848° N, - 2.5544° W, Scotland, and two from Skomer Island in Wales in 2017. Black guillemot (*Cepphus grylle*; n = 5) eggs were collected from Flatey Island, 65.37611°N 22.91194°W, Breiðafjörður, Iceland in 2017. Little auk (*Alle alle;* n = 5) and Brünnich's guillemot (*Uria lomvia;* n = 5) eggs were collected in Norway; little auk eggs from Bear Island, Bjørnøya, 74.3686°N 19.0309°E, Svalbard in 2017, and Brünnich's guillemot eggs from Bjørnøya in 2012 – 13. Cassin's auklet (*Ptychoramphus aleuticus;* n = 5 in 2004) and rhinoceros auklet (*Cerorhinca monocerata;* n = 5 in 2018) eggs were collected in Canada from Triangle Island, 50.8643° N, 129.0820° W, British Columbia. Ancient murrelet (*Synthliboramphus antiquus;* n = 5), Crested auklet (*Aethia cristatella;* n = 3), horned puffin (*Fratercula coniculata;* n = 4), tufted puffin (*Fratercula cirrhata;* n = 5), least auklet (*Aethia pusilla;* n = 4), parakeet auklet (*Aethia psittacula;* n = 3) and whiskered auklet (*Aethia pygmaea;* n = 4) eggs were collected in Alaska, USA in 2017 from three island sites; Aiktak, 54.1835° N, 164.8341° W, Buldir, 52.3602° N, 175.9173° E, and Chowiet, 56.0313° N, 156.7005° W. Five Scripps's murrelet (*Synthliboramphus scrippsi*) eggs were collected in the USA from Santa Barbara Island, 33.4756° N, 119.0373° W, California in 2017. Japanese murrelet (*Synthliboramphus wumizisume)* eggs (2 reasonably complete eggshells, but 5 in total by using fragments from multiple eggs) were collected from Biro-jima Island, 32.4647° N,

131.7307° E, Japan in 2013 – 14. This selection of species covers 5 out of the 6 Alcid tribes, and 9 out of the 10 extant genera.

The majority of our samples were intact eggshells where we could measure egg length breadth and obtain a silhouette for shape analysis. Some broken eggshells could be reconstructed satisfactorily with masking tape, typically because the egg was carefully broken in half, or in large fragments and could easily be put back together. Any eggshells that were reconstructed were imaged so that the masking tape didn't obscure the egg outline or the images were carefully edited prior to analysis to remove any masking tape from the edge of the egg.

Some samples arrived in the UK damaged or fragmented, and we could not obtain size and shape parameters for 3/5 Cassin's auklet eggs, 3/4 least auklet eggs, 2/3 parakeet auklet eggs, 1/3 crested auklet eggs, and all of the whiskered auklet and Japanese murrelet eggshells. These were samples that were either (a) fragile and damaged in transit, (b) from partial or fragmented eggs, (c) from de-predated eggs or (d) from hatched eggs (e.g. 2 least auklet, 2 parakeet auklet, 1 crested auklet and all whiskered auklet eggs). The common guillemot eggs collected in Ireland, Cassin's auklet, Scripps's murrelet, and some of the rhinoceros auklet eggs were stored frozen before they were emptied of their contents and sent to Sheffield, UK for shell thickness analysis.

Not all eggs were taken fresh prior to the start of incubation and as a result, some eggshell thinning may have occurred in some samples. However, our focal measure was effective eggshell thickness which is likely unaffected by eggshell thinning due to changes in thickness primarily only occurring at the tips of the mammillary bodies (e.g. Soler e*t al.* 2019). Where possible and in most cases, for measurements of total, true shell or mammillary layer thickness we measured mammillary bodies that maintained their rotund shape and appeared to be undissolved. In cases where the membranes were no longer attached to the shell either due to eggshell thinning or because samples were heat treated and the membranes had dehydrated and sheared from the shell, we measured the membrane and true shell separately and used the sum of these values in the preliminary comparative analyses of total shell thickness presented here.

Shape parameters

Listed below is a summary of the shape parameters used and how they are calculated, for more information on shape and size parameters see Biggins *et al.* (2018).

1. Elongation is how long the egg is relative to its breadth, measured by taking the maximum length of the egg and dividing it by the egg's maximum breadth. Larger values mean that an egg is more elongate.
2. Asymmetry is a measure of how asymmetrical the egg is around the maximum breadth of the egg. Asymmetry is calculated by taking the length from the tip of the pointed end of the egg to the maximum breadth of the egg and dividing that by the maximum length of the egg. Larger values mean that an egg is more asymmetric.
3. Taper is a measure of how much the pointed end of the egg tapers to a point from the maximum breadth. It is calculated by dividing the diameter of a circle fitted to the pointed end of the egg by the maximum breadth of the egg. Larger values mean that the pointed pole is more rounded and smaller values indicate that the egg tapers sharply to a point.
4. Blunt end sphericity is a measure of how close to half a sphere (or a circle, since it is in 2D) the blunt end of the egg is. A departure from 1 means that the egg is more pointed or ovate instead of being circular or spherical at the blunt pole. It is calculated by dividing the diameter of a circle fitted to the blunt end of the egg by the maximum breadth of the egg. Smaller numbers mean that the blunt end is more pointed.
5. Elongation at the blunt end of the egg is calculated by dividing twice the length from the maximum breadth of an egg to the blunt end of the egg by the maximum breadth of the egg. Larger values mean that the blunt end is more elongate.

Taper, sphericity, and elongation at the blunt end are not default outputs from the script provided in Biggins *et al.* (2018) but they can be calculated using the same measurements (see Figure S1). We did not use a measure included in previous papers on common guillemot and auk egg shape (e.g. Biggins *et al.* 2018; Birkhead *et al.* 2019) called "Polar Asymmetry" which compares both ends of the egg as we were not interested in how bicone the eggs were here. Instead we were interested in how the specific shape at each end of the egg may be related to variation in eggshell thickness.

See Table 1 in Biggins *et al.* (2018) for a description of various shape parameters. In that table, taper is called “cloacal” and blunt end sphericity is called “infundibular”. Here we try to use more intuitive names for these parameters that actually describe the differences in observed egg shape (taper and blunt end sphericity).

References

Biggins, J. D., Thompson, J. E. and Birkhead, T. R., (2018). Accurately quantifying the shape of birds’ eggs. *Ecology and Evolution*. **8**(19), 9728-9738.

Birkhead, T. R., Thompson, J. E., Biggins, J. D. and Montgomerie, R., (2019). The evolution of egg shape in birds: selection during the incubation period. *Ibis.* **161**(3), 605-618.

Soler, M., Rodríguez-Navarro, A. B., Pérez-Contreras, T., García-Ruiz, J. M. and José Soler, J., (2019). Great spotted cuckoo eggshell microstructure characteristics can make eggs stronger. *Journal of Avian Biology*. https://doi.org/10.1111/jav.02252

Issues with analysing and interpreting percentage thickness differences

Variation in ratios and percentage differences come from differences in two variables instead of just one which can lead to problems with interpreting differences. For example, a percentage difference of 10% for an egg with a blunt end thickness of 100µm is 10µm. This could mean that the equator is 10µm thicker than the blunt end or that the blunt end is 10µm thinner than the equator. Or it could mean that each region varies in approximately 5µm (equator + 5µm; blunt - 5µm) from the thickness we would expect for an egg of that size or incubated by a bird of a specific size. This makes interpreting what that 10% actually means difficult, as it could mean three different things which is particularly problematic if this newly created variable is being used in further analyses.

We found a lot of variation in the relative difference in thickness at the equator compared to the blunt end within a single species (common guillemot: mean ± SD; 36% ± 11; range 16.5 – 65.5%, n = 55). But contrary to expectations, this variation was largely attributable to changes in thickness at the blunt end (Spearman's rank correlation: $r_s = -0.552$, $p < 0.0001$) rather than also to variation in thickness at the equator of the eggs ($r_s = 0.142$, $p = 0.300$). Studying the relative difference in thickness between the equator and blunt end may not be a good measure if researchers are interested in whether a specific region (i.e. the equator) is particularly thick or thin, as (1) there can be a lot of variation within a single species and (2) it does not necessarily represent variation relating to thickness at a single region of interest (i.e. the equator). This is particularly problematic here as we were interested in studying thickening at the equator in relation to our main hypotheses; that enhanced thickness at the equator (compared to what we would predict based on the size of the egg or incubating parent's mass) relates to the incubation substrate or egg shape. Therefore, we did not use the relative difference between the blunt end and equator in any of our analyses.

Furthermore, relative measures (ratios or percentage differences) mask the absolute differences which are likely more important when looking at eggshell thickness, particularly in relation to egg strength. This is particularly important as reasonably small

differences in thin-shelled eggs could lead to large percentage differences, whereas reasonably larger differences in thick-shelled eggs may be overlooked because there are only small percentage differences between the blunt end and equator. For example, an eggshell with a blunt end thickness of 100μm could have a 20% increase in thickness at the equator which translates to a 20μm difference between regions, but an eggshell with a blunt end thickness of 500μm could have the same percentage increase that translates to a 100μm difference between the equator and blunt end. Although these differences are both 20%, the absolute changes in thickness are likely more important in how the shell would function, especially in providing increased strength.

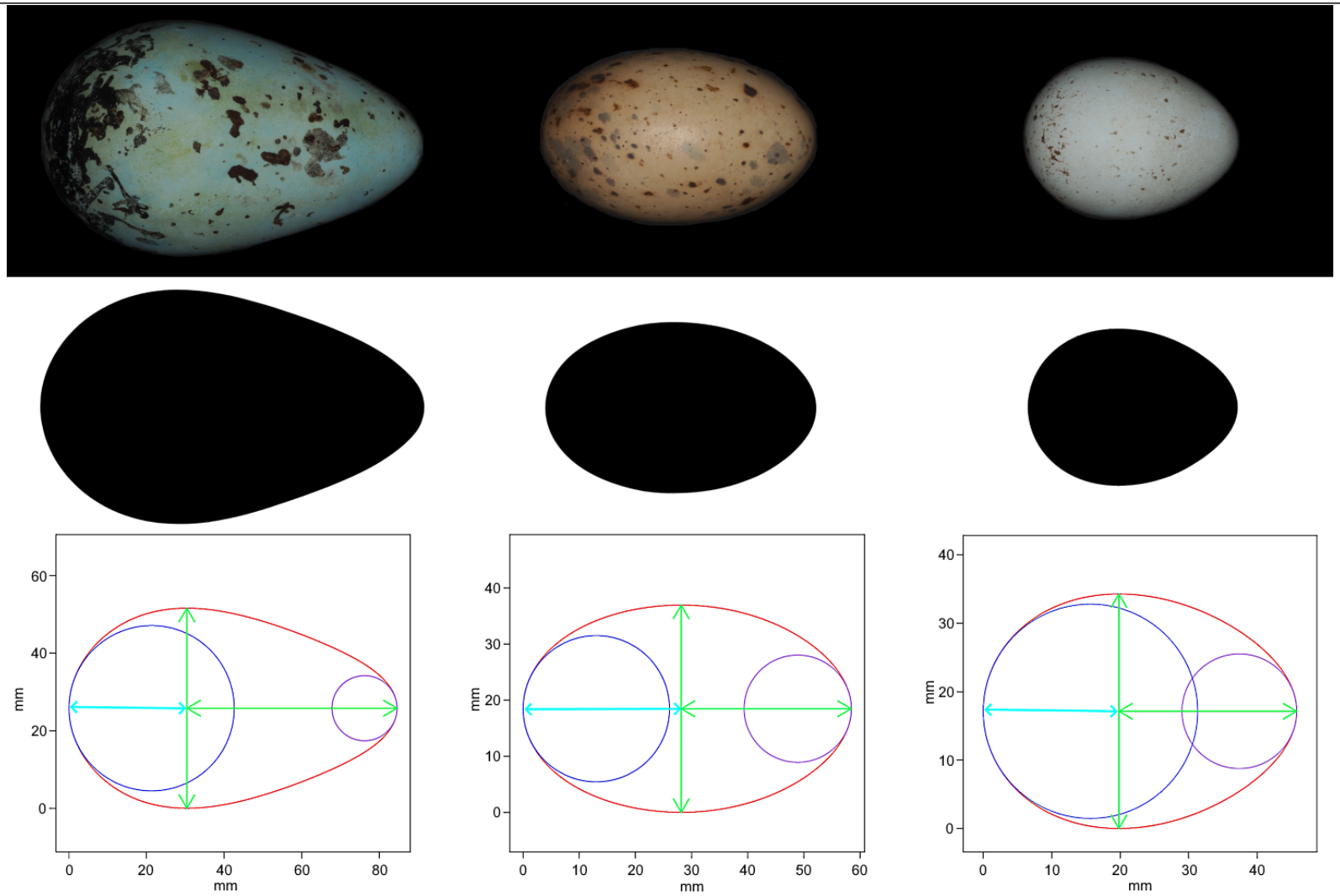

Figure S1. Measuring Alcid egg shapes. Top: images of a common guillemot, ancient murrelet and little auk egg (left to right). These eggs were selected as they show a range of shapes and sizes of eggs used in this study. Common guillemot eggs are highly asymmetric, elongate and large, ancient murrelet eggs are less asymmetric, elongate and are medium sized, and little auk eggs are slightly asymmetric, less elongate and small. Middle row: egg silhouettes obtained by imaging the eggs on a light box. Bottom row: fitted egg outlines (red) illustrating the circles fitted to each end of the egg (blue and purple), the vertical green arrow is the maximum breadth, the horizontal green arrow is the length from the maximum breadth to the pointed end of the egg and the cyan arrow is the length from the maximum breadth to the blunt end of the egg. These lengths and the diameter of the circles are used to calculate the shape of an egg.

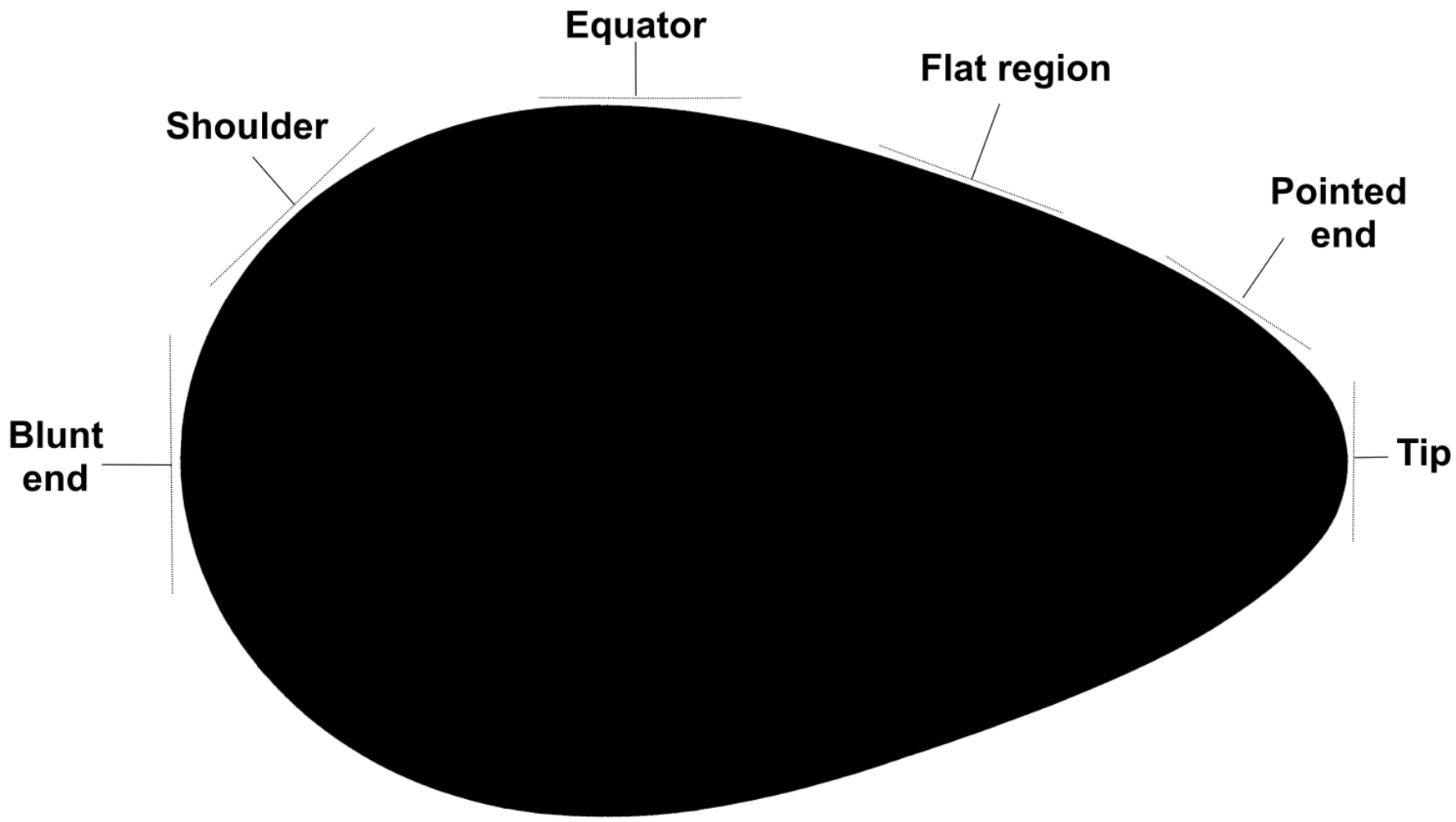

Figure S2. The regions of an egg. For most of our comparisons we compared the blunt end to the equator and pointed end. However, in ten common guillemot eggs we also sampled fragments from the shoulder, flat region and tip of the egg. We defined the equator as the maximum breadth of the egg and sampled just below this region, slightly towards the flat region and pointed end. This is different to the actual equator of the egg (i.e. the middle point), however we needed to sample a defined area rather than a region of the egg which may be more subjective (e.g. the “middle”).

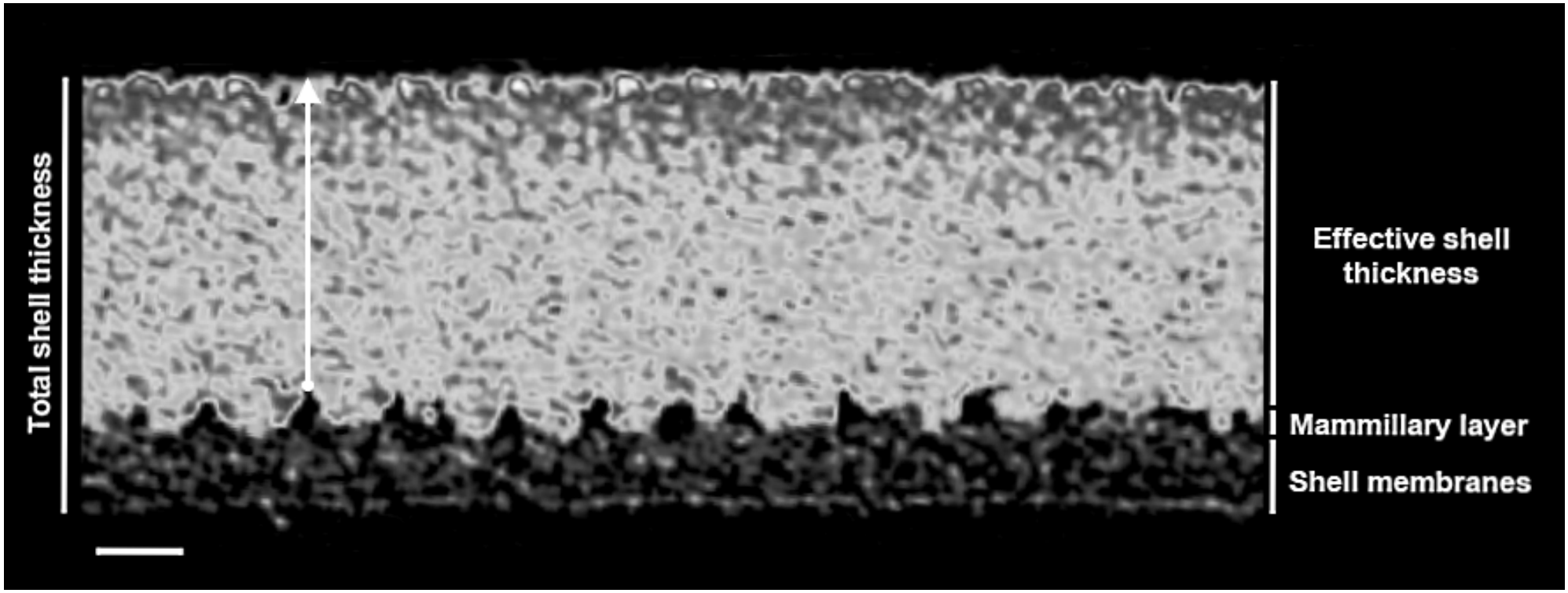

Figure S3. Measuring effective shell thickness on a cross-section of common guillemot eggshell taken using X-ray micro-computed tomography. To measure effective shell thickness I haphazardly selected a mammillary body (from the 3D image stack) and scrolled through the cross-sectional image stack to find the highest point of fusion between a neighbouring mammillary body (see white circle). I then drew a straight line outwards (white line with arrow indicating surface) to the exterior surface and measured this length as the effective shell thickness. Mammillary bodies were haphazardly selected by the measurer closing their eyes, randomly positioning the mouse cursor on the eggshell fragment (aiming for the inner surface) and scrolling through the image stack. Whichever mammillary body was closest to the cursor when the measurer opened their eyes was the randomly selected mammillary body we measured from. This process was repeated a total of ten times. To avoid measuring the same distance twice, each time the field of view (i.e. area of eggshell on screen) was different. This was achieved by (1) zooming in on the fragment starting with the first measure on the left most section of eggshell, then viewing the adjacent area of eggshell to the right for the next location and so on for the next 8 locations, and by (2) scrolling through the eggshell cross section in the same direction. As a result, our haphazard selection provided measurements from approximately the whole area of shell that was scanned. Scale bar = 100µm. Figure adapted from Figure S2 in the Supplementary Materials of Birkhead *et al.* (2017).

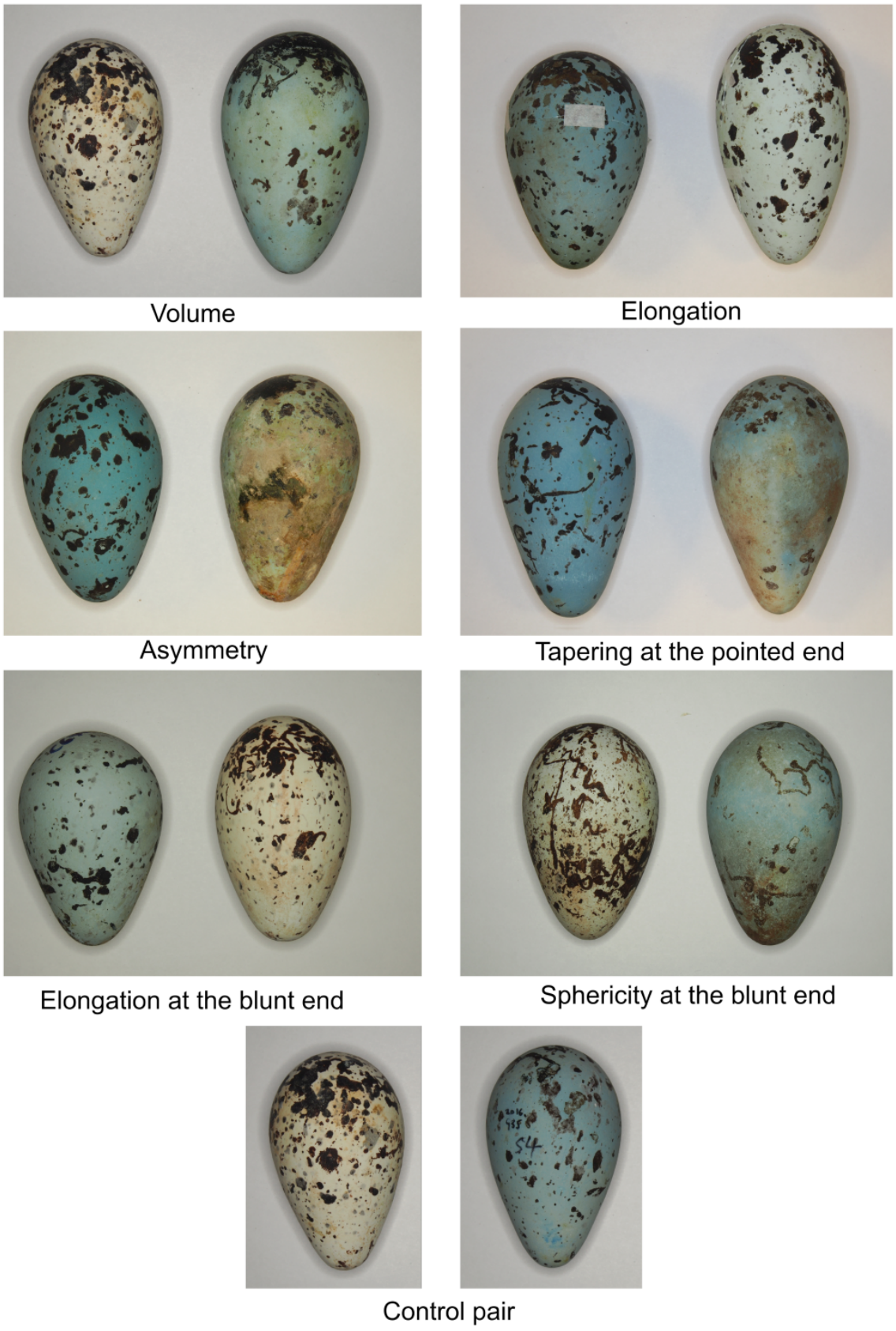

Figure S4. Examples of pairs of common guillemot eggs used to assess the relationship between egg shape, size and eggshell thickness. Each pair is an example of eggs matched on most egg traits but that vary in one parameter. The parameter they differ in is labelled below each pair.

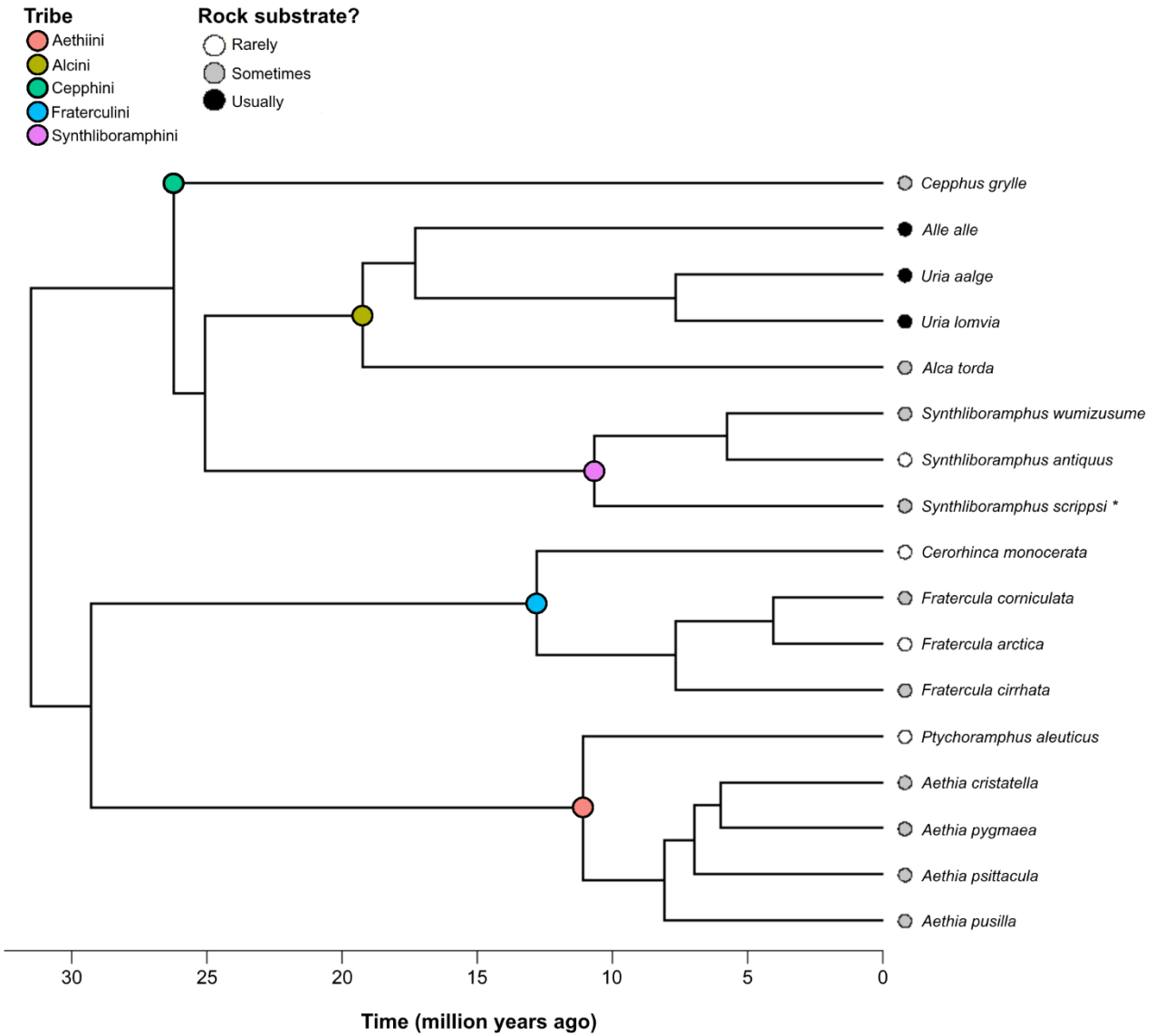

Figure S5. Phylogenetic tree of extant Alcids from Weir and Mursleen (2013), pruned to leave only the species represented in our dataset. *S. wumizusume* and *A. pygmaea* were excluded from comparative analyses due to missing data on egg size and shape because no whole eggshells were imaged. **S. Scrippsi* previously called *S. hypoleucus scrippsi.*

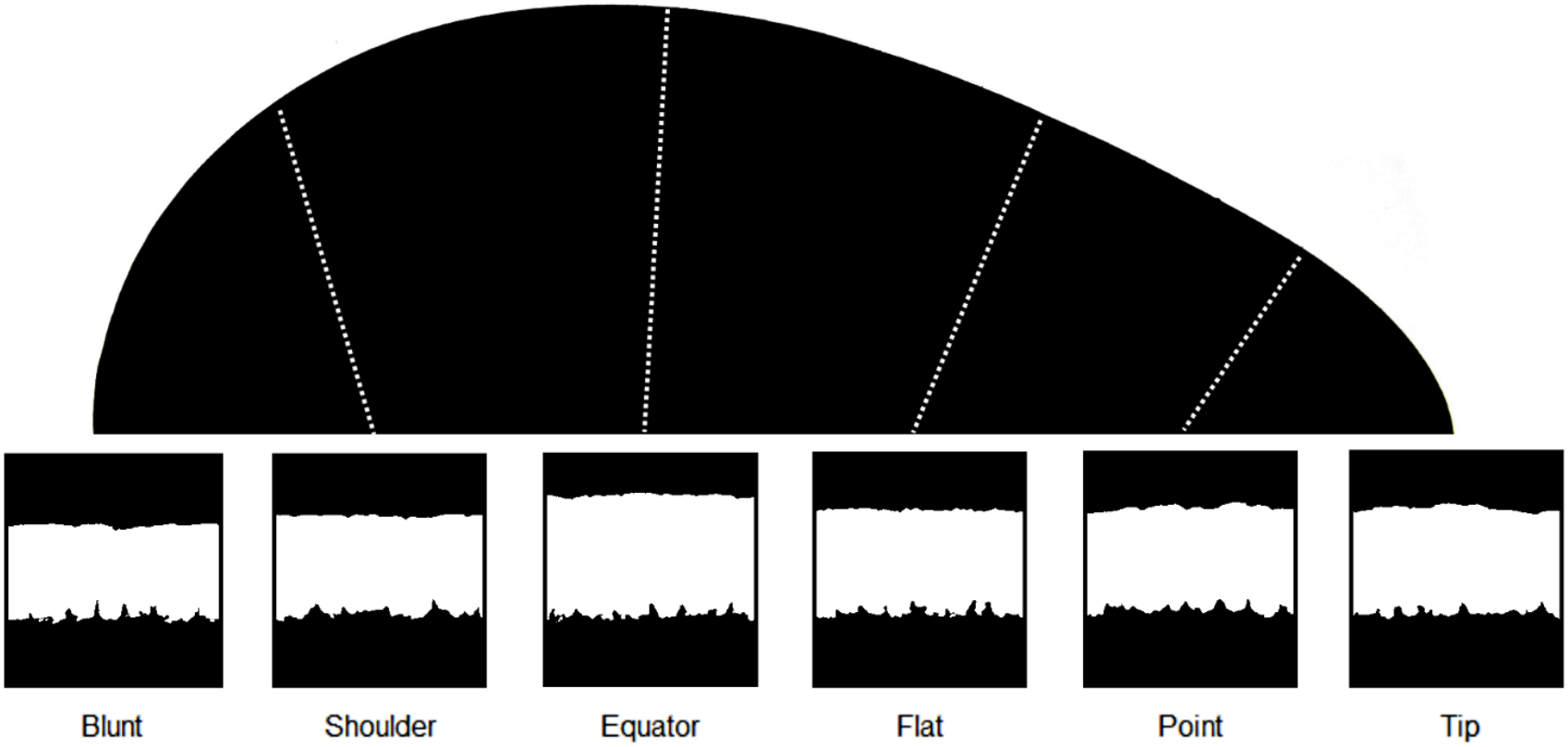

Figure S6. Variation in eggshell thickness along a common guillemot's egg. The length of each shell is 1mm.

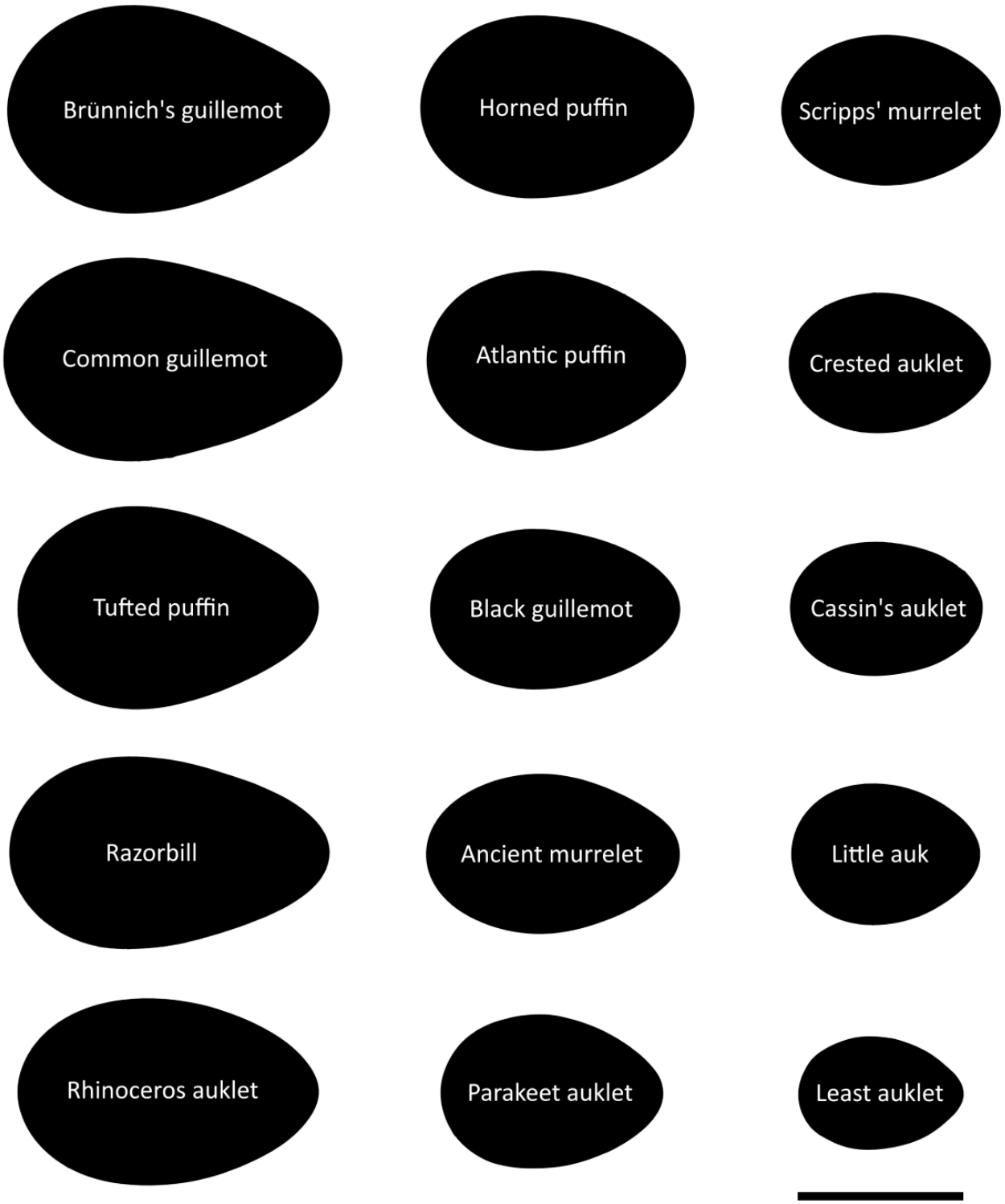

Figure S7. Variation in egg size between Alcids. Each egg was selected to most closely represent the mean volume for that species in our study. The images are ranked from largest (Brünnich's guillemot – top left) to smallest (least auklet – bottom right) egg by volume. Egg silhouettes were obtained by taking a picture of a levelled egg on a light box (see Materials and Methods). Scale bar = 40mm.

Table S1. Intraspecific eggshell thickness (µm) Spearman's rank correlations across eggshell fragments from 55 common guillemot eggs.

Thickness parameter	Membrane	Mammillary	Effective	True shell
Mammillary layer	**0.338**	-		
Effective	*0.127*	**0.398**	-	
True shell	0.165	**0.502**	**0.989**	-
Total[1]	**0.415**	**0.547**	**0.949**	**0.964**

n.s. p > 0.05, p < 0.05, p < 0.01, **p < 0.001**.
[1] n = 150 fragments as the membrane was no longer attached in 15 fragments and could not be directly measured. n = 165 fragments (55 eggs with one fragment per region) for all other comparisons.

Table S2. Interspecific eggshell thickness (µm) Spearman's rank correlations across eggshell fragments from 17 species of Alcid.

Thickness parameter	Membrane	Mammillary	Effective	True shell
Mammillary layer	**0.553**	-		
Effective	**0.553**	**0.754**	-	
True shell	**0.566**	**0.820**	**0.990**	-
Total[1]	**0.765**	**0.820**	**0.966**	**0.979**

n.s. p > 0.05, p < 0.05, p < 0.01, **p < 0.001**.
[1] n = 207 fragments as the membrane was no longer attached in 27 fragments and could not be directly measured. n = 234 fragments (78 eggs in total across all species, with one fragment per region) for all other comparisons.

Table S3. Spearman's rank correlations between different shape parameters across common guillemot eggs (n = 55).

	Volume (cm^3)	Elongation	Asymmetry	Taper	Sphericity
Elongation	*0.095*	-			
Asymmetry	*0.011*	*0.238*[1] *0.08*	-		
Taper	*0.155*	*-0.144*	*-0.214*	-	
Sphericity	*-0.003*	**-0.476**	*0.215*	*0.204*	-
Blunt end elongation	*0.093*	**0.671**	**-0.456**	*-0.033*	**-0.673**

n.s. p > 0.05, p < 0.05, p < 0.01, **p < 0.001**.
[1] p-value reported below r_s as 0.05 < p < 0.1

Table S4. Relationships between egg shape and effective shell thickness (μm) at the blunt end of common guillemot eggs after controlling for egg volume.

Egg shape parameter	Estimate		t	p	Adjusted R^2	$F_{(2,52)}$	p
	intercept	470	3.81	0.0004			
Elongation	Volume	1.03	1.47	0.149	0.065	2.88	0.065
	Elongation	-133	-1.99	0.052			
	intercept	353	1.3	0.190			
Asymmetry	Volume	0.929	1.28	0.207	- 0.0004	0.89	0.415
	Asymmetry	-141	-0.35	0.728			
	intercept	228	3.11	0.003			
Taper	Volume	0.762	1.05	0.298	0.031	1.85	0.167
	Taper	157	1.41	0.166			
	intercept	294	3.05	0.004			
Sphericity	Volume	0.939	1.29	0.201	- 0.002	0.94	0.398
	Sphericity	-39.5	-0.46	0.648			
	intercept	392	3.53	0.0009			
Elongation at the blunt end	Volume	1.02	1.43	0.160	0.034	1.95	0.153
	Blunt end elongation	-115	-1.47	0.147			

Table S5. Relationships between egg shape and effective shell thickness (μm) at the equator of common guillemot eggs after controlling for egg volume.

Egg shape parameter	Estimate		t	p	Adjusted R^2	$F_{(2,52)}$	p
	intercept	468	3.87	0.0003			
Elongation	Volume	2.28	3.33	0.002	0.184	7.08	0.002
	Elongation	-129	-1.98	0.054			
	intercept	650	2.55	0.014			
Asymmetry	Volume	2.16	3.11	0.003	0.162	6.21	0.004
	Asymmetry	-599	-1.56	0.125			
	intercept	226	3.19	0.002			
Taper	Volume	1.99	2.84	0.007	0.168	6.45	0.003
	Taper	182	1.68	0.099			
	intercept	279	2.95	0.005			
Sphericity	Volume	2.19	3.09	0.003	0.123	4.79	0.012
	Sphericity	-15.0	-0.18	0.859			
	intercept	326	2.95	0.005			
Elongation at the blunt end	Volume	2.23	3.15	0.003	0.130	5.04	0.010
	Blunt end elongation	-51.7	-0.67	0.507			

Table S6. Relationships between egg shape and effective shell thickness (μm) at the pointed end of common guillemot eggs after controlling for egg volume.

Egg shape parameter	Estimate		t	p	Adjusted R^2	$F_{(2,52)}$	p
	intercept	542	3.17	0.003			
Elongation	Volume	2.66	2.75	0.008	0.170	6.53	0.003
	Elongation	-232	-2.53	0.015			
	intercept	1063	3.00	0.004			
Asymmetry	Volume	2.42	2.51	0.015	0.174	6.69	0.003
	Asymmetry	-1382	-2.58	0.013			
	intercept	126	1.23	0.225			
Taper	Volume	2.24	2.20	0.032	0.106	4.19	0.021
	Taper	232	1.48	0.146			
	intercept	299	2.22	0.031			
Sphericity	Volume	2.51	2.49	0.016	0.097	3.89	0.027
	Sphericity	-153	-1.28	0.207			
	intercept	240	1.50	0.139			
Elongation at the blunt end	Volume	2.54	2.47	0.017	0.072	3.10	0.053
	Blunt end elongation	-53.2	-0.48	0.637			

Table S7. Linear mixed effects model (using lme in the nlme package and controlling for egg identity as a random factor) combining individually important factors based on Tables S4-S6 and the Results in Chapter 2.

	Value		Standard error	t	p	$F_{(d.f.)}$	$\chi^2_{(d.f.)}$	p
Region	Blunt	326	304	1.07	0.285	Intercept: $8222_{(1,106)}$		
	Equator	428	269	1.59	0.114	Region: $258_{(2,106)}$	$515_{(2)}$	< 0.0001
	Point	869	269	3.23	0.002			
Interaction: Region & Asymmetry	Blunt	65.2	442	0.148	0.883	Asymmetry: $4.30_{(1,50)}$	Asymmetry: $1.99_{(1)}$	0.158
	Equator	-481	424	-1.13	0.260	Region & Asymmetry: $4.55_{(2,106)}$	Region & Asymmetry: $9.11_{(2)}$	0.011
	Point	-1269	424	-2.99	0.004			
Volume		1.82	0.658	2.77	0.008	$8.11_{(1,50)}$	$7.67_{(1)}$	0.006
Elongation		-139	63.0	-2.20	0.033	$6.00_{(1,50)}$	$4.84_{(1)}$	0.028
Taper		109	105	1.04	0.306	$1.07_{(1,50)}$	$1.07_{(1)}$	0.301

This is a reduced model where non-significant interactions between size or shape parameters and region were removed.

Table S8. Descriptive statistics for effective eggshell thickness (µm) for common guillemot egg groups.

Group		Effective eggshell thickness (µm) at the			Pattern	$F_{(2,8)}$	p
		Blunt end	Equator	Pointed end			
Control	A	364 ± 38.9	500 ± 45.1	431 ± 51.7	E > P > B	77.4	< 0.001
	B	326 ± 49.3	454 ± 39.9	410 ± 27.9	E > P > B	35.7	< 0.001
Volume	Small	338 ± 19.8	430 ± 32.9	368 ± 37.6	E > P = B	12.6	0.003
	Large	368 ± 32.4	495 ± 25.4	432 ± 29.7	E > P > B	35.6	< 0.001
Elongation	Rotund	393 ± 67.1	509 ± 33.5	459 ± 46.9	E > P > B	30.6	< 0.001
	Elongate	366 ± 49.6	461 ± 29.6	400 ± 55.0	E = P = B	6.9 (1.07, 4.29)*	0.0180 (0.0535)*
Asymmetry	Low (more symmetrical)	358 ± 22.8	496 ± 38.8	463 ± 49.3	E > P > B	58.8	< 0.001
	High (less symmetrical)	353 ± 55.6	496 ± 56.0	399 ± 92.4	E > P > B	31.0	< 0.001
Taper	Rounded point	373 ± 33.3	498 ± 24.8	422 ± 47.9	E > P > B	40.8	< 0.001
	Tapered point	343 ± 27.7	466 ± 24.8	417 ± 39.7	E > P > B	19.0	< 0.001
Sphere	More spherical blunt end	329 ± 65.1	463 ± 43.2	395 ± 74.4	E > P > B	30.5	< 0.001
	More pointed blunt end	353 ± 14.2	483 ± 34.1	451 ± 53.1	E = P > B	22.9	< 0.001
Elongation at the blunt end[1]	Rounded blunt end	350 ± 30.3	466 ± 46.2	415 ± 69.3	E > P > B	17.8	< 0.001
	More elongate and pointed blunt end	337 ± 42.2	476 ± 43.2	399 ± 53.2	E > P > B	29.9 (1.12,5.59)*	< 0.001 (0.002)*

> or < post-hoc test with Tukey contrasts $p < 0.05$ after significant repeated measures ANOVA.
[1] d.f. = 2,10, n = 6.
*Greenhouse-Geisser corrected p-value and d.f. due to violation of sphericity assumption.

Table S9. Relationships between egg shape and true shell thickness (μm) at the blunt end of common guillemot eggs after controlling for egg volume.

Egg shape parameter	Estimate		t	p	Adjusted R^2	$F_{(2,52)}$	p
	intercept	566	4.39	< 0.0001			
Elongation	Volume	1.30	1.78	0.0811	0.102	4.06	0.023
	Elongation	-162	-2.34	0.0234			
	intercept	453	1.61	0.113			
Asymmetry	Volume	1.18	1.54	0.131	0.012	1.34	0.271
	Asymmetry	-219	-0.52	0.609			
	intercept	270	3.52	0.0009			
Taper	Volume	0.980	1.29	0.204	0.054	2.55	0.088
	Taper	188	1.60	0.115			
	intercept	333	3.25	0.002			
Sphericity	Volume	1.19	1.55	0.127	0.009	1.24	0.298
	Sphericity	-24.7	-0.27	0.787			
	intercept	464	3.97	0.0002			
Elongation at the blunt end	Volume	1.29	1.71	0.093	0.056	2.60	0.084
	Blunt end elongation	-134	-1.64	0.108			

Table S10. Relationships between egg shape and true shell thickness (μm) at the equator of common guillemot eggs after controlling for egg volume.

Egg shape parameter	Estimate		t	p	Adjusted R^2	$F_{(2,52)}$	p
	intercept	550	4.32	< 0.0001			
Elongation	Volume	2.50	3.46	0.001	0.200	7.76	0.001
	Elongation	-145	-2.11	0.040			
	intercept	735	2.73	0.009			
Asymmetry	Volume	2.36	3.22	0.002	0.171	6.59	0.003
	Asymmetry	-642	-1.58	0.121			
	intercept	276	3.70	0.0005			
Taper	Volume	2.17	2.93	0.005	0.184	7.09	0.002
	Taper	208	1.83	0.073			
	intercept	321	3.21	0.002			
Sphericity	Volume	2.40	3.19	0.002	0.132	5.10	0.001
	Sphericity	3.49	0.04	0.969			
	intercept	394	3.38	0.001			
Elongation at the blunt end	Volume	2.44	3.26	0.002	0.141	5.44	0.007
	Blunt end elongation	-61.8	-0.76	0.454			

Table S11. Relationships between egg shape and true shell thickness (μm) at the pointed end of common guillemot eggs after controlling for egg volume.

Egg shape parameter	Estimate		t	p	Adjusted R^2	$F_{(2,52)}$	p
	intercept	630	3.55	0.0008			
Elongation	Volume	3.27	3.24	0.002	0.223	8.74	0.0005
	Elongation	-274	-2.85	0.006			
	intercept	1107	2.95	0.005			
Asymmetry	Volume	3.00	2.92	0.005	0.197	7.61	0.001
	Asymmetry	-1413	-2.49	0.016			
	intercept	140	1.30	0.200			
Taper	Volume	2.77	2.58	0.013	0.148	5.68	0.006
	Taper	279	1.69	0.097			
	intercept	311	2.18	0.034			
Sphericity	Volume	3.09	2.88	0.006	0.121	4.70	0.013
	Sphericity	-137	-1.08	0.287			
	intercept	305	1.82	0.075			
Elongation at the blunt end	Volume	3.14	2.91	0.005	0.111	4.37	0.018
	Blunt end elongation	-89.7	-0.76	0.450			

Table S12. Pairwise comparisons of common guillemot true shell (µm) thickness

Group	Blunt end			Equator			Pointed end		
	$t_{(d.f. = 4)}$	p	Mean of the differences (µm)	$t_{(d.f. = 4)}$	p	Mean of the differences (µm)	$t_{(d.f. = 4)}$	p	Mean of the differences (µm)
Control	0.79	0.476	31.4	1.62	0.181	55.1	0.91	0.414	33.4
Volume	2.03	0.112	32.1	12.9	0.0002	**73.4**	2.95	0.042	**79.8**
Elongation	-1.69	0.166	-34.6	-3.30	0.030	**-50.0**	-3.73	0.020	**-67.3**
Asymmetry	-0.46	0.670	-13.9	0.01	0.994	0.217	-1.13	0.322	-64.1
Taper	2.01	0.115	31.5	3.98	0.016	**37.1**	0.61	0.575	15.8
Sphere	0.63	0.561	21.6	0.63	0.566	20.3	1.84	0.139	60.9
Elongation at the blunt end[1]	-1.01	0.360	-22.0	0.29	0.780	6.86	-0.69	0.521	-28.3

Bold indicates significant difference.
[1] d.f. = 5, n = 6.

Table S13. Relationships between egg shape and total shell thickness (μm) at the blunt end of common guillemot eggs after controlling for egg volume.

Egg shape parameter	Estimate		t	p	Adjusted R^2	$F_{(2,52)}$	p
	intercept	720	4.76	< 0.0001			
Elongation	Volume	1.39	1.61	0.113	0.109	4.29	0.019
	Elongation	-208	-2.54	0.014			
	intercept	485	1.46	0.151			
Asymmetry	Volume	1.24	1.36	0.180	-0.001	0.97	0.385
	Asymmetry	-137	-0.27	0.786			
	intercept	343	3.79	0.0004			
Taper	Volume	0.98	1.09	0.281	0.051	2.46	0.096
	Taper	237	1.72	0.092			
	intercept	423	3.49	0.001			
Sphericity	Volume	1.25	1.37	0.177	-0.0007	0.98	0.382
	Sphericity	-32.0	-0.30	0.768			
	intercept	610	4.46	< 0.0001			
Elongation at the blunt end	Volume	1.38	1.57	0.124	0.067	2.94	0.062
	Blunt end elongation	-189	-1.97	0.054			

Table S14. Relationships between egg shape and total shell thickness (µm) at the equator of common guillemot eggs after controlling for egg volume.

Egg shape parameter	Estimate		t	p	Adjusted R^2	$F_{(2,52)}$	p
	intercept	635	4.48	< 0.0001			
Elongation	Volume	2.85	3.54	0.0009	0.206	8.02	0.0009
	Elongation	-161	-2.10	0.0404			
	intercept	662	2.18	0.0342			
Asymmetry	Volume	2.72	3.27	0.0019	0.154	5.90	0.0049
	Asymmetry	-434	-0.94	0.350			
	intercept	316	3.89	0.0003			
Taper	Volume	2.41	2.99	0.0043	0.225	8.86	0.0005
	Taper	299	2.41	0.0196			
	intercept	374	3.35	0.0015			
Sphericity	Volume	2.74	3.27	0.0019	0.139	5.37	0.0076
	Sphericity	14.9	0.15	0.881			
	intercept	502	3.90	0.0003			
Elongation at the blunt end	Volume	2.82	3.39	0.0013	0.160	6.16	0.0040
	Blunt end elongation	-104	-1.15	0.254			

Table S15. Relationships between egg shape and total shell thickness (μm) at the pointed end of common guillemot eggs after controlling for egg volume.

Egg shape parameter	Estimate		t	p	Adjusted R^2	$F_{(2,52)}$	p
	intercept	900	4.72	< 0.0001			
Elongation	Volume	3.33	3.07	0.00336	0.262	10.6	0.0001
	Elongation	-372	-3.62	0.00067			
	intercept	1100	2.56	0.0133			
Asymmetry	Volume	3.00	2.56	0.0133	0.135	5.22	0.0086
	Asymmetry	-1220	-1.88	0.0655			
	intercept	257	2.12	0.0389			
Taper	Volume	2.76	2.30	0.0257	0.115	4.49	0.0158
	Taper	278	1.50	0.139			
	intercept	354	2.20	0.0323			
Sphericity	Volume	3.07	2.54	0.0140	0.078	3.28	0.0457
	Sphericity	-42.6	-0.30	0.767			
	intercept	557	3.03	0.0038			
Elongation at the blunt end	Volume	3.22	2.72	0.0088	0.121	4.71	0.0131
	Blunt end elongation	-210	-1.63	0.110			

Table S16. Pairwise comparisons of common guillemot total shell thickness (µm).

Group	Blunt end			Equator			Pointed end		
	$t_{(d.f. = 4)}$	p	Mean of the differences (µm)	$t_{(d.f. = 4)}$	p	Mean of the differences (µm)	$t_{(d.f. = 4)}$	p	Mean of the differences (µm)
Control	0.87	0.432	41.6	1.59	0.188	64.7	0.27	0.797	14.5
Volume	0.95	0.398	25.3	7.01	0.002	**70.1**	1.78	0.150	68.5
Elongation	-2.01	0.115	-40.6	-3.95	0.017	**-54.7**	-6.34	0.003	**-92.2**
Asymmetry	-0.20	0.823	-7.66	0.26	0.811	9.04	-1.02	0.367	-56.2
Taper	2.06	0.108	41.8	5.63	0.005	**62.3**	-0.13	0.906	-3.46
Sphere	0.86	0.441	25.9	0.46	0.672	14.3	0.86	0.440	35.3
Elongation at the blunt end[1]	-1.13	0.309	-32.2	-0.21	0.845	-6.33	-1.01	0.357	-47.8

Bold indicates significant difference.
[1] d.f. = 5, n = 6.

Table S17. Regional effective thickness to total shell thickness ratios for the Alcidae.

Species	Effective to total shell thickness ratio at the			Pattern	$F_{(d.f.)}$	p
	Blunt end	Equator	Pointed end			
Ancient murrelet	0.61 ± 0.040	0.61 ± 0.039	0.62 ± 0.029	P = E = B	$0.16_{(2,8)}$	0.851
Atlantic puffin	0.69 ± 0.048	0.66 ± 0.029	0.62 ± 0.031	**B > P B = E, E = P**	$6.53_{(2,8)}$	0.021
Black guillemot	0.65 ± 0.030	0.65 ± 0.032	0.62 ± 0.039	E = B = P	$3.76_{(2,8)}$	0.070
Brünnich's guillemot	0.66 ± 0.047	0.72 ± 0.021	0.64 ± 0.021	**E > B = P**	$18.6_{(2,8)}$	< 0.001
Cassin's auklet	0.59 ± 0.021	0.57 ± 0.012	0.56 ± 0.013	**B > P B = E, E = P**	$4.75_{(2,8)}$	0.044
Common guillemot	0.71 ± 0.023	0.74 ± 0.013	0.68 ± 0.027	**E = B > P**	$8.78_{(2,8)}$	0.0096 (0.021)*
Crested auklet	0.60 ± 0.023	0.59 ± 0.060	0.58 ± 0.053	B = E = P	$0.44_{(2,4)}$	0.672
Horned puffin	0.68 ± 0.032	0.66 ± 0.016	0.62 ± 0.031	B = E = P	$4.00_{(2,6)}$	0.070
Japanese murrelet	0.62 ± 0.019	0.62 ± 0.034	0.63 ± 0.019	B = P = E	$0.64_{(2,12)}$	0.542
Least auklet	0.58 ± 0.046	0.55 ± 0.023	0.54 ± 0.023	B = E = P	$2.94_{(2,6)}$	0.129
Little auk	0.66 ± 0.024	0.64 ± 0.050	0.60 ± 0.041	**B = E > P**	$19.3_{(2,8)}$	0.0009
Parakeet auklet	0.62 ± 0.025	0.58 ± 0.007	0.54 ± 0.030	B = E = P	$6.82_{(2,4)}$	0.051
Razorbill	0.69 ± 0.027	0.71 ± 0.023	0.68 ± 0.028	E = B = P	$3.11_{(2,8)}$	0.100
Rhinoceros auklet	0.67 ± 0.011	0.65 ± 0.036	0.64 ± 0.083	B = E = P	$0.76_{(2,8)}$	0.497
Scripps' murrelet	0.65 ± 0.027	0.66 ± 0.021	0.65 ± 0.019	E = B = P	$0.22_{(2,8)}$	0.805
Tufted puffin	0.68 ± 0.033	0.64 ± 0.033	0.59 ± 0.011	**B > E > P**	$18.7_{(2,8)}$	0.001
Whiskered auklet	0.59 ± 0.025	0.53 ± 0.041	0.51 ± 0.018	**B > E = P**	$16.4_{(2,6)}$	0.004

N.B. the membranes were separate to the shell for some species (e.g. whiskered auklet) which may explain some of the sub 60% results as the measures (membrane & calculated total thickness) are possibly overestimates. Bold patterns indicate significant differences (repeat measures ANOVA, > or < indicates post-hoc tests with Tukey contrasts $p < 0.05$).
*Greenhouse-Geisser corrected d.f. (1.04, 4.16) and p-value due to violation of sphericity.

Table S18. Regional total eggshell thickness (μm) for the Alcidae

Species	Total eggshell thickness (μm) at the			Pattern	$F_{(d.f.)}$	p
	Blunt end	Equator	Pointed end			
Significant variation in thickness along their eggs						
Ancient murrelet	259 ± 19.9	284 ± 4.69	283 ± 12.2	**E = P > B**	$10.6_{(2,8)}$	0.006
Black guillemot	346 ± 12.0	351 ± 16.7	380 ± 16.3	**P > E = B**	$9.78_{(2,8)}$	0.007
Brünnich's guillemot	490 ± 48.2	591 ± 36.1	574 ± 83.1	**E = P > B**	$12.3_{(2,8)}$	0.004
Cassin's auklet	239 ± 12.5	263 ± 15.1	269 ± 11.7	**P = E > B**	$11.9_{(2,8)}$	0.004
Common guillemot	559 ± 36.6	688 ± 22.8	638 ± 50.4	**E > P > B**	$39.5_{(2,8)}$	< 0.001
Least auklet	207 ± 11.5	224 ± 14.1	235 ± 13.5	**P = E > B**	$11.1_{(2,6)}$	0.010
Little auk	283 ± 27.0	315 ± 34.3	315 ± 33.6	**E = P > B**	$29.0_{(2,8)}$	< 0.001
Razorbill	401 ± 24.8	461 ± 18.6	486 ± 60.5	**P = E > B**	$8.41_{(2,8)}$	0.012
Rhinoceros auklet	311 ± 17.4	354 ± 21.3	342 ± 13.3	**E = P > B**	$11.2_{(2,8)}$	0.005
Scripps' murrelet	271 ± 31.1	289 ± 19.4	287 ± 24.4	**E = P > B**	$4.54_{(2,8)}$	0.048
Tufted puffin	422 ± 30.1	424 ± 28.2	448 ± 13.4	**P > E = B**	$5.55_{(2,8)}$	0.031
Whiskered auklet	255 ± 8.6	267 ± 9.0	281 ± 12.3	**P > E > B**	$29.3_{(2,6)}$	< 0.001
Non-significant variation in thickness along their eggs						
Atlantic puffin	299 ± 21.2	319 ± 8.97	335 ± 23.7	P = E = B	$3.54_{(2,8)}$	0.079
Crested auklet	346 ± 66.7	450 ± 117	391 ± 56.2	E = P = B	$1.37_{(2,4)}$	0.353
Horned puffin	347 ± 25.1	365 ± 15.0	377 ± 20.8	P = E = B	$2.62_{(2,6)}$	0.152
Japanese murrelet	250 ± 14.6	261 ± 7.3	260 ± 15.9	E = P = B	$1.11_{(2,12)}$	0.361
Parakeet auklet	300 ± 19.2	321 ± 25.7	338 ± 25.9	P = E = B	$5.17_{(2,4)}$	0.078

N.B. total thickness at blunt end may be lower in some cases because the air cell has formed and reduced thickness at the blunt end by ~ 10 – 20μm (based on scanned and measured air-cells). Whereas the membranes are likely not separated at the equator and the point. Bold patterns indicate significant differences (repeat measures ANOVA, > or < indicates post-hoc tests with Tukey contrasts $p < 0.05$).

Table S19. Best fitting phylogenetically controlled linear model at the blunt end of Alcid eggs for total shell thickness (µm).

Factor		Estimate	t	p	Partial R^2
Adult mass		0.265	9.15	< 0.001	0.884
	Rock: Usually	256	9.74	< 0.001	
Incubation substrate	Rock: Sometimes	-37.0	-1.74	0.109	0.452
	Rock: Rarely	-76.2	-3.16	0.009	

AIC = 150.7, Lambda < 0.001, full model r^2 = 0.929.

Table S20. Best fitting phylogenetically controlled linear model at the equator of Alcid eggs for total shell thickness (µm).

Factor		Estimate	t	p	Partial R^2
Adult mass		0.349	7.19	< 0.001	0.858
	Rock: Usually	280	8.32	< 0.001	
Incubation substrate	Rock: Sometimes	-76.3	-2.45	0.032	0.358
	Rock: Rarely	-96.9	-2.73	0.020	

AIC = 159.9, Lambda = 0.4, full model r^2 = 0.922.

Table S21. Best fitting phylogenetically controlled linear model at the pointed end of Alcid eggs for total shell thickness (µm).

Factor		Estimate	t	p	Partial R^2
Adult mass		0.336	8.97	< 0.001	0.876
	Rock: Usually	268	7.70	< 0.001	
Incubation substrate	Rock: Sometimes	-40.2	-1.45	0.176	0.326
	Rock: Rarely	-76.3	-2.41	0.035	

AIC = 156.6, Lambda = 0.375, full model r^2 = 0.926.

Table S22. Regional effective thickness to true shell thickness ratios for the Alcidae.

Species	Effective to total shell thickness ratio at the			Pattern	$F_{(d.f.)}$	p
	Blunt end	Equator	Pointed end			
Ancient murrelet	0.80 ± 0.021	0.79 ± 0.032	0.80 ± 0.031	B = P = E	$0.91_{(2,8)}$	0.440
Atlantic puffin	0.82 ± 0.033	0.80 ± 0.023	0.77 ± 0.017	B = E = P	$4.85_{(2,8)}$	0.042 (0.087)*
Black guillemot	0.80 ± 0.044	0.79 ± 0.025	0.78 ± 0.032	B = E = P	$2.00_{(2,8)}$	0.200
Brünnich's guillemot	0.82 ± 0.029	0.84 ± 0.014	0.80 ± 0.020	**E > B = P**	$12.21_{(2,8)}$	0.004
Cassin's auklet	0.78 ± 0.010	0.75 ± 0.022	0.73 ± 0.003	**B > E = P**	$16.83_{(2,8)}$	0.001
Common guillemot	0.85 ± 0.018	0.86 ± 0.017	0.83 ± 0.035	**E = B > P**	$6.86_{(2,8)}$	0.018
Crested auklet	0.81 ± 0.027	0.80 ± 0.034	0.79 ± 0.044	B = E = P	$0.10_{(2,4)}$	0.904
Horned puffin	0.83 ± 0.008	0.81 ± 0.012	0.81 ± 0.031	B = E = P	$1.60_{(2,6)}$	0.277
Japanese murrelet	0.81 ± 0.036	0.80 ± 0.029	0.81 ± 0.029	B = P = E	$0.11_{(2,12)}$	0.894
Least auklet	0.76 ± 0.037	0.80 ± 0.030	0.80 ± 0.016	E = P = B	$1.92_{(2,6)}$	0.227
Little auk	0.81 ± 0.016	0.79 ± 0.017	0.76 ± 0.046	**B = E > P**	$8.24_{(2,8)}$	0.011
Parakeet auklet	0.79 ± 0.027	0.82 ± 0.005	0.81 ± 0.015	E = P = B	$1.66_{(2,4)}$	0.298
Razorbill	0.84 ± 0.023	0.84 ± 0.014	0.85 ± 0.016	P = E = B	$0.44_{(2,8)}$	0.659
Rhinoceros auklet	0.83 ± 0.023	0.83 ± 0.019	0.79 ± 0.034	B = E = P	$2.65_{(2,8)}$	0.131
Scripps' murrelet	0.82 ± 0.032	0.80 ± 0.034	0.82 ± 0.012	P = B = E	$0.66_{(2,8)}$	0.541
Tufted puffin	0.82 ± 0.025	0.80 ± 0.028	0.77 ± 0.019	**B > P, B=E, E=P**	$9.14_{(2,8)}$	0.009
Whiskered auklet	0.78 ± 0.027	0.81 ± 0.052	0.79 ± 0.026	E = P = B	$1.18_{(2,6)}$	0.369

Bold patterns indicate significant differences (repeat measures ANOVA, > or < indicates post-hoc tests with Tukey contrasts $p < 0.05$).
*Greenhouse-Geisser corrected d.f. (1.07, 4.27) and p-values due to violation of sphericity assumption.

Table S23. Regional true shell thickness (μm) for the Alcidae

Species	True shell thickness (μm) at the			Pattern	$F_{(d.f.)}$	p (adjusted)*
	Blunt end	Equator	Pointed end			
Significant variation in thickness along their eggs						
Ancient murrelet	198 ± 7.5	219 ± 5.5	217 ± 11.1	**E = P > B**	$16.1_{(2,8)}$	0.002
Black guillemot	281 ± 14.8	288 ± 6.1	301 ± 11.6	**P > B P=E, E=B**	$5.07_{(2,8)}$	0.038
Brünnich's guillemot	395 ± 40.3	504 ± 23.0	455 ± 58.5	**E > P > B**	$18.5_{(2,8)}$	0.001
Cassin's auklet	180 ± 7.9	201 ± 11.5	206 ± 7.3	**P = E > B**	$16.8_{(2,8)}$	0.001
Common guillemot	469 ± 34.7	593 ± 19.6	524 ± 34.7	**E > P > B**	$27.4_{(2,8)}$	< 0.001
Crested auklet	257 ± 42.3	264 ± 25.2	285 ± 36.0	**P > E = B**	$7.50_{(2,4)}$	0.045
Little auk	232 ± 18.8	256 ± 25.6	251 ± 21.4	**E = P > B**	$13.6_{(2,8)}$	0.003
Razorbill	329 ± 16.2	388 ± 19.4	392 ± 47.3	**P = E > B**	$11.3_{(2,8)}$	0.005
Whiskered auklet	193 ± 4.0	175 ± 9.1	181 ± 13.6	**B > P = E**	$11.6_{(2,6)}$ (1.02, 3.07)	0.009 (0.041)*
Non-significant variation in thickness along their eggs						
Atlantic puffin	249 ± 12.3	266 ± 18.1	268 ± 12.9	P = E = B	$2.46_{(2,8)}$	0.147
Horned puffin	286 ± 18.4	295 ± 6.8	290 ± 11.2	E = P = B	$0.48_{(2,6)}$	0.639
Japanese murrelet	194 ± 6.9	201 ± 8.5	203 ± 8.1	P = E = B	$2.11_{(2,12)}$	0.164
Least auklet	158 ± 13.1	153 ± 16.6	159 ± 15.1	P = B = E	$0.25_{(2,6)}$	0.784
Parakeet auklet	233 ± 15.1	225 ± 18.0	226 ± 25.0	B = P = E	$1.30_{(2,4)}$ (1.00, 2.00)	0.368 (0.373)*
Rhinoceros auklet	255 ± 18.2	278 ± 12.0	276 ± 33.8	E = P = B	$4.01_{(2,8)}$	0.062
Scripps' murrelet	217 ± 25.0	237 ± 15.0	225 ± 18.5	E = P = B	$4.10_{(2,8)}$	0.059
Tufted puffin	347 ± 28.4	340 ± 25.1	341 ± 10.7	B = E = P	$0.39_{(2,8)}$ (1.05, 4.21)	0.689 (0.574)*

Bold patterns indicate significant differences (> or < indicates post-hoc test with Tukey contrasts $p < 0.05$).
*Greenhouse-Geisser corrected d.f. and p-values due to violation of sphericity assumption.

Table S24. Best fitting phylogenetically controlled linear model at the blunt end of Alcid eggs for true shell thickness (µm).

Factor		Estimate	t	p	Partial R^2
Adult mass		0.236	11.3	< 0.001	0.916
	Rock: Usually	198	10.4	< 0.001	
Incubation substrate	Rock: Sometimes	-33.5	-2.18	0.052	0.540
	Rock: Rarely	-64.4	-3.68	0.004	

AIC = 141.1, Lambda < 0.001, full model r^2 = 0.951.

Table S25. Best fitting phylogenetically controlled linear model at the equator of Alcid eggs for true shell thickness (µm).

Factor		Estimate	t	p	Partial R^2
Adult mass		0.269	8.25	< 0.001	0.866
Elongation		374	2.15	0.057	0.280
	Rock: Usually	-308	-1.21	0.255	
Incubation substrate	Rock: Sometimes	-81.2	-3.70	0.004	0.565
	Rock: Rarely	-111	-4.53	0.001	

AIC = 151.7, Lambda < 0.001, full model r^2 = 0.955.

Table S26. Best fitting phylogenetically controlled linear model at the pointed end of Alcid eggs for true shell thickness (µm).

Factor		Estimate	t	p	Partial R^2
Adult mass		0.278	8.82	< 0.001	0.871
	Rock: Usually	211	7.30	< 0.001	
Incubation substrate	Rock: Sometimes	-48.2	-2.08	0.061	0.271
	Rock: Rarely	-66.5	-2.52	0.029	

AIC = 152.2, Lambda = 0.182, full model r^2 = 0.926.

Table S27. Comparison of shell thickness values obtained using microCT (our study) to published values obtained using traditional methods.

Species	True shell thickness (µm)					Total shell thickness (µm)					
	Zimmerman and Hipfner (2007)	Our study			Belopol'skiĭ (1961) (range)	Ar and Rahn (1985)	Maurer *et al.* (2012)			Our study	
		Blunt	Equator	Point			Blunt	Equator	Point	Blunt	Equator	Point
Ancient murrelet	270	198 ± 7.5	219 ± 5.5	217 ± 11.1	-	-	-	-	-	259 ± 19.9	284 ± 4.69	283 ± 12.2
Atlantic puffin	-	249 ± 12.3	266 ± 18.1	268 ± 12.9	150 (140-150)	310	263 ± 26.5	274 ± 33.8	297 ± 23.9	299 ± 21.2	319 ± 8.97	335 ± 23.7
Black guillemot	-	281 ± 14.8	288 ± 6.1	301 ± 11.6	170 (160-190)	-	304 ± 22.0	321 ± 5.9	348 ± 9.3	346 ± 12.0	351 ± 16.7	380 ± 16.3
Brünnich's guillemot[1]	-	395 ± 40.3	504 ± 23.0	455 ± 58.5	300 (220-340) 500 (460-530)[1]	555	-	-	-	490 ± 48.2	591 ± 36.1	574 ± 83.1
Cassin's auklet	200 ± 1	180 ± 7.9	201 ± 11.5	206 ± 7.3	-	230	-	-	-	239 ± 12.5	263 ± 15.1	269 ± 11.7
Common guillemot[2]	540 ± 5	469 ± 34.7	593 ± 19.6	524 ± 34.7	310 (260-360)	660	497 ± 52.6	614 ± 51.8	592 ± 88.8	559 ± 36.6	688 ± 22.8	638 ± 50.4
Little auk	-	232 ± 18.8	256 ± 25.6	251 ± 21.4	240 (230-260)	-	-	-	-	283 ± 27.0	315 ± 34.3	315 ± 33.6
Razorbill	-	329 ± 16.2	388 ± 19.4	392 ± 47.3	280 (270-320)	-	367 ± 24.8	437 ± 20.1	464 ± 31.2	401 ± 24.8	461 ± 18.6	486 ± 60.5

Table continued on next page

Species	True shell thickness (µm)					Total shell thickness (µm)							
	Zimmerman and Hipfner (2007)	Our study			Belopol'skiĭ (1961) (range)	Ar and Rahn (1985)	Maurer *et al.* (2012)			Our study		
		Blunt	Equator	Point			Blunt	Equator	Point	Blunt	Equator	Point
Rhinoceros auklet	280 ± 2	255 ± 18.2	278 ± 12.0	276 ± 33.8	-	-	-	-	-	311 ± 17.4	354 ± 21.3	342 ± 13.3
Tufted puffin	320 ± 3	347 ± 28.4	340 ± 25.1	341 ± 10.7	-	360	-	-	-	422 ± 30.1	424 ± 28.2	448 ± 13.4

[1] values presented for two localities; East Murman and Nova Zemlya.

[2] for all 55 common guillemot eggs studied true shell thickness: blunt end: 427µm ± 41µm; equator: 554µm ± 43µm; pointed end: 499µm ± 60.0µm, total shell thickness, blunt end: 517µm ± 48µm; equator: 647µm ± 47µm; pointed end: 614µm ± 66.5µm.

Techniques used:

Belopol'skiĭ (1961) - measures taken from Kaaftanovskii (1941) or measured by L.O. Belopol'skiĭ, technique used is not specified.

Ar and Rahn (1985) – the measured thickness of dried eggshell using a ball-point caliper, averaged per egg then per species.

Zimmerman and Hipfner (2007) – true shell thickness measured on fresh eggshells with calipers (membranes were removed using boiling sodium hydroxide), species mean shell thickness values reported.

Maurer *et al.* (2012) – modified micrometer used to measure total shell thickness (the eggshell with membranes) of historical museum specimens.

Here, we do not compare our values to those presented by Schönwetter (1960 – 92) because his values are actually an index calculated from eggshell mass and egg dimensions, and not directly measured shell thickness values (Maurer *et al.* 2010; Maurer *et al.* 2012).

Appendix A4:

Supplementary materials for Chapter 3

Supplementary results

Statistical analysis of pore density differences between species

Between different species' eggs, pore density varied significantly (MANOVA, Pillai's Trace = 1.37, $F_{(48,174)}$ = 3.06, $p < 0.0001$). Brünnich's guillemot (*Uria lomvia*), common guillemot (*Uria aalge*), razorbill (*Alca torda*), and black guillemot (*Cepphus grylle*) eggs typically had a higher density of pores at the blunt end than the other Alcid species studied here, although not all differences between species were significant (one-way ANOVA: $F_{(16,58)}$ = 5.70, $p < 0.001$; Fig 3). *U. lomvia* had higher pore density at the blunt end than *S. antiquus, F. arctica, P. aleuticus, A. cristatella, F. corniculata, A. pusilla, A. alle, C. monocerata* and *S. scrippsi* (post-hoc tests with Tukey contrasts $p < 0.05$). *U. aalge* eggs had higher blunt end pore density than *S. scrippsi* and *S. antiquus* ($p < 0.05$). *A. torda* eggs had higher pore density at the blunt end than *C. monocerata, S. scrippsi, A. alle, F. corniculata, A. cristatella, P. aleuticus* and *S. antiquus* ($p < 0.05$). *C. grylle* had higher pore density at the blunt end than *S. antiquus, P. aleuticus, F. corniculata, C. monocerata* and *S. scrippsi* ($p < 0.05$), and nearly to *A. cristatella* ($p = 0.062$) and *A. alle* ($p = 0.067$).

Brünnich's guillemot, common guillemot, and razorbill eggs typically had a lower density of pores at the equator relative to other Alcids, but few differences were significant (one-way ANOVA: $F_{(16,58)}$ = 3.39, $p < 0.001$; Fig 3). The pore density at the equator of *U. lomvia* eggs was lower than *C. grylle* and *A. alle* ($p < 0.05$). *U. aalge* eggs had lower equator pore density than *A. alle* and nearly *C. grylle* ($p = 0.062$).

There was considerable variation in pore density at the pointed end across the Alcids eggs, but only Scripps's murrelet (*Synthliboramphus scrippsi)* and little auk (*Alle alle*) eggs differed from each other significantly, with little auk eggs typically having a higher density of pores at the pointed end than Scripps's murrelet eggs (one-way ANOVA: $F_{(16,58)}$ = 1.88, $p = 0.042$; post-hoc tests with Tukey contrasts $p < 0.05$; Fig 3).

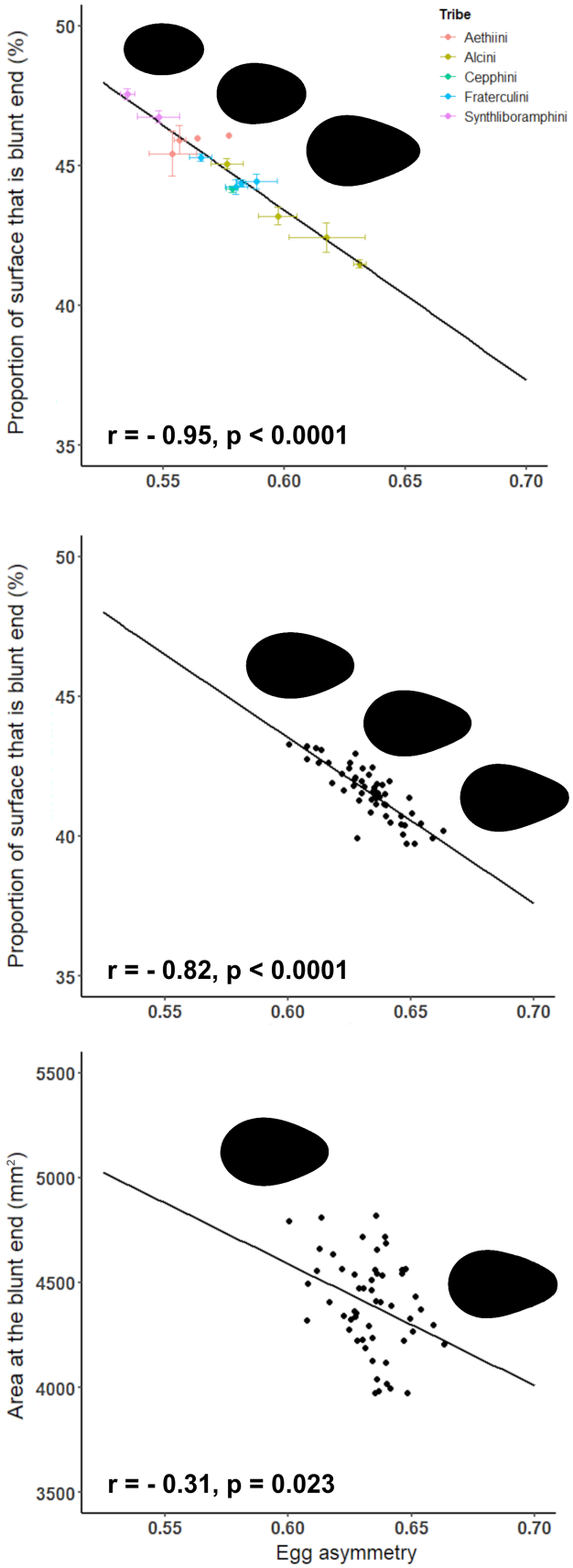

Figure S1. The relationship between egg asymmetry and the proportion of surface area that is blunt end across species (top), common guillemot eggs (middle) and actual differences in blunt end surface area across common guillemot eggs (bottom). The egg was split in two at the equator to define the blunt and pointed end. Correlation results annotated on graphs (Pearson's product moment for across species n = 15, Spearman's rank for common guillemot eggs n = 55).

Table S1. Egg size and shape correlations (Spearman's rank) with pore density at each region of common guillemot eggs (n = 55).

Parameter	Pore density per mm² at the		
	Blunt end	**Equator**	**Pointed end**
Volume	*-0.045*	*-0.182*	*-0.125*
Elongation	*0.257*[1] *0.058*	*-0.197*	*-0.226*[1] *0.097*
Asymmetry	*0.112*	*-0.012*	*0.173*
Taper	*0.016*	*0.137*	*0.029*
Sphere	*-0.103*	*0.137*	*0.194*
Elongation at the blunt end	*0.169*	*-0.078*	-0.281

n.s. p > 0.05, $p < 0.05$, $p < 0.01$, **p < 0.001**.
[1] $0.1 > p > 0.05$ r_s then p-value reported.

Table S2. Descriptive statistics (mean ± SD) of pore density for guillemot egg groups and repeated measures ANOVA results.

Group		Pore density per mm^2 at the			Pattern	$F_{(2,8)}$	p
		Blunt end	Equator	Pointed end			
Control	A	1.11 ± 0.25	0.60 ± 0.16	0.74 ± 0.29	B = E = P	4.35	0.053
	B	1.30 ± 0.47	0.70 ± 0.22	0.95 ± 0.43	B > E. E = P, B = P	4.92	0.041
Volume	Small	1.27 ± 0.57	0.71 ± 0.27	0.94 ± 0.47	B = E = P	2.25	0.167 (0.205)*
	Large	1.01 ± 0.25	0.55 ± 0.13	0.77 ± 0.12	B > E. B = P, E = P	7.24	0.016
Elongation	Rotund	0.97 ± 0.10	0.62 ± 0.03	0.75 ± 0.23	B > E = P	7.59	0.014
	Elongate	1.24 ± 0.35	0.52 ± 0.02	0.58 ± 0.11	B > E = P	21.2	< 0.001
Asymmetry	Low (more symmetrical)	1.43 ± 0.40	0.63 ± 0.09	0.83 ± 0.27	B > E = P	12.7	0.003
	High (less symmetrical)	1.52 ± 0.48	0.54 ± 0.18	0.88 ± 0.20	B > P > E	33.7	< 0.001
Taper	Rounded point	1.09 ± 0.13	0.72 ± 0.23	0.62 ± 0.35	B > E = P	9.87	< 0.001
	Pointed point	1.10 ± 0.09	0.63 ± 0.11	0.61 ± 0.16	B > E = P	22.5	< 0.001
Elongation at the blunt end	Rounded blunt end	1.32 ± 0.49	0.55 ± 0.19	0.78 ± 0.29	B > E = P	14.9	< 0.001
	Elongate, more pointed blunt end	1.35 ± 0.32	0.50 ± 0.13	0.55 ± 0.10	B > E = P	30.5	< 0.001
Sphericity	More spherical	1.38 ± 0.56	0.60 ± 0.12	0.84 ± 0.18	B > E = P	10.3	0.006
	Less spherical	1.05 ± 0.27	0.59 ± 0.13	0.73 ± 0.38	B = E = P	3.57	0.078

> or < post-hoc test with Tukey contrasts $p < 0.05$

[1] df = 2,10, n = 6.

*Greenhouse-Geisser adjusted p-value and d.f. (1.07,4.28) due to violation of sphericity assumption

Table S3. Pairwise comparisons of common guillemot eggshell pore density (per mm^2)

Group	Blunt end			Equator			Pointed end		
	$t_{(d.f. = 4)}$	p	Mean of the differences	$t_{(d.f. = 4)}$	p	Mean of the differences	$t_{(d.f. = 4)}$	p	Mean of the differences
Control	-1.33	0.253	-0.196	-0.71	0.515	-0.100	-0.76	0.491	-0.210
Volume	-1.12	0.324	-0.263	-1.02	0.367	-0.162	-0.92	0.411	-0.169
Elongation	1.95	0.123	0.270	-7.00	0.002	**-0.102**	-1.17	0.309	-0.168
Asymmetry	0.23	0.828	0.081	-1.27	0.274	-0.090	0.34	0.750	0.052
Taper	-0.13	0.904	-0.009	0.70	0.525	0.087	0.058	0.957	0.011
Sphericity	-1.67	0.171	-0.326	-0.23	0.832	-0.015	-0.510	0.637	-0.110
Elongation at the blunt end[1]	0.12	0.913	0.034	-0.56	0.603	-0.052	-1.59	0.173	-0.231

Bold indicates significant difference.
[1] df = 5, n = 6.

Table S4. Relationship between egg shape and size and pore density across the Alcidae

Region	Egg trait	Estimate		t	p	R^2	lambda
Blunt	Asymmetry	intercept	-4.37	-3.82	0.002	0.652	0.378
		slope	8.84	4.45	< 0.001		
	Elongation	intercept	-0.653	-0.29	0.776	0.266	0.941
		slope	0.924	0.62	0.548		
	Volume	intercept	0.384	2.31	0.038	0.492	0.830
		slope	0.006	2.60	0.022		
Equator	Asymmetry	intercept	2.26	1.79	0.097	0.094	< 0.001
		slope	-2.55	-1.63	0.266		
	Elongation	intercept	2.71	1.78	0.098	0.110	< 0.001
		slope	-1.29	-1.26	0.228		
	Volume	intercept	0.980	8.46	< 0.001	0.202	< 0.001
		slope	-0.003	-1.81	0.093		
Point	Asymmetry	intercept	0.704	0.69	0.500	< 0.001	< 0.001
		slope	0.030	0.02	0.987		
	Elongation	intercept	2.24	1.93	0.075	0.117	< 0.001
		slope	-1.02	-1.31	0.212		
	Volume	intercept	0.746	7.55	< 0.001	0.006	< 0.001
		slope	-0.0004	-0.28	0.787		

Table S5. Relationship between egg size and calculated total pore number across the Alcidae

Total pore number calculation (equivalent pore density ratio)*	Lambda	Estimate		t	p	Full model R^2	Egg volume R^2	Phylogeny R^2
Equal weighting (B:E:P x SA)	< 0.001	Intercept	1813	3.32	0.006	0.809	0.809	< 0.001
		Slope	65.5	7.41	< 0.001			
Twice the weight at the equator (B:2E:P x SA)	< 0.001	Intercept	2278	3.79	0.002	0.728	0.728	< 0.001
		Slope	57.4	5.90	< 0.001			
Moderate (~ B:2.5or3E:P x SA)[1]	< 0.001	Intercept	2513	3.85	0.002	0.661	0.661	< 0.001
		Slope	53.2	5.03	< 0.001			
Realistic (~ B:6E:1or2P x SA)[1]	< 0.001	Intercept	2852	4.07	0.001	0.564	0.564	< 0.001
		Slope	46.5	4.09	0.001			
Conservative (~ B:16E:5.5P x SA)[1]	0.002	Intercept	3057	4.08	0.001	0.485	0.484	< 0.001
		Slope	42.4	3.50	0.004			

*where B, E and P is blunt end, equator and pointed end pore density and SA is surface area.
[1]Approximate ratios that provide average pore density values for an egg that when multiplied by eggshell surface area provides similar, equivalent results to our new scaling methods (see Materials and Methods).

Table S6. Relationship between egg size, incubation period and calculated total pore number across the Alcidae

Total pore number calculation (equivalent pore density ratio)*	Estimate		t	p
Equal weighting (B:E:P x SA)	intercept	2265	1.30	0.218
	Volume	66.6	6.70	< 0.001
	Incubation period	-14.2	-0.28	0.788
Twice the weight at the equator (B:2E:P x SA)	intercept	1585	0.83	0.423
	Volume	55.8	5.12	< 0.001
	Incubation period	21.78	0.38	0.708
Moderate (~ B:2.5or3E:P x SA)[1]	intercept	1304	0.63	0.538
	Volume	50.40	4.29	0.001
	Incubation period	38.0	0.62	0.546
Realistic (~ B:6E:1or2P x SA)[1]	intercept	293	0.14	0.892
	Volume	40.5	3.38	0.005
	Incubation period	80.5	1.29	0.222
Conservative (~ B:16E:5.5P x SA)[1]	intercept	-314	-0.15	0.887
	Volume	34.6	2.80	0.016
	Incubation period	106	1.65	0.126

*where B, E and P is blunt end, equator and pointed end pore density and SA is surface area.
[1]Approximate ratios that provide average pore density values for an egg that when multiplied by eggshell surface area provides similar, equivalent results to our new scaling methods (see Materials and Methods).

Table S7. Comparison of pore density and total number between our study, Zimmerman and Hipfner (2007) and Ar and Rahn (1985).

Species	Pore density per cm^2				Predicted total pore number				
	Zimmerman and Hipfner (2007)	Our study			Zimmerman and Hipfner (2007)	Ar and Rahn (1985)	Our study		
		Blunt	Equator	Point			Moderate	Realistic	Conservative
Ancient murrelet	49	38.0 ± 19.1	81.6 ± 16.2	81.4 ± 25.6	2994	-	4543 ± 382	4866 ± 391	5060 ± 402
Atlantic puffin	-	69.1 ± 24.3	91.2 ± 41.9	68.7 ± 34.8	-	7482	6179 ± 976	6315 ± 1058	6397 ± 1112
Brünnich's guillemot	-	124.8 ± 25.4	48.4 ± 14.1	60.2 ± 26.7	-	7639	7263 ± 583	6406 ± 489	5898 ± 445
Cassin's auklet	49.0 ± 10.1	52.6 ± 24.8	97.6 ± 25.6	73.5 ± 26.1	2200	3315	3919 ± 591	4064 ± 542	4151 ± 513
Common guillemot	36.2 ± 3.8	102.4 ± 9.9	54.8 ± 8.1	62.0 ± 34.2	4235	7727	6986 ± 531	6484 ± 592	6183 ± 632
Razorbill	-	113.8 ± 14.3	61.4 ± 18.1	61.0 ± 28.3	-	7236	6910 ± 564	6377 ± 676	6057 ± 745
Rhinoceros auklet	43.4 ± 12.4	51.5 ± 28.0	96.1 ± 26.9	72.6 ± 23.8	3832	-	7233 ± 881	7617 ± 931	7848 ± 972
Tufted puffin	44.7 ± 6.3	71.9 ± 15.0	71.0 ± 15.4	88.2 ± 13.6	4358	10717	7310 ± 189	7351 ± 265	7376 ± 318

N.B. our value for pore density at the equator of common guillemot egg similar to measure reported in Tyler (1969) – 55 pores per cm^2. Our value for Cassin's auklet eggs is higher than those reported by Ar and Rahn (1985) and Roudybush *et al.* (1980) – 3295 ± 152 and Zimmerman and Hipfner's (2007) value of 2200 is considerably lower than all three values.

Appendix A5:

Supplementary materials for Chapter 4

Figure S1. Images illustrating the conditions within a guillemot breeding colony. Note the puddles of water and debris on the ledges. All images were taken at sites on Skomer Island, Wales, UK by T.R.B. Additional images and videos of guillemots incubating their eggs can be seen on Wildscreen Arkive e.g. https://www.arkive.org/guillemot/uria-aalge/image-A24724.html and https://www.arkive.org/guillemot/uria-aalge/video-09c.html.

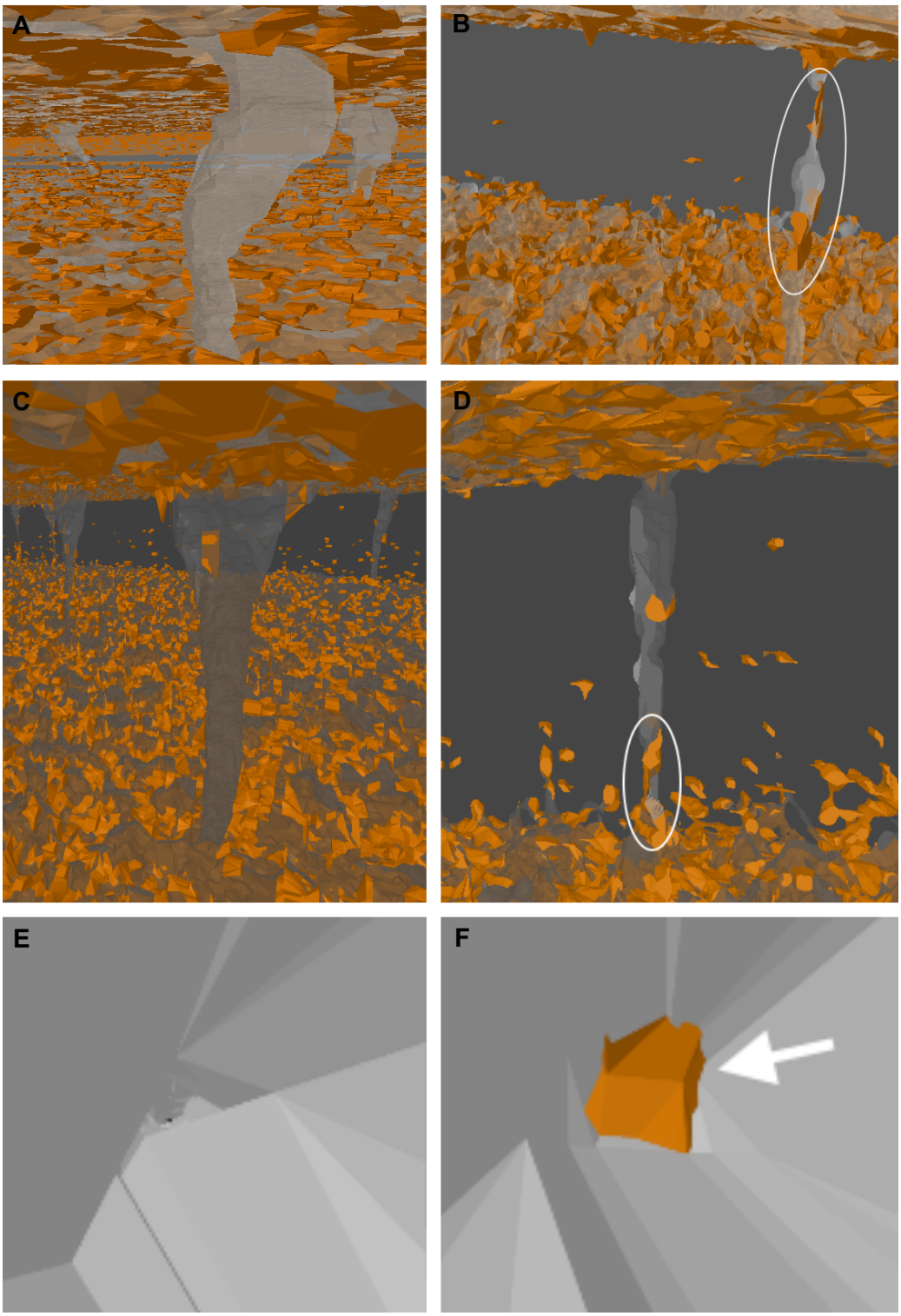

Figure S2. Examples of unblocked (A, C, E) and blocked (B, D, F) eggshell models, created from microCT data. The orange model represents the debris (and other organic matter like the shell membranes) and the translucent grey-white model represents the eggshell. The top two rows of images (A, B, C, D) show a cross section through the shell with the shell transparent and the pore channels (empty air space) visible in translucent grey. The top of the image is the exterior surface of the shell. The bottom two images (E, F) are the view looking down through a pore channel from near the exterior surface of the shell. The black dot in the middle of the E is the empty space on the other side of the pore channel (i.e. looking through the pore opening on the inner surface of the shell). The white circles and arrow highlight blockages within a pore channel caused by debris. All pores were checked for blockages both ways, but only pores that had a solid block i.e. no air spaces in the orange debris model (illustrated by the arrow) were considered blocked.

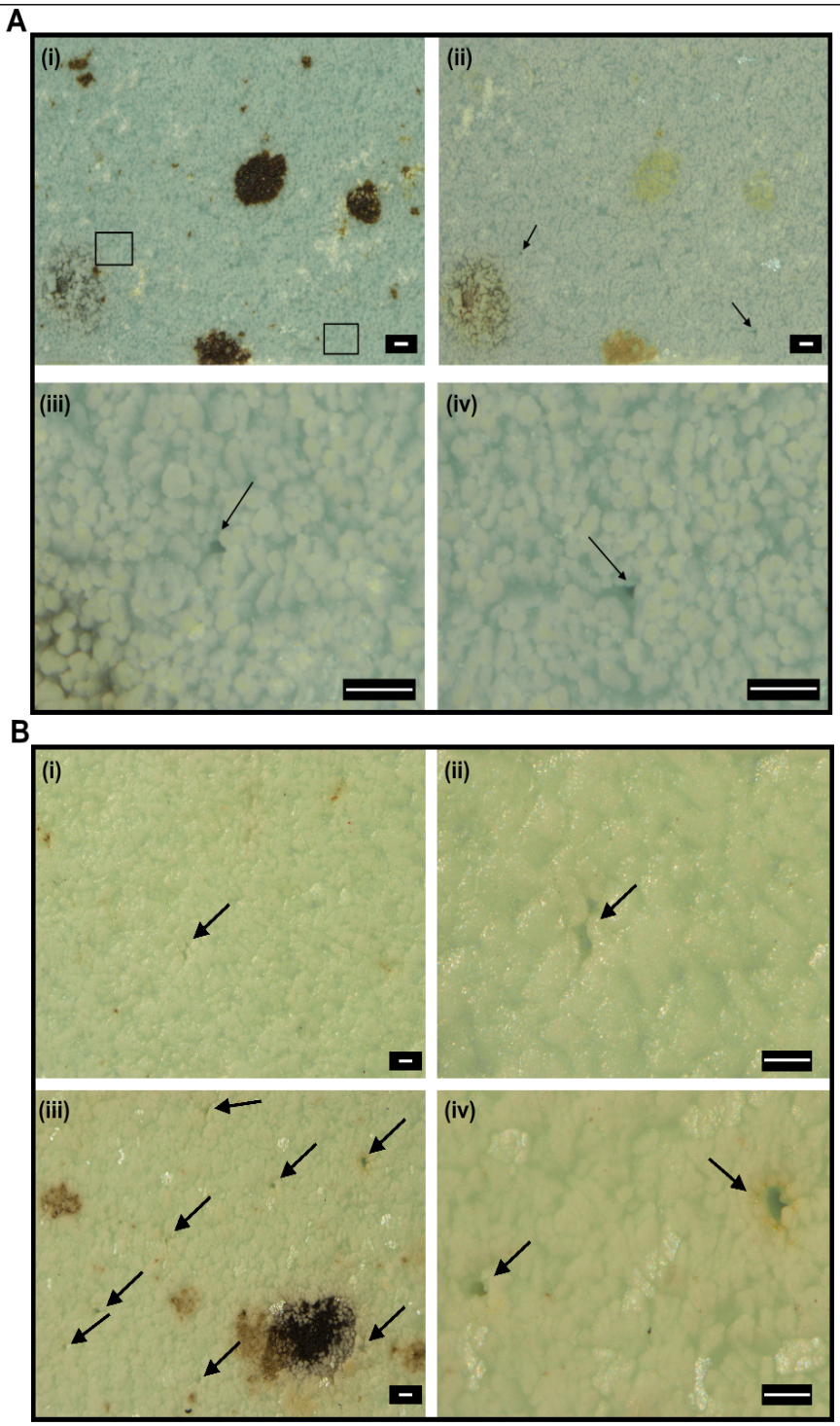

Figure S3. Removal of shell accessory material with bleach (A) and the natural variation in shell accessory material presence over pores between eggs (B). **A** - (i) Untreated eggshell. Rectangles mark where two pores are that only become visible after treatment with bleach because they are covered in SAM. (ii) Eggshell treated with bleach. The SAM have been removed from the eggshell, and as a result, there is much more definition in the shell surface topography, pigment has been removed and pores (indicated with black arrows) are now visible because they are no longer covered in SAM. (iii) A higher magnification image of the open pore visible on the left hand side of top right image. (iv) A higher magnification image of the open pore visible on the right hand side of the top right image. **B** - Images (i) and (ii) are from one of the eggs used in our study that showed a low proportion of blocked pores after debris application and (iii) and (iv) are from one of the eggs used that had the highest proportion of blocked pores after debris application. In images (i) and (ii), only one pore is clearly visible and it is covered in shell accessory materials (ii), whereas the pores in the other egg are not covered by shell accessory material (iii and iv), which may explain why this egg showed such a high proportion of blocked pores when debris was applied to the surface. All images were taken at a clean region of the equator of each egg and these imaging locations (i and iii) were haphazardly selected. Arrows indicate the location of visible pores. Scale bars = 100µm.

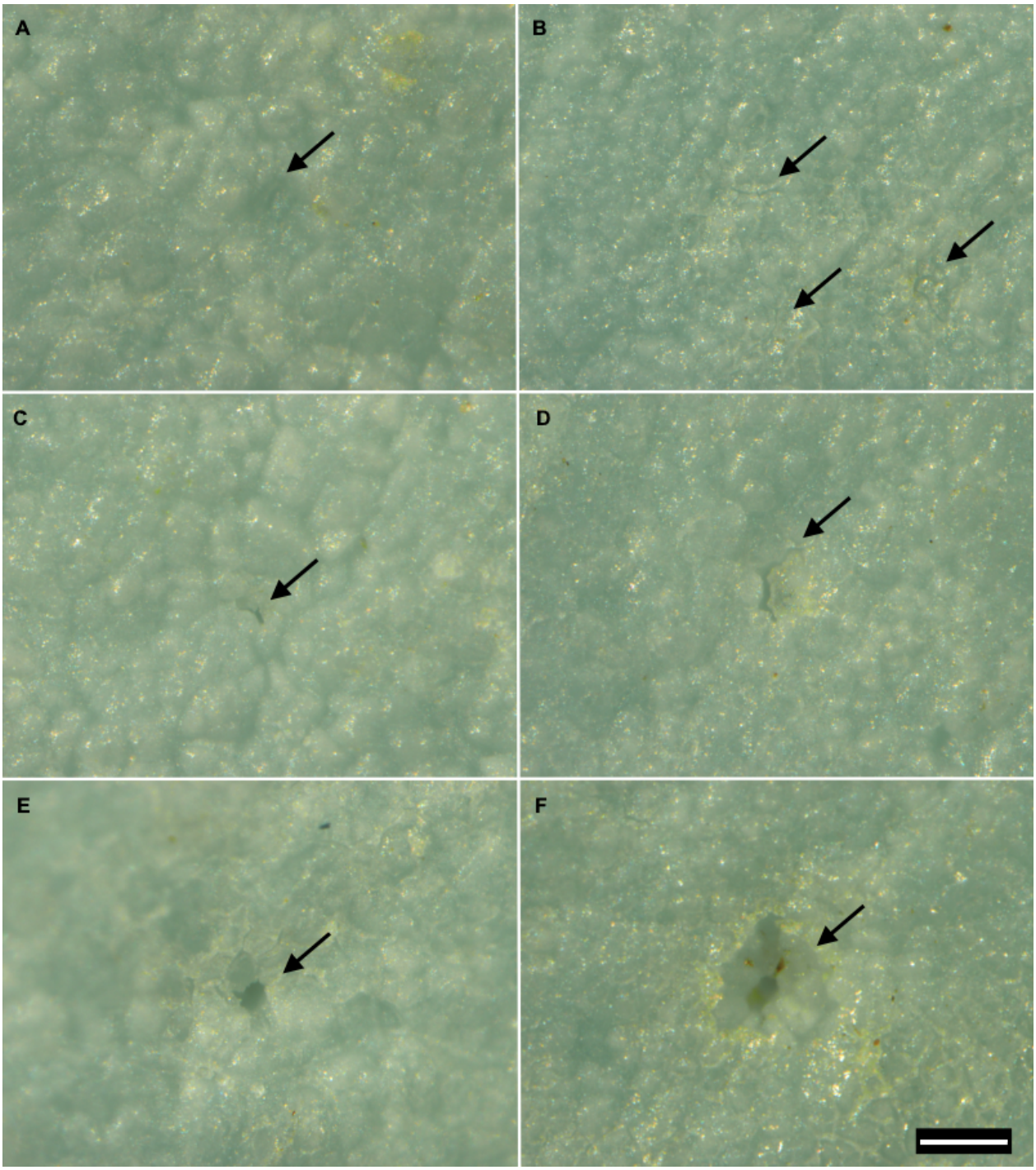

Figure S4. Natural variation in shell accessory material cover over pores. A – F show a sequence of pores starting with one that is fully covered in shell accessory material (A) to pores that have shell accessory material covering them but it is cracked to differing degrees (B – D), to pores that are open with the shell accessory material completely cracked or damaged meaning they are no longer covered (E – F). Arrows indicate the location of visible pores. All images are from the same egg and are at the same scale – see scale bar on image F. Scale bar = 100µm.

Datasets

Below are datasets 1 and 2. These contain the data we collected and analysed in this paper. To access the data used for Table 1 please refer to the following reference:

Hoyt, D. F., Board, R. G., Rahn, H. and Paganelli, C. V., (1979). The eggs of the Anatidae: conductance, pore structure, and metabolism. *Physiological Zoology*. **52**, 438-450.

Dataset 1: The effect of debris on eggshell gas conductance and pore blockages.

ID	Clean gas conductance	Dirty gas conductance	Difference in conductance	Relative difference in conductance (%)	Pore number	Blocked pores	Blocked pores (%)	Average true shell thickness (µm)	Average pore length (µm)	Average thickness of debris (µm)	Average thickness of debris covering pores (µm)
G107	10.31098	10.55226	0.24128	2.34	13	3	23.08	445.249	389.342	299.312	315.299
G114	4.196583	4.768366	0.571783	13.62	11	2	18.18	413.796	351.176	218.746	155.243
G129	8.694998	7.435982	-1.259016	-14.48	12	4	33.33	384.065	324.896	179.077	155.838
G16	12.90546	9.1036	-3.80186	-29.46	32	23	71.88	425.195	376.768	473.303	470.233
G20	14.37053	10.52241	-3.84812	-26.78	40	28	70	400.731	351.007	263.407	261.079
G105	14.74378	14.22333	-0.52045	-3.53	24	13	54.17	386.198	330.678	249.206	224.340
G106	11.6527	10.32138	-1.33132	-11.42	37	14	37.84	347.584	302.236	633.628	695.597
G116	21.72172	20.22435	-1.49737	-6.89	52	26	50	408.248	361.531	198.325	207.693
G123	8.405391	6.660318	-1.745073	-20.76	39	23	58.97	440.979	357.482	221.920	264.848
G126	13.44856	7.803131	-5.645429	-41.98	35	22	62.86	360.403	326.294	301.522	268.721

N.B. Average true shell thickness measures are not the same as average pore length values.

Dataset 2: The effect of shell accessory material removal with bleach on the percentage of pores blocked by debris in an eggshell fragment.

ID	Treatment	Blocked pores	Proportion of pores blocked	Blocked pores (%)
G107	Control	0	0	0
G107	SAM removal (Bleach)	6	0.40	40
G114	Control	2	0.133	13.3
G114	SAM removal (Bleach)	7	0.467	46.7
G129	Control	3	0.2	20
G129	SAM removal (Bleach)	7	0.467	46.7
GE2	Control	1	0.067	6.7
GE2	SAM removal (Bleach)	3	0.2	20
GE6	Control	3	0.2	20
GE6	SAM removal (Bleach)	5	0.333	33.3

Appendix A6:

Supplementary materials for Chapter 5

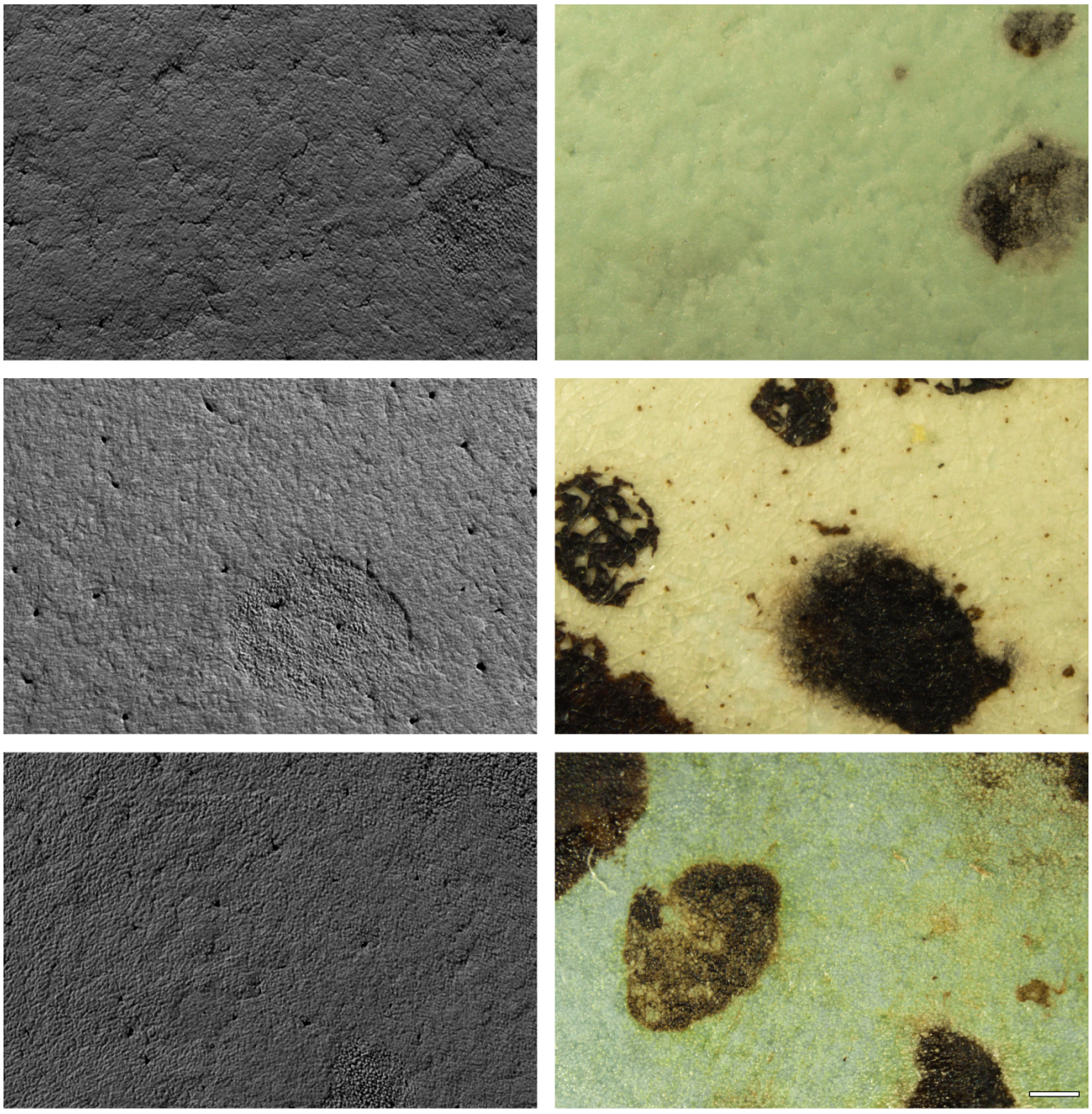

Figure S1. Volumetric reconstructions and optical images showing variation in roughness within an eggshell fragment. Note that not all surface patterning relates to patches of additional surface roughness. This is likely because many patches of pigments are found within or on top of the shell accessory material layer and not incorporated into the surface layers of the crystalline shell. Volumetric reconstructions (left) are approximately to the same scale as the optical images (right), scale bar = 500μm.

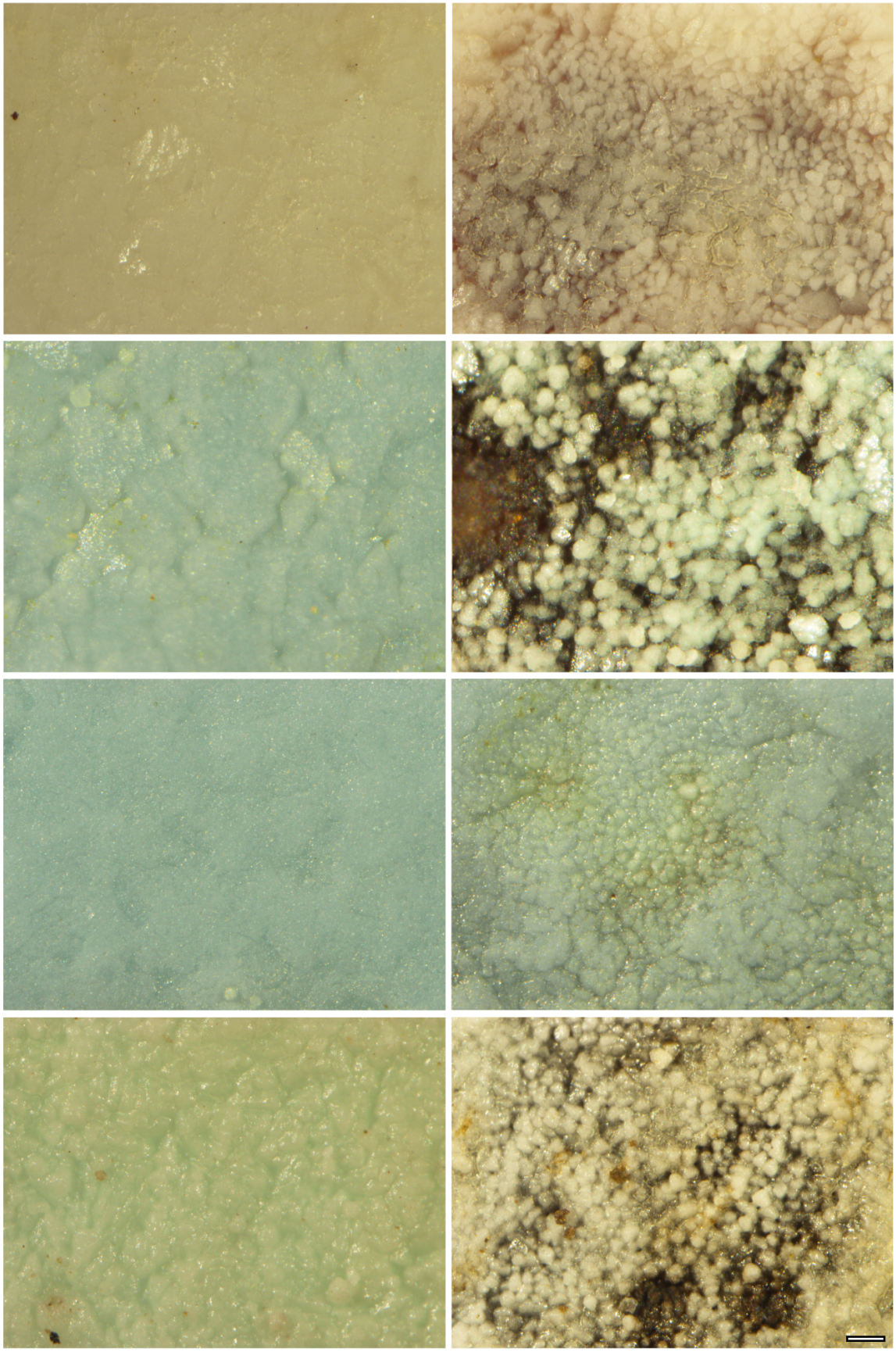

Figure S2. Variation in surface structure relating to pigment. Paired fragments from four eggs showing the influence dark pigment within the eggshell surface layers can have on the surface structure morphology and the resulting roughness. Scale bar = 100μm.

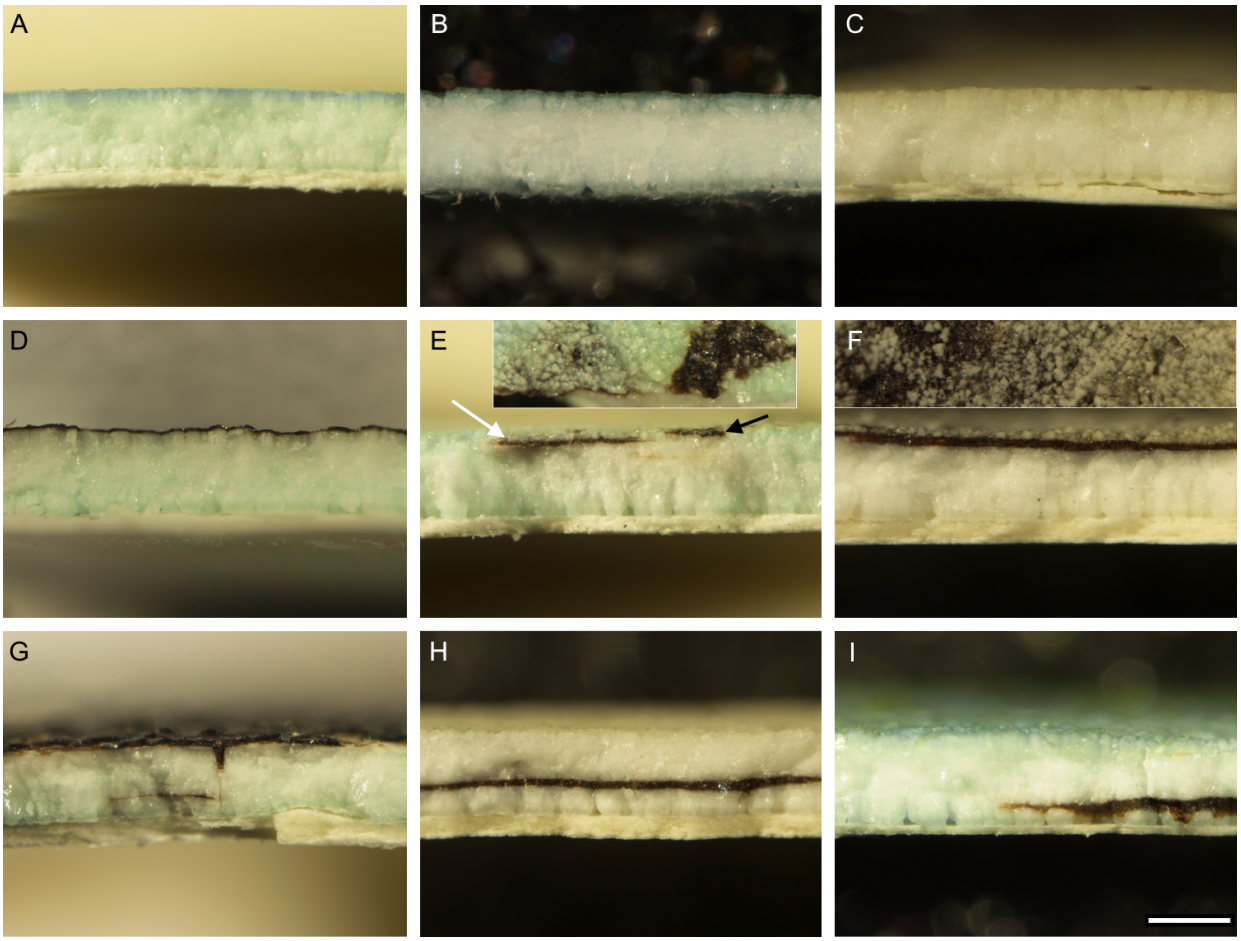

Figure S3. Cross sections of common guillemot eggshell illustrating variation in colour, patterning and therefore pigment within the shell. Blue pigment can be seen in the outer surface layers (top) of the shell (A, B, D, E, I) as well as it being incorporated into the inner mammillary surface layer (e.g. B, D, E, G, I). On top of the outer surface is shell accessory material – often a thin translucent layer (B). Pale eggs may or may not contain pigment in the outer and inner surface (C). Dark black-brown pigment patterning may rest on the surface of the shell (D) or be incorporated into the rest of the shell accessory material (G). Pigment patches associated with shell patterning may also reside in the surface of the shell or just below (E, F) and when pigment occurs here, it appears to be associated with changes in surface structure, especially localised roughness (E, F – see surface images above cross-sections). In (E), a dark pigment patch resides within the shell surface (white arrow) and an adjacent pigment patch rests on the surface of the shell and is incorporated into the shell accessory material layer (black arrow). Dark black-brown pigment may also penetrate gas exchange pores and penetrate the thickness of the shell (G) or be incorporated in the thickness of the shell anywhere from the outer to the inner surface (E – I). All edges imaged were from snapped eggshells. Scale bar = 500µm.

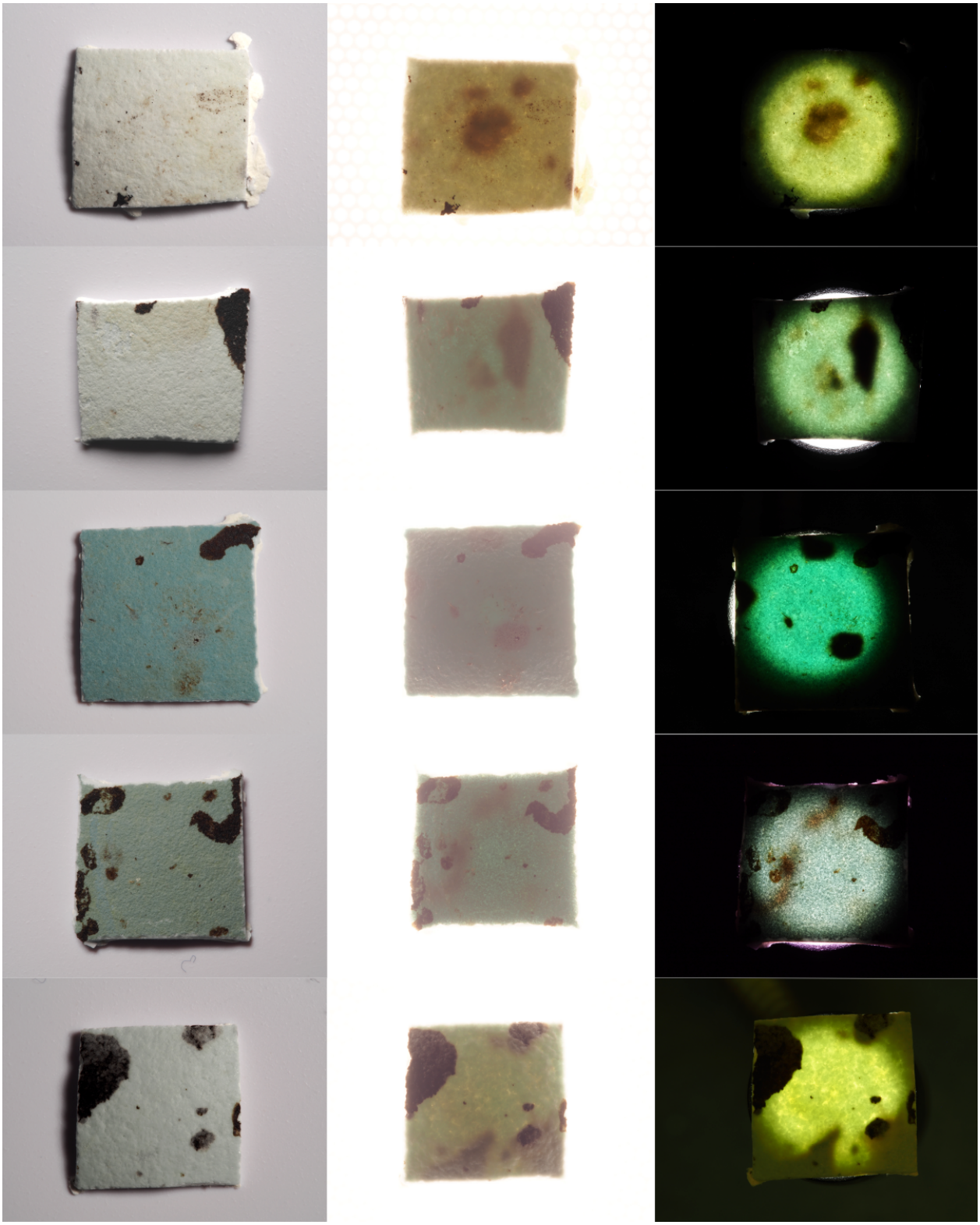

Figure S4. Examples of different types of lighting to allow visualisation of the surface colour and pattern (left), the surface and pigment in the shell (middle) or primarily the pigment patches in the shell (right). Images are not to scale.

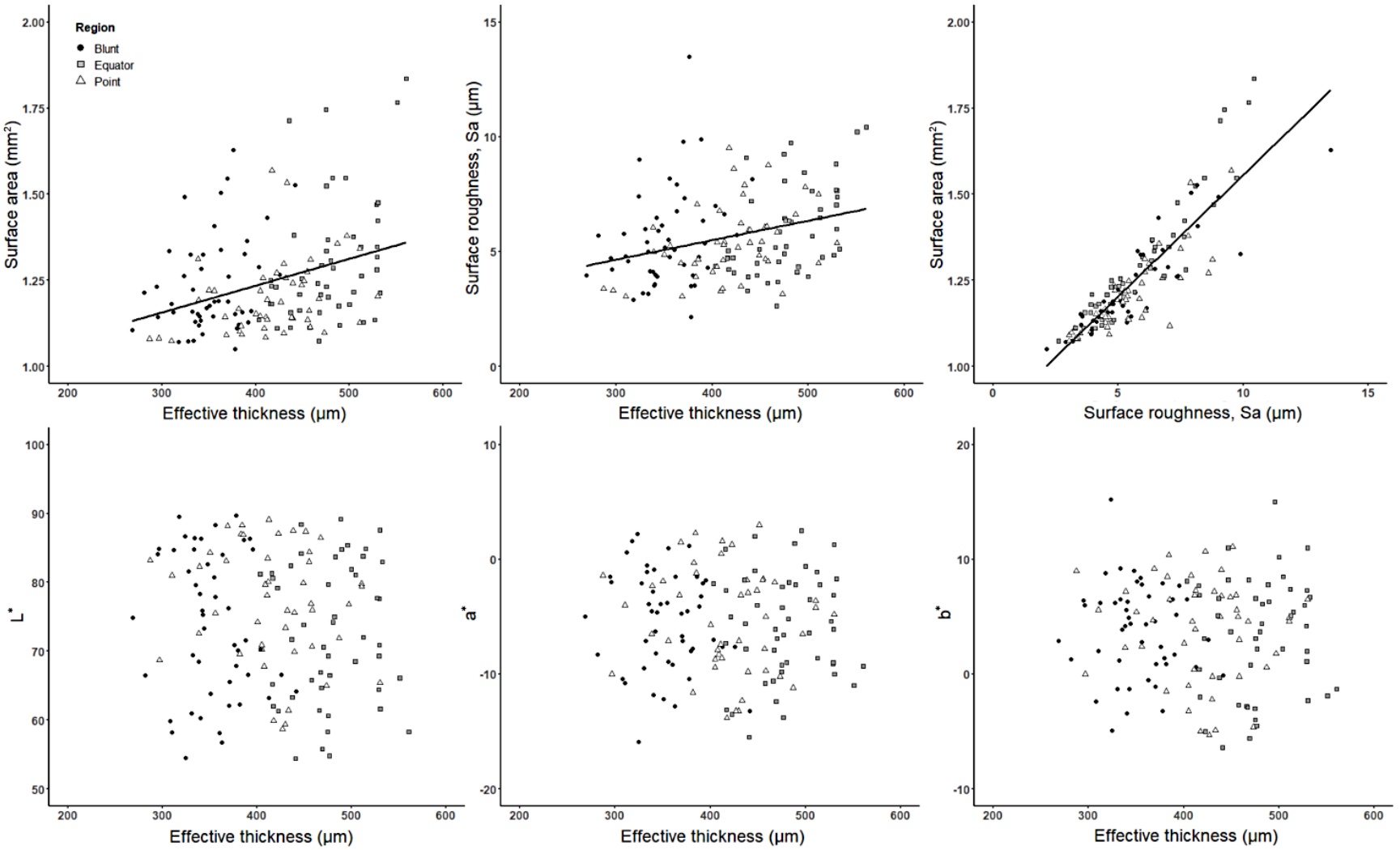

Figure S5. Effective eggshell thickness relationships with surface area (top left) and surface roughness (top middle). Surface roughness vs surface area (top right). There is no significant relationship between colour (bottom row) and effective thickness of common guillemot eggshell. Black lines are lines of best fit for significant correlations across all fragments. See Table 2 in Chapter 5 for correlations across all fragments.

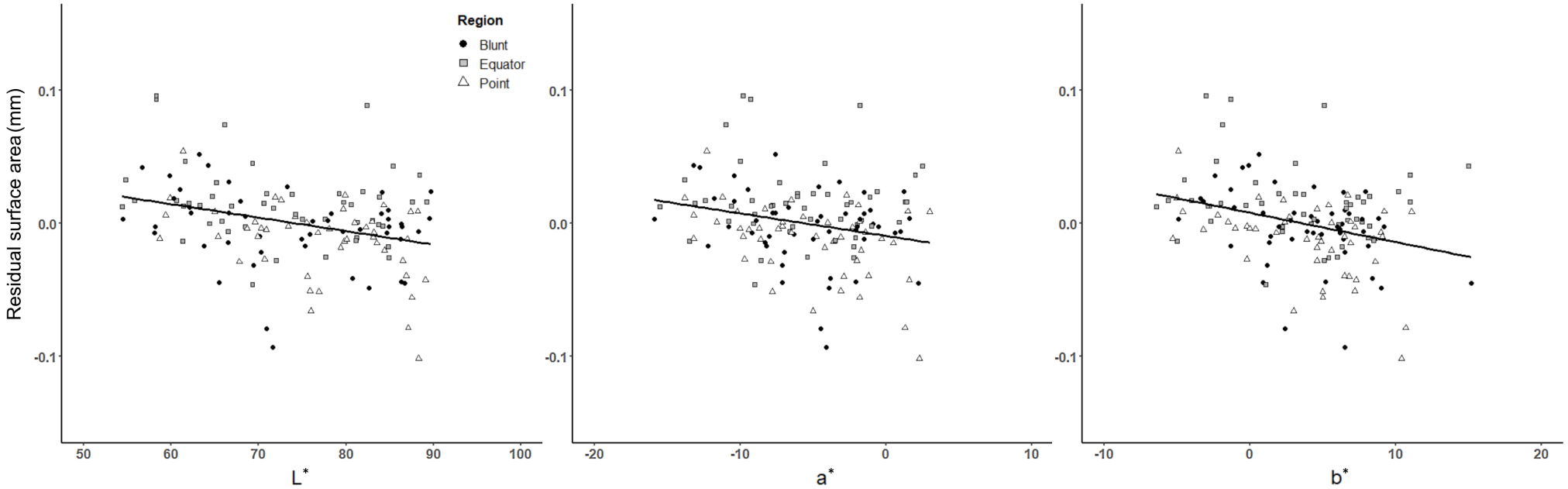

Figure S6. Relationship between colour (L*, a* and b*) and residual surface area. Black lines are the lines of best fit for all fragments. See Table 2 in Chapter 5 for correlations across all fragments.

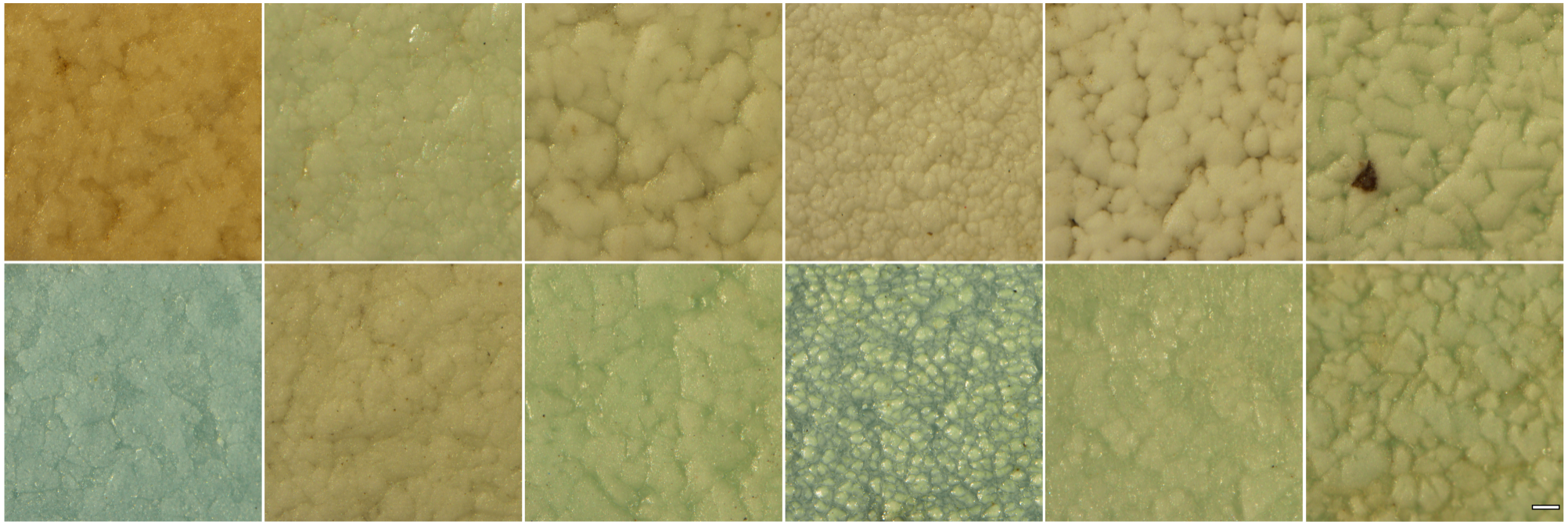

Figure S7. Preliminary comparison of variation in Alcid eggshell surfaces to variation exhibited within common guillemots. Top, auk eggshell surfaces (left to right; ancient murrelet, little auk, black guillemot, rhinoceros auklet, Atlantic puffin and razorbill), bottom; common guillemot shell surfaces. Scale bar = 100μm.

Table S1. Relationships between egg colour and effective shell thickness (μm) after controlling for egg volume, elongation and region using a generalized linear mixed model (glmer – gaussian family with log link) with egg identity as a random factor.

Colour	Value			Standard error	t	p	$F_{(d.f.)}$	$\chi^2_{(d.f.)}$	p
L*		Blunt	5.99	0.196	30.5	< 0.001			
	Region	Equator	0.308	0.021	15.0	< 0.001	$113_{(2)}$	$227_{(2)}$	< 0.001
		Point	0.170	0.022	7.74	< 0.001			
	Volume		0.00450	0.00060	7.57	< 0.001	$13.7_{(1)}$	$57.2_{(1)}$	< 0.001
	Elongation		-0.365	0.114	-3.20	0.001	$10.0_{(1)}$	$10.2_{(1)}$	0.001
	L*		0.000493	0.000689	0.72	0.474	$0.3_{(1)}$	$0.5_{(1)}$	0.474
a*		Blunt	6.06	0.198	30.6	< 0.001			
	Region	Equator	0.308	0.021	15.0	< 0.001	$113_{(2)}$	$229_{(2)}$	< 0.001
		Point	0.171	0.022	7.86	< 0.001			
	Volume		0.00464	0.00059	7.81	< 0.001	$13.9_{(1)}$	$60.9_{(1)}$	< 0.001
	Elongation		-0.387	0.117	-3.33	< 0.001	$10.0_{(1)}$	$11.1_{(1)}$	< 0.001
	a*		0.00201	0.00186	1.08	0.279	$1.1_{(1)}$	$1.2_{(1)}$	0.279
b*		Blunt	6.04	0.194	31.2	< 0.001			
	Region	Equator	0.309	0.021	15.1	< 0.001	$114_{(2)}$	$230_{(2)}$	< 0.001
		Point	0.172	0.022	7.89	< 0.001			
	Volume		0.00458	0.00059	7.76	< 0.001	$13.9_{(1)}$	$60.2_{(1)}$	< 0.001
	Elongation		-0.385	0.116	-3.33	< 0.001	$10.1_{(1)}$	$11.1_{(1)}$	< 0.001
	b*		0.00217	0.00178	1.22	0.223	$1.4_{(1)}$	$1.5_{(1)}$	0.223

Performed on subset (n = 142 fragments) excluding dirty fragments.

Table S2. Spearman's rank correlations between external eggshell colour and mammillary layer thickness (μm).

Variable	Mammillary layer thickness (all regions)[1]	Mammillary layer thickness at the blunt end[2]	Mammillary layer thickness at the equator[2]	Mammillary layer thickness at the pointed end[2]
L*	*0.021*	*-0.136*	*0.078*	*0.125*
a*	*0.031*	*-0.064*	*0.012*	*0.124*
b*	*0.026*	*-0.059*	*0.177*	*0.171*

n.s. p > 0.05, p < 0.05, p < 0.01, **p < 0.001**.
[1]Performed on subset (n = 142 fragments) excluding dirty fragments.
[2]Performed on subset (n = 42 eggs, 3 fragments per egg) excluding dirty eggs.

Table S3. Relationships between egg colour and mammillary layer thickness (μm) after controlling for egg volume, elongation and region using a generalized linear mixed model (glmer – gaussian family with log link) with egg identity as a random factor.

Colour		Value		Standard error	t	p	$F_{(d.f.)}$	$\chi^2_{(d.f.)}$	p
L*	Region	Blunt	4.42	0.255	17.3	< 0.0001	$6.91_{(2)}$	$13.7_{(2)}$	0.001
		Equator	0.0845	0.0259	3.26	0.001			
		Point	0.0839	0.0262	3.96	0.001			
	Volume		0.00364	0.00092	3.96	< 0.0001	$4.13_{(1)}$	$15.7_{(1)}$	< 0.0001
	Elongation		-0.390	0.146	-2.67	0.008	$6.33_{(1)}$	$7.12_{(1)}$	0.008
	L*		0.00137	0.00097	1.42	0.157	$1.44_{(1)}$	$2.00_{(1)}$	0.157
a*	Region	Blunt	4.60	0.257	17.9	< 0.0001	$7.01_{(2)}$	$14.5_{(2)}$	0.0007
		Equator	0.0844	0.0258	3.28	0.0001			
		Point	0.0879	0.0258	3.39	0.0007			
	Volume		0.00374	0.00091	4.10	< 0.0001	$4.15_{(1)}$	$16.8_{(1)}$	< 0.0001
	Elongation		-0.434	0.150	-2.89	0.004	$6.56_{(1)}$	$8.35_{(1)}$	0.004
	a*		0.00411	0.00247	1.67	0.096	$2.73_{(1)}$	$2.77_{(1)}$	0.096
b*	Region	Blunt	4.54	0.252	18.0	< 0.0001	$6.89_{(2)}$	$14.4_{(2)}$	0.0007
		Equator	0.0848	0.0259	3.27	0.001			
		Point	0.0881	0.0260	3.38	0.0007			
	Volume		0.00344	0.00091	3.77	0.0002	$4.13_{(1)}$	$14.2_{(1)}$	0.0002
	Elongation		-0.401	0.149	-2.70	0.007	$6.33_{(1)}$	$7.26_{(1)}$	0.007
	b*		0.00288	0.00237	1.21	0.225	$1.45_{(1)}$	$1.47_{(1)}$	0.225

Performed on subset (n = 142 fragments) excluding dirty fragments.

Table S4. Spearman's rank correlations at the blunt end of common guillemot eggs.

Variable	Effective thickness (µm)	L*	a*	b*	Surface area (mm^2)
L*	*-0.104*	-			
a*	*-0.115*	**0.904**	-		
b*	*-0.045*	**0.783**	**0.775**	-	
Surface area (mm^2)	*0.250[1], 0.086*	-0.355	*-0.241[1], 0.098*	*-0.168*	-
Mean roughness, Sa (µm)	*0.261[1], 0.073*	*-0.257[1], 0.078*	*-0.193*	*-0.054*	**0.910**
Residual surface area (mm)	*0.069*	*-0.271[1], 0.062*	*-0.182*	-0.373	*0.200*

Performed on subset (n = 48 fragments) excluding dirty fragments. *n.s. p > 0.05*, p < 0.05, p < 0.01, **p < 0.001**.
[1] 0.1 > p > 0.05 r_s and p-value reported.

Table S5. Spearman's rank correlations at the equator of common guillemot eggs.

Variable	Effective thickness (µm)	L*	a*	b*	Surface area (mm^2)
L*	*0.121*	-			
a*	*0.045*	**0.934**	-		
b*	*0.120*	**0.863**	**0.898**	-	
Surface area (mm^2)	**0.413**	*-0.152*	*-0.106*	*-0.125*	-
Mean roughness, Sa (µm)	**0.537**	*-0.104*	*-0.109*	*-0.107*	**0.937**
Residual surface area (mm)	*-0.035*	*-0.188*	*-0.037*	*-0.141*	**0.511**

Performed on subset (n = 48 fragments) excluding dirty fragments. *n.s. p > 0.05*, p < 0.05, p < 0.01, **p < 0.001**.

Table S6. Spearman's rank correlations at the pointed end of common guillemot eggs.

Variable	Effective thickness (µm)	L*	a*	b*	Surface area (mm^2)
L*	*-0.158*	-			
a*	*-0.117*	**0.910**	-		
b*	*-0.108*	**0.702**	**0.815**	-	
Surface area (mm^2)	0.367	-0.309	*-0.248[1], 0.097*	*-0.128*	-
Mean roughness, Sa (µm)	**0.423**	*-0.100*	*-0.044*	*0.068*	**0.835**
Residual surface area (mm)	*-0.204*	-0.340	-0.369	-0.368	*0.191*

Performed on subset (n = 46 fragments) excluding dirty fragments. *n.s. p > 0.05*, p < 0.05, p < 0.01, **p < 0.001**.
[1] 0.1 > p > 0.05 r_s and p-value reported.

Table S7. Linear mixed models (lmer with REML) controlling for region and egg identity between egg colour, thickness (µm) and surface structure (Box-Cox transformed surface area, mm^2).

	Estimate		Standard error	t	$F_{(d.f.)}$	$x^2_{(d.f.)}$	p
	Blunt	0.216	0.062	3.47			
Region	Equator	-0.00910	0.00874	-1.04	20.9 (2)	9.57 (2)	0.008
	Point	-0.0168	0.0063	-2.67			
Effective thickness		0.000195	0.000062	3.17	14.0 (1)	10.0 (1)	0.002
L*		-0.00194	0.00065	-2.97	5.16 (1)	8.80 (1)	0.003
a*		0.00271	0.00168	1.61	3.98 (1)	2.59 (1)	0.107
b*		0.000302	0.001218	0.25	0.06 (1)	0.06 (1)	0.804

Performed on subset (n = 142 fragments) excluding dirty fragments.

Table S8. Generalized linear model (GLM with Gamma family and identity link) between egg colour, thickness (μm) and residual surface area after accounting for variation in the height roughness profile (Sa).

	Estimate		Standard error	t	p	χ^2 (d.f.)	p
	Blunt	1.080	0.052	20.8	<0.001		
Region	Equator	0.0204	0.00876	2.32	0.022	14.6 (2)	0.0007
	Point	-0.00552	0.00685	-0.81	0.422		
Effective thickness		-0.0000249	0.0000530	-0.47	0.640	0.223 (1)	0.637
L*		-0.000754	0.000568	-1.33	0.186	1.77 (1)	0.183
a*		0.00188	0.00137	1.38	0.172	1.90 (1)	0.168
b*		-0.00236	0.00098	-2.40	0.018	5.70 (1)	0.017

Performed on subset (n = 142) excluding dirty fragments.

N.B. A generalized linear model was used here because the generalized mixed effects model would not converge when egg identity was included as a random factor. This is possibly because egg identity explains a small amount of variance (in the model presented in Table S7 variance explained by egg ID was 0.0008573) when region is also included in the model and causes singular fits in other models (e.g. the model presented in Table S7).

Table S9. Egg shape and size correlations (Spearman's rank, n = 55 eggs) with surface area, mm^2.

Parameter	Surface area (mm^2) at the		
	Blunt end	**Equator**	**Pointed end**
Volume	*0.251[1], 0.065*	*0.187*	*0.257[1], 0.058*
Elongation	*-0.196*	*-0.137*	*-0.243[1], 0.074*
Asymmetry	*-0.083*	*-0.140*	*-0.257[1], 0.058*
Taper	*0.081*	*0.104*	*0.134*

n.s. p > 0.05, p < 0.05, p < 0.01, **p < 0.001**.
[1] 0.1 > p > 0.05 r_s and p-value reported.

Table S10. Egg shape and size correlations (Spearman's rank, n = 42 eggs) with L*.

Parameter	L* at the		
	Blunt end	**Equator**	**Pointed end**
Volume	-0.352	*-0.247*	*-0.217*
Elongation	*0.117*	*0.102*	*0.099*
Asymmetry	*0.012*	*-0.043*	*0.069*
Taper	*-0.073*	*-0.088*	*-0.206*

n.s. p > 0.05, p < 0.05, p < 0.01, **p < 0.001**.

Table S11. Egg shape and size correlations (Pearson's product moment, n = 42 eggs) with a*.

Parameter	a* at the		
	Blunt end	**Equator**	**Pointed end**
Volume	*-0.263, 0.092*	*-0.245*	*-0.213*
Elongation	*0.289, 0.063*	*0.269, 0.085*	*0.262, 0.094*
Asymmetry	*0.046*	*-0.002*	*0.033*
Taper	*-0.079*	*-0.008*	*-0.125*

n.s. p > 0.05, p < 0.05, p < 0.01, **p < 0.001**.
[1] 0.1 > p > 0.05 r_s then p-value reported.

Table S12. Egg shape and size correlations (Pearson's product moment, n = 42 eggs) with b*.

Parameter	b* at the		
	Blunt end	**Equator**	**Pointed end**
Volume	*-0.121*	*-0.155*	*-0.204*
Elongation	*0.126*	*0.206*	*0.182*
Asymmetry	*-0.024*	*-0.010*	*0.113*
Taper	*0.044*	*-0.010*	*-0.155*

n.s. p > 0.05, p < 0.05, p < 0.01, **p < 0.001**.

Appendix A7:

Preliminary comparative analysis of eggshell surface structure across the auks

Preliminary comparative analysis of eggshell surface structure across the auks

In this appendix, I present preliminary comparisons of surface structure between members of the Alcidae. Alcids exhibit huge diversity in egg traits, including shape, size, colour and patterning (Gaston & Jones 1998), and incubate their egg(s) in a wide range of conditions, providing an opportunity to investigate whether the fine-scale eggshell surface structure depends on the environment in which eggs are incubated.

Materials and Methods

Eggs from 17 Alcid species, covering 9 of 10 extant Alcid genera and 5 out of the 6 tribes, were collected under licence from a range of field sites around the world between 2004 – 2018 (see Appendix A3). Eggs were emptied of their contents and rinsed with distilled water, air-dried and those collected outside the UK were heat treated at 56ºC to eliminate microbes (required for importation) before transportation to the UK. For most species (12/17), I then examined the surface structure of fragments (0.5 – 1cm^2) from the equatorial region of 5 different eggshells. In some species, fewer eggs were examined due to limited sample size (4 eggs n = 3, 3 eggs n = 1, 2 eggs n = 1; see Chapter 2). I also examined 5 eggshell fragments from the Kittlitz's murrelet, *Brachyramphus brevirostris*, a species from the single unrepresented tribe in our main dataset. These samples were provided by Robin Corcoran. However, since the region of the egg these five fragments were from was unknown, I only examined eggshell surface structure qualitatively for this species and did not include it in broader quantitative comparative analyses. See chapter 2 for details on X-ray micro-computed tomography scanning and chapter 5 for information on height map creation and optical imaging.

Statistical comparisons

Linear regressions were used to investigate the relationship between surface structure (surface area, surface roughness and maximum surface structure height) and effective eggshell thickness across the Alcidae. I controlled for phylogenetic relatedness using

Pagel's lambda model (Ho & Ane 2014). I used the extant Alcidae phylogenetic tree (Weir & Mursleen 2013), pruned to leave only the species represented in our dataset, and species mean values were used for each variable included in our analyses. R^2 values for full models, including any phylogenetic effects, and partial R^2 values associated with individual predictors were calculated using the "R2.lik" function in the R package 'rr2' (Ives 2019). I investigated differences between incubation substrate (usually, sometimes or rarely on rock – see Chapter 2) and tribes using a similar approach, adding the categorical variable (substrate or tribe) into the phylogenetically controlled linear models with surface area. I present models that include effective thickness as well as those that do not. Absolute surface area variation may determine eggshell surface properties therefore I was interested in whether this varied in relation to incubation substrate or between tribes, but I also performed the same comparisons after controlling for eggshell thickness in case variation in eggshell thickness was the underlying driver of any variation in surface roughness.

Results

Variation in eggshell surface structure within the Alcidae

All members of the Alcid family studied here typically possessed some degree of surface structure, but there was variation both within and between species (Fig. 1 – 8). The *Fraterculini* (puffins) tended to exhibit surfaces with pits rather than peaks, but this is not always the case, with certain members, e.g. the rhinoceros auklet, possessing variable surfaces typified by peaks rather than pits (Fig. 1 – 3). Likewise, although *Synthliboramphus* murrelets typically possess relatively smooth shell surfaces, I found examples of eggs with surface texture (Fig. 1, 2 & 4). The *Alcini* (little auk, razorbill and *Uria sp.* guillemots) typically possessed visually rough surfaces but varied in their surface morphology (Fig. 1, 2 & 5). While I found considerable variation in surface structure between the *Alcini* and the rest of the Alcidae, it is important to note that I found a similar amount of variation in surface structure between common guillemot eggs alone (see Chapter 5).

As in common guillemot eggs, I also found variation in roughness within small areas of shell for other species. Locally rough areas of shell surface appeared to be associated with surface level pigmentation in the black guillemot and razorbill (Fig. 8). The location of pigment within the shell varied in some species (Fig. 8 – 10), as it does within the common guillemot eggshell (see Chapter 5 and Appendix A6). Indeed, even the white or beige eggs laid by the *Fraterculini* can have dark pigment within their shell structure as previously noted by Harrison in 1966 (Fig. 10). Furthermore, observations show that white or beige common guillemot and razorbill eggs can have a blue inner surface, as can beige or brown ancient murrelet and Japanese murrelet eggs (Fig. 10; see Chapter 5 and A6).

Shell thickness, incubation substrate and surface roughness

Across species, the shell surface area related strongly to effective shell thickness (Fig. 11). This may be because the surface of the shell constitutes 6 – 28% of its effective thickness (13µm – 92µm in height; mean of species' means 14.4%, 32.9µm), so eggs with thicker shells can have a greater surface area primarily due to an increase in the height of surface features (pits or peaks) rather than any differences in their number, width, or shape. Indeed, effective shell thickness is strongly correlated with maximum surface height ($R^2 = 0.711$, $F = 40.4$, d.f. = 1,15, $p < 0.0001$) and height based surface roughness, Sa ($R^2 = 0.807$, $F = 67.8$, d.f. = 1,15, $p < 0.0001$). Sa and the maximum surface height are also related to the shell surface area (height: $R^2 = 0.698$, $F = 37.9$, d.f. = 1,15, $p < 0.0001$; Sa: $R^2 = 0.872$, $F = 110$, d.f. = 1,15, $p < 0.0001$).

Effective thickness and phylogeny explained 91% of the variation in surface area across species (Surface area = 0.000645*effective thickness + 0.938; $t_{intercept} = 57.2$, $t_{slope} = 10.6$, $p_{intercept \& slope} < 0.0001$; $R^2 = 0.911$; lambda = 0.458). Partial R^2 values (thickness $R^2 = 0.883$, phylogeny $R^2 = 0.108$) indicate that the scaling relationship between effective thickness and surface area is largely independent of phylogeny. Although including incubation substrate in the phylogenetic linear model between effective shell thickness and surface area reduced the AIC value from -76.8 to -79.2 and increased the R^2 value to 0.939, there were no significant differences between substrate categories (lambda = 0.508; rarely on rock compared to usually; estimate = -0.0200, t = -1.03, p = 0.322, rarely

compared to sometimes; estimate = -0.0148, t = 1.47, p = 0.165). However, species that usually incubate their egg on rock tended to be rougher than those that sometimes incubate on rock, but this difference only approached significance (estimate = 0.0349, t = 2.03, p = 0.063). Partial R^2 values indicate that the effect of phylogeny (R^2 = 0.162) and incubation substrate (R^2 = 0.317) is relatively small compared to the effect of effective shell thickness (R^2 = 0.865) on surface area. I found similar non-significant patterns when I did not control for variation in effective thickness across species (lambda = 1; rarely on rock compared to usually; estimate = -0.087, t = -1.73, p = 0.106, rarely compared to sometimes; estimate = 0.004, t = 0.213, p = 0.835; sometimes compared to usually; estimate = -0.091, t = -1.91, p = 0.077; full model R^2 = 0.582; incubation substrate partial R^2 = 0.207).

Differences in surface roughness between tribes

After controlling for the relationship between surface area and effective eggshell thickness, eggs laid by the *Fraterculini* and *Synthliboramphini* were significantly smoother than *Aethini* eggs (*Aethini* as reference; *Fraterculini* estimate = -0.0330, t = -2.48, p = 0.031; *Synthliboramphini* estimate = -0.0309, t = -2.34, p = 0.039; AIC = 79.7, lambda < 0.0001; R^2 = 0.953). Eggs laid by the *Fraterculini* tended to be smoother than those laid by the *Alcini*, but this difference only approached significance (*Alcini* as reference; *Fraterculini* estimate = -0.0319, t = -2.01, p = 0.069). When differences between tribes were assessed without controlling for effective shell thickness, the surface of eggs laid by the *Alcini* were significantly rougher than all other tribes (lambda < 0.001; R^2 = 0.655; *Aethiini* as reference; estimate = -0.124, t = -3.95, p = 0.002; *Cepphini* as reference; estimate = -0.114, t = -2.18, p = 0.05; *Fraterculini* as reference; estimate = -0.111, t = -3.33, p = 0.006; *Synthliboramphini* as reference; estimate = -0.148, t = -4.13, p = 0.001).

Discussion

Here, I show that there is large variation in eggshell surface structure across the Alcidae. Eggshell thickness and phylogeny accounted for 91% of the variation in eggshell surface area across the Alcids, showing the importance of accounting for eggshell thickness and phylogeny in future comparative studies of eggshell surface microstructure. It remains

unclear why there is morphological variation in eggshell surface structure within and between species but some suggestions are made below.

Ecological benefits

As suggested in chapter 5, a rough shell surface may be beneficial in helping shell accessory materials adhere to the eggshell and also in minimising wear and abrasion during incubation. Possessing a rough eggshell surface could thus be especially important in the guillemots (*Uria sp.*) that incubate their egg on dirty, bare rock cliff ledges without a nest but less important for species that breed in dirt burrows where the substrate is less abrasive. This may explain differences between tribes found here. For example, *Alcini* (*Uria sp.* guillemots, razorbill and little auk) eggs had rougher surfaces than all other tribes and typically incubate their eggs on rocky substrates, but this may also relate to *Alcini* laying eggs with relatively thick shells, especially at the equator (Chapter 2). *Aethiini* auklets tend to incubate in crevices potentially on rock, whereas members of the *Fraterculini* and *Synthliboramphini* tend to incubate in burrows on softer substrates and have smoother shells than the Aethiini after controlling for eggshell thickness. Additionally, Kittlitz's murrelet, *Brachyramphus brevirostris*, incubates its egg in a pebble nest and the surface of its eggshell appears rougher than other murrelet shells, although this may be due to phylogenetic differences (*Brachyramphini* vs *Synthliboramphini* murrelets). However, I did not find any significant differences between species that usually, sometimes or rarely incubate on rock, so it remains unclear if variation in surface morphology and roughness across bird eggs is adaptive in any specific environments.

Egg colour

Although I did not analyse egg colour in relation to eggshell structure across the Alcids due to limited sample size (n < 5 eggs per species), the variation I observed across Alcids was somewhat consistent with the idea that egg colouration relates to surface structure. Alcids that lay blue-green eggs (*Uria sp.* guillemots, black guillemots, and little auks), have eggshells that often appear visually rougher than those of species that lay browner eggs (e.g. *Synthliboramphus* murrelets, which have previously been noted to have a

smooth surface layer of pigment; Harrison 1966). However, those species with white eggs had variable surface textures and I found too much variation both within and between species to draw any valid comparative conclusions across the Alcids. As is the case in the common guillemot, I found evidence that patches of pigment pattern within the surface of some species shells – the razorbill and black guillemot – are associated with localised areas of surface texture that differ from the rest of the shell (Fig. 8). This suggests pigments may disrupt calcium crystal formation across multiple species in the Alcidae and not solely in the common guillemot. Rigorous tests of the relationships between eggshell surface structure, pigment content, and egg colouration, both within and between species, will be an important future step. The role of shell accessory material in both colour and eggshell roughness should also be carefully considered in such studies.

Further study

Our preliminary study highlights the need for wider taxonomic study of eggshell surface structure to avoid erroneous claims of unique species-specific surface structures. For example, the presence of “nodes” or peaks in the Australian brush turkey (Grellet-Tinner *et al.* 2017) were said to be unique but here, I show other species’ eggshells possess peaks of variable sizes on their surface too. Furthermore, given the large intraspecific variation in eggshell surface structure I have observed, large samples sizes are likely required to capture this variation and better understand its significance. As surface structure is putatively related to egg colouration (Chapter 5), gloss (Igic *et al.* 2015) and UV reflectance (Fecheyr-Lippens *et al.* 2015), techniques involving optical methods (e.g. extended depth of field microscopy and light interferometry) should be used with caution, since variation in colour or gloss could impact roughness measures. The use of microCT is ideal for studying the surface structure of the calcium carbonate shell, with, where possible, a small imaging pixel resolution. I found 4μm pixel size is suitable for capturing large scale variation in microstructure, but it may not detect smaller-scale variation in microstructures with low Z-heights, so I recommend using smaller pixel sizes where possible.

References

Fecheyr-Lippens, D. C., Igic, B., D'Alba, L., Hanley, D., Verdes, A., Holford, M., Waterhouse, G. I. N., Grim, T., Hauber, M. E. and Shawkey, M. D., (2015). The cuticle modulates ultraviolet reflectance of avian eggshells. *Biology Open.* **4**(7), 753-759.

Gaston, A. J. and Jones, I. L., (1998). *Bird Families of the World series: The Auks.* Oxford, UK: Oxford University Press.

Grellet-Tinner, G., Lindsay, S. and Thompson, M. B., (2017). The biomechanical, chemical and physiological adaptations of the eggs of two Australian megapodes to their nesting strategies and their implications for extinct titanosaur dinosaurs. *Journal of Microscopy.* **267**(2), 237-249.

Harrison, C. J. O., (1966). Variation in the distribution of pigment within the shell structure of birds' eggs. *Journal of Zoology*. **148**(4), 526-539.

Ho, L. S. T. and Ané, C., (2014). A Linear-Time Algorithm for Gaussian and Non-Gaussian Trait Evolution Models. *Systematic Biology.* **63**(3), 397-408.

Igic, B., Fecheyr-Lippens, D., Xiao, M., Chan, A., Hanley, D., Brennan, P. R. L., Grim, T., Waterhouse, G. I. N., Hauber, M. E. and Shawkey, M. D., (2015). A nanostructural basis for gloss of avian eggshells. *Journal of The Royal Society Interface.* **12**(103), 20141210.

Ives, A. R., (2019). R^2s for correlated data: phylogenetic models, LMMs, and GLMMs. *Systematic Biology.* **68**(2), 234-251.

Weir, J. T. and Mursleen, S., (2013). Diversity-dependent cladogenesis and trait evolution in the adaptive radiation of the auks (Aves: Alcidae). *Evolution*. **67**(2), 403-416.

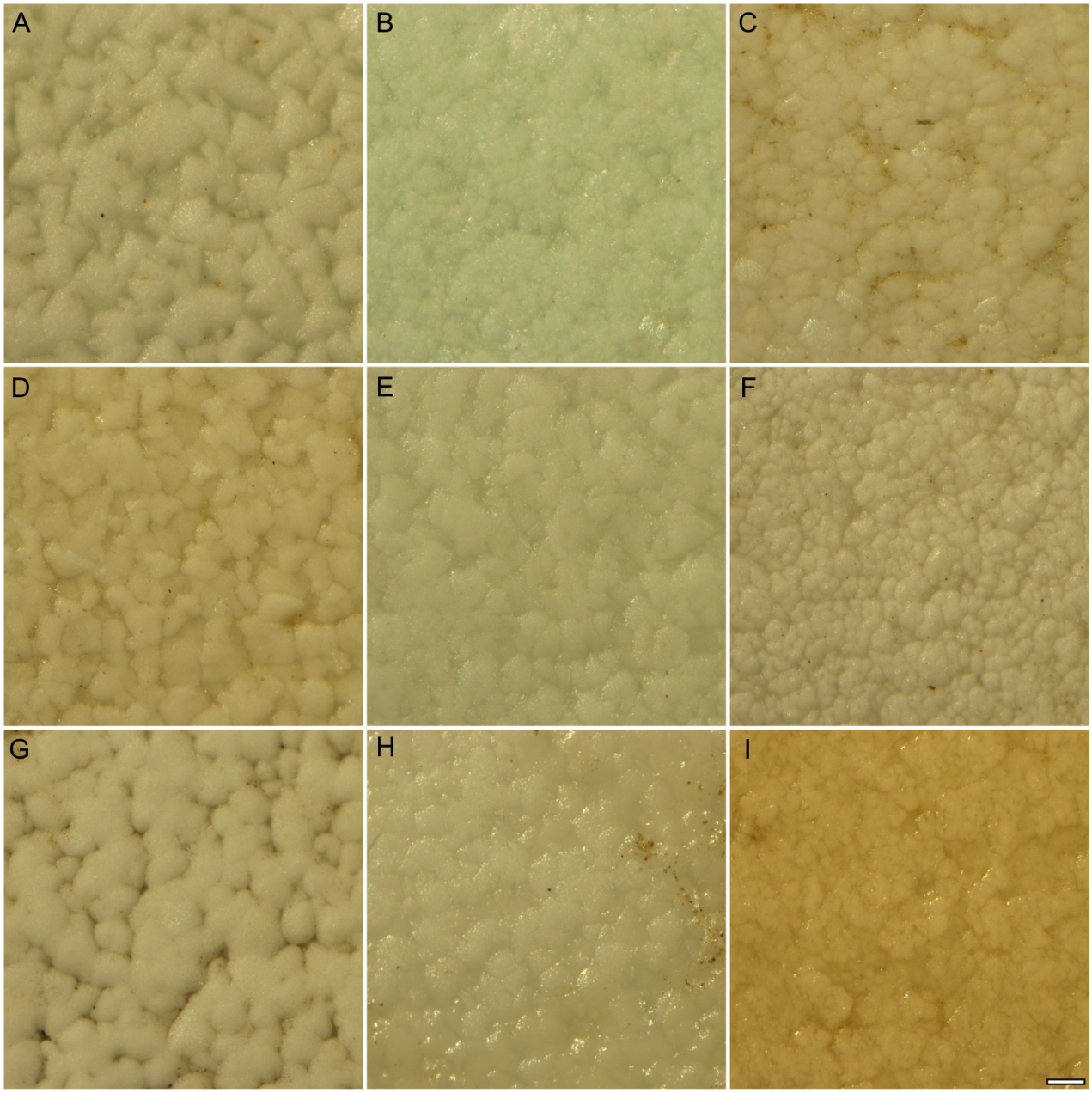

Figure 1. Optical microscope images showing variation in surface structure across the Alcidae. (A) Razorbill (*Alca torda)*, (B) little auk (*Alle alle),* (C) whiskered auklet (*Aethia pygmaea)*, (D) Kittlitz's murrelet (*Brachyramphus brevirostris),* (E) black guillemot (*Cepphus grylle),* (F) rhinoceros auklet (*Cerorhinca monocerata),* (G) Atlantic puffin (*Fratercula arctica),* (H) Cassin's auklet *(Ptychoramphus aleuticus)* and (I) ancient murrelet (*Synthliboramphus antiquus)*. All images are 1mm^2 and scale bar = 100µm. See Fig. 2 for corresponding microCT height maps.

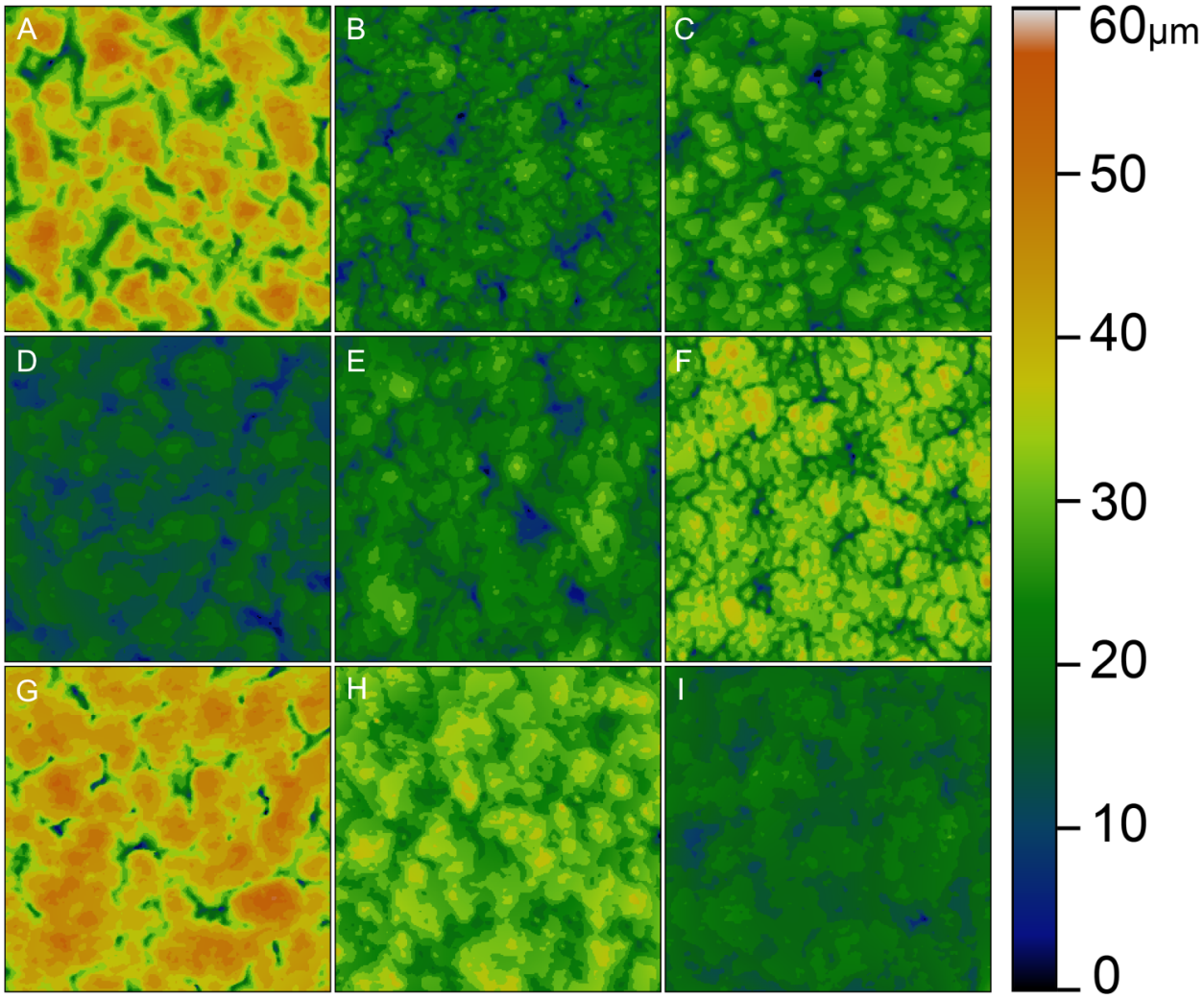

Figure 2. Height maps created from microCT data showing variation in surface structure across the Alcidae corresponding to optical images in Fig. 1. (A) Razorbill (*Alca torda*), (B) little auk (*Alle alle*), (C) whiskered auklet (*Aethia pygmaea*), (D) Kittlitz's murrelet (*Brachyramphus brevirostris*), (E) black guillemot (*Cepphus grylle*), (F) rhinoceros auklet (*Cerorhinca monocerata*), (G) Atlantic puffin (*Fratercula arctica*), (H) Cassin's auklet (*Ptychoramphus aleuticus*) and (I) ancient murrelet (*Synthliboramphus antiquus*). All images are 1mm^2.

Figure 3. Examples of variation in eggshell surface structure in the *Fraterculini*. Atlantic puffin (top), tufted puffin (middle) and rhinoceros auklet (bottom). *N.B*. horned puffin eggshells have surface structure similar to tufted puffin eggshell. Scale bar = 100µm

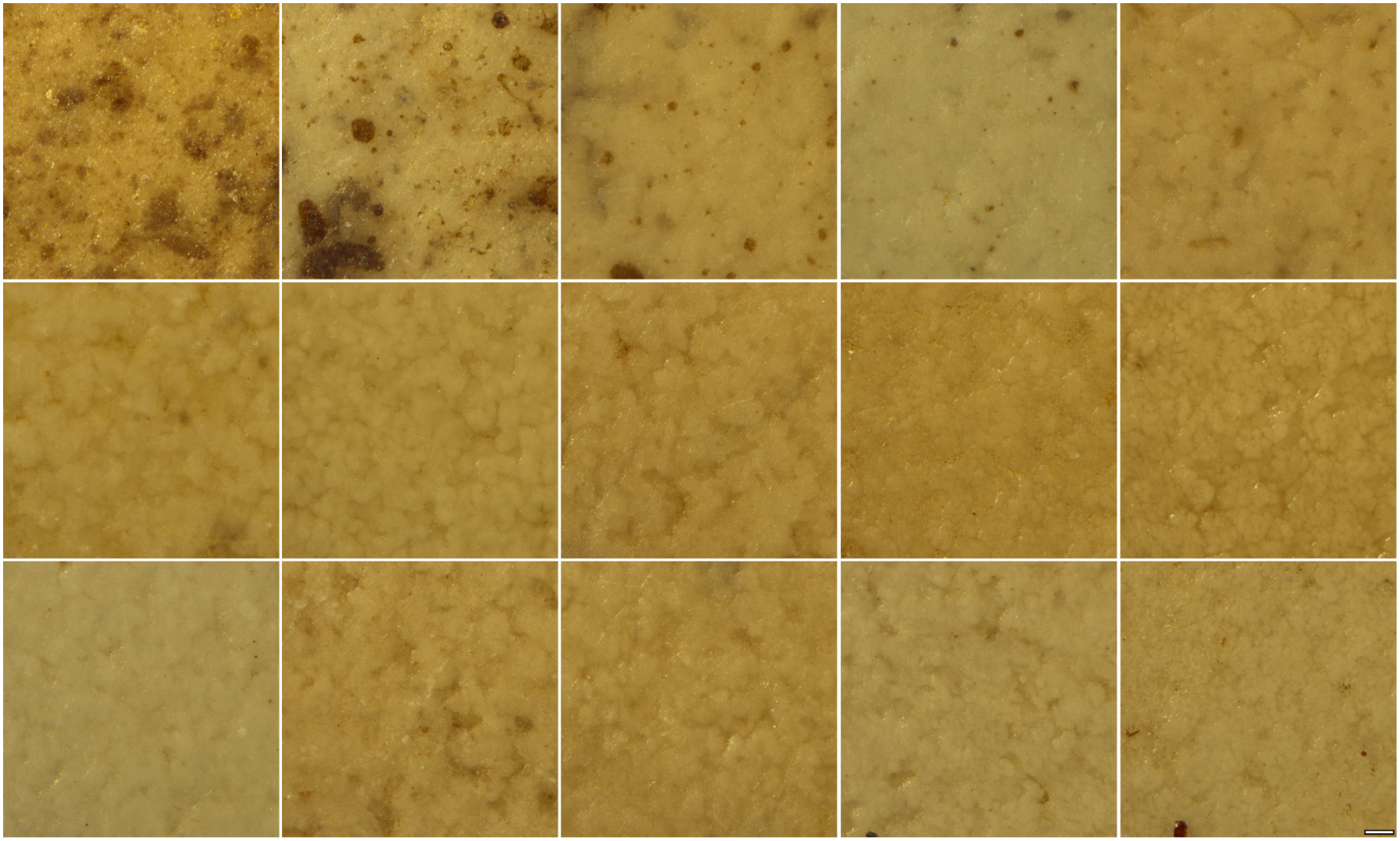

Figure 4. Examples of variation in eggshell surface structure in the *Synthliboramphini.* Scripps's murrelet (top), ancient murrelet (middle), Japanese murrelet (bottom). Scale bar = 100µm.

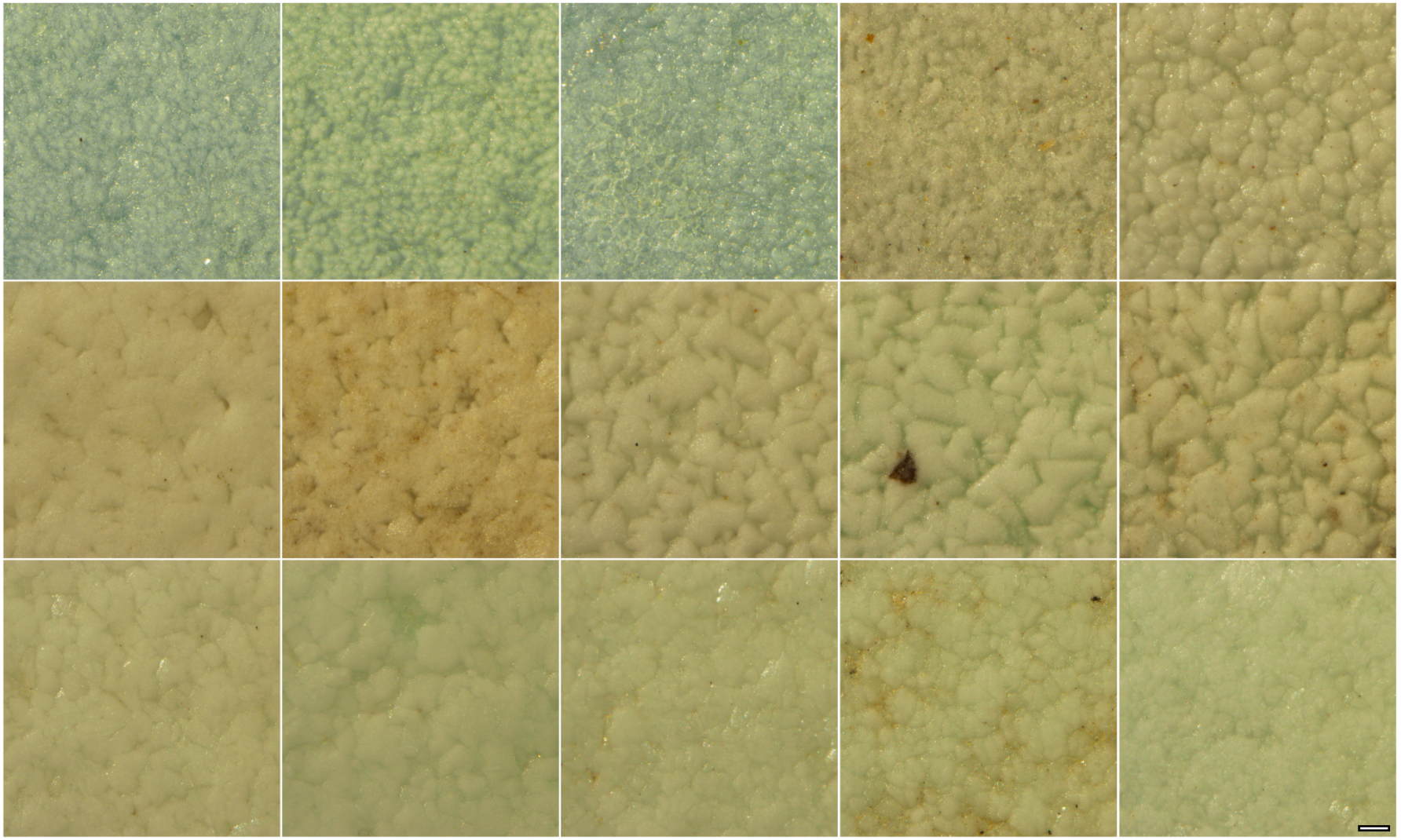

Figure 5. Examples of variation in eggshell surface structure in the *Alcini.* Brünnich's guillemot (top), razorbill (middle) and little auk (bottom). Scale bar = 100μm.

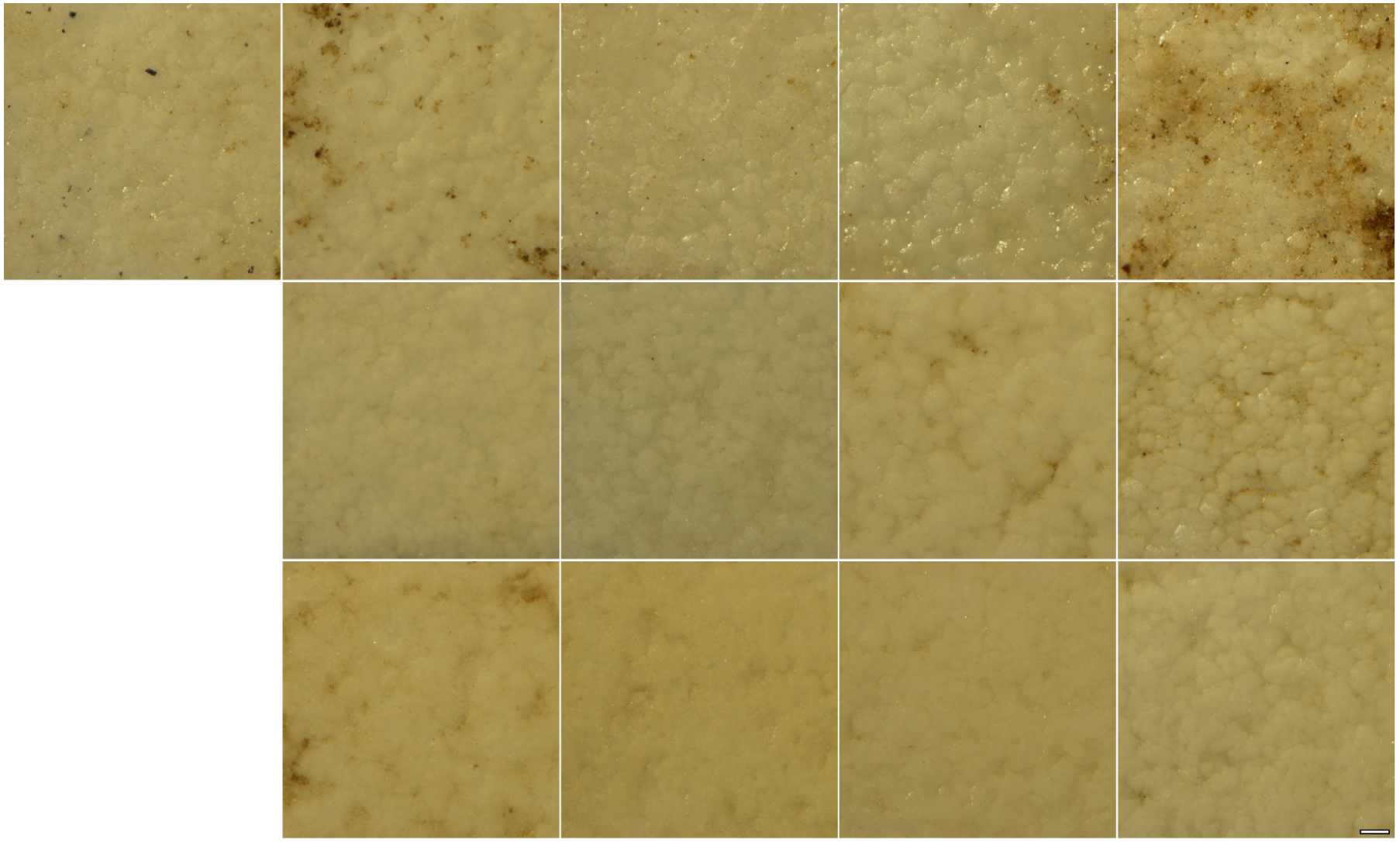

Figure 6. Examples of variation in eggshell surface structure in the *Aethinii*. Cassin's auklet (top), whiskered auklet (middle), least auklet (bottom). Scale bar = 100µm.

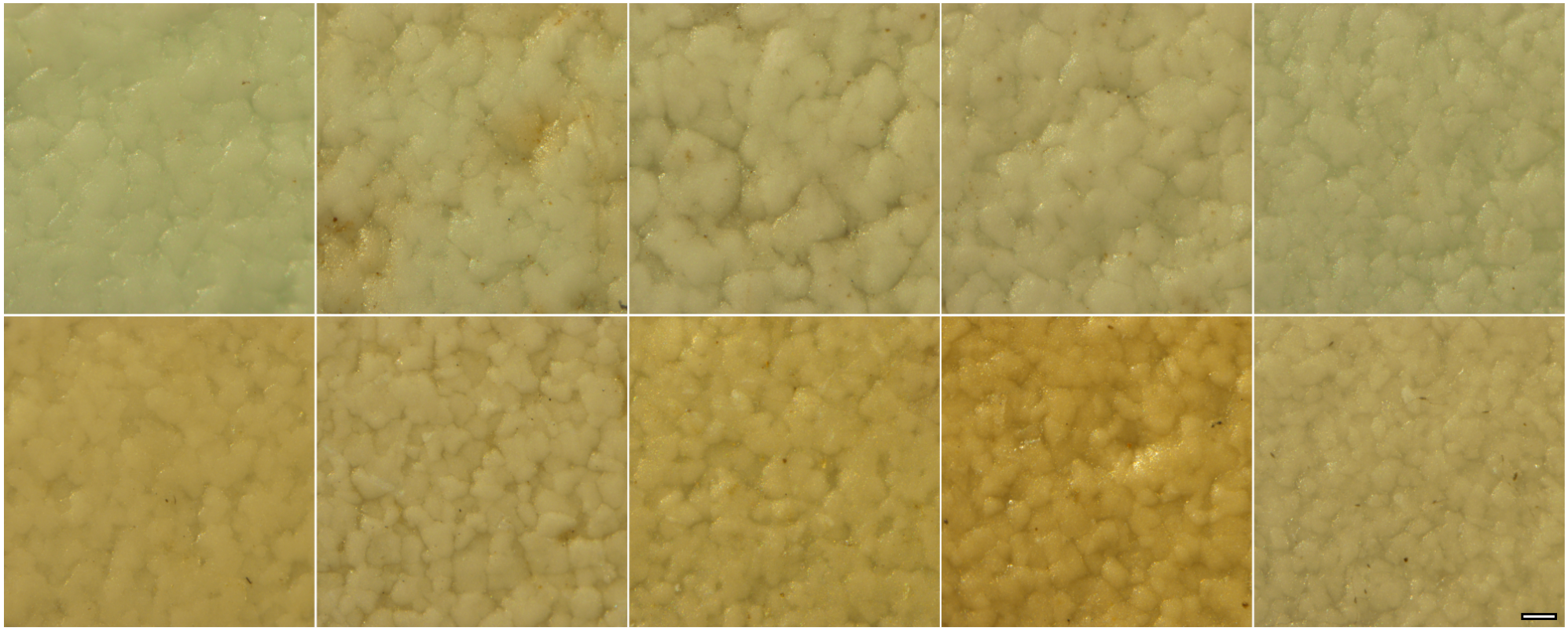

Figure 7. Examples of variation in eggshell surface structure between black guillemot (top) and Kittlitz's murrelet (bottom). Scale bar = 100µm.

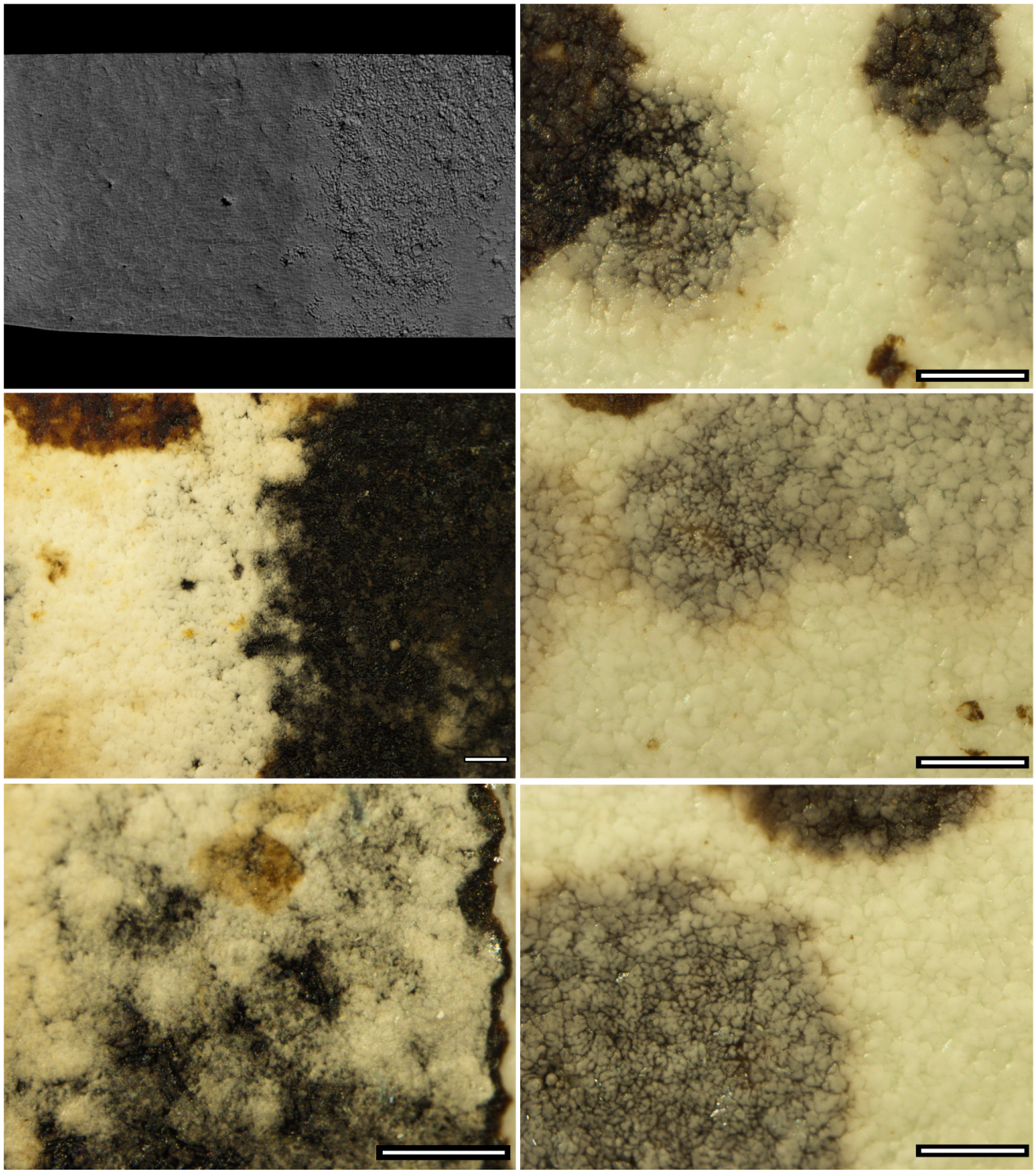

Figure 8. Surface level pigment and roughness variation in razorbill and black guillemot eggs. Left, volumetric reconstruction from microCT data (top) and the corresponding optical image (middle), and example of surface level pigmentation in razorbill eggshell (bottom). Right hand side, variation in pigmentation and surface roughness in black guillemot eggs. Scale bar = 500µm.

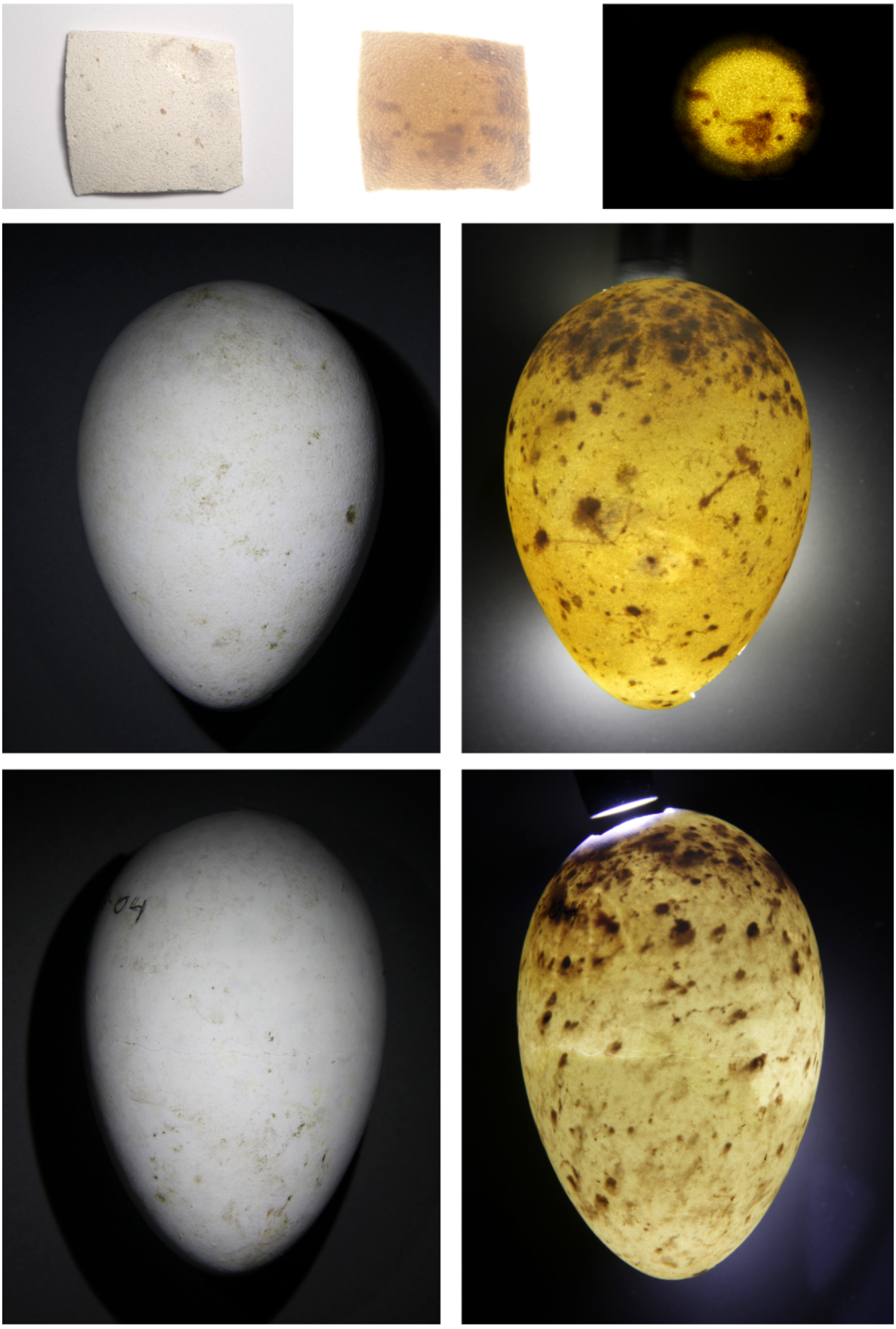

Figure 9. Pigment within *Fraterculini* eggshells. Top, pigment within Atlantic puffin eggshell. Middle, pigment visible in horned puffin eggshell when the egg is illuminated from the inside. Bottom, pigment in rhinoceros auklet eggshell. Images are not to scale.

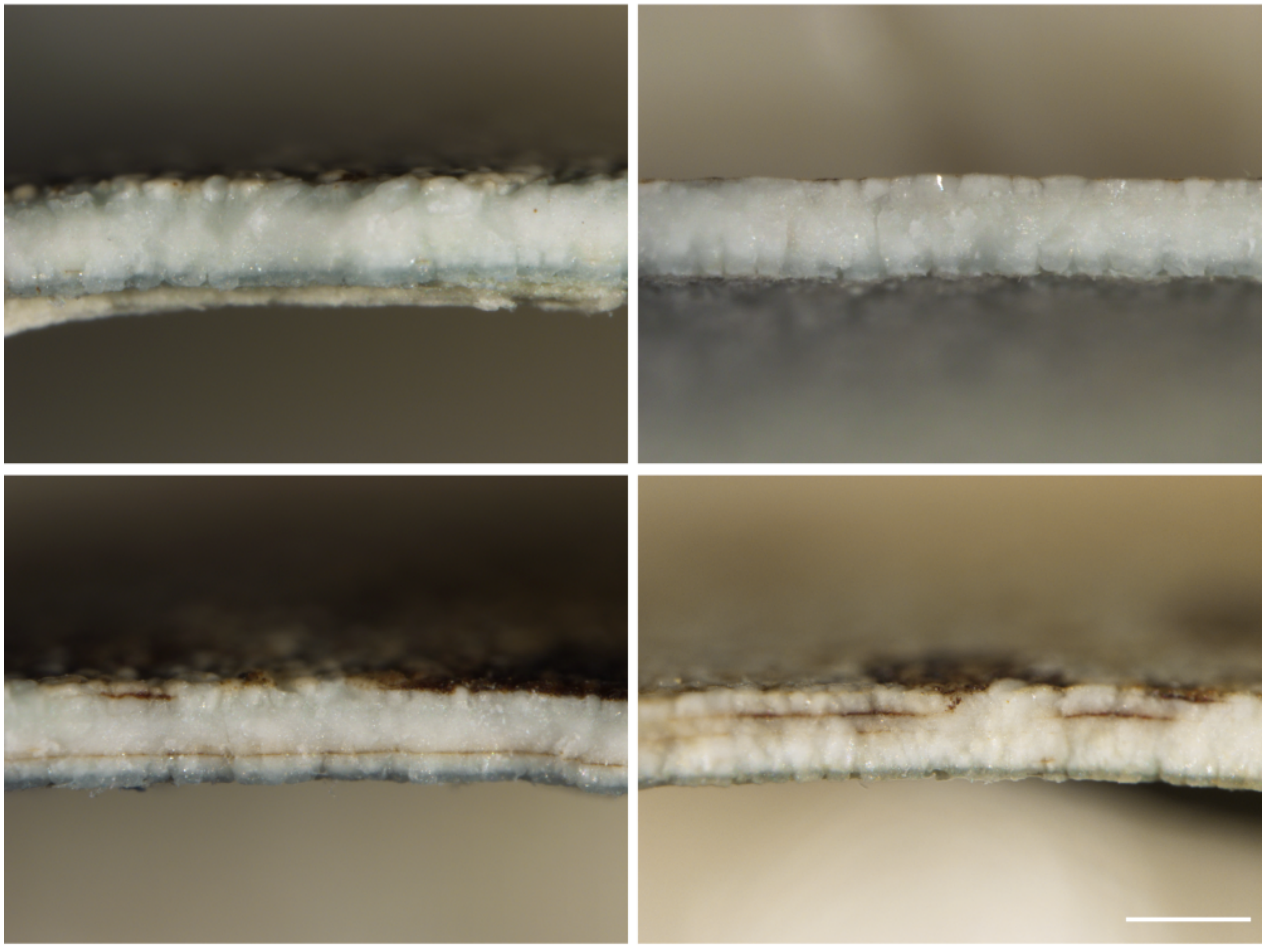

Figure 10. Pigment distribution through razorbill eggshell. Dark (brown/black) pigment patches can be found throughout the razorbill's shell and the inner (bottom) mammillary layer may be a different colour from the rest of the shell, including a translucent grey – blue colour. Scale bar = 500µm.

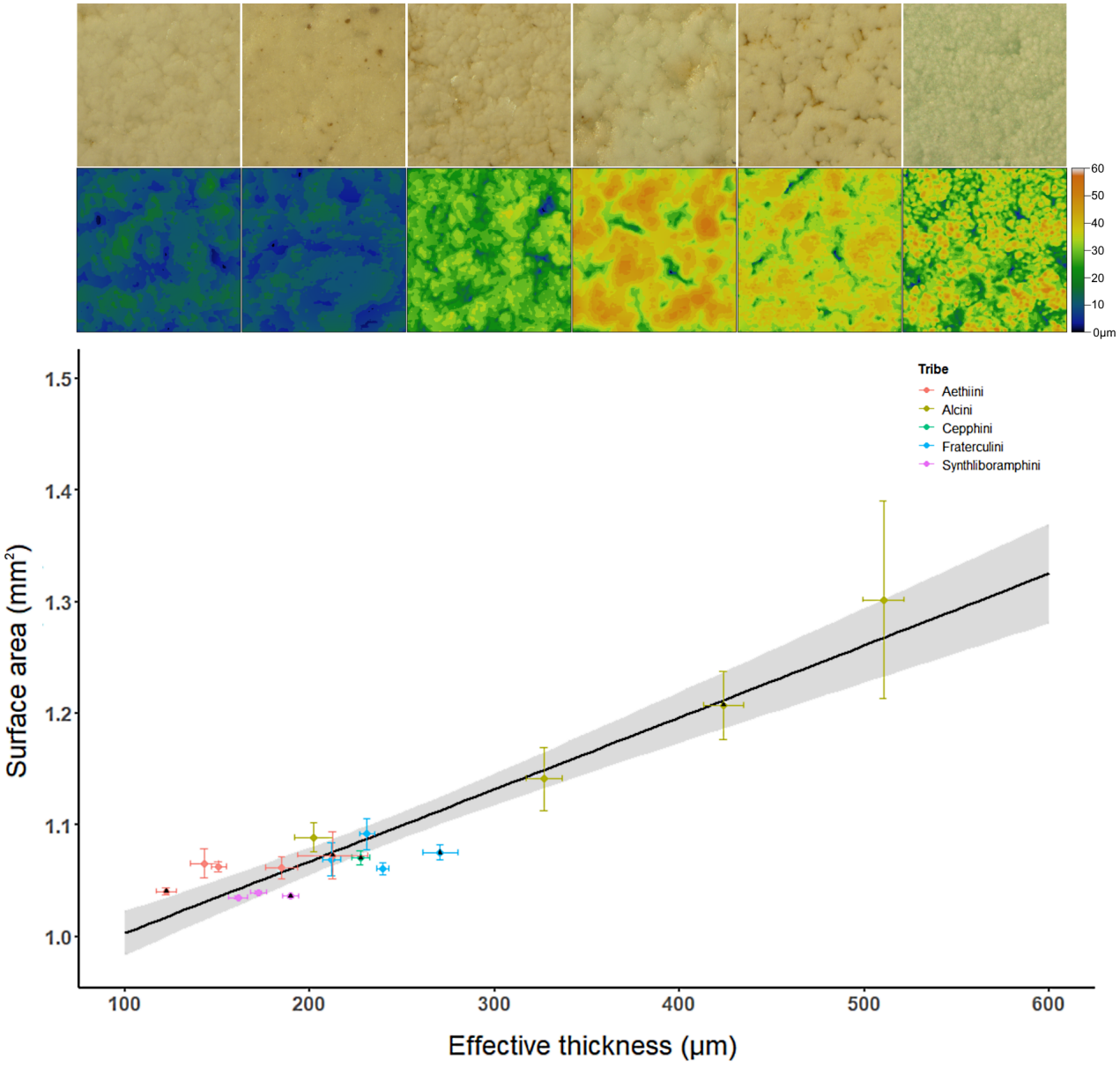

Figure 11. The relationship between effective eggshell thickness and surface area across the Alcidae. $R^2 = 0.894$, $F_{(1,15)} = 135$, $p < 0.0001$. Images were selected to demonstrate variation across the auk tribes, indicated by black triangle. Left to right, least auklet (*Aethia pusilla),* Scripps's murrelet (*Synthliboramphus scrippsi),* crested auklet (*Aethia cristatella),* black guillemot (*Cepphus grylle),* tufted puffin (*Fratercula cirrhata*) and Brünnich's guillemot (*Uria lomvia).* All images 1mm^2. Points are the mean with standard error bars. Black line is the regression relationship with the confidence interval (grey).